# DROUGHT IN THE SOUTHEASTERN UNITED STATES AND THE EFFECTS ON HYDROLOGICAL, PHYSIOCHEMICAL, NUTRIENT AND MACROINVERTEBRATE METRICS

by

KELSEY LAYMON

(Under the Direction of Darold Batzer)

## ABSTRACT

Drought occurs naturally due to variability in rainfall, but the frequency and severity of drought is increasing in many regions due to climate change (Trenberth et al., 2014). Hydrological drought has wide-ranging impacts on water quality, nutrients, carbon, and biota. This study investigated the effects of hydrological drought on historical streamflow patterns, water quality and macroinvertebrate metrics. We found that drought conditions affect water quality metrics, with changes in physicochemical, nutrient and carbon metrics. These changes were complex due to the regulation of the river and inputs from point and non-point sources. Further, we found that historical streamflows records showed broad declines over the southeastern U.S. with impacts being ecoregion specific. Additionally, these changes were spatially complex and likely from a range of causative factors. Finally, we found that streamflow declines were evident in individual basins and related to precipitation and drainage area. Given

the uncertainty of climate change and the predicted increased frequency and severity of drought in the future, investigations into changes induced by drought are increasingly important.

INDEX WORDS: aquatic insect, connectivity, floodplain, rivers, low flow, oxbow lakes, Savannah River, streams.

# DROUGHT IN THE SOUTHEASTERN UNITED STATES AND THE EFFECTS ON HYDROLOGICAL, PHYSIOCHEMICAL, NUTRIENT AND MACROINVERTEBRATE METRICS

By

KELSEY A. WILBANKS

BS, University of Alabama at Birmingham, 2013

MS, Georgia Southern University, 2018

A Dissertation Submitted to the Graduate Faculty of The University of Georgia in Partial Fulfillment of the Requirements for the Degree

DOCTOR OF PHILOSOPHY

ATHENS, GEORGIA

2024

# DROUGHT IN THE SOUTHEASTERN UNITED STATES AND THE EFFECTS ON HYDROLOGICAL, PHYSIOCHEMICAL, NUTRIENT AND MACROINVERTEBRATE METRICS

by

KELSEY WILBANKS

Major Professor: Darold P. Batzer

Committee: Stephen W. Golladay

Amy D. Rosemond

Electronic Version Approved:

Ron Walcott
Vice Provost for Graduate Education and Dean of the Graduate School
The University of Georgia
December 2024

# DEDICATION

I would like to dedicate my dissertation to my family. For those that supported me and are long past and those that support me today. To my mom and grandma, that were educators and encouraged me to always ask questions and not be afraid of learning something new. Their life-long learning and passion for education inspired me to always be open to the pursuit of knowledge. Also, for my husband, Brock and my son, Colin for their continued support. Brock's support gives me confidence to accomplish the impossible and Colin's innocence and spirit inspires me to work hard to provide a better future for him. Without their support every day, I would not be where I am today.

# ACKNOWLEDGEMENTS

I would like to thank my advisor, Dr. Darold Batzer for his guidance, dependability and unwavering support. His patience and gentle guidance allowed me to follow my own path of interests and grow as a scientist. His respect and treatment of me as a colleague provides the highest standard of how professors should treat their graduate students. I have thoroughly enjoyed my time working with him and thank him for his continued support. He is a god of gods.

I would also like to thank my committee members, Dr. Amy Rosemond and Dr. Stephen Golladay. They have provided insight and perspective into my research that helped to grow my research even further. Additionally, their mentorship, inclusion and kindness has made the graduate student process less daunting.

Lastly, I would like to thank my lab mates, Sophie Reindl and Gabriela Cardona Rivera. Sophie was a great help in the field and her cheerful disposition, adaptability and sense of humor made difficult tasks enjoyable. I would like to thank Gabriela for her guidance navigating the interworking of all things UGA and our lab. Her tenacity, dedication and hard work are an inspiration.

Lastly, I would like to acknowledge the organizations that have provided funding for my research including the Georgia Environmental Protection Division and the Savannah-Upper Ogeechee Water Council. Barbara Stitt with GA EPD was an excellent grants administrator and her assistance with grant coordination and deliverables was greatly appreciated. Further, I'd like to acknowledge the Savannah-Upper Ogeechee Water Council for their continued support of my research.

# TABLE OF CONTENTS

# LIST OF TABLES

Page

# LIST OF FIGURES

Page

# CHAPTER 1

# INTRODUCTION

Freshwater ecosystems are critical habitats for maintaining biodiversity and providing ecosystem services. Despite this, freshwater ecosystems are one of the most threatened in the world, with 83% of freshwater species and 30% of freshwater ecosystems lost since 1970 (Tickner et al. 2020). Climate change and anthropogenic activities have led to the degradation of the freshwater ecosystems. Reductions in water quantities and changes in water qualities will have social, economic and environmental impacts.

Climate change is affecting water resources through increased surface temperatures and evaporation rates, decreased snowpack and increased variability in precipitation patterns. This results in more extreme weather events, including an increase in the frequency and severity of drought (Dai 2013, Trenberth et al. 2014). Recent studies have indicated global declines in streamflows (Zhang et al. 2023) as well as in the southeastern United States (U.S.) (van Vliet et al. 2013, Stephens and Bledsoe 2020, Dudley et al. 2020). Further, water demands will be exacerbated by increasing populations (i.e., the Southeast is expected to grow by 29% from 2010 to 2040) and associated anthropogenic activities (Sutton et al. 2021).

Drought conditions can have deleterious effects on freshwater ecosystems. Drought reduces freshwater levels and alters the timing and magnitude of flows (Mosley 2015). These alterations impact the physical, physicochemical, chemical and biological functioning of streams and rivers (Mosley 2015). However, the response to drought ultimately depends on the local environment and becomes increasingly complex in regulated systems. Given the complexity of changes that occur with drought, a more complete understanding of the effects of drought are

increasingly important. Understanding the impacts of drought will guide and assist policymakers, water managers, and stakeholders in creating solutions to reduce growing water resource problems.

This study aimed to understand drought in the southeastern U.S. and its effects on the hydrological processes, physiochemical metrics, nutrients and macroinvertebrates. First, I assessed macroinvertebrates in a hydrologically variable environment. Second, I evaluated the effects of reduced flow on the physicochemical, nutrients and carbon metrics for a major river in the southeastern U.S. Finally, I assessed long-term streamflow trends for streams and rivers in ecoregions for Georgia, South Carolina and North Carolina, and basins of the South Atlantic-Gulf Drainage. These studies highlight the complexity of drought and its effects on streams and rivers, as well as the challenges facing freshwater ecosystems due to the uncertainty about climate changes and interactions with anthropogenic drivers. Further, our studies emphasized the need for management, planning and mitigation as drought becomes more prevalent in the future.

LITERATURE CITED

Dai, A. 2013. Increasing drought under global warming in observations and models. Nature climate change. 3(1):52-58.

Mosley, L.M. 2015. Drought impacts on the water quality of freshwater systems; review and integration. Earth-Science Reviews. 140:203-214.

Dudley, R.W., R.M. Hirsch, S.A. Archfield, A.G. Blum, and B. Renard. 2020. Low streamflow trends at human-impacted and reference basins in the United States. Journal of Hydrology. 580:124254.

Mosley, L.M. 2015. Drought impacts on the water quality of freshwater systems; review and integration. Earth-Science Reviews, 140:203-214.

Stephens, T.A., and B.P. Bledsoe. 2020. Low-flow trends at Southeast United States streamflow gauges. Journal of Water Resource Planning Management. 146:04020032.

Sutton, C., S. Kumar, M.K. Lee, and E. Davis. 2021. Human imprint of water withdrawals in the wet environment: A case study of declining groundwater in Georgia, USA. Journal of Hydrology: Regional Studies. 35:100813.

Tickner, D., J.J. Opperman, R. Abell, M. Acreman, A.H. Arthington, S.E. Bunn, S.J. Cooke, J. Dalton, W. Darwall, G. Edwards, and I. Harrison. 2020. Bending the curve of global freshwater biodiversity loss: an emergency recovery plan. BioScience. 70(4):330-342.

Trenberth, K.E., A. Dai, G. Van Der Schrier, P.D. Jones, J. Barichivich, K.R. Briffa, and J. Sheffield. 2014. Global warming and changes in drought. Nature Climate Change. 4(1):17-22.

Van Vliet, M.T., Franssen, W.H., Yearsley, J.R., Ludwig, F., Haddeland, I., Lettenmaier, D.P. and Kabat, P., 2013. Global river discharge and water temperature under climate change. Global Environmental Change, 23(2), pp.450-464.

Zhang, Y., H. Zheng, X. Zhang, L. R. Leung, C. Liu, C. Zheng, Y. Guo, F. H. Chiew, D. Post, D. Kong, and H. E. Beck. 2023. Future global streamflow declines are probably more severe than previously estimated. Nature Water 1:261-271.

# CHAPTER 2

## FLOODING EFFECTS ON AQUATIC INVERTEBRATES IN OXBOW LAKES OF A SOUTHEASTERN USA RIVER FLOODPLAIN

Wilbanks, K.A. and D.L. Mullis. Accepted by Hydrobiologia. Reprinted here with permission of publisher 2022.

## ABSTRACT

We investigated the relative importance of connectivity to the main river channel and the influence of flooding on macroinvertebrate distributions in oxbow lakes of a southeastern USA river floodplain. Invertebrate assemblages were described in four oxbow lakes located on the Savannah River; two with continuous connection to the main stem river (i.e., high connectivity) and two that were only connected during a significant flood event (i.e., low connectivity). Invertebrate assemblages were sampled 25 times over a major flooding event (before, during and after) in 2014-2015 to determine the influence of lateral hydrological connection. Community response (pseudo-$F_{1,19}$ =1.06, $p<0.01$) showed differences in oxbow lakes before, during and after flooding. Assemblages did not differ between high and low connectivity lakes before or after flooding in community response or any individual metrics. However, during flooding, oxbow lakes with high connectivity differed in Tolerance and Habit metrics, and oxbows lakes with low connectivity differed in Composition, Tolerance and Functional Feeding Group metrics. Post-flood, invertebrate assemblages quickly reverted back to pre-flood conditions. Although flooding affected invertebrate assemblages, with impacts being greatest in oxbows with low connectivity, responses were short-lived and pre-flood conditions soon reestablished.


## INTRODUCTION

River floodplains are comprised of a mosaic of ecosystems and habitats. A prominent component of floodplains are oxbow lakes, which are small lakes located in an abandoned meander loop of a river. They enrich the floodplain heterogeneity by increasing the physical, hydrological and habitat diversity, and are a unique link between aquatic and terrestrial environments (Gallardo et al. 2014).

Oxbow lakes that are newly formed are often hydrologically connected longitudinally to the parent river by inlet and outlet channels, which allows for the exchange nutrients, algae and the migration of swimming organisms (Ward & Stanford 1995, Obolewski et al. 2016). Oxbow lakes import and retain

nutrient-rich sediments from the surrounding landscape and act as sinks for contaminants in suspension (Constantine et al. 2010). The alteration of nutrients and algae by riverine water inputs determines the structure and function of aquatic communities and contributes to the diversity and production of organisms within the oxbow lakes. Longitudinal connectivity to the parent river has been described as a critical component in maintaining biodiversity and structuring the biotic community (Gallardo et al. 2009, 2014, Obolewski et al. 2015). Older oxbow lakes often have lost their connection to the river and are particularly susceptible to retention of nutrients and pollutants (Gallardo et al. 2009, Obolewski et al. 2016). Oxbow lakes that are not connected to the parent river have been reported to have low richness of zooplankton (Frisch et al. 2004) and fish (Ward et al. 1999, Sheaves et al. 2007). However, retention of these nutrients and biota can be exchanged with the parent river through lateral hydrological connectivity.

Periodic overbank flooding, or lateral hydrological connectivity reestablishes the exchange of energy, nutrients, and organisms from oxbow lakes to the parent river (Paillex et al. 2013). The level of hydrological connectivity can range from isolated waterbodies, which are only inundated during the most extreme floods (e.g., low connectivity), to highly connected habitats, which are located near the main channel and maintain near permanent connection to the parent river (e.g., high connectivity) (Gallardo et al. 2014). In addition, flood pulse variation (i.e., duration, frequency, amplitude and rate of change) creates high spatiotemporal heterogeneity and impacts the exchange of materials and organisms (Bhattacharya et al. 2016). This is crucial for the dispersal of aquatic organisms between interconnected habitats, thus affecting the distribution of organisms (Sheaves et al. 2007, Gallardo et al. 2009, Batzer & Boix 2018). Batzer et al. (2018) showed a combination of lateral and longitudinal connectivity are important drivers of abiotic and biotic conditions in southeastern USA floodplains.

Oxbow lakes are highly productive environments and can have substantially higher production than the parent river or the surrounding terrestrial landscape (Tockner & Stanford 2002), and additionally, are important habitats for aquatic biodiversity (Reckendorfer et al. 2006, Pan et al. 2014). Oxbow lakes provide biota refuge from high flows, predators and disturbances, and an area to recover from floods or droughts (Glińska-Lewczuk & Burandt 2011). Therefore, aquatic insect communities have been shown to

respond to variability in hydrodynamics in floodplains (Batzer & Boix 2018). For example, predators and deposit feeders have been shown to respond positively to reduced flows, and thus, may be expected in higher abundance in low connectivity oxbow lakes (Gallardo et al. 2014). Whereas shredders, scrapers and filter feeders have been shown to respond positively to high flows and are well adapted to exploit the limited food resources of frequently flooded habitats (Gallardo et al. 2014). For southeastern USA river floodplains, Batzer et al. (2018) developed a conceptual model for invertebrate distributions. Aquatic communities in the lower- reach floodplains experience predictable seasonal flooding, and the organisms in these communities are well adapted for floods. Further, Batzer et al. (2018) described patterns of redistribution during flooding and found that strong predation pressure prevented incursions of lotic invertebrates, suggesting a community of obligate wetland organisms in southeastern USA floodplains. However, across a range of rivers and regions, the redistribution of aquatic invertebrates during flooding appears complex (Sheldon & Thoms 2006, Reese & Batzer 2007).

This study aimed to compare macroinvertebrate assemblage response to hydrological connectivity in oxbow lakes of the Savannah River floodplain. We predicted (1) invertebrate assemblages would differ in high and low connectivity oxbow lakes at baseflow. We hypothesized that obligate wetland taxa would dominate in low connectivity oxbow lakes due to the lack of riverine inputs and lotic taxa would be more prevalent in high connectivity oxbow lakes due to the frequent exchange of water via the parent river. (2) A flood event, which connected the river channel to the main expanse of the floodplain, would significantly affect invertebrate assemblages in oxbow lakes, with impacts being the greatest in the low connectivity oxbow lakes. We hypothesized that inputs of riverine water would significantly affect conditions in low connectivity oxbow lakes whereas inputs of riverine water would not significantly affect high connectivity oxbow lakes as they would have similar environmental conditions before and during flooding. (3) A flood event would have long-term impacts on invertebrate assemblages in oxbow lakes, beyond the duration of the flood. We predicted that invertebrate assemblages would reorganize with the onset flooding, but the reorganization after the flood would take at least several months for wetland

taxa to reestablish. Furthermore, we predicted low connectivity assemblages would experience greater reorganization and require more time for recovery.

## MATERIALS AND METHODS

*Study Sites*

We studied four oxbow lakes located in the lower portion of the Savannah River, in the southeastern USA Coastal Plain ecoregion. The Savannah River is approximately 484 kilometers (km) long, drains an area of 25,511 $km^2$ and forms the border between South Carolina and Georgia. The hydrology of the Savannah River has been greatly altered by dams including J. Strom Thurmond Dam located 175 river km upstream from our study area. Flow dynamics and water levels are controlled by J. Strom Thurmond Dam which was built in 1952. According to Sanders et al. (1990), flood frequency analyses showed flooding prior to the J. Strom Thurmond Dam impoundment exceeded all floods since 1952, even when adjusted for regulation. Thus, oxbow lakes do not experience as frequent or intense overbank flooding as they would have prior to the J. Strom Thurmond dam installation. During late 1800s, the Savannah River was channelized for navigation, cutting through numerous bends, and leaving many cut off channels. Maintenance of the Savannah River for commercial shipping ended in 1979. Four of these cut off channels (i.e., oxbow lakes) were selected for this study, two with constant longitudinal hydrological connection and two with no lateral hydrological connection during normal hydrology (Figure 2.1). Three of the lakes were located in Tuckahoe Wildlife Management Area (i.e., TWMA) in Screven County, Georgia and one was located across the river in Allendale County, South Carolina.

Possum Eddy Lake (i.e., 3.9 hectares) was located furthest upstream and Whirligig Lake (i.e., 2.91 hectares) was located furthest downstream. Conyers (i.e., 3.94 hectares) and Miller Lakes (i.e., 7.79 hectares) were in the middle (Figure 2.1; Table 2.1). Possum Eddy and Conyers Lakes had no longitudinal hydrological connection with the main channel of the Savannah River, except during floodstage (hereafter, low connectivity). Miller and Whirligig Lakes always retained some level of longitudinal

hydrological connection to the main river channel (hereafter, high connectivity) on their downstream arms.

Oxbow lakes in this study differed in morphology (Table 2.1, Figure 2.1). Lengths ranged from 500 – 1,000 meters (m), and sinuosities ranged from 1.2 to 5.6 (i.e., 1.0 represents completely straight). Possum Eddy and Conyers Lakes were shallow, averaging 2.0 m and 1.5 m, respectively, and Miller and Whirligig Lakes were deeper, averaging 3.0 m and 3.6 m, respectively. Adjacent floodplain habitat was dominated by willow (*Salix spp.*), bald cypress [*Taxodium distichum* (L.) Rich.] and variety of oaks (*Quercus spp.*), and canopy cover over the lakes was minimal.

*Study design and sampling*

Water quality and macroinvertebrates were sampled from July 2015 to June 2016 for a total of 25 samples across the four oxbow lakes. Water quality measurements, including temperature (°C), conductivity (μS $cm^{-1}$), pH and dissolved oxygen (DO; mg $L^{-1}$ and % saturation) were recorded using a portable multiparameter sonde (YSI 6600). Each measurement was taken just below the water surface, in the middle of each oxbow lake and prior to each sampling event for macroinvertebrates.

During the winter of 2015 and 2016, warmer than usual winter temperatures combined with an influx of warm tropical moisture created heavy rainfall across central and southern United States. Flash flooding and runoff was widespread in the Savannah River basin. Discharge ($m^3$ $s^{-1}$) measurements obtained from USGS gage 02197500, approximately 13.4 river kilometers upstream of Possum Eddy Lake, indicated that over-bank flooding occurred (i.e., flood stage was a gage height of approximately 4.3 m and a discharge of 453 $m^3$ $s^{-1}$) and all four oxbow lakes became connected to the main river channel.

Non-flood flows occurred from 1 June 2015 to 3 Nov 2015 (i.e., before) and high (4 samples) and low (4 samples) connectivity lakes were sampled at an average discharge of 180 ± 0.3 $m^3$ $s^{-1}$ (Figure 2.2). Flooding occurred from 4 November 2015 to 28 February 2016, with two major rising limbs, peak segments and falling limbs (i.e., during). The first rising limb began in early November 2015 and peaked

at 691 $m^3 s^{-1}$ during mid-November. The falling limb occurred during late December 2015 and reached its lowest flow at 233 $m^3 s^{-1}$, but immediately ascended into another major rising limb which peaked at 1,161 $m^3 s^{-1}$ during mid-January. Flooding had a reoccurrence interval of 7.8 years from a historical record of 92 years and oxbow lakes were continuously inundated for 115 days. High (4 samples) and low (2 samples) connectivity lakes were sampled at an average of 664 ± 5.5 $m^3 s^{-1}$ during the flood. Overbank flooding from the Savannah River into the oxbow lakes occurred from 4 November 2015 to 28 February 2016 and flow entered on the upstream arms of Possum Eddy and Conyers Lakes. Miller Lake was hydrologically connected on the downstream arm at baseflow with an approximate 17 m wide connection to the Savannah River, which increased to 67 m wide during flooding. Additionally, overbank flooding occurred on the upstream arm in Miller Lake. Whirligig Lake, at baseflow, was connected to the Savannah River on the downstream arm with an approximate 40 m wide connection that increased to 105 m wide during flooding. Oxbow lakes were still recognizable during flooding because large trees (e.g., *Salix spp.*, *Taxodium distichum*, *Quercus spp*.) dominated the floodplain and created distinguishable habitat. Flood conditions ended in late February 2016 and flows remained low until June 2016 (i.e., after). After flooding, high (6 samples) and low (5 samples) connectivity lakes were sampled at a discharge of 253 ± 1.5 $m^3 s^{-1}$.

To determine the structure of benthic assemblages living in the oxbow lakes, the lakes were divided into sampling areas (i.e., upstream arm, middle section, and downstream arm) and habitats (i.e., banks/rootwads, woody debris, leaf packs, soft/sandy sediments and submerged macrophytes). Macroinvertebrates were sampled using a D-frame dip net and sampling areas and habitats were sampled with equal level of effort for a total of 20-jabs according to GA Environmental Protection Agency standard operating procedures (GA DNR EPD 2007). The 20-jabs were partitioned to represent all habitat types present and dispersed to include a range of habitat types. During flooding, the height at which sampling occurred was elevated by approximately 2 m in Possum Eddy, 1 m in Conyers, 4 m in Miller and 3 m in Whirligig Lakes. Subsamples across sections and habitats were combined into composite

representative samples in the field from each lake and placed into a sieve bucket with a 500-µm mesh. Samples were rinsed in the field and then preserved in 95% ethanol, stored in plastic bags and transported to the laboratory for processing. In the laboratory, macroinvertebrates were washed a second time using a 500-µm sieve. A randomized 200 ± 20 organisms were sorted from each sample, following U.S. Environmental Protection Agency Standard Operating Procedures for sorting and subsampling (USEPA 2008). Macroinvertebrates were identified to lowest possible taxonomic level (i.e., ranging from genus for some insects, and order for some non-insects).

Common metrics used to describe invertebrate assemblages were calculated using GA DNR EPD (2007) procedures and included Richness, Composition, Environmental Tolerance, Functional Feeding Group (FFG) and Habitat Preference metrics. Environmental Tolerance, Functional Feeding Group and Habitat Preferences were obtained for each taxon from a GA DNR EPD (2012) taxa list. Richness metrics included Total Taxa, EPT Taxa, Trichoptera Taxa and Diptera Taxa. Composition metrics included % EPT, % Non-Insect, % Oligochaeta and % Gastropoda. Tolerance metrics included % Tolerant Individuals, Tolerant Taxa numbers, % Intolerant Individuals, Intolerant Taxa numbers and % Dominant Individuals. Tolerance ranges from 0-10, and a taxon was determined to be tolerant if the tolerance value was ≥ 7, and intolerant if the tolerance value was ≤ 3. Functional Feeding Group metrics included % Collector-gatherer, % Collector-filterer, % Scraper, % Shredder, % Predator and % Unknown, and Habitat Preference metrics included % Clinger, % Climber, % Burrower, % Sprawler, % Swimmer, % Skater and % Unknown.

*Data analyses*

Timing of the flood resulted in 8 samples collected before the flood, 6 samples collected during the flood, and 11 samples collected after the flood, with both high and low connectivity lakes being sampled in roughly equal proportions during each period. Permutational Analysis of Variance (i.e., PERMANOVA) results indicated significant differences (pseudo-$F_{1,19} = 1.06$, $p < 0.01$; Figure 3) between

temporal periods. Therefore, pairwise comparisons between lake treatment (i.e., high and low connectivity) were divided by flood stage into a before flooding event (i.e., before), during flooding event (i.e., during) and after flooding event (i.e., after).

For univariate metrics (i.e., water quality measures, individual invertebrate metrics), data was statistically contrasted spatially between oxbow lakes (i.e., high vs. low connectivity) within each temporal period (i.e., before, during and after), using a 1-way Analysis of Variance (ANOVA) with an a priori $\alpha$ of 0.05. Further, we compared temporal periods (i.e., before, during and after) within the oxbow lakes (i.e., high and low connectivity) using a 2- way ANOVA. For these temporal comparisons, we used Tukey-Kramer post hoc test ($\alpha$ =0.05) to determine how assemblages changed over time.

Multivariate PERMANOVA ($\alpha$ =0.05) was used to determine differences in overall community structure, and Nonmetric Multi-Dimensional Scaling (NMDS) was used to visualize patterns of assemblages among oxbow lakes over the study period. Data were square-root transformed prior to multivariate analyses and ordinations were run with a Bray-Curtis distance matrix for a maximum of 999 permutations. Similarity Percentage Analysis (SIMPER) was used to determine invertebrate taxa driving the differences. R (Version 3.6) was used to run ANOVAs (R Core Team 2020) and the vegan package (Oksanen et al. 2017) was used to perform Permutational Analysis of Variance (PERMANOVA), Nonmetric Multi-Dimensional Scaling (NMDS) with species vectors (envfit function) and Similarity Percentage Analysis (SIMPER).

## RESULTS

We found that the flood had a widespread impact on invertebrate communities, with assemblages in both high and low connectivity lakes during the flood being significantly different (pseudo-$F_{2,19}$= 1.06, $p < 0.01$; Figure 2.3) than those either before or after the flood. Taxa most influenced by the flood included *Labrundinia* (Diptera: Chironomidae), *Crangonyx* (Amphipoda: Crangonyctidae), *Polypedilum* (Diptera: Chironomidae) and *Corynoneura* (Diptera: Chironomidae).

*Conditions Before the Flood*

Prior to the flood, we did not detect any significant differences between high and low connectivity lakes for temperature, pH or DO (Appendix 2.2). However, conductivity (μS $cm^{-1}$) in high connectivity oxbow lakes was significantly higher than low connectivity oxbow lakes ($F_{1,6} = 17.38$, $p < 0.01$). Invertebrate community structure was not significantly different between high and low connectivity oxbow lakes. There were no differences between lakes for any of the individual invertebrate metrics including Richness, Composition, Tolerance, Functional Feeding Group and Habitat Preference metrics (Table 2.2).

*Conditions During the Flood*

During the flood, we did not detect any significant differences between high and low connectivity oxbow lakes for temperature, conductivity, pH or DO (Appendix 2.2). Overall, invertebrate community structure was not significantly different between high and low connectivity oxbow lakes. Richness and Habitat Preference metrics were similar between high and low connectivity oxbow lakes during flooding. However, Compositional, Tolerance and Functional Feeding Group metrics varied between high and low connectivity oxbow lakes during flooding. Composition metrics including % EPT ($F_{1,4} = 10.59$, $p = 0.03$; Figure 2.4a) and % Gastropoda ($F_{1,4} = 9.11$, $p = 0.04$; Figure 2.4b) were higher in low connectivity oxbow lakes. The genera *Stenonema* (Ephemeroptera: Heptageniidae), *Ephemerella* (Ephemeroptera: Ephemerellidae), *Eurylophella* (Ephemeroptera: Ephemerellidae) and *Baetis* (Ephemeroptera: Baetidae) comprised the majority (67.2%) of EPT taxa. Further, % Intolerant Individuals ($F_{1,4} = 7.98$, $p = 0.05$; 2. 4c) was 69% higher in low connectivity oxbow lakes. The genera *Ephemerella* (Ephemeroptera: Ephemerellidae), *Eurylophella* (Ephemeroptera: Ephemerellidae) and *Heptagenia* (Ephemeroptera: Heptageniidae) comprised the majority (68.2%) of intolerant individuals. The Functional Feeding Group metric, % Scrapers ($F_{1,4} = 9.35$, $p = 0.04$, Figure 2.4d) was 74% higher in low connectivity oxbow lakes. The freshwater snail orders Physidae and Planorbidae, and the genus *Stenonema* (Ephemeroptera: Heptageniidae) comprised the majority (76.9%) of the scrapers.

*Conditions After the Flood*

After the flood, we did not detect any significant differences between high and low connectivity oxbow lakes for temperature, conductivity, pH or DO (Appendix 2.2). Community structure (i.e., PERMANOVA) was not significantly different between high and low connectivity oxbow lakes. Further, Richness, Composition, Tolerance, Functional Feeding Group and Habitat Preference metrics were similar between high and low connectivity oxbow lakes after flooding.

*Changes in High Connectivity Lakes over Time*

Over the duration of the study, we did not detect any significant temporal (i.e., before, during and after) differences in high connectivity oxbow lakes for conductivity, pH or DO (Appendix 2.2). However, as expected due to seasonality, water temperature (°C) decreased during flooding ($F_{2,11} = 9.66$, $p < 0.01$), which occurred during the winter months. We found significant (pseudo-$F_{2,11}=2.75$, $p < 0.01$; Figure 2.3) differences in community structure among time periods; before and during flooding exhibited 72.3% dissimilarity, after and during flooding exhibited 70.6% dissimilarity, and before and after flooding were the most similar, exhibiting 57.3% dissimilarity (Table 2.3). Richness, Composition, Functional Feeding Group and Habitat Preference metrics in high connectivity oxbow lakes were similar among the three time periods. However, Tolerant Taxa ($F_{2,11} = 9.95$, $p < 0.01$; Figure 2.5a) and % Tolerant Individuals ($F_{2,11} = 5.89$, $p = 0.02$; Figure 2.5b) were less common during flooding. *Endochironomus* (Diptera: Chironomidae), *Glyptotendipes* (Diptera: Chironomidae), *Hyalella* (Amphipoda: Hyalellidae) and *Trepobates* (Hemiptera: Gerridae) comprised a large percentage (44.2%) of Tolerant individuals. Conversely, % Dominant individuals (i.e., *Polypedilum*) ($F_{2,11} = 5.74$, $p = 0.02$; Figure 2.5c), which comprised 16.8% of the total assemblage, were higher during flooding. % Clingers ($F_{2,11} = 4.92$, $p = 0.03$, 2. 5d) were significantly lower during flooding and 90.7% of these individuals were *Endochironomus* (Diptera: Chironomidae).

*Changes in Low Connectivity Lakes over Time*

There was no significant temporal (i.e., before, during and after) differences in low connectivity oxbow lakes for DO (Appendix 2.2). However, as expected due to seasonality, water temperature decreased during flooding ($F_{2,8}$ = 7.96, p = 0.01; Figure 2.6a) similar to the observations in high connectivity oxbow lakes (Figure 2.6). In addition, conductivity ($F_{2,8}$ = 12.15, p < 0.01; Figure 2.6b) and pH ($F_{2,8}$ = 5.21, p = 0.04; Figure 2.6c) decreased during flooding. We found significant (pseudo-$F_{2,8}$ = 2.46, p = 0.01) differences in community structure among temporal periods in the low connectivity oxbow lakes. Before and during flooding exhibited 71.1% dissimilarity, after and during flooding exhibited 71.2% dissimilarity, and before and after flooding were the most similar with 52.0% dissimilarity (Table 2.3). Richness and Habitat Preference metrics in low connectivity oxbow lakes were similar among the three time periods. However, the Composition metric, % Gastropoda ($F_{2,8}$ = 10.4, p <0.01, Figure 2.7a) was higher during flooding. Gastropods were comprised primarily of freshwater snails in Family Physidae (mean: 68.0 ± 9.1%). However, also included families Planorbidae and Lymnaeidae snails. Further, % Tolerant Individuals ($F_{2,8}$ = 10.4, p < 0.01; Figure 7b), Intolerant Taxa ($F_{2,8}$ = 160.36, p < 0.01; Figure 7c), % Intolerant Individuals ($F_{2,8}$ = 3,694, p < 0.01; Figure 2.7d) and % Dominant Individuals ($F_{2,8}$ = 4.95, p = 0.04; Figure 2.7e) varied among temporal periods. In addition, % Scrapers ($F_{2,8}$ = 7.54, p = 0.01; Figure 2.7f) and % Predators ($F_{2,8}$ = 5.65, p = 0.03; Figure 2.7g) differed among temporal periods. Scrapers were largely comprised of family Physidae (Gastropoda) and the beetle larvae, *Cyphon* (Coleoptera: Scirtidae). Predators were comprised of a number of taxa but notably *Enallagma* (Odonata: Coenagrionidae), Trombidiformes (Arachnida), *Procladius* (Chironomidae: Tanypodinae) and *Trepobates* (Hemiptera: Gerridae).

## DISCUSSION

Our study assessed whether connectivity to the main river channel affected the invertebrate assemblages in oxbow lakes and how a large flooding event altered invertebrate assemblages in oxbow lakes of the Savannah River floodplain. We found connectivity to the main river channel during baseflow

had minimal control on the assemblage of invertebrates. We hypothesized that macroinvertebrates would differ based on abiotic factors (e.g., oxbow age, flow, water quality), favoring small-bodied, short-lived, stress tolerant organisms in isolated or low connectivity oxbow lakes (Sheldon et al. 2010, Gallardo et al. 2014) and favoring larger, longer lived, and stress intolerant organisms that are more commonly found in lotic environments, in high connectivity oxbow lakes (Amoros & Bornette 2002). We also hypothesized that richness and functional feeding groups would differ based on the availability of food resources, with increased taxonomic richness as well as shredders, scrapers and filter feeders responding positively to flowing water (i.e., high connectivity oxbows) (Statzner & Beche 2010). Previous studies have indicated that river-oxbow connectivity has major effects on the habitat quality (Gallardo et al. 2008, Obolewski and Glińska-Lewczuk 2011), hydrology (Pan et al. 2014) and the diversity and distribution of macroinvertebrates (Amoros & Bornette 2002, Reckendorfer et al. 2006). Additionally, the age, depth, type of water body, and historical and evolutionary factors have been shown to drive taxonomic compositions (Bonda et al. 2006, Obolewski et al. 2015). Therefore, it is somewhat surprising that our findings did not show any richness, functional feeding group or compositional metric differences between high and low connectivity oxbow lakes before flooding, as has been shown by others (Gallardo et al. 2008, Paillex et al. 2013, Obolewski et al. 2015). However, we found Chironomidae larvae to be the dominant organism, suggesting that both high and low connectivity oxbow lakes favored small-bodied, short-lived organisms (Sheldon et al. 2010) that thrive in a hydrologically variable environment (Anderson & Ferrington 2013). Our data supports the conceptual model presented in Batzer et al. (2018), suggesting that Coastal Plain floodplains are mostly controlled by internal processes and the communities within them function independently from the river channel. Despite the connection to the main stem of the river, oxbow lakes functioned similarly to each other, suggesting the assemblage of organisms occupying the oxbow lakes were uniquely adapted to survive in floodplain habitats. However, in our study the ecotonal interactions and wetland processes became less dominant during flooding, thus allowing for the shift of community composition.

We also hypothesized that flooding would impact the assemblage of macroinvertebrates within oxbow lakes, and impacts would be greatest in low connectivity oxbow lakes that otherwise do not receive inputs of riverine water. During flooding, all oxbow lakes became well connected to the river channel creating similar environmental conditions across the entire expanse of the floodplain. Rising flood waters allowed oxbow lakes to become hospitable and accessible for aquatic organisms that otherwise would not be able to withstand the abiotic or biotic constraints (Batzer and Wissinger 1996). In our study, the response of high and low connectivity changes in macroinvertebrate assemblage (i.e., specifically Chironomidae taxa) was unexpected, as one would expect similar changes with flooding (Reese & Batzer 2007). For example, EPT richness has previously been shown to peak in highly connected oxbow lakes (Paillex et al. 2009, Gallardo et al. 2008), and therefore, it is surprising that EPT richness was significantly higher in low connectivity oxbow lakes since both types were well connected during flooding (Chanut et al. 2019). Our findings corroborated the findings of Arrington and Winemiller (2006), who found that most taxa reorganized in oxbow lakes in a predictable manner throughout seasonal water level changes. The shift in assemblages could be attributed to a various mechanisms including colonization dynamics, species-specific evolutionary constraints (Resh & Rosenberg 1984), refugia seeking (Matthaei & Townsend 2000), biotic interactions (Arscott et al. 2005) or foraging strategies (Gallardo et al. 2009, McInerney et al. 2017). For example, a disproportional biotic shift observed was the decrease of predators in low connectivity oxbow lakes. Floodplains in the lower portion of rivers have been described as having a strong community of invertebrate predators (Gallardo et al. 2014, Batzer et al. 2018), but with an influx of macroinvertebrates exploiting the low connectivity oxbow lake from external habitats, predators may have become less dominant. Fewer predators may have allowed for habitat exploitation with less predation risk. Another disproportional biotic shift observed was the strong snail response to flooding, which has not been previously reported. Snails were not common in the oxbow lakes, either before or after the flood, but were present during flooding, especially in low connectivity oxbow lakes. Pulmonate snails have been found to be ubiquitous in completely lentic floodplains because their pulmonary respiration allows for survival under low oxygen conditions (Reckendorfer et al. 2006,

Guan et al. 2017). Instead, snails were only present during flooding or lotic conditions in low connectivity oxbow lakes. Some snail taxa are capable of aestivation in soil during dry periods (Strong et al. 2008), which might explain their reemergence during a wet period, but not their disappearance after the flood waters receded. Although flooding caused a redistribution of invertebrates in the Savannah River floodplain lakes, it was not uniform, and those changes did not persist.

After flooding receded, macroinvertebrate assemblages quickly reverted back to the pre-flooding community, yet another unexpected result. We had hypothesized that flooding would have long term impacts, but recovery occurred within two weeks after the falling limb of the hydrograph. Matthaei & Townsend (2000) indicated changes in floodplain communities persisted 5 months after floodwaters had receded and Dube et al. (2017) indicated increased richness persisted for at least 3 months after flooding receded. Our findings may be due to a variety of abiotic components (e.g., heat stress, dissolved oxygen fluctuations, etc.) not measured in our study that inhibited organism persistence after the flood. Batzer et al. (2018) assessed the progressive longitudinal changes of floodplains and found a unique assemblage of macroinvertebrates associated with Piedmont headwater streams, mid-reach Piedmont river channels, and large Coastal Plain river channels. They found that the communities in the Coastal Plain floodplains were dominated by obligate wetland fauna, well adapted to withstand flood-pulse variability (e.g., by spending low water periods as dessication-resistant stages in soil and leaf litter, or by life history strategies) and capable of exploiting these habitats. Flooding occurs frequently in the Coastal Plain ecoregion, where our study was conducted, and therefore, flooding is a regular seasonal event, for which the organisms have developed adaptations.

In the oxbow lakes of the Savannah River floodplain, hydrological connectivity had less than expected control on the assemblage of aquatic invertebrates. Our results indicate that connectivity to the main river channel does not dramatically affect macroinvertebrate assemblages. While large floods have clear impacts on oxbow lake invertebrates, the invertebrate fauna appears to be well adapted to seasonal hydrological variability, and quickly reestablishes. This does not mean that connectivity is unimportant, however. Non-natural breaks in connectivity, from human controls on flows or creation of non-natural

breaks in connectivity (e.g. dikes), likely will have more impacts (see Gallardo et al. 2008, Guan et al. 2017) than natural variation in connectivity. Further, connectivity between the floodplain and river channels may have important impacts on the channel (an aspect not addressed by our study). Our study indicates that invertebrate assemblages in oxbow lakes are unique and resilient, and that oxbow lakes are not simply ecotones between river channels and floodplains but constitute a unique and valuable habitat onto themselves.

## ACNOWLEDGEMENTS

Funding for this project was provided by the USGS State Water Resources Research Act Program Project ID 2015SC98B and the City of Augusta, City of Aiken and Columbia County municipalities. We thank Darold P. Batzer for his guidance and support framing and editing this manuscript. Field assistance was provided by Matthew Erickson, Nicole Hiabach, Jason Moak, Chalisa Nestell, and Liam Wolff.

**REFERENCES**

Amoros, C. & G. Bornette, 2002. Connectivity and biocomplexity in waterbodies of riverine floodplains. Freshwater Biology 47(4):761-776.

Anderson, A.M. & L.C. Ferrington, 2013. Resistance and resilience of winter-emerging Chironomidae (Diptera) to a flood event: implications for Minnesota trout streams. Hydrobiologia 707(1):59-71.

Arrington, D.A. & K.O. Winemiller, 2006. Habitat affinity, the seasonal flood pulse, and community assembly in the littoral zone of a Neotropical floodplain river. Journal of the North American Benthological Society 25(1):126-141.

Arscott, D.B., K. Tockner & J.V. Ward, 2005. Lateral organization of aquatic invertebrates along the corridor of a braided floodplain river. Journal of the North American Benthological Society 24(4): 934-954.

Batzer, D.P. & S.A Wissinger, 1996. Ecology of insect communities in nontidal wetlands. Annual Review of Entomology 41(1):75-100.

Batzer, D.P. & D. Boix, 2018. Invertebrates in freshwater wetlands. Springer Cham 451-492.

Batzer, D.P., G.B. Noe, L. Lee & M. Galatowitsch, 2018. A floodplain continuum for Atlantic coast rivers of the Southeastern US: Predictable changes in floodplain biota along a river's length. Wetlands 38(1):1-3.

Bhattacharya, R., S. Hausmann, J.B. Hubeny, P. Gell & J.L. Black, 2016. Ecological response to hydrological variability and catchment development: insights from a shallow oxbow lake in Lower Mississippi Valley, Arkansas. Science of the Total Environment 569:1087-1097.

Bonada, N., N. Prat, V.H Resh & B. Statzner, 2006. Developments in aquatic insect biomonitoring: a comparative analysis of recent approaches. Annual Review Entomology 51(1) 495-523.

Chanut, P.C., T. Datry, C. Gabbud & C.T. Robinson, 2019. Direct and indirect effects of flood regime on macroinvertebrate assemblages in a floodplain riverscape. Ecohydrology 12(5): e2095.

Constantine, J.A., T. Dunne, H. Piegay & G. Mathias Kondolf, 2010. Controls on the alluviation of oxbow lakes by bed-material load along the Sacramento River, California. Sedimentology 57(2): 389-407.

Dube, T., L. DeNecker, J.H. Van Vuren, V. Wepener, N.J. Smit & L. Brendonck, 2017. Spatial and temporal variation of invertebrate community structure in flood-controlled tropical floodplain wetlands. Journal of Freshwater Ecology 32(1): 1-15.

Frisch, D., B.S. Libman, S.J. D'Surney & S.T. Threlkeld. 2004. Diversity of floodplain copepods (Crustacea) modified by flooding: species richness, diapause strategies and population genetics. Archiv fur Hydrobiologie 162(1): 1-18.

Gallardo, B., M. García, Á. Cabezas, E. González, M. González, C. Ciancarelli & F.A. Comín, 2008. Macroinvertebrate patterns along environmental gradients and hydrological connectivity within a regulated river-floodplain. Aquatic Sciences 70(3): 248-258.

Gallardo, B., S. Gascon, M. García & F.A. Comín, 2009. Testing the response of macroinvertebrate functional structure and biodiversity to flooding and confinement. Journal of Limnology 68(2):315-326.

Gallardo, B., S. Dolédec, A. Paillex, D.B. Arscott, F. Sheldon, F. Zilli, S. Mérigoux, E. Castella & F.A. Comín, 2014. Response of benthic macroinvertebrates to gradients in hydrological connectivity: a comparison of temperate, subtropical, Mediterranean and semiarid river floodplains. Freshwater Biology 59(3): 630-648.

GA Environmental Protection Agency (GA DNR EPD), 2012. GAEPD Taxa list with functional feeding group (FFG), habit, and tolerance values. Environmental Protection Division, https://epd.georgia.gov/macroinvertebrate-bioassessment-standard-operating-procedures-sop-and-metric-spreadsheets.

GA Environmental Protection Agency (GA DNR EPD), 2007. Macroinvertebrate biological assessment of wadeable streams in Georgia –standard operating procedures. Environmental Protection Division,

epd.georgia.gov/macroinvertebrate-bioassessment-standard-operating-procedures-sop-and-metric-spreadsheets.

Glińska-Lewczuk, K. & P. Burandt, 2011. Effect of river straightening on the hydrochemical properties of floodplain lakes: Observations from the Łyna and Drwęca Rivers, N Poland. Ecological Engineering 37(5): 786-795.

Guan, Q., H. Wu, K. Lu, X. Lu & D.P. Batzer, 2017. Longitudinal and lateral variation in snail assemblages along a floodplain continuum. Hydrobiologia 792(1):345-356.

Matthaei, C.D. & C.R. Townsend, 2000. Long-term effects of local disturbance history on mobile stream invertebrates. Oecologia 125(1): 119-126.

McInerney, P.J., R.J. Stoffels, M.E. Shackleton & C.D. Davey, 2017. Flooding drives a macroinvertebrate biomass boom in ephemeral floodplain wetlands. Freshwater Science 36(4):726-738.

Obolewski, K. & K. Glińska-Lewczuk, 2011. Effects of oxbow reconnection based on the distribution and structure of benthic macroinvertebrates. Clean–soil, Air, Water 39(9): 853-862.

Obolewski, K., K. Glińska-Lewczuk & A. Strzelczak, 2015. Does hydrological connectivity determine the benthic macroinvertebrate structure in oxbow lakes?. Ecohydrology 8:1488-1502.

Obolewski, K., K. Glińska-Lewczuk, P. Burandt, S. Kobus, A. Strzelczak & C. Timofte, 2016. Response of the fish community to oxbow lake restoration in a low-gradient river floodplain. Environmental Engineering & Management Journal (EEMJ) 15(6).

Oksanen, J.F., G. Blanchet, M. Friendly, R. Kindt, P. Legendre, D. McGlinn, P.R. Minchin, R.B. O'Hara, G.L. Simpson, P. Solymos, M.H.H. Stevens, E. Szoecs & H. Wagner, 2017. Vegan: Community Ecology Package. R package version 2.4-5. https://CRAN.R-project.org/package=veganR Core Team. R: A language and environment for statistical computing. R Foundation for Statistical Computing, Vienna, Austria. URL https://www.R-project.org/.

Pan, B., H. Wang & H. Wang, 2014. A floodplain-scale lake classification based on characteristics of macroinvertebrate assemblages and corresponding environmental properties. Limnologica-Ecology and Management of Inland Waters 49:10-17.

Paillex, A., S. Dolédec, E. Castella & S. Mérigoux, 2009. Large river floodplain restoration: predicting species richness and trait responses to the restoration of hydrological connectivity. Journal of Applied Ecology 46(1): 250-258.

Paillex, A., S. Dolédec, E. Castella, S. Mérigoux & D.C. Aldridge, 2013. Functional diversity in a large river floodplain: anticipating the response of native and alien macroinvertebrates to the restoration of hydrological connectivity. Journal of Applied Ecology 50 (1): 97-106.

R Core Team (2020). R: A language and environment for statistical computing. R Foundation for Statistical Computing, Vienna, Austria. https://www.R-project.org/.

Reckendorfer, W., C. Baranyi, A. Funk & F. Schiemer, 2006. Floodplain restoration by reinforcing hydrological connectivity: expected effects on aquatic mollusc communities. Journal of Applied Ecology 43(3): 474-484.

Reese, E.G. & D.P. Batzer, 2007. Do invertebrate communities in floodplains change predictably along a river's length?. Freshwater Biology 52(2): 226-239.

Resh, V.H. & D.M. Rosenberg. 1984. The ecology of aquatic insects. Praeger Publishers. New York, NY, USA.

Sanders Jr, C.L.., H.E. Kubik, J.T. Hoke Jr. & W.H. Kirby, 1990. Flood Frequency of the Savannah River at Augusta, Georgia. Department of the Interior, US Geological Survey.

Statzner, B. and L.A. Beche, 2010. Can biological invertebrate traits resolve effects of multiple stressors on running water ecosystems?. Freshwater Biology 55:80-119.

Sheaves M, R. Johnston & K. Abrantes, 2007. Fish fauna of dry tropical and subtropical estuarine floodplain wetlands. Marine and Freshwater Research 58(10):931-43.

Sheldon, F. & M.C. Thoms, 2006. Relationships between flow variability and macroinvertebrate assemblage composition: data from four Australian dryland rivers. River Research and Applications 22(2): 219-238.

Sheldon, F., S.E. Bunn, J.M. Hughes, A.H. Arthington, S.R. Balcombe & C.S. Fellows, 2010. Ecological roles and threats to aquatic refugia in arid landscapes: dryland river waterholes. Marine and Freshwater Research 61(8):885-895.

Strong, E.E., O. Gargominy, W.F. Ponder & P. Bouchet, 2008. Global diversity of gastropods (Gastropoda; Mollusca) in freshwater. Hydrobiologia 595(1): 149-166.

Tockner, K. & J.A. Stanford, 2002. Riverine flood plains: present state and future trends. Environmental Conservation 29(3): 308-330.

Ward, J.V. and J.A. Stanford, 1995. Ecological connectivity in alluvial river ecosystems and its disruption by flow regulation. Regulated Rivers: Research & Management, 11(1):105-119.

Ward, J.V., K. Tockner & F. Schiemer, 1999. Biodiversity of floodplain river ecosystems: ecotones and connectivity. River Research and Applications 15(1-3): 25-139.

US Environmental Protection Agency (USEPA), 2008. National rivers and streams assessment: laboratory methods manual. Office of Water and Office of Research and Development EPA-841-B-07-010. Washington, D.C., U.S.A.

Table 2.1: Morphological parameters of Possum Eddy, Conyers, Miller and Whirligig lakes on the Savannah River floodplain. Possum Eddy and Conyers (i.e., low connectivity) lakes were only hydrologically connected to the main stem of the Savannah River during flooding events whereas Miller and Whirligig (i.e., high connectivity) lakes maintained hydrological connection to the main stem of the Savannah River for the entirety of the study. Coordinates (GPS), sinuosity, maximum length (m), maximum and minimum width (m), average depth (m), average volume ($m^3$) and distance of upstream and downstream arm to the river (m) for each lake are included.

| | | Possum Eddy | Conyers | Miller | Whirligig |
|---|---|---|---|---|---|
| GPS coordinates | | 32.877138, -81.478933 | 32.841680, -81.448688 | 32.804420, -81.432423 | 32.792687, -81.420184 |
| Sinuosity S=D/a-b | | 1.2 | 1.2 | 5.6 | 1.5 |
| Area (hectares) | | 3.90 | 3.94 | 7.79 | 2.91 |
| Length (m) | | 476.2 | 538.4 | 926.5 | 676.0 |
| Width (m) | Min | 26.6 | 28.1 | 62.4 | 11.1 |
| | Max | 132.8 | 54.8 | 161.3 | 128.6 |
| Low flow (m) connection width | | 0 | 0 | 72.8 | 90.3 |
| Depth (m) | | 2.0 | 1.5 | 3.0 | 3.6 |
| Volume ($m^3$) | | 25,334 | 22,694 | 173,441 | 27,013 |
| Distance from River (m) | Upstream arm (a) | 67.5 | 199.3 | 91.9 | 336.2 |
| | Downstream arm (b) | 169.2 | 252.6 | 0 | 0 |

Table 2.2: Summary of metrics (mean ± SE) used to assess assemblages within the oxbow lakes of the Savannah River floodplains. Metrics include Richness, Composition, Tolerance, Functional Feeding Group and Habit Metrics, before, during and after flooding for high and low connectivity oxbow lakes.

| | | Before | | During | | After | |
|---|---|---|---|---|---|---|---|
| Metric Group | Metric | High | Low | High | Low | High | Low |
| Richness | Total Taxa | 26.0 ± 3.2 | 26.5 ± 3.7 | 18.0 ± 2.2 | 25.0 ± 0.0 | 24.8 ± 2.5 | 26.4 ± 2.9 |
| | EPT Taxa | 1.8 ± 0.3 | 1.8 ± 0.5 | 2.5 ± 1.6 | 7.0 ± 0.0 | 2.7 ± 0.5 | 2.6 ± 0.5 |
| | Trichoptera Taxa | 0.5 ± 0.3 | 1.0 ± 0.4 | 0.5 ± 0.5 | 1.0 ± 0.0 | 1.5 ± 0.5 | 1.4 ± 0.5 |
| | Diptera Taxa | 8.0 ± 2.0 | 11.5 ± 2.3 | 10.0 ± 1.4 | 8.0 ± 2.0 | 9.5 ± | 10.2 ± |
| Composition | %EPT | 7.5 ± 4.1 | 8.9 ± 3.5 | 2.7 ± 1.4 | 11.7 ± 3.0 | 4.6 ± 1.4 | 6.1 ± 1.8 |
| | % Non-Insect | 18.6 ± 7.3 | 24.3 ± 4.3 | 25.0 ± 6.2 | 40.5 ± 12.2 | 17.3 ± 2.9 | 20.5 ± 2.2 |
| | % Gastropoda | 5.7 ± 4.1 | 6.0 ± 2.1 | 5.0 ± 1.7 | 15.6 ± 4.0 | 3.0 ± 0.6 | 2.4 ± 0.6 |
| | % Oligochaeta | 2.0 ± 0.7 | 3.6 ± 2.2 | 7.0 ± 4.3 | — | 1.0 ± 0.8 | 3.9 ± 2.2 |
| Tolerance | Tolerant Taxa | 17.3 ± 1.9 | 17.5 ± 1.3 | 8.0 ± 1.2 | 10.0 ± 1.0 | 14.3 ± 1.1 | 16.0 ± 1.6 |
| | % Tolerant Individuals | 64.8 ± 9.6 | 78.6 ± 4.1 | 37.9 ± 11.1 | 48.6 ± 14.5 | 73.4 ± 3.4 | 73.1 ± 4.7 |
| | Intolerant Taxa | — | — | 1.3 ± 0.6 | 3.5 ± 0.5 | 0.5 ± 0.2 | — |
| | % Intolerant Individuals | — | — | 1.1 ± 0.6 | 3.6 ± 0.1 | 0.5 ± 0.3 | — |

| | | | | | | | |
|---|---|---|---|---|---|---|---|
| | % Dominant Individuals | 13.9 ± 3.9 | 6.4 ± 3.3 | 36.9 ± 9.6 | 31.0 ± 13.8 | 10.4 ± 3.9 | 8.5 ± 3.4 |
| Functional | % Collector | 21.5 ± 8.0 | 24.7 ± 5.3 | 28.8 ± 5.5 | 25.3 ± 0.1 | 18.6 ± 2.8 | 14.7 ± 5.5 |
| Feeding Group | % Filterer | 7.4 ± 3.0 | 16.5 ± 3.6 | 2.6 ± 1.9 | 0.9 ± 0.9 | 9.8 ± 2.0 | 17.4 ± 9.2 |
| | % Scraper | 8.4 ± 4.7 | 8.3 ± 1.2 | 7.1 ± 2.5 | 27.7 ± 9.2 | 6.1 ± 1.5 | 7.6 ± 2.8 |
| | % Shredder | 26.0 ± 4.5 | 15.8 ± 4.3 | 48.8 ± 1.2 | 37.2 ± 10.8 | 36.6 ± 6.9 | 31.5 ± 8.3 |
| | % Predator | 35.4 ± 13.2 | 34.4 ± 6.2 | 12.4 ± 5.2 | 8.4 ± 0.8 | 28.8 ± 5.9 | 27.6 ± 3.0 |
| Habit | % Clingers | 13.4 ± 6.1 | 6.8 ± 2.2 | 3.5 ± 1.9 | 11.4 ± 2.7 | 22.7 ± 4.1 | 17.1 ± 3.2 |
| | % Climbers | 11.3 ± 3.2 | 8.3 ± 2.9 | 0.9 ± 0.8 | 3.4 ± 2.7 | 7.4 ± 3.1 | 12.2 ± 4.4 |
| | % Burrowers | 6.3 ± 2.6 | 9.7 ± 3.3 | 4.4 ± 3.6 | 1.7 ± 1.7 | 8.1 ± 1.5 | 5.7 ± 1.5 |
| | % Sprawlers | 10.1± 5.8 | 19.5 ± 5.1 | 21.9 ± 4.5 | 5.5 ± 4.3 | 7.3 ± 3.7 | 8.0 ± 2.4 |
| | % Swimmers | 3.3 ± 1.4 | 1.0 ± 1.0 | 2.7 ± 1.6 | 3.0 ± 1.3 | 5.5 ± 2.1 | 1.6 ± 0.7 |
| | % Skaters | 14.2 ± 8.5 | 1.5 ± 1.2 | — | — | 3.7 ± 2.1 | 3.3 ± 2.2 |

Table 2.3: Summary of similarity percentage (SIMPER) results including the mean contribution (%) to overall dissimilarity and the ordered cumulative contribution (%) of the five most influential taxa (order:genus) contributing to temporal changes (i.e., before, during and after flooding), for high and low connectivity oxbow lakes of the Savannah River.

| Oxbow | Temporal Comparison | Taxon | Contribution (%) | Cumulative (%) |
|---|---|---|---|---|
| High | Before:During | Hemiptera: *Rheumatobates* | 4.1 | 5.7 |
| | | Hemiptera: *Trepobates* | 4.1 | 10.4 |
| | | Diptera: *Polypedilum* | 3.2 | 14.8 |
| | | Diptera: *Endochironomus* | 3.1 | 19.1 |
| | | Diptera: *Labrundinia* | 3.0 | 23.3 |
| | During:After | Diptera: *Polypedilum* | 5.0 | 7.1 |
| | | Diptera: *Endochironomus* | 3.7 | 12.3 |
| | | Diptera: *Labrundinia* | 3.5 | 17.2 |
| | | Amphipoda: *Hyalella* | 3.3 | 21.9 |
| | | Diptera: *Corynoneura* | 3.3 | 26.5 |
| | Before:After | Hemiptera: *Rheumatobates* | 3.4 | 5.9 |
| | | Hemiptera: *Trepobates* | 2.9 | 11.0 |
| | | Ephemeroptera: *Caenis* | 2.3 | 15.1 |
| | | Diptera: *Polypedilum* | 2.1 | 18.7 |
| | | Hirudinea | 1.9 | 22.0 |
| Low | Before:During | Amphipoda: *Crangonyx* | 4.4 | 6.2 |
| | | Diptera: *Polypedilum* | 4.0 | 11.8 |
| | | Diptera: *Glyptotendipes* | 3.8 | 17.2 |
| | | Ephemeroptera: *Stenonema* | 2.9 | 21.2 |

| | | | |
|---|---|---|---|
| | Ephemeroptera: *Caenis* | 2.7 | 25.0 |
| During:After | Amphipoda: *Crangonyx* | 4.6 | 6.4 |
| | Diptera: *Polypedilum* | 3.7 | 11.6 |
| | Diptera: *Endochironomus* | 3.4 | 16.4 |
| | Diptera: *Glyptotendipes* | 3.1 | 20.8 |
| | Ephemeroptera: *Stenonema* | 3.0 | 25.0 |
| Before:After | Diptera: *Glyptotendipes* | 3.1 | 5.9 |
| | Trombidiformes | 2.1 | 10.0 |
| | Ephemeroptera: *Caenis* | 2.0 | 13.9 |
| | Diptera: *Endochironomus* | 1.9 | 17.5 |
| | Diptera: *Polypedilum* | 1.6 | 20.6 |

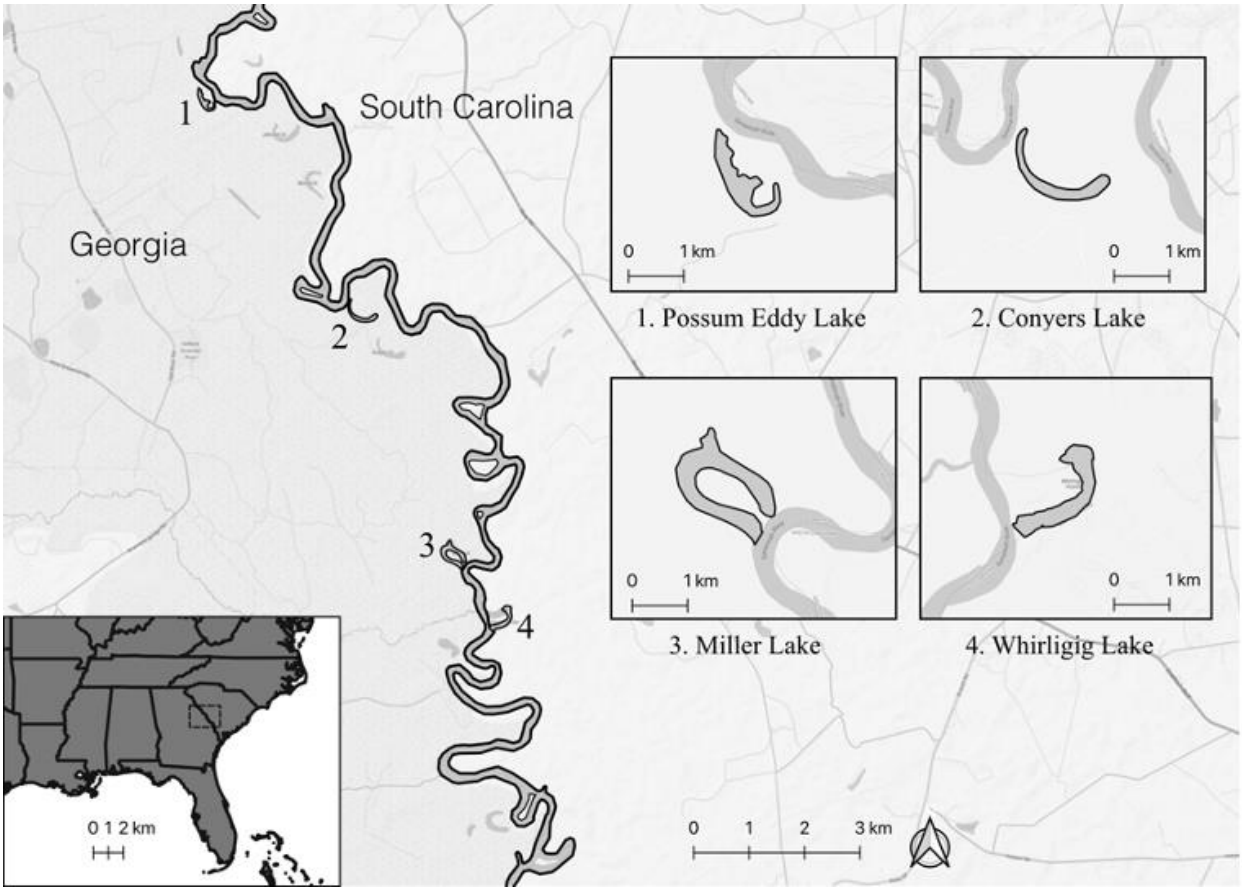


Figure 2.1: Study sites located along the Savannah River including Possum Eddy Lake (32.804420, -81.432423), located fartherest north and denoted as 1, Conyers Lake (32.841680, -81.448688), located downstream of Possum Eddy Lake and denoted as 2, Miller Lake (32.804420, -81.432423) located downstream of Conyers Lake and denoted as 3, and Whirligig Lake (32.792687, -81.420184), located farthest downstream and denoted as 4. The Savannah River forms the border between Georgia and South Carolina, USA.

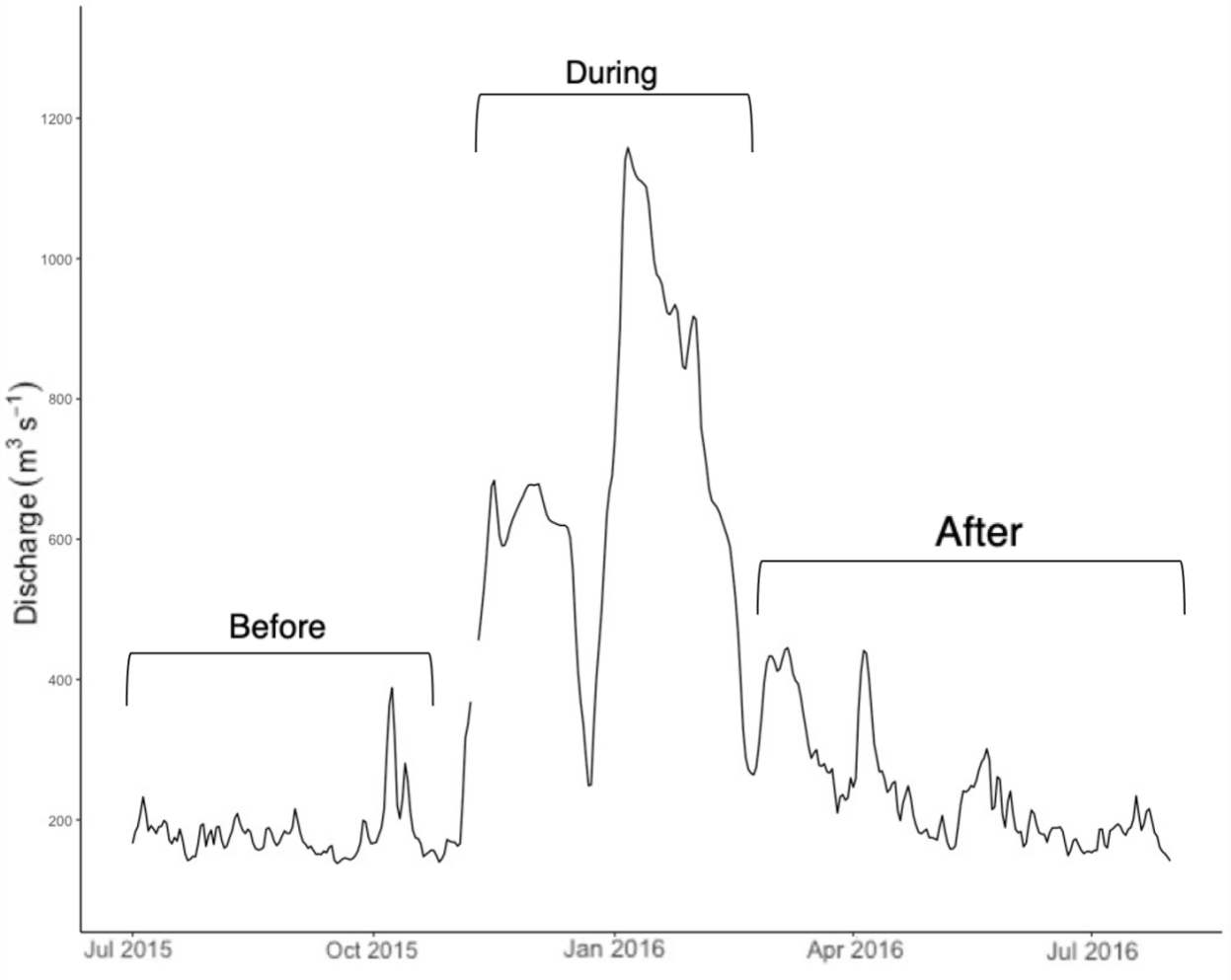


Figure 2.2:Average daily discharge ($m^3 s^{-1}$) from USGS gage (02197500) on the Savannah River for the sampling period of July 2015 to June 2016. Sampling before flooding (n = 8) occurred from late June 2015 to late October 2015 as indicated by the "Before" bracket, sampling during flooding (n = 6) occurred from early November 2015 to late February 2016 as indicated by the "During" bracket and sampling after flooding (n = 11) occurred from early March 2016 to late June 2016 as indicated by the "After" bracket. Overbank flooding from the Savannah River occurred into the oxbow lakes from 4 November 2015 to 28 February 2016 at a gage height of 4.3 m and a discharge of 453 $m^3 s^{-1}$.

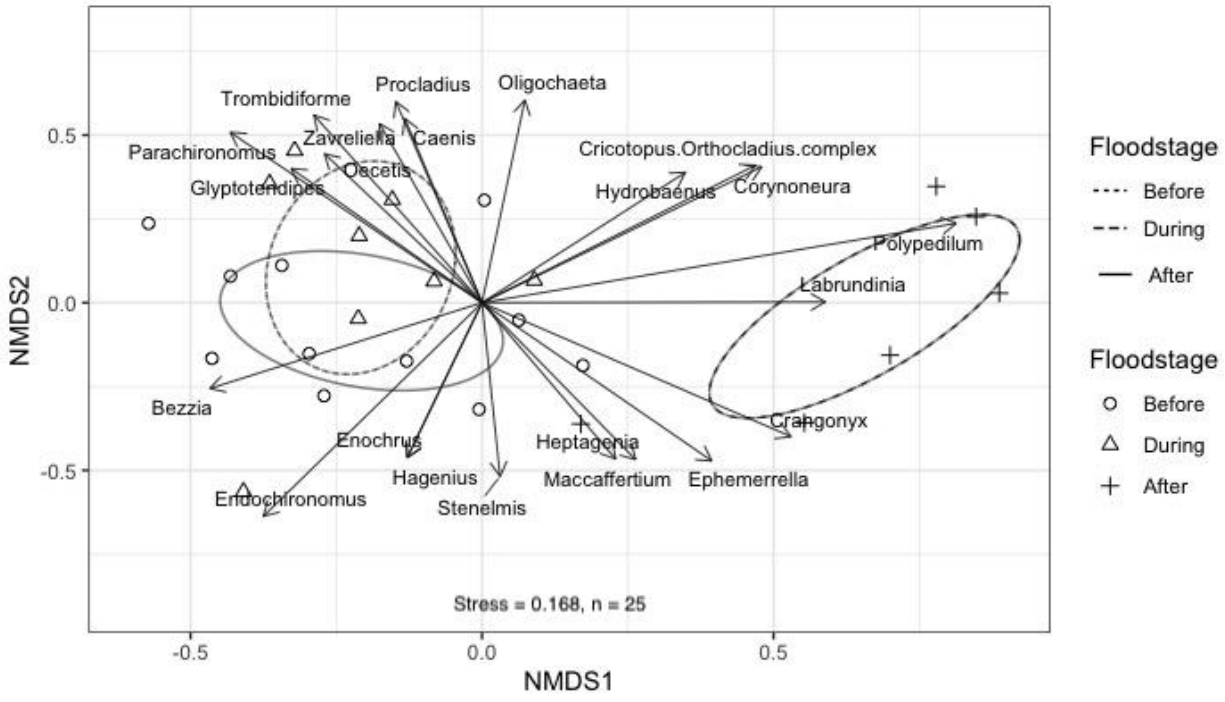


Figure 2.3: Non-metric multidimensional scaling (NMDS) ordination using Bray-Curtis similarity matrix for assemblages in high and low connectivity oxbow lakes. Triangles represent before flooding, crosses represent during flooding, and open circles represent after flooding. Ellipses represent 95% confidence intervals for each floodstage. Arrows indicate significant ($p < 0.05$) taxa contributing to differences and the length of arrows increase with correlation coefficient. PERMANOVA indicted significant differences in assemblages among time periods (pseudo-$F_{2,19} = 1.06$, $p < 0.01$).

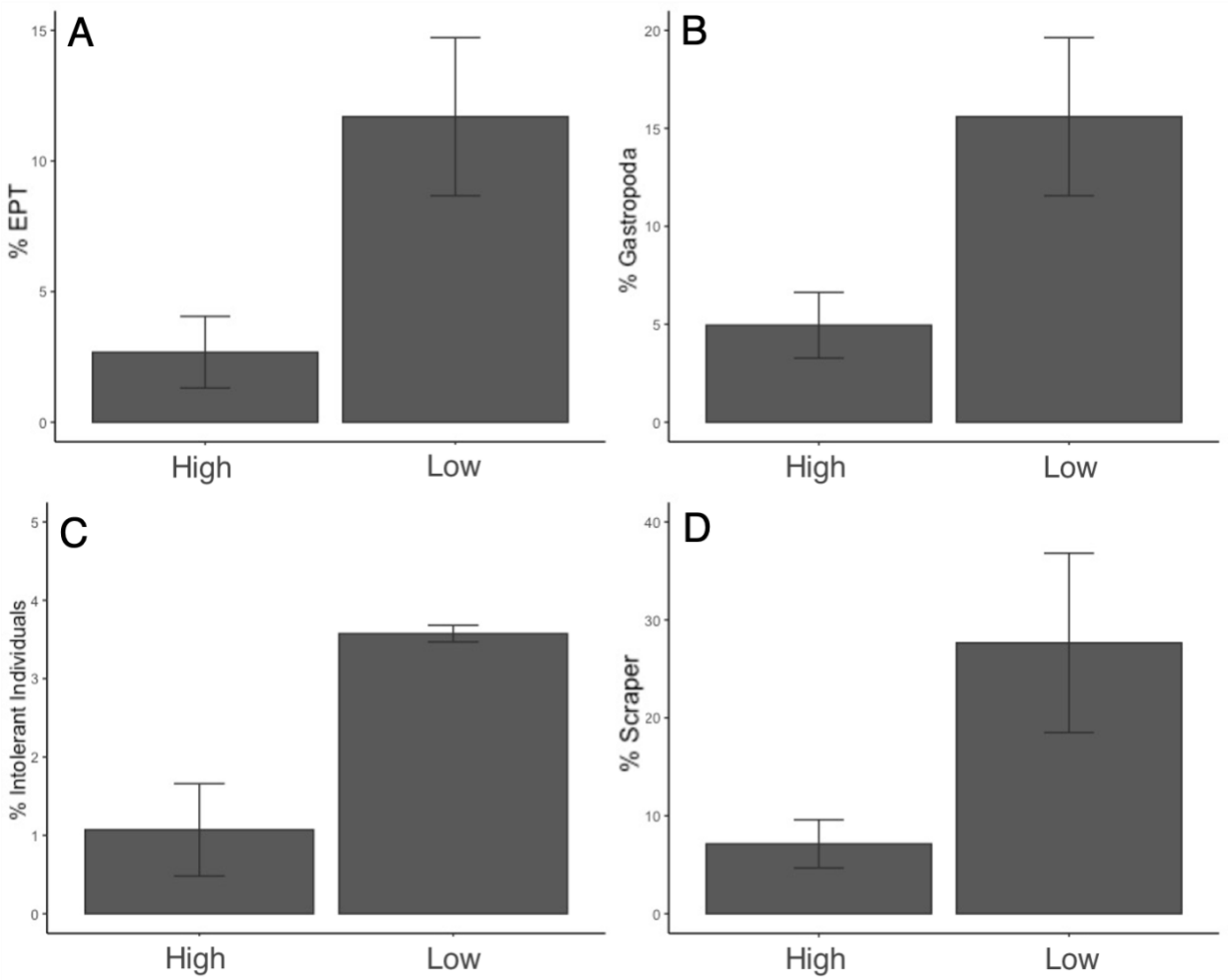


Figure 2.4:Average (± SE) metrics during flooding for high and low connectivity oxbow lakes in the Savannah River floodplain: (A) % EPT ($F_{1,4} = 10.59$, $p = 0.04$), (B) % Gastropoda ($F_{1,4} = 9.11$, $p = 0.04$), (C) % Intolerant Individuals ($F_{1,4} = 7.98$, $p = 0.05$), (D) % Scraper ($F_{1,4} = 9.35$, $p = 0.04$).

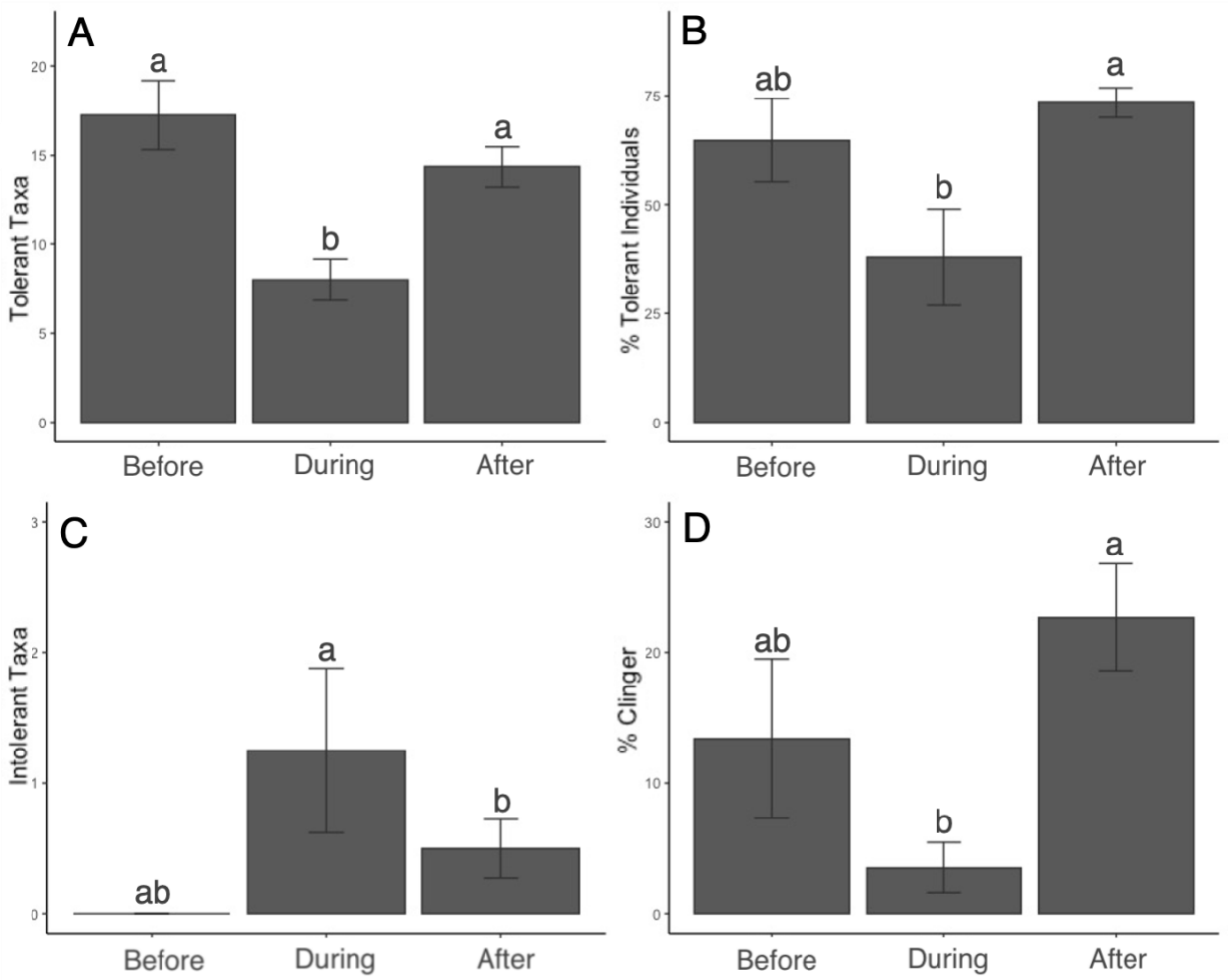


Figure 2.5:Average (± SE) metrics before, during and after flooding for high connectivity oxbow lakes in the Savannah River floodplain: (A) Tolerant Taxa ($F_{2,11} = 9.95$, $p < 0.01$), (B) % Tolerant Individuals ($F_{2,11} = 5.89$, $p = 0.02$), (C) Intolerant Taxa ($F_{2,11} = 5.74$, $p = 0.02$), (D) % Clinger ($F_{2,11} = 4.92$, $p = 0.03$). Small letters indicate significant Tukey's HSD-Test ($p > 0.05$).

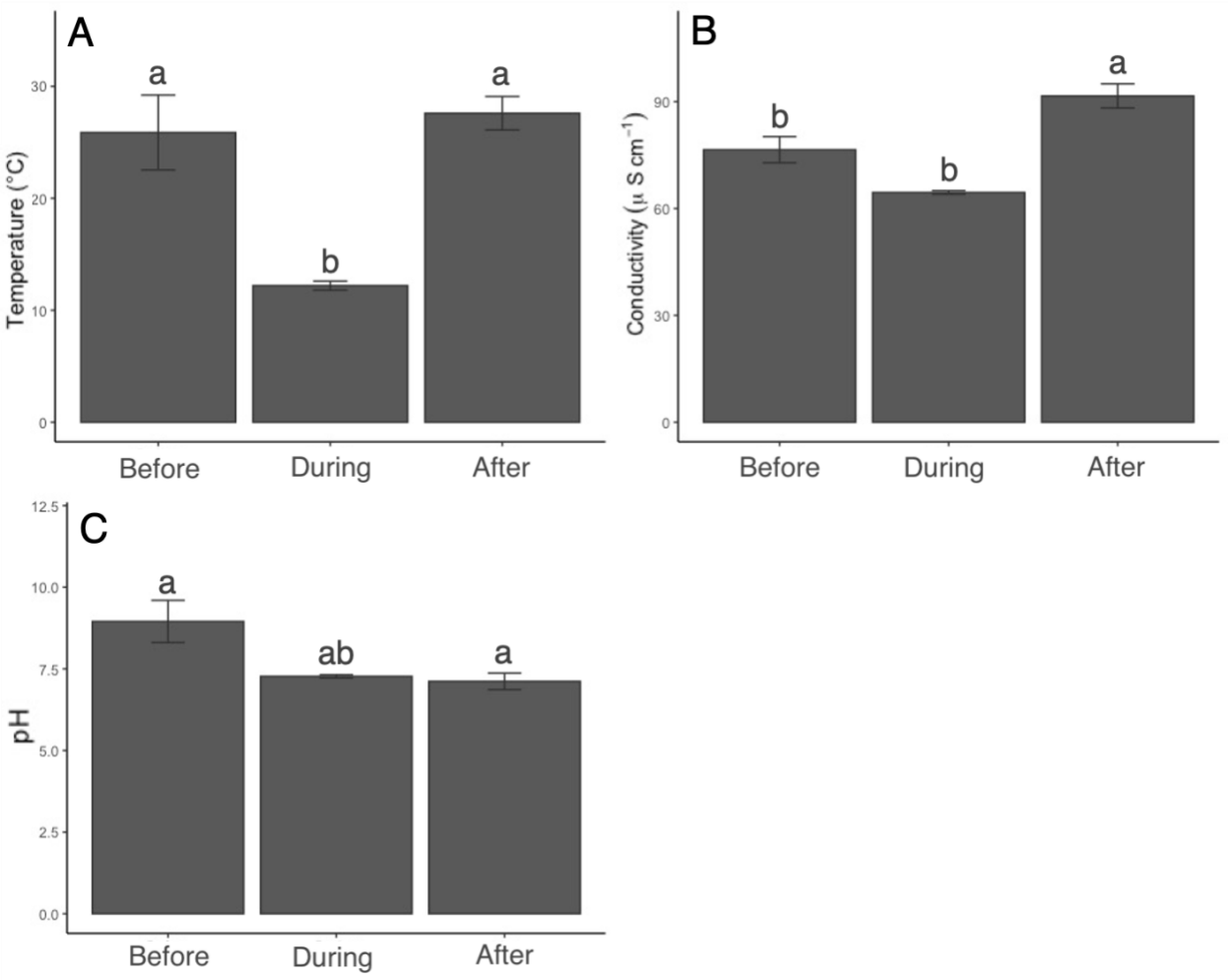


Figure 2.6: Water quality parameters for low connectivity oxbow lakes: (A) Temperature (°C) ($F_{2,8}$ = 7.96, p = 0.01), (B) Conductivity (µS cm-1) ($F_{2,8}$ = 12.15, p < 0.01) and (C) pH ($F_{2,8}$ = 5.21, p < 0.01). Small letters indicate significant Tukey's HSD-Test (p > 0.05).

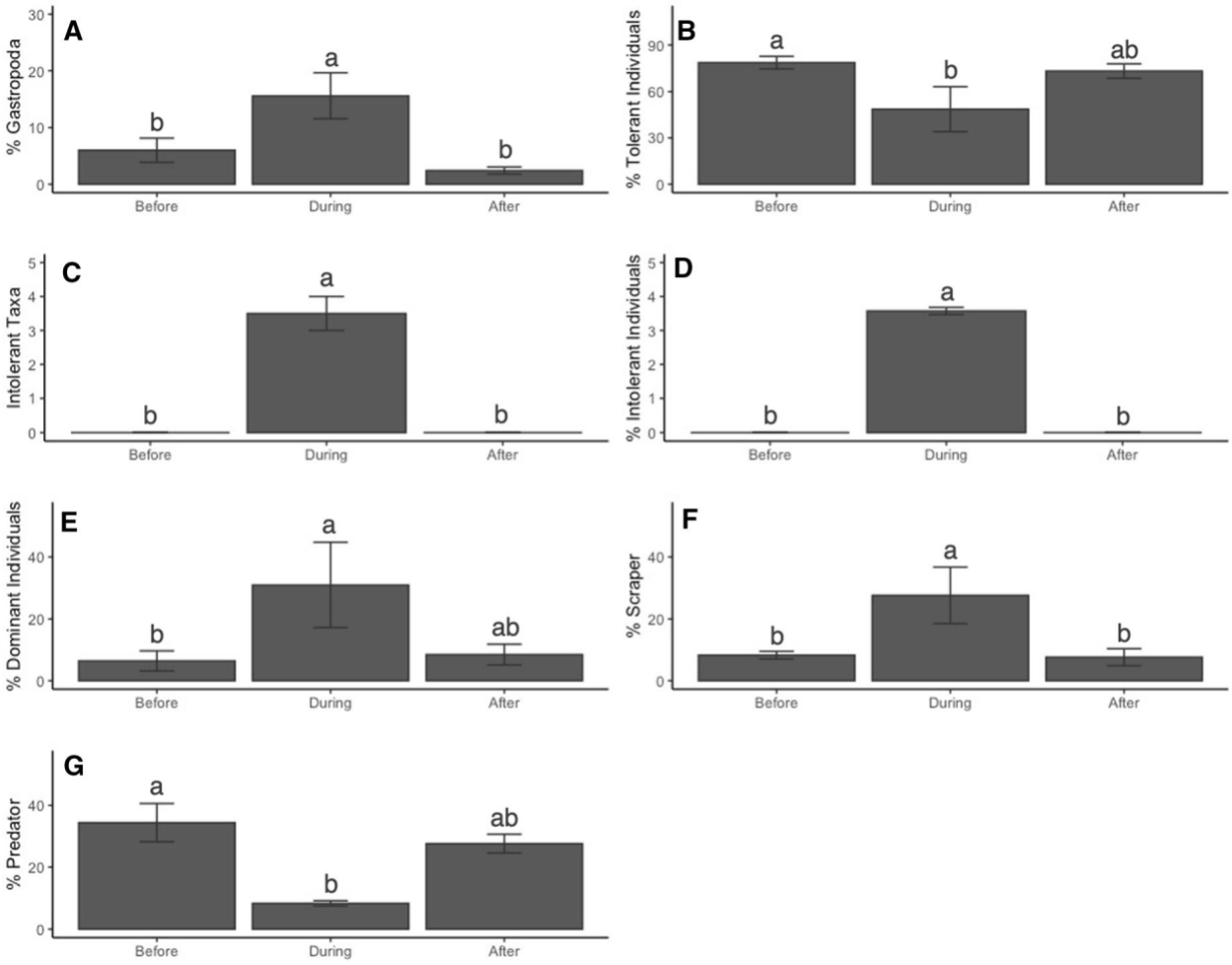


Figure 2.7:Average (± SE) metrics before, during and after flooding for low connectivity oxbow lakes in the Savannah River floodplain: (A)% Gastropoda ($F_{2,8} = 10.40$, $p < 0.01$), (B) % Tolerant Individuals ($F_{2,8} = 4.69$, $p = 0.05$), (C) Intolerant Taxa ($F_{2,8} = 160.36$, $p < 0.01$), (D) % Intolerant Individuals ($F_{2,8} = 3{,}694.78$, $p < 0.01$), (E) % Dominant Individuals ($F_{2,8} = 4.95$, $p = 0.04$), (F) % Scraper ($F_{2,8} = 11.96$, $p = 0.01$) and (G) % Predator ($F_{2,8} = 11.96$, $p = 0.03$). Small letters indicate significant Tukey's HSD-Test ($p > 0.05$).

# CHAPTER 3

## EFFECTS OF DROUGHT ON THE PHYSICOCHEMICAL, NUTRIENT AND CARBON METRICS OF FLOWS IN THE SAVANNAH RIVER, GEORGIA, USA

Wilbanks, K.A., and D.P. Batzer. Accepted by River Research and Application. Reprinted here with permission of publisher August 6, 2023

**ABSTRACT**

Hydrological drought has wide-ranging impacts on water quality, nutrient and carbon metrics, and given the uncertainty of climate change and the predicted increased frequency and intensity of drought in the future, investigations into changes induced by drought become increasingly important. This study compared physicochemical parameters (temperature, conductivity, pH and DO), nutrients (TN, $NO_X$ [$NO_2$ + $NO_3$], $NH_3$ and TP) and carbon (TOC and DOC) between hydrological drought conditions (2006–2008) and hydrological normal conditions (2016–2019) at five sites along the lower Savannah River (Georgia, USA). While we had predicted that water temperatures would increase from drought, we instead found temperature was significantly lower during drought conditions. Levels of pH and DO were significantly higher during drought. Further, TN, TOC and DOC concentrations were significantly lower during drought, but $NO_X$ concentrations were significantly higher during drought. Conductivity varied at the lower river sites, being significantly higher during drought at sites located below the city of Augusta, GA. These complex changes could be attributed to volume reductions coupled with an increase in the percentage of total flow originating from groundwater as well as limnetic reservoir inputs, persistent point source pollution, reduced natural catchment inputs and/or reduced floodplain interactions. The changes that occurred during drought may be disruptive to aquatic life, not only from reduced water quantity but also due to a scarcity of some biologically essential materials and lower food resources, combined with artificially high levels of some other potentially stressful materials.

# 1. INTRODUCTION

Drought, or a prolonged period of abnormally low rainfall, occurs naturally due to variability in rainfall, but the frequency and severity of drought is increasing in many regions due to climate change (Trenberth *et al.*, 2014). Further, anthropogenic influences (e.g., extraction of water for consumption) will exacerbate the effects of drought on aquatic ecosystems, and reductions in water quantities will have social, economic and environmental impacts (Mosley, 2015).

In large river systems, physicochemical processes during drought vary considerably. The responses of physicochemical processes to drought vary across different river systems, and a range of responses have been observed in temperature, dissolved oxygen and salinity (Whitehead *et al.*, 2009). Longer residence times and reduced water volumes typically cause increased water temperatures, lowered dissolved oxygen concentrations, increased salinity and changes in other water quality measures (Sprague, 2005; Baurès *et al.*, 2013). Dissolved oxygen is inversely related to temperature, and thus, responses of dissolved oxygen have ranged widely following changes in temperature (Zieliński *et al.*, 2009; Ylla *et al.*, 2010). Water temperature increases from 1 to 2 ºC during drought have been observed (Zieliński *et al.*, 2009; Hrdinka *et al.*, 2012), and extreme temperature increases (7 ºC) have also been noted (Ha *et al.*, 1999). Further, major ions have been shown to increase during drought and these findings were attributed to reduced dilution of more saline groundwater inputs and increased evapotranspiration (Hrdinka *et al.*, 2012). Although some physicochemical responses have been frequently documented during drought, efforts to assess changes in nutrient concentrations have been less extensive.

Predictions of rising global air temperatures and increased drought forecast an increase in nutrient loads (Whitehead *et al.*, 2009). However, the response of nutrients to drought has been mixed and varies among river systems. Reduced water volume and reduced dilution of point source pollution have been shown to increase nutrient concentrations (Van Vliet & Zwolsman, 2008), especially where wastewater or industrial effluent is present (Andersen *et al.*, 2004; Battaglin & Chapin 2022). Increased nutrients have been observed with reduced groundwater dilution or reduced river connection to the floodplains

(Golladay & Battle, 2002). Although, mixed responses of different nutrients to drought within the same system have also been observed (Sprague, 2005; Wilbers *et al*., 2009; Zieliński *et al.*, 2009). Low flows and longer residence times may facilitate an increased internal recycling of nutrients and primary production, which could account for decreased water column nutrients during drought (Hosen *et al.*, 2019). Further, reduced catchment inputs and low turbidity may result in greater primary production, especially where algae are light limited (Andersen *et al*., 2004; Baurès *et al.*, 2013).

Carbon dynamics in larger river systems during drought also have varied considerably. Much of our understanding of carbon dynamics is associated with flooding and the resultant mobilization of carbon stores (Whitworth *et al.*, 2012), and few studies have emphasized carbon dynamics during drought. After floods recede, carbon and nutrients return to the main river channel and thus have been found in higher concentrations during low flows (Baurès *et al.*, 2013). In contrast, some studies of drought noted decreased carbon concentrations because of reduced catchment inputs and reduced transportation of organic matter downstream (Zielinski *et al.*, 2009; Ylla *et al.*, 2010). A system's response to drought ultimately depends on the local environment and becomes increasingly complex where industrial, municipal and agricultural water usage, as well as hydroelectric power generation, is important.

This study compares physicochemical attributes (temperature, conductivity, pH and dissolved oxygen), nitrogen (TN, $NO_X$, $NH_3$), total phosphorus (TP) and carbon (TOC and DOC) levels between hydrological drought conditions (defined here as 2006–2008) and hydrological normal conditions (defined here as 2016–2019) at five sites on the Savannah River, Georgia, USA. We hypothesized that (1) physicochemical metrics during drought, especially water temperature and dissolved oxygen concentrations, would be impacted by flow reductions because drier periods are typically associated with hotter air temperatures. We predicted that increased air temperatures, increased evapotranspiration rates and reduced water volumes would result in an increase in water temperature and a decrease in dissolved oxygen. Further, persistent point source pollution and reduced water volume would increase ionic concentrations; and (2) dissolved nutrients and carbon would increase with reduced flows because levels of nutrients and carbon will not change, but a reduced volume would result in higher nutrient

concentrations. We predicted nitrogen and phosphorus concentrations would increase during drought from point source pollution. While concentrations of dissolved chemicals may increase, we predicted that material fluxes might decrease due to decreased flow volumes, or at least remain the same, if inputs did not change.

The Savannah River is a large river system supporting many industrial, municipal and recreational water uses and has experienced variability in drought conditions throughout the course of this study. Changes in nutrient load and physical parameters on large river systems like the Savannah River such as, increased water temperatures (Bonacina et al. 2023), nitrogen levels (Beketov 2004) and water acidification (Ganong et al. 2021) have been shown to negatively impact aquatic life. Likewise, these changes can largely affect the people and industries that rely on these systems to maintain a certain standard of water quality. Given this, an understanding of the impact that drought conditions have on these parameters is important not just from an ecological standpoint, but a social and economic one, as well.

## 2. METHODS

### 2.1 Study sites

The Savannah River is a major river in the southeastern United States and forms the border between South Carolina and Georgia. The drainage basin extends from the southeastern portion of the Appalachian Mountains, where the Tugaloo and Chattooga Rivers converge to form the headwaters of the Savannah River. The Savannah River is approximately 484 km long, drains an area of 27,390 $km^2$ and supports two major cities in Georgia: Augusta located mid-watershed near the Fall line (transition between the Piedmont and Coastal Plain) and Savannah located at the mouth of the river and the Atlantic Ocean, where the Savannah River drains. The natural hydrology of the Savannah River has been greatly altered by dams, with the largest of the dams, J. Strom Thurmond Dam, located near the Fall line and upstream from our study area, and ultimately affecting all flows in the mid and lower river to some extent. The Savannah River watershed is altered by agriculture, silviculture, municipalities, industries and energy generation. Silviculture is an especially significant industry in the Savannah River basin, with

approximately 890,000 hectares of commercial forested land. As of 2018, there were 177 industries and municipalities authorized to discharge wastewater in the basin (Georgia River Networks, 2018).

Five study sites were selected for this study, located in the middle and lower portions of the Savannah River (Figure 3.1, Appendix 3.A). Site 1 (325 river kilometers; hereafter RKM) was the most upstream site and Site 5 (98 RKM) was the most downstream site. Site 1 was approximately 7 RKM below the Augusta Diversion Dam at the base of a rocky shoals. Site 2 was located 12 RKM downstream from the Horse Creek confluence, whose watershed drains the cities of North Augusta and Aiken, South Carolina. Site 3 was located 18 RKM downstream from New Savannah Bluff Lock and Dam, 12 RKM downstream from the Butler Creek confluence, whose watershed drains Augusta, GA, and 4.3 RKM downstream from a large pulp and paper mill. Site 4 was located 6.4 RKM downstream of Plant Vogtle, a nuclear electric generating plant. Site 5 was located in the lower Coastal Plain ecoregion near Clyo, Georgia. Our study sites spanned the majority of the lower river, from the Fall line across the Coastal Plain to the upper extent of any tidal influences.

**2.2 Drought**

In Georgia, maximum daily air temperature (ºC) during the 2006–2008 study period averaged 25.6 ± 0.8 ºC and minimum daily air temperature averaged 10.8 ± 0.2 ºC. During the 2016–2019 study period, maximum daily air temperature averaged 26.2 ± 0.2 ºC and minimum daily air temperature averaged 12.4 ± 0.2 ºC (NOAA Station USW00003820). Maximum daily air temperature was statistically similar between the two study periods, but average minimum temperature was significantly ($F_{1,2554}$ = 21.86, $p < 0.01$) lower during the 2006–2008 study period (Appendix 3.B). However, during the 2006–2008 study period, Georgia experienced considerable precipitation deficits. Total precipitation averaged 81.3 ± 5.1 millimeters (mm) per month for the 2006–2008 study period and 106.7 ± 7.6 mm per month for the 2016–2019 study period, a difference of 23.8% (Young *et al.*, 2020).

Drought data were obtained from the U.S. Drought Monitor, which combines the Palmer Drought Severity Index, the Standardized Precipitation Index and other climatological inputs (Akyuz, 2017). The

2006–2008 study period was significantly drier for all drought metrics (Figure 3.2). A particularly intense period of drought occurred the week of December 11, 2007, when exceptional drought (D4) conditions affected 49.9% of Georgia land (Akyuz, 2017). Therefore, the 2006–2008 study period encompassed significant drought conditions (i.e., D1-4 were $p < 0.01$), while the 2016–2019 study period had near normal rainfall. Hereafter, "drought" conditions refer to the 2006–2008 period and "normal" conditions refer to the 2016–2019 period.

**2.3 Savannah River hydrology**

Discharge data were gathered from the U.S. Geological Survey (USGS) gage at Augusta (#02197000) for Site 1 (USGS, 2006). Site 1 was located approximately 25 RKM upstream of the USGS gage at Augusta. Discharge from the Horse Creek gage (#02196690), a major tributary approximately 8 RKM downstream from Site 1 but upstream from the Augusta gage, was subtracted to estimate discharge at Site 1. Discharge from the Augusta gage (#02197000) was used to estimate discharge at Sites 2 and 3; no significant tributaries flow into the Savannah between that gage and these sampling sites. Discharge from the Waynesboro gage (#021973269) was used to estimate discharge at Site 4 and discharge from the Clyo gage (#021973269) was used to estimate discharge at Site 5. We calculated average daily discharge yield ($m^3\ km^{-2}\ s^{-1}$) by obtaining drainage area ($km^2$) from the associated USGS gage and dividing it from daily discharge ($m^3 s^{-1}$). Average discharge during the drought period was found to be significantly lower than the normal period across sites ($F_{1,220} = 6.22$, $p = 0.01$; Figure 3.3). Discharge for the drought study period averaged $150.0 \pm 8.9\ m^3\ s^{-1}$ at the uppermost gage and increased to $193.1 \pm 10.3\ m^3\ s^{-1}$ at the lowest gage. In contrast, discharge for the normal study period averaged $206.3 \pm 23.0\ m^3\ s^{-1}$ at the uppermost gage and $262.8 \pm 25.7\ m^3\ s^{-1}$ at the lowest gage, an approximate 27% difference at the uppermost and lowest gage between drought and normal periods. The current Savannah River Drought Plan establishes a minimum daily average release from Thurmond dam of $107.6\ m^3 s^{-1}$ (USACE, 2012). This minimum was established so that municipalities and industries downstream of the dam would be in

compliance with state permitting requirements for the dilution of wastewater and to ensure adequate river flows for industrial water supply.

**2.4 Field methods**

We collected monthly field measurements and discrete water samples from February 2006 to January 2008 and from May 2016 to December 2019. Field measurements of temperature (°C), dissolved oxygen (mg $L^{-1}$ and % saturation), pH and specific conductance (µS $cm^{-1}$) were collected using a YSI multiparameter sonde (Yellow Springs Instruments, Yellow Springs, OH). Following USGS protocol (USGS, 2006), samples were collected in the field using non-isokinetic pump sampling methods. A portable pump was used to collect a depth-integrated sample by continuously lowering and raising the pump vertically in the water column at a constant rate. One vertical sample was obtained in well-mixed areas or the thalweg of the river for each sampling event. Samples were collected in acid-rinsed polypropylene bottles, stored on ice, transported to the laboratory and processed within 48 hours.

Extensive quality control measures were used to maintain data consistency (USGS, 2006). Field blank and replicate samples were collected for each sample batch, which was every 5 samples or at least once per month. Results from blank samples were used to indicate contamination across samples and replicate samples were used to indicate variability from the collection, processing and laboratory analyses.

In the laboratory, samples were transferred to a churn splitter (Phinizy Center for Water Sciences; Augusta, Georgia) and homogenized to ensure the particulate organic material was evenly distributed. Aliquots were separated for each analyte and preserved with sulfuric acid to a pH ≤ 2 for subsequent analyses. For dissolved organic carbon (DOC), samples were filtered through a 0.45 µm glass fiber filter prior to analysis. Samples were stored between 4 °C and 6 °C until the time of analysis.

**2.5 Analytical methods**

Samples were analyzed within 28 days for total nitrogen (TN), ammonia ($NH_3$), nitrate + nitrite ($NO_X$), total phosphorus (TP), total organic carbon (TOC) and dissolved organic carbon (DOC). Samples from the 2006–2008 study period were analyzed by Pace Analytical (Columbia, SC, USA), and samples from the 2016–2019 study period were analyzed by Pace Analytical and Phinizy Center for Water Science (Augusta, GA, USA). $NO_X$, $NH_3$ and TP were determined by colorimetric analysis with a discrete analyzer (Seal Analytical v. 4, Mequon, WI), and TOC and DOC were determined by combustion catalytic oxidation and non-dispersive infra-red detection by a total organic analyzer (TOC-L) with TN module with a chemiluminescence detector (Shimadzu v. 1.04, Columbia, MD). Methods used to analyze included Environmental Protection Agency (EPA) method 350.1 for the determination of $NH_3$ (USEPA, 1993a); method 353.2 for the determination of $NO_X$ (USEPA, 1993b), method 365.1 for the determination of TP (USEPA, 1993c), and method 415.1 for the determination of TOC and DOC (USEPA, 1974). Prior to 2018, EPA method 351.2 was used to determine TN (USEPA,1993d), and from 2018–2019, a comparable method, American Standard Methods D8083 was used because of safety concerns working with mercury (ASTM, 2016). In each analysis batch quality control consisted of a calibration control blank and a calibration control verification to check for instrument drift, a laboratory-fortified matrix to determine instrument repeatability and accuracy, a laboratory fortified duplicate to determine the precision of the instrument and certified reference material to determine the analysis accuracy (Eaton *et al.*, 1998). During 2016–2019, samples were externally verified by Pace Analytical at least once per year.

**2.6 Data analyses**

To assess the effects of discharge on nutrient concentrations, mass flux (kg $day^{-1}$) was used to account for reduced flow rates during drought, integrating concentration and daily discharge averages. This was achieved by gathering average daily discharge for each sampling date from the nearest USGS gage (Appendix 3.A) and then calculating mass flux for each nutrient (Aulenbach *et al.*, 2007). Mass flux ($\Phi$) was calculated as the product of constituent concentration (C) and discharge (Q) integrated over time (t):

$$\Phi = C(t)Q(t)dt$$

The following equation was used to convert nutrient concentrations into kilograms per day (Goolsby *et al.*, 1999):

$$Concentration\ \left(\frac{mg}{L}\right) x\ flow\ \left(\frac{m^3}{s}\right) x\ 8.64\ x\ 10^{-3} = \frac{kilograms}{day}$$

Data were organized by Julian date and grouped by drought conditions (2006–2008) and normal conditions (2016–2019). Data was blocked by historical flow seasonality (Benke, 2001) to ensure equal number of samples were collected during both natural high flow and low flow periods. The natural high flow period was 1 December to 31 May, and the natural low flow period was 1 June to 30 November. We calculated means, medians, minimums, maximums, standard deviations (SD), standard errors (SE) and coefficients of variation (CV) to summarize each metric. Data were then compared using a 2-way Analysis of Variance (ANOVA), with time period (i.e., drought, normal) and sampling sites (i.e., 1–5) as the factors (*a priori* $\alpha = 0.05$). Goodness of Fit Tests were used to ensure normal distributions of data, and Levene Tests were used to ensure equal variances. If metrics were found to have significant interactions between the time periods and the sites, a series of 1-way ANOVAs were used to assess the effect of time period within each of the 5 sites. When a significant effect of site was indicated by the 2-way ANOVAs, we used Tukey -HSD tests to separate site means. R (Version 3.6; R Core Team, 2020) was used to run 1-way and 2-way ANOVAs, Goodness of Fit Tests, Levene Tests and Tukey tests.

## 3 RESULTS

### 3.1 Drought impacts on physicochemical parameters

Mean water temperature (ºC) was found to be significantly lower during the drought period than the normal period ($F_{1,220} = 4.27$, $p = 0.04$; Figure 3.4A). Variation in water temperature, as reflected by coefficient of variation (CV), was highest at site 3, at 74.1% during drought and 103.9% during normal conditions and decreased steadily downstream with Site 5 exhibiting the lowest CV of 17.7% during

drought and 50.7% during normal conditions (Appendix 3.C). Dissolved oxygen levels were higher during drought for both concentration (mg $L^{-1}$) ($F_{1,220} = 11.74$, $p < 0.01$; Figure 3.4B) and saturation (%) ($F_{1,220} = 6.72$, $p = 0.01$, Figure 3.4C). Levels of pH were significantly higher at all sites during drought ($F_{1,220} = 11.99$, $p < 0.01$; Figure 3.5A). Electrical conductivity (µS $cm^{-1}$) was found to have a significant interaction between time periods (i.e., drought and normal periods) and sites ($p < 0.01$, Figure 3.5B); thus, a series of 1-way ANOVAs for each site was used to determine impacts of drought. Sites 1 and 2 did not differ in conductivity between time periods ($p > 0.05$), but sites 3 ($F_{1,47} = 12.56$, $p < 0.01$), 4 ($F_{1,47} = 12.96$, $p < 0.01$) and 5 ($F_{1,34} = 17.60$, $p < 0.01$) had higher conductivity during drought than normal conditions (Figure 3.5B).

### 3.2 Drought impacts on nutrient and carbon parameters

Nitrogen concentrations, including total nitrogen (TN), ammonia ($NH_3$), and nitrate + nitrite ($NO_X$), were found to vary between drought and normal hydrological conditions (Figure 6, Appendix 3.D). TN concentration (mg-N $L^{-1}$) was significantly lower during drought ($F_{1,220} = 5.23$, $p = 0.02$; Figure 3.6A), as was TN flux (kg-N $day^{-1}$) ($F_{1,220} = 11.29$, $p < 0.01$; Figure 3.6B). $NO_X$ concentration (mg-N $L^{-1}$) was significantly higher during drought ($F_{1,219} = 4.04$, $p = 0.05$; Figure 3.6C), but $NO_X$ flux (kg-N $day^{-1}$) was similar between drought and normal conditions (Figure 3.6D). Concentrations (mg $L^{-1}$) and flux (kg $day^{-1}$) of $NH_3$ and TP were similar between drought and normal conditions (Figure 3.6E and 3.6F; and 3.6G and 3.6H, respectively).

TOC concentration ($F_{1,220} = 49.95$, $p < 0.01$; Figure 3.7A) and flux ($F_{1,220} = 29.88$, $p < 0.01$; Figure 3.7B), and DOC concentration ($F_{1,220} = 30.22$, $p < 0.01$; Figure 3.7C) and flux ($F_{1.220} = 21.95$, $p < 0.01$, Figure 3.7D), were significantly lower during drought. DOC constituted 96% of TOC in the Savannah River.

## 4 DISCUSSION

A drought event in the Savannah River of the southeastern United States had a great effect not only on physicochemical conditions, but also on the dynamics of important nutrients. Drought conditions caused a shift in flow dynamics, and the concentrations and flux of nutrients. Changes in these nutrients during drought were complex and a variety of mechanisms could account for these shifts.

We had hypothesized that water temperatures would increase and dissolved oxygen levels would decrease during drought due to flow reductions. However, water temperatures instead decreased and dissolved oxygen levels increased during the drought. Maximum air temperatures in our study area were similar between the time periods, although minimum air temperatures were significantly lower during drought. For reference, we assessed water temperatures in the Ogeechee River, an adjacent, largely unregulated, free-flowing river in Georgia, and found no differences in water temperature between drought and normal hydrological periods (Appendix 3.C). Thus, the observed differences in the Savannah River were likely attributable to the regulation of the upstream large reservoir (Thurmond Dam). A higher percentage of total flows in the river likely originated from hypolimnetic discharges through the dam during drought (Sprague, 2005). To corroborate this, we assessed temperature variation (as reflected by coefficients of variation) and found the least variability at the most upstream site, closest to the dam, and a steady increase in the temperature variability longitudinally during drought (i.e., sites became more variable as the regulatory impacts of the dam waned) (Appendix 3.E). Controlled flows from the dam dominated total flows near the dam, which caused decreased water temperature levels and variability, a common observation for dams (Ruhi *et al.*, 2018). We predicted that DO levels would be related to water temperature, and this was true, although, like for temperature, inversely to our prediction. We found that DO increased during drought conditions. We did not find any similar instances in the literature, but we found several studies reported no changes in DO levels (Caruso, 2002; Hrdinka *et al.*, 2012). They attributed the lack of temperature increases to similar air temperature and dilution from cooler reservoir inputs, point sources, or groundwater downstream.

Additionally, we predicted drought would cause increased pH and conductivity with reduced water volumes and inputs of point source pollutants. We found that pH and conductivity, at some

locations, were higher during the drought, similar to findings by Sprague (2005) and Zieliński *et al.* (2009). Elsewhere, higher pH and dissolved ions during drought have been attributed to more saline and more alkaline (bicarbonate) groundwater inputs, coupled with decreased dilution and flushing from precipitation (Mosley *et al.*, 2012; Mosley, 2015), and in some cases to point source pollution (Van Vliet & Zwolsman, 2008). We found that conductivity was only elevated downstream from the city of Augusta (Sites 3-5), which suggested that anthropogenic inputs of ions from Augusta might be involved. This pattern was observed in both time periods but was exacerbated during drought.

We also hypothesized that reduced flows would increase the concentrations of dissolved nutrients and carbon, but that flux would decrease with reduced water volumes. This hypothesis was observed for nitrate + nitrite but was not observed for any of the other nutrients. Increased nutrients during drought commonly occurs in rivers where point sources (e.g., industrial, domestic, agricultural or wastewater discharge) of nutrients predominate (Sprague, 2005; Baurès *et al.*, 2013). Higher concentrations of nitrate and nitrite during drought probably indicates a decreased dilution of effluent from municipal and industrial sources. This was corroborated by flux calculations, as they were similar between drought and normal conditions, suggesting unchanging effluent discharge. However, ammonia and phosphorus did not follow this trend. Ammonia is the most bioavailable form of nitrogen, and phosphorus is a limiting nutrient in freshwater systems. Therefore, they may have been utilized by primary producers and assimilated into biomass before detection, which has been reported by others (Caruso, 2002; Caramujo *et al.*, 2008; Nguyen *et al.* 2020).

Contrary to our original hypothesis, we found that total nitrogen and carbon levels were reduced during drought. In low gradient streams, nitrogen and carbon that originates from the terrestrial landscape can accumulate in floodplains and wetlands (Batzer & Sharitz, 2014; Richardson *et al.* 2018). The flood-pulse concept (Junk *et al.*, 1989) emphasized the importance of river-floodplain exchanges. During drought, rivers receive reduced overland flows and catchment inputs, and floodplain connection declines. This reduced connectivity with terrestrial landscapes and floodplains is considered a likely mechanism for decreased nutrients in river waters during drought (Golladay & Battle, 2002; Hunt *et al.*, 2005). This has

been corroborated by the mobilization of these stored nutrients and carbon during floods (Kaushal *et al.*, 2014; Frazar *et al.*, 2019). Nutrient dynamics are obviously complex during drought, and in our study were likely complicated by flow regulation, and by point source and non-point source pollution.

The results of this study indicate that drought conditions affect water quality metrics, but not always in consistent or expected ways. Our observations were likely related to several mechanisms, including volume reduction, persistent point source pollution, reduced natural catchment inputs, and reduced floodplain interactions. Although we were not aware of what management actions were implemented in response to drought, we acknowledge that management efforts to mitigate changes in regulated nutrients may have affected differences between our study time periods. Given the sensitivity of aquatic life, especially macroinvertebrates, to minute changes in water chemistry, drought was likely disruptive to aquatic biological communities, especially those which may be affected by changes in pH and total nitrogen, considering the differences seen between normal and drought conditions. Likewise, animals which feed on these more sensitive organisms may have been affected. That said, impacts during drought were dynamic and complex, and a more complete understanding of these interactions in large rivers will become increasingly important with the anticipated increases in intensity, frequency and duration of drought disturbances in the future.

## ACKNOWLEDGEMENTS

This work was performed in collaboration with Phinizy Center for Water Sciences.

Funding for this project was provided by the City of Augusta, City of Aiken and Columbia County municipalities through the Phinizy Center for Water Sciences, USDA Hatch Program, US Environmental Protection Agency and the Georgia Environmental Protection Division, Regional Water Plan SEED Grant, Contract Number: 761–200119. The preparation of this manuscript was financed in part through a cooperative agreement with Augusta, Georgia/Augusta Utilities Department. The following should be acknowledged for their efforts: Gene Eidson, Matthew Erickson, Oscar Flite, Nicole Hiabach, Natt

Hobbs, Katie Johnson, Brian Metts, Jason Moak, Damon Mullis, Chalisa Nestell, Stephen Sefick and Liam Wolff.

**DATA AVAILABILITY STATEMENT**

The authors confirm that the data supporting the findings of this study are available from the corresponding author, KAW, upon reasonable request.

## REFERENCES

Akyuz, F.A. (2017). Drought Severity and Coverage Index. United States Drought Monitor. https://droughtmonitor.unl.edu/About/AbouttheData/DSCI.aspx.

American Society for Testing and Materials International (ASTM). (2016). Method D8083: Standard Test Method for Total Nitrogen, and Total Kjeldahl Nitrogen (TKN) by Calculation, in Water by High Temperature Catalytic Combustion and Chemiluminescence Detection. West Conshohocken, PA.

Andersen, C.B., Lewis, G.P., & Sargent, K.A. (2004). Influence of wastewater-treatment effluent on concentrations and fluxes of solutes in the Bush River, South Carolina, during extreme drought conditions. Environmental Geosciences. 11(1): 28–41.

Aulenbach, B. T., Buxton, H.T., Battaglin, W.A & Coupe, R.H. (2007). Streamflow and nutrient fluxes of the Mississippi-Atchafalaya River Basin and subbasins for the period of record through 2005: U.S. Geological Survey. Open-File Report 2007–1080, https://toxics.usgs.gov/pubs/of-2007-1080/index.html

Battaglin, W.A. and Chapin, T.W., 2022. Identifying nutrient sources and sinks to the South Platte River and Cherry Creek, Denver, CO, during low-flow conditions in 2019–2020. River Research and Applications. DOI: 10.1002/rra.4060

Batzer, D.P. & Sharitz, R.R. (2014). Ecology of freshwater and estuarine wetlands, 2nd Edition. University of California Press.

Baurès, E., Delpla, S. Merel, Thomas, M.F., Jung, A.V., & Thomas, O. (2013). Variation of organic carbon and nitrate with river flow within an oceanic regime in a rural area and potential impacts for drinking water production. Journal of Hydrology. 477(1): 86–93.

Beketov, M., 2004. Different sensitivity of mayflies (Insecta, Ephemeroptera) to ammonia, nitrite and nitrate: linkage between experimental and observational data. Hydrobiologia, 528(1-3), pp.209-216.

Benke, A.C. (2001). Importance of flood regime to invertebrate habitat in an unregulated river–floodplain ecosystem. Journal of the North American Benthological Society. 20(2): 225–240.

Bonacina, L., Fasano, F., Mezzanotte, V. and Fornaroli, R., 2023. Effects of water temperature on freshwater macroinvertebrates: a systematic review. Biological Reviews, 98(1), pp.191-221.

Caramujo, M.J., Mendes, C.R.B., Cartaxana, P., Brotas, V., &. Boavida, M.J. (2008). Influence of drought on algal biofilms and meiofaunal assemblages of temperate reservoirs and rivers. Hydrobiologia. 598(1): 77–94.

Caruso, B.S. (2002). Temporal and spatial patterns of extreme low flows and effects on stream ecosystems in Otago, New Zealand. Journal of Hydrology. 257(1-4): 115–133.

Eaton A.D., Clesceri, L.S., Greenberg, A.E., & Franson, M.H. (1998). Standard methods for the examination of water and wastewater. American Public Health Association, American Water Works Association, and Water Environment Federation. Washington, D.C., 23rd edition.

Frazar, S., Gold, A.J., Addy, K., Moatar, F., Birgand, F., Schroth, A.W., Kellogg, D.Q., & Pradhanang, S.M. (2019). Contrasting behavior of nitrate and phosphate flux from high flow events on small agricultural and urban watersheds. Biogeochemistry. 145(1–2): 141–160.

Ganong, C., Oconitrillo, M.H. and Pringle, C., 2021. Thresholds of acidification impacts on macroinvertebrates adapted to seasonally acidified tropical streams: potential responses to extreme drought-driven pH declines. PeerJ, 9, p.e11955.

Georgia River Networks. (2018). Savannah River. https://garivers.org/savannah-river/. 10 September 2020.

Golladay, S.W., & Battle, J. (2002). Effects of flooding and drought on water quality in gulf coastal plain streams in Georgia. Journal of Environmental Quality. 31(4): 1266–1272.

Goolsby, D. A., Battaglin, W.A., Lawrence, G.B., Artz, R.S., Aulenbach, B.T., Hooper, R.P., Keeney, D.R., & Stensland, G.J. (1999). Flux and sources of nutrients in the Mississippi-Atchafalaya River Basin. National Oceanic and Atmospheric Administration National Ocean Service Coastal Ocean Program.

Ha, K., Cho, E.A., Kim, H.W., & Joo, G.J. (1999). Microcystis bloom formation in the lower Nakdong River, South Korea: importance of hydrodynamics and nutrient loading. Marine and Freshwater Research. 50(1): 89–94.

Hosen, J.D., Aho, K.S., Appling, A.P., Creech, E.C., Fair, J.H., Hall Jr, R.O., Kyzivat, E.D., Lowenthal, R.S., Matt, S., Morrison, J., & Saiers, J.E. (2019). Enhancement of primary production during drought in a temperate watershed is greater in larger rivers than headwater streams. Limnology and Oceanography. 64(4): 1458–1472.

Hrdinka, T., Novický, O., Hanslík, E., & Rieder, M. (2012). Possible impacts of floods and droughts on water quality. Journal of Hydro-environment Research. 6(2): 145–150.

Hunt, C.W., Loder, T., & Vörösmarty, C. (2005). Spatial and temporal patterns of inorganic nutrient concentrations in the Androscoggin and Kennebec Rivers, Maine. Water, Air, and Soil Pollution. 163(1-4): 303–323.

Junk, W.J., Bayley, P.B., & Sparks, R.E. (1989). The flood pulse concept in river-floodplain systems. Canadian special publication of fisheries and aquatic sciences. 106(1): 110–127.

Kaushal, S.S., Mayer, P.M., Vidon, P.G., Smith, R.M., Pennino, M.J., Newcomer, T.A., Duan, S., Welty, C., & Belt, K.T. (2014). Land use and climate variability amplify carbon, nutrient, and contaminant pulses: a review with management implications. Journal of the American Water Resources Association. 50(3): 585–614.

Mosley, L.M., Zammit, B., Leyden, E., Heneker, T.M., Hipsey, M.R., Skinner D., & Aldridge, K.T. (2012). The impact of extreme low flows on the water quality of the Lower Murray River and Lakes (South Australia). Water Resources Management. 26(13): 3923–3946.

Mosley, L.M. (2015). Drought impacts on the water quality of freshwater systems; review and integration. Earth-Science Reviews. 140(1): 203–214.

Nguyen, T.T., Némery, J., Gratiot, N., Garnier, J., Strady, E., Nguyen, D.P., Tran, V.Q., Nguyen, A.T., Cao, S.T. and Huynh, T.P., 2020. Nutrient budgets in the Saigon–Dongnai River basin: Past to future inputs from the developing Ho Chi Minh megacity (Vietnam). River Research and Applications. 36(6): 974-990. DOI: 10.1002/rra.3552

R Core Team (2020). R: A language and environment for statistical computing. R Foundation for Statistical Computing, Vienna, Austria. https://www.R-project.org/.

Richardson, W.B., Bartsch, L.A., Bartsch, M.R., Kiesling, R. and Lafrancois, B.M., 2018. Nitrogen cycling in large temperate floodplain rivers of contrasting nutrient regimes and management. River Research and Applications, 35(5): 529-539. DOI: 10.1002/rra.3267

Ruhi A., Dong, X., McDaniel, C.H., Batzer, D.P., & Sabo, J.L. (2018). Detrimental effects of a novel flow regime on the functional trajectory of an aquatic invertebrate metacommunity. Global Change Biology. 24(8):3749–65.

Sprague, L.A. (2005). Drought effects on water quality in the South Platte River basin, Colorado. Journal of the American Water Resources Association. 41(1): 11–24.

Trenberth, K.E., Dai, A., Van Der Schrier, G., Jones, P.D., Barichivich, J., Briffa, K.R., & Sheffield., J. (2014). Global warming and changes in drought. Nature Climate Change. 4(1): 17–22.

U.S. Army Corps of Engineers (USACE). (2012). Savannah River Basin Drought Management Plan. http://www.sas.usace.army.mil/reports.html.

U.S. Environmental Protection Agency. (1974). Method 415.1: Organic Carbon, Total (Combustion or Oxidation). Cincinnati, OH.

U.S. Environmental Protection Agency. (1993a). Method 350.1: Nitrogen, Ammonia (Colorimetric, Automated Phenate), Revision 2.0. Cincinnati, OH.

U.S. Environmental Protection Agency. (1993b). Method 353: Determination of nitrate-nitrite nitrogen by automated colorimetry. Revision 2.0. Cincinnati, OH.

U.S. Environmental Protection Agency. (1993c). Method 365.1: determination of phosphorus by semi-automated colorimetry. Revision 2.0. Cincinnati, OH.

U.S. Environmental Protection Agency. (1993d). Method 351.2: determination of total kjeldahl nitrogen by semi- automatedcolorimetry. Revision 2.0. Cincinnati, OH.

U.S. Geological Survey (USGS). (2006). National field manual for the collection of water-quality data. U.S. Geological Survey Techniques of Water Resources Investigations, Book 9. Chapter 4.1.3B. https://pubs.er.usgs.gov/publication/twri09

Van Vliet, M.T.H., & Zwolsman, J.J.G. (2008). Impact of summer droughts on the water quality of the Meuse river. Journal of Hydrology. 353(1–2): 1–17.

Whitehead, P.G., Wilby, R.L., Battarbee, R.W., Kernan, M., & Wade, A.J. (2009). A review of the potential impacts of climate change on surface water quality. Hydrological Sciences Journal. 54(1): 101–123.

Whitworth, K. L., Baldwin, D.S., & Kerr, J.L. (2012). Drought, floods and water quality: drivers of a severe hypoxic blackwater event in a major river system (the southern Murray–Darling Basin, Australia). Journal of Hydrology. 450: 190–198.

Wilbers, G.J., Zwolsman, G., Klaver, G. & Hendriks, A.J. (2009). Effects of a drought period on physico-chemical surface water quality in a regional catchment area. Journal of Environmental Monitoring. 11(6): 1298–1302.

Ylla, I., Sanpera-Calbet, I., Vázquez, E., Romaní, A.M., Munoz, I., Butturini, A., & Sabater, S. (2010). Organic matter availability during pre-and post-drought periods in a Mediterranean stream. Hydrobiologia. 657: 217–232.

Young, A.H., Knapp, K.R., Inamdar, A., Hankins, W., & Rossow, W.B. (2020). The International Satellite Cloud Climatology Project H-Series climate data record product. Earth System Science Data. 10(1): 583–593. doi.org/10.5194/essd-10-583-2018.

Zieliński, P., Gorniak, A., & Piekarski, M.K. (2009). The effect of hydrological drought on chemical quality of water and dissolved organic carbon concentrations in lowland rivers. Polish Journal of Ecology. 57(2): 217–227.

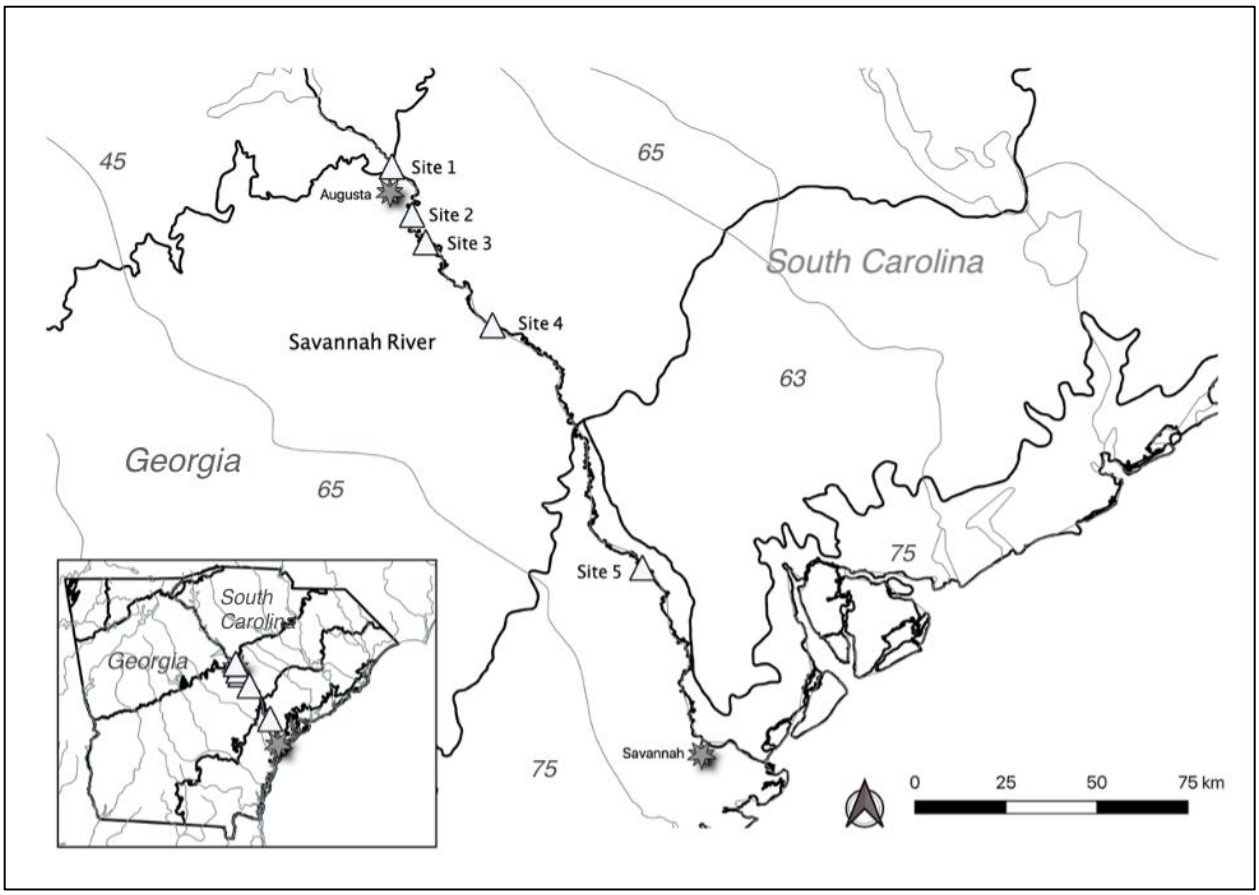


Figure 3.1: Study sites on the Savannah River included Site 1 (33.50277, -81.99067), Site 2 (33.38391, -81.93174), Site 3 (33.31791, -81.89093), Site 4 (33.11608, -81.69772) and Site 5 (32.52474, -81.26239). The Savannah River forms the border between Georgia and South Carolina, USA. EPA level III ecoregions are indicated with black lines including 45 (Piedmont), 63 (Middle Atlantic Coastal Plain), 65 (Southeastern Plains) and 75 (Southern Coastal Plain), and gray lines indicate other river systems. The trainstion between the Piedmont ecoregion and Southeastern Plains ecoregion is known as the Fall line.

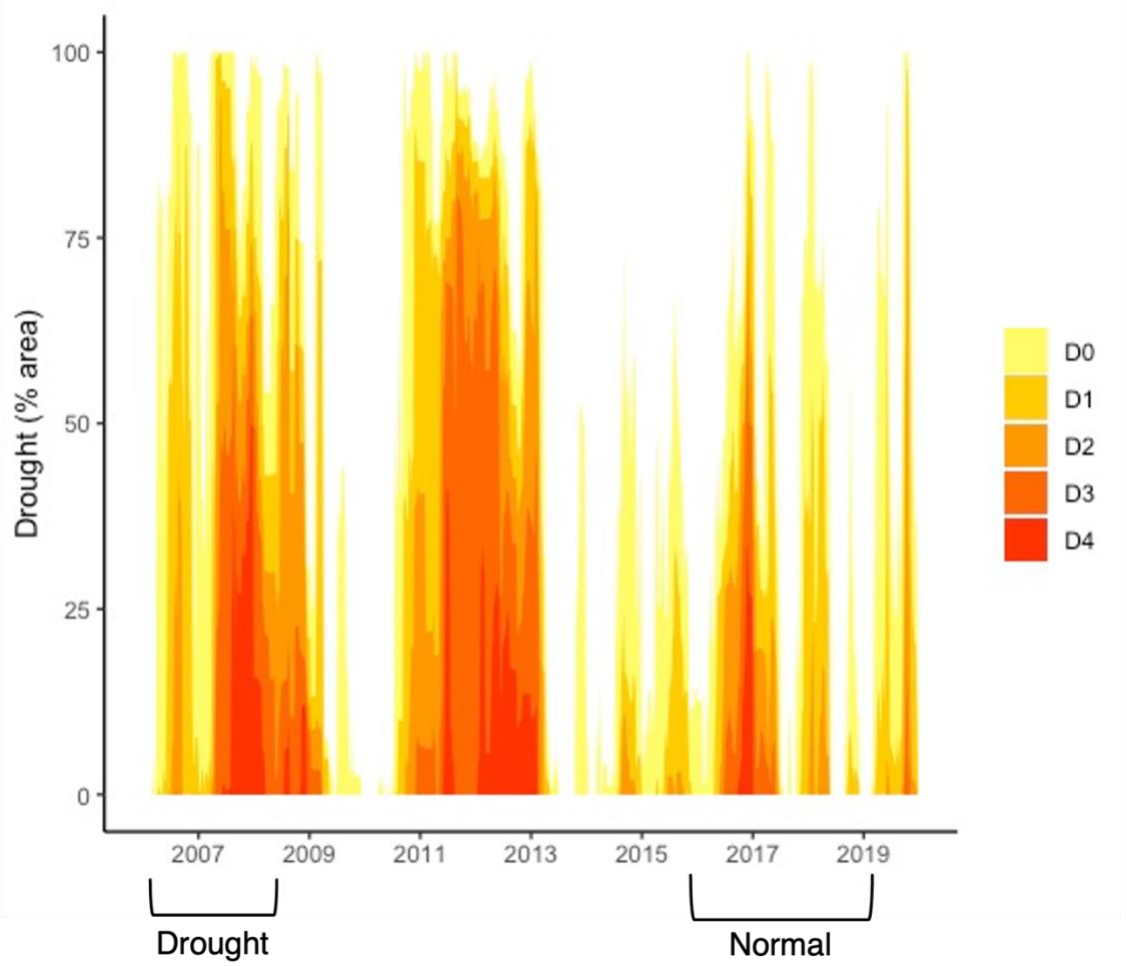


Figure 3.2: Area (% area) of Georgia experiencing drought from 2006–2019. Bracket indicates study periods (drought [2006-2008] or normal [2016-2019]). Data were obtained from the US Drought Monitor. Drought was significantly higher during 2006-2008 for abnormally dry (D0), moderate drought (D1), severe drought (D2), extreme drought (D3) and exceptional drought (D4) and significantly lower during 2016–2019 for no instances of drought.

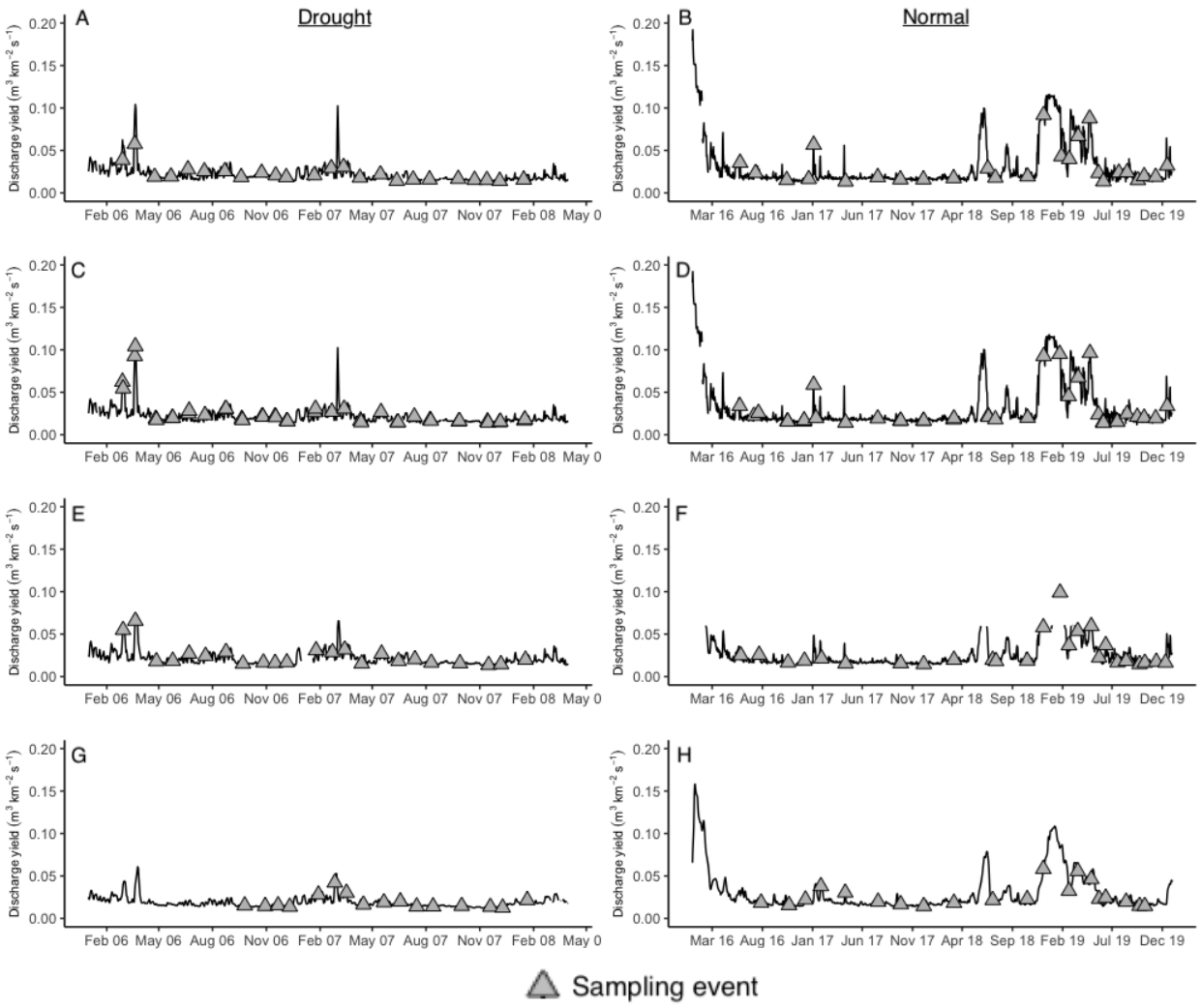


Figure 3.3: Average daily discharge yield ($m^3$ $km^{-2}$ $s^{-1}$) from the 2006-2008 study period (drought period; left column) and the 2016–2019 study period (normal period; right column) for (A and B) Site 1 (USGS #02197000 & USGS #02196690), (C and D) Sites 2 and 3 (USGS #02197000), (E and F) Site 4 (USGS #021973269) and (G and H) Site 5 (USGS #021973269). Gray triangles indicate sampling events. Average discharge was found to be significantly different between drought and normal periods across all sites.

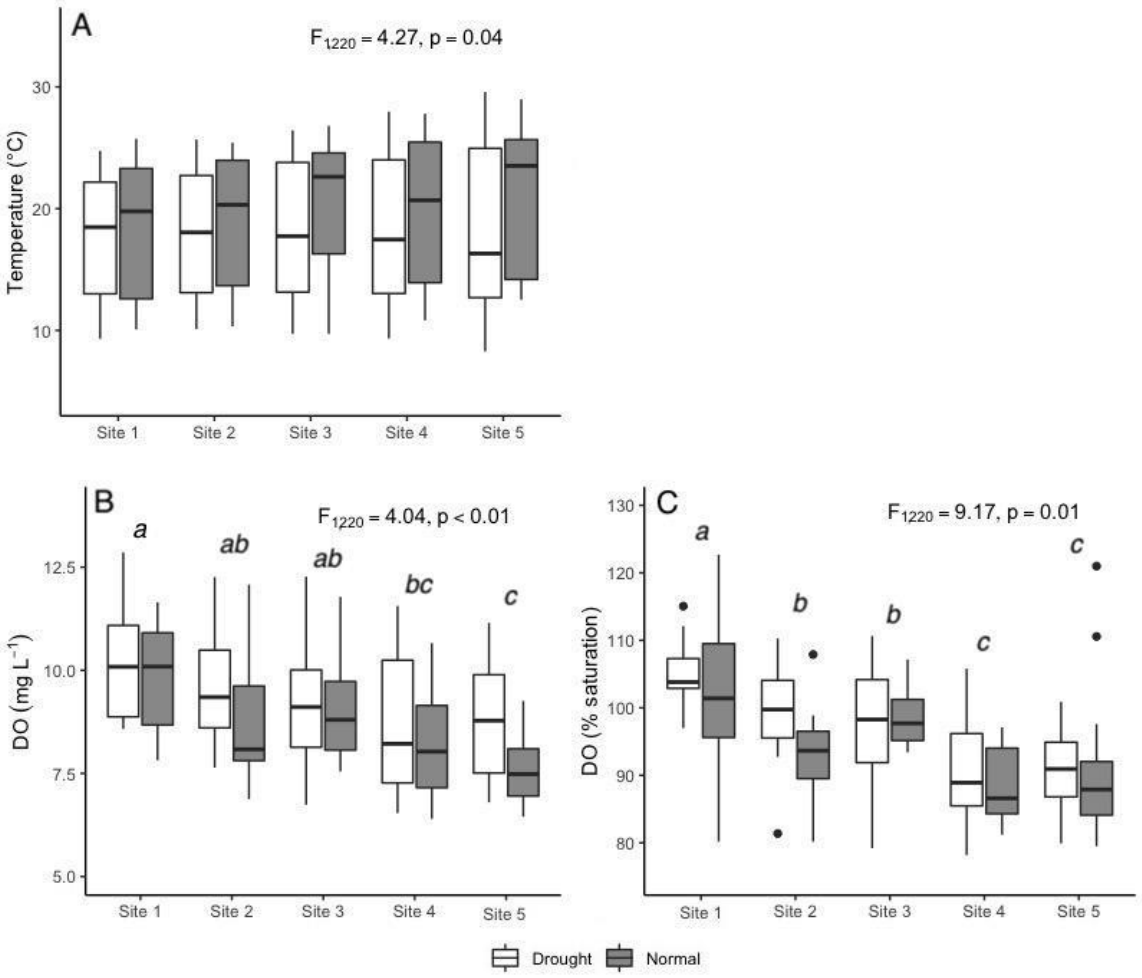


Figure 3.4: (A) Water temperature (ºC), (B) dissolved oxygen (DO) (mg $L^{-1}$) and (C) dissolved oxygen (DO) (% saturation). Box and whisker plots in white represent the drought period and box and whisker plots in gray represent the normal period. The bottom and top of each box are the 25$^{th}$ and 75$^{th}$ percentiles of the samples, the line in the middle of each box is the median, whiskers extend above and below each box to 1.5 times the interquartile range and observations beyond the whisker length are marked as outliers with an individual symbol. Where site effects were significant ($p < 0.05$), Tukey-HSD tests were used to separate means (indicated by small letters), and sites indicated by the same letter are not different. The most extreme values are not shown for figure clarity.

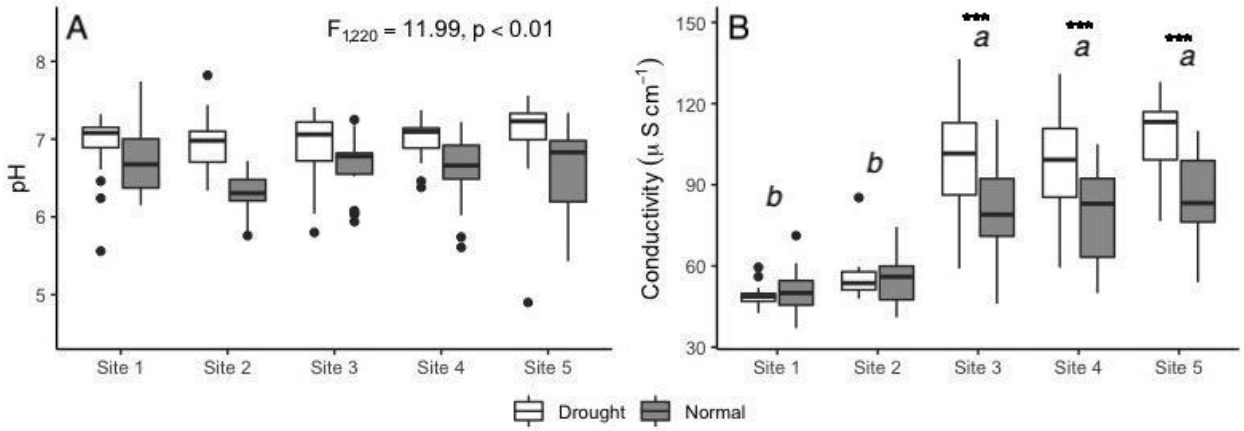


Figure 3.5: Physicochemical ionic metrics including (A) pH and (B) overall conductivity (µS cm$^{-1}$). For conductivity, a significant interaction existed between sites and time periods, so a series of 1-way ANOVAs were used; Sites 1 and 2 were similar between time periods, but sites 3, 4 and 5 were significant (denoted as ***). Box and whisker plots in white represent the drought period and box and whisker plots in gray represent the normal period. The bottom and top of each box are the 25$^{th}$ and 75$^{th}$ percentiles of the samples, the line in the middle of each box is the median, whiskers extend above and below each box to 1.5 times the interquartile range and observations beyond the whisker length are marked as outliers with an individual symbol. Where site effects were significant ($p < 0.05$), Tukey-HSD tests were used to separate means (indicated by small letters), and sites indicated by the same letter are not different. The most extreme values are not shown for figure clarity.

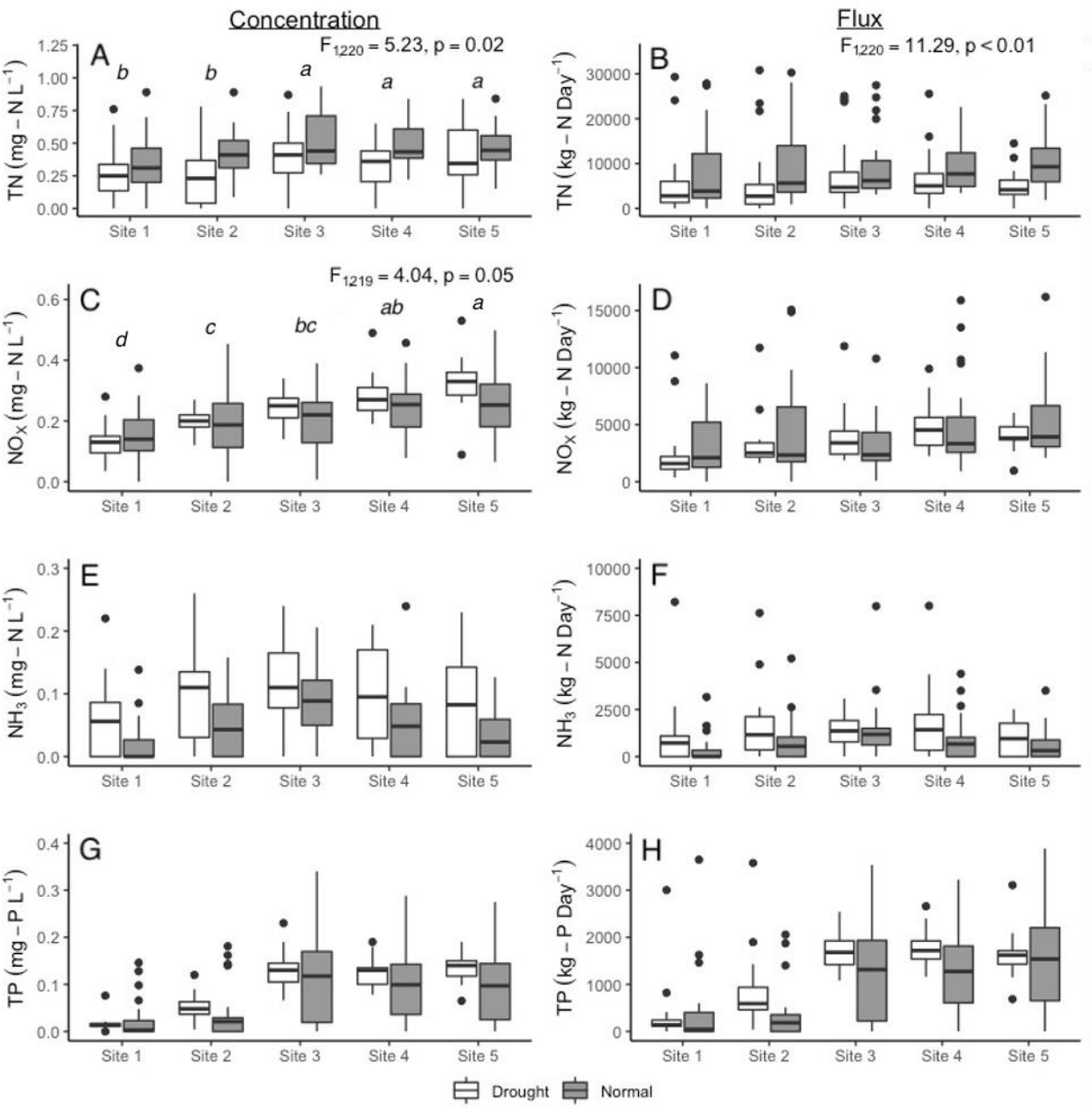


Figure 3.6: Nutrient metrics including (A) total nitrogen (TN) concentrations (mg-N $L^{-1}$), (B) total nitrogen flux (kg-N $day^{-1}$), (C) $NO_X$ (nitrate +nitrite) concentrations (mg-N $L^{-1}$), (D) nitrate + nitrite flux (kg-N $day^{-1}$), (E) ammonia ($NH_3$) concentration (mg-N $L^{-1}$), (F) ammonia flux (kg-N $day^{-1}$), (G) total phosphorus (TP) concentration (mg-P $L^{-1}$) and (H) total phosphorus flux (kg-P $day^{-1}$). Box and whisker plots in white represent drought conditions and box and whisker plots in gray represent normal conditions. The bottom and top of each box are the 25$^{th}$ and 75$^{th}$ percentiles of the samples, the line in the

middle of each box is the median, whiskers extend above and below each box to 1.5 times the interquartile range, and observations beyond the whisker length are marked as outliers with an individual symbol. Where site effects were significant ($p < 0.05$), Tukey-HSD tests were used to separate means (indicated by small letters), and sites indicated by the same letter are not different. The most extreme values are not shown for figure clarity.

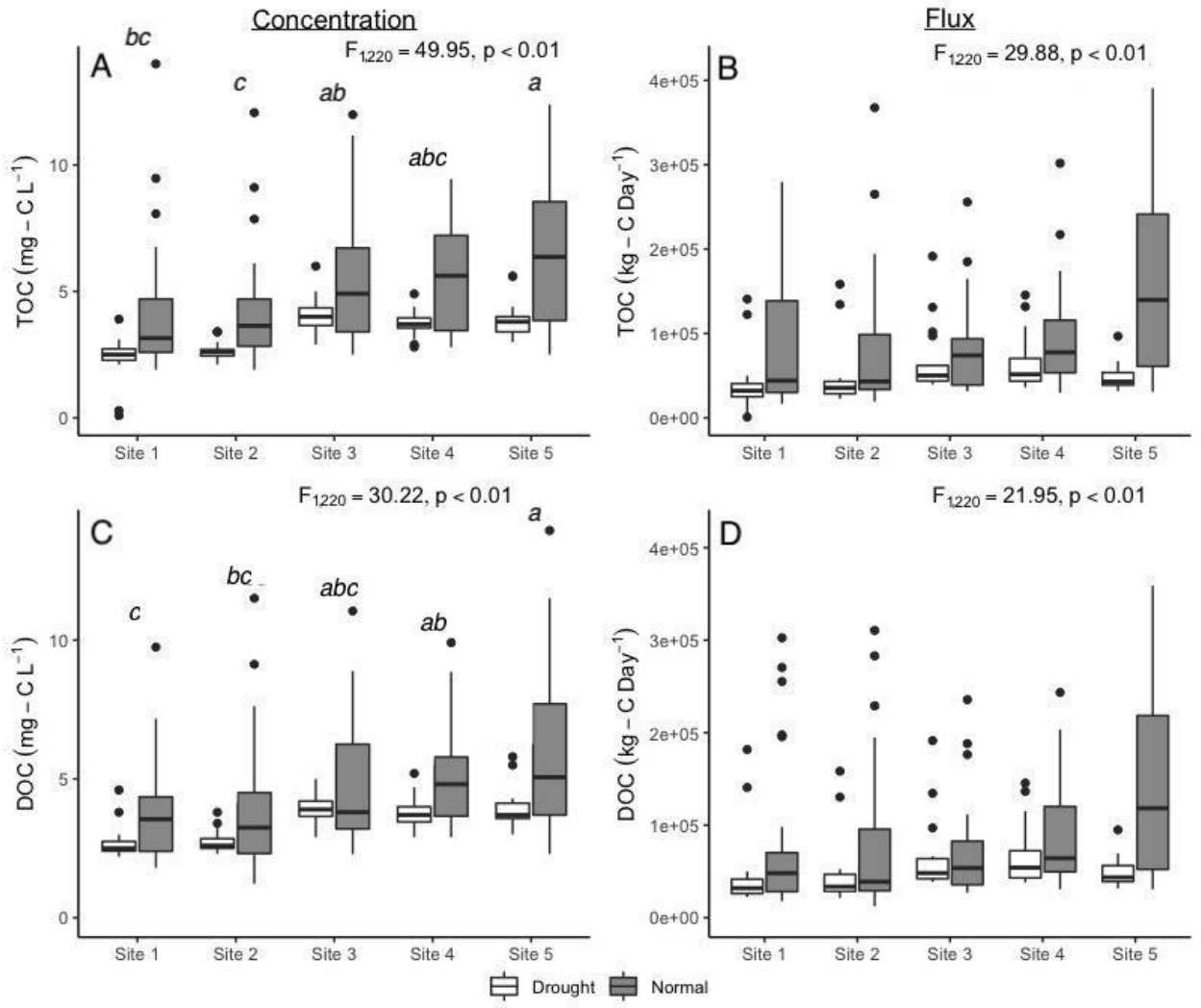


Figure 3.7: (A) Total organic carbon (TOC) concentrations (mg-C $L^{-1}$), (B) total organic carbon flux (kg-C $day^{-1}$), (C) dissolved organic carbon (DOC) concentration (mg-C $L^{-1}$) and (D) dissolved organic carbon flux (mg-C $L^{-1}$). Box and whisker plots in white represent the drought conditions and box and whisker plots in gray represent the normal conditions. The bottom and top of each box are the 25$^{th}$ and 75$^{th}$ percentiles of the samples respectively, the line in the middle of each box is the median, whiskers extend above and below each box to 1.5 times the interquartile range, and observations beyond the whisker length are marked as outliers with an individual symbol. Where site effects were significant ($p$ < 0.05), Tukey-HSD tests were used to separate means (indicated by small letters), and sites indicated by the same letter are not different. The most extreme values are not shown for figure clarity.

# CHAPTER 4

## SPATIAL VARIABILITY OF LONG-TERM STREAMFLOW TRENDS IN THE SOUTHEASTERN UNITED STATES

Wilbanks, K.A., C.R. Jackson, and D.P. Batzer. Submitted to River Research and Application, September 1, 2024.

## ABSTRACT

We assessed long-term discharge trends for 189 streams and rivers from the Mountain, Piedmont, Southeastern Plains and Coast ecoregions of Georgia, South Carolina and North Carolina, U.S.A. Trends over time of average annual discharge volumes (gages with 50+ years of data), average annual groundwater levels (gages with 30+ years of data; n = 143), total annual precipitation (n = 275 stations), average annual temperature maximums (n = 207 stations) and average annual temperature minimums (n = 204 stations) (all with 50+ years of data) were statistically assessed using Mann-Kendall analyses. Decreasing trends were observed at 72% of sites and 22% of those sites had significant decreases in streamflow. Patterns of streamflow were significantly associated with ecoregion ($X^2 = 34.3$, df = 6, $p < 0.01$) and stream size ($F_{3,196} = 9.1$, $p < 0.01$). Using contingency tests, we assessed the relationships between discharge and factors that might be influencing changes in discharge (including groundwater, precipitation and temperature). The Mountain ecoregion showed unchanging streamflow conditions that were somewhat associated with precipitation patterns. In contrast, the Piedmont, Southeastern Plains and Coast ecoregions showed drying streamflow conditions that were associated with a combination of groundwater and/or climate factors, depending on the area. In the Southeastern U.S., streamflows are broadly declining but changes are spatially complex, likely from a range of causative factors, and impacts are ecoregion specific.

# 1 INTRODUCTION

Changes in the volume of water in streams and rivers (discharge) have been observed in several global (van Vliet et al., 2013; Alfieri et al., 2020), national (Sagarika et al., 2014; Dudley et al., 2020; Hodgkins et al., 2020), and regional studies (Rodgers et al., 2020; Botero-Acosta et al., 2022). Recent studies indicate that discharge (also referred to as streamflow, which we use interchangeably with discharge in the manuscript) in the Southeastern United States (U.S.) have declined over the last 25 – 50 years (van Vliet et al., 2013; Stephens and Bledsoe, 2020), and water demands here are expected to increase with increasing populations (i.e., the Southeast is expected to grow by 29% from 2010 to 2040) (Sutton et al., 2021). Understanding spatial variability in changing streamflows, as well as the causative factors driving these changes, is important as climate and human modifications are expected to alter freshwater systems in the future.

Streamflows are altered through a number of climate related factors including precipitation, air temperatures and evapotranspiration (Paul et al., 2019). Precipitation has a direct influence on changes in annual streamflow (Rice et al., 2015) but impacts on streamflow can be complicated by differences in basin size, topography, soils, geology, vegetation and various climate characteristics (Bales et al., 2018; Franzen et al., 2020). Annual precipitation in the Southeastern region is among the highest in the U.S. (1016 to 1270 mm/year on average) (Ingram et al., 2013; USGCRP, 2017; Sutton et al., 2021). However, precipitation is highly spatially and seasonally variable even within regions (Rice et al., 2015; USGCRP, 2017). Further, warming air temperatures have been linked to intensification of water cycling (Paul et al., 2019), and the Southeastern U.S. has experienced an increase of 0.7 – 1.0 °C in average annual temperature from 1986 to 2016 (USGCRP, 2017). Additionally, increased temperatures generally lead to increased evapotranspiration rates, which have been shown to play an important role in water holding capacities and water budgets. Water balance and streamflow changes depend on the tradeoff between changes in precipitation and evapotranspiration (Douville et al., 2013; Heerspink et al., 2020). Thus, climate change has a complicated relationship to streamflow changes.

In addition to climate changes, streamflows are altered through human activities. Rapid population growth intensifies anthropogenic drivers, such as groundwater withdrawals (de Graaf et al., 2019), consumption (Lin et al., 2019), reservoirs (Chai et al., 2019; Allawi et al., 2019; Brogan et al., 2022), land use changes (e.g., deforestation, urbanization and agriculture) (Silva et al., 2021; Aragaw et al., 2021; Kayitesi et al., 2022) and others. Groundwater accounts for up to 40% of freshwater supplies and withdrawals affect the timing, quantity and quality of streamflows (de Graaf et al., 2019; Mohan et al., 2023). Groundwater withdrawals may lead to unreliable water availability, changes in freshwater supplies, and decreased streamflows.

Reservoirs attenuate and disrupt downstream streamflow dynamics by altering hydrographs directly and increasing evapotranspiration (Williams and Wolman, 1984; Poff et al., 1997; Brogan et al., 2022). The eastern U.S. has numerous reservoirs, contributing to decreased streamflows downstream (Downing et al., 2006; Brogan et al., 2022). Reservoir surfaces substantially increase evaporation rates (Cooley et al., 2021; Zhao et al., 2022). Finally, land use changes, such as increased deforestation, growing urbanization and agriculture can alter water balances (e.g., Andréassian 2004; Younger et al., 2020; Silva et al., 2021). Anthropogenic drivers modulate streamflow through numerous mechanisms and may perhaps drive streamflow changes through their cumulative impacts, even more so than those from climate change.

This study aimed to understand historic, long-term spatial patterns of streamflows in the Southeastern U.S., specifically Georgia and the Carolinas. (1) We predicted that streamflows would show long-term decreases due to both climate change (e.g., increases in average air temperatures, changing precipitation patterns or increased evapotranspiration rates) and human actions (e.g., impoundments, population growth, consumption, land use changes, groundwater withdrawals, etc.). (2) We hypothesized that streamflows in the Mountain ecoregion would be disproportionally impacted whereas those in coastal regions would be minimally impacted by global increases in air temperature since air temperature increases (leading to higher evapotranspiration rates) are expected to be greatest at higher latitudes and inland areas, with smaller increases occurring near the coast (Paul et al., 2019). (3) Additionally, we

predicted that streamflow trends would be linked to groundwater trends and would be most pronounced in areas where groundwater pumping is the greatest, corresponding with land use changes (i.e., areas of extensive agriculture or urban growth) (Sutton et al., 2021).

## 2 MATERIAL & METHODS

### *2.1 Study Area*

We focused on streams and rivers in the Southeastern United States including Georgia, South Carolina and North Carolina (Figure 4.1; Appendix 4.A: Table 4.1). The western portion of our study area was bordered by the Appalachian Mountain range and the eastern portion of our study area encompassed the plains and coast which extended to the Atlantic Ocean. North Carolina, the northern most state in our study area, included 60,920 linear kilometers (km) of rivers and streams within 17 river basins, with 12 of those basins flowing into the Atlantic Ocean and five ultimately emptying into the Gulf of Mexico (*NWSRS, 2022*). South Carolina included 46,116 km of rivers and streams within eight river basins, which all flow into the Atlantic Ocean. Georgia, the most southern state in our study area, included 111,925 km of rivers and streams within 14 drainage basins, seven which drain into the Atlantic Ocean and seven which drain into the Gulf of Mexico (*NWSRS, 2022).*

Ecoregions are broad areas with relatively homogenous characteristics like soils, climate and land cover and were used to group sites in our study (Omernik and Griffith, 2014). These classifications were obtained from the United States Geological Survey (USGS). We categorized our study area geographically into the Mountains (Blue Ridge, Ridge and Valley, and Southwestern Appalachians), Piedmont, Southeastern Plains, and Coastal ecoregions (Southern Coastal Plains and Middle Atlantic Coastal Plains) (USGS, 2016).

The climate of the Southeastern U.S. is a humid subtropical environment that is generally mild but can experience extreme weather events (Ingram et al., 2013). Temperatures in the Southeastern U.S. decrease with increased elevation and latitude, while precipitation decreases away from the coast. Historical records suggest that temperatures overall have increased since the 1970s (Ingram et al., 2013).

Mean annual precipitation is predicted to increase across the northern portion of the Southeast and decrease across the southern portion of the Southeast throughout the 21st century (Ingram et al., 2013).

### *2.2 Data Collection*

Daily discharge ($m^3\ s^{-1}$) and groundwater level (depth (m) to water level) were gathered from the USGS. For discharge analysis, we used time series from 1957 (the date when most major dam building in the Southeast was complete) to 2022, for gages where at least 50 years of data recordings were available, to present; time periods ranged from 50 to 66 total years across a total of 189 sites. Data sets for 88% of sites were continuous with no gaps; 12% of the data sets had gaps ranging from 1 to 15 years, although linear trends remained evident despite gaps. Data sets from gages largely affected by flows through major dams (defined as locations where the reservoirs contributed > 50% of discharge) were not included, as they would reflect localized conditions. Groundwater levels were collected from sites with a minimum of 30 years of data, spanning from 1957 at the earliest to 2022, for a total of 143 sites. Data ranged from 30 to 66 years. Information including drainage area ($km^2$), watershed hydrologic unit code (HUC) and location coordinates were collected from the USGS National Water Information System (USGS, 2016). Discharge and groundwater data were downloaded using the dataRetrieval package in R studio (RStudio Team, 2020; De Cicco et al., 2022).

Climate data, including total annual precipitation (mm) and snowfall (mm), temperature maximums (°C) and temperature minimums (°C) were gathered from the National Oceanic and Atmospheric Administration (NOAA) National Centers for Environmental Information (Menne et al. 2012b). Stations with a minimum of 50 years of data, spanning between 1957 at the earliest to 2022, were utilized for a total of 275 stations for precipitation, 207 stations for temperature maximum and 204 stations for temperature minimum. Total annual precipitation was calculated by summing average daily precipitation and average daily snowfall for each year. We used the Global Historical Climatological Network daily (GHCNd) package to download and summarize climate data in R studio (Menne et al., 2012a; RStudio Team, 2020).

### *2.3 Data Analysis*

Data were summarized into annual means or annual totals to describe temporal trends. Averages were reported with standard errors (mean ± SE). Mann-Kendall analysis (Helsel et al., 2020), a non-parametric regression, was used to statistically (*a priori* $\alpha = 0.05$) describe trends of discharge ($m^3 s^{-1}$; n = 189 stream gages), groundwater level (depth (m) below surface level; n = 143 wells), total precipitation (mm, n = 275 rain gages), temperature maximums (ºC, n = 207 weather stations) and temperature minimums (ºC, n = 204 weather stations) over time (years of record). Mann-Kendall results were then used to group sites by trends into 1) significantly decreasing (negative $\tau$, $p \leq 0.05$), 2) decreasing trend ($\tau < -2\%$, but $p > 0.05$), 3) no change ($\tau$ between -2% and +2%), 4) increasing trend ($\tau > +2\%$, but $p > 0.05$) or 5) significantly increasing (positive $\tau$, $p \leq 0.05$). Data were mapped using QGIS software (version 3.8.2 - Zanzibar, QGIS Development Team, 2009) to visualize spatial distributions of trends, create figures and determine the ecoregion where each metric was collected. A Chi-squared goodness of fit test was used to determine if discharge distributions deviated from a hypothesized even distribution of tendencies (i.e., decreasing, no change, and increasing, all at similar rates). To assess if trend patterns for discharge differed among ecoregions, Pearson's Chi-square test of independence was used. For both tests, the standardized residuals of the Chi-square test cells were used to interpret significant associations, with absolute values $\geq 2$ being considered major contributors (Sharpe, 2015). Analysis of Variance (ANOVA) was used to explain relationships between drainage area, ecoregion and discharge trends.

In addition, we used Chi-square tests to describe the relationships between discharge patterns in individual ecoregions and factors that might be influencing those changes in discharge, such as groundwater level, total precipitation, temperature maximums and temperature minimums. A negative $\tau$ (slope) from Mann-Kendall tests was used to describe drier conditions [i.e., lower discharge, groundwater, and precipitation and higher temperatures (causing an increase in evapotranspiration)] and a positive $\tau$ was used to describe wetter conditions (the reverse for potential causative factors). A Chi-square p-value

≥ 0.50 was used to describe a strong association, a p-value < 0.5 and > 0.05 was used to describe a weak association, and a p-value ≤ 0.05 was used to indicate complete independence (i.e., changes in discharge were not consistent with changes in possible causative factors, such as discharge was declining but precipitation was increasing). R studio (version 2022.12.0+353; RStudio Team, 2020) with the R Stats Package was used to run all data analyses (R Core Team, 2013) and the ggplot2 package to make figures (Wickham 2016).

## 3 RESULTS

### *3.1 Long-term streamflow trends*

Discharge ($m^3s^{-1}$; n = 189) analysis (Appendix 4.C - Appendix 4.F) revealed decreased streamflow ($\tau$ < -2%) at 136 sites (72%), no changes ($\tau$ between -2% and +2%) at 32 sites (17 %) and increased streamflow ($\tau$ > +2%) at 21 sites (11%). Decreases were significant at 42 sites (22%) and increases were significant at 2 sites (1%). Standardized residuals (*r*) from the Chi-square goodness-of-fit analyses, with a hypothesized even distribution among decreasing, no change and increasing discharge, indicated that decreasing discharges were most pronounced in the Piedmont (*r* = 7.2), Southeastern Plains (*r* = 6.5) and Coast (*r* = 5.8) ecoregions, whereas the Mountain ecoregion (all *r* between -2 and +2) did not show any bias for changes in discharge (Table 4.1; $X^2$ = 177.4, df = 11, p < 0.01). Correspondingly, sites in the Piedmont (*r* = -3.7), Southeastern Plains (*r* = -3.1) and Coast ecoregions (*r* = -2.9) were less likely than expected to exhibit no changes in discharge or to exhibit an increase in discharge (-3.5, -3.4, -2.9, respectively).

We also found significant spatial trends in annual stream discharge among ecoregions (Figure 4.1, Table 4.2; Pearson's Chi-squared test of independence: $X^2$ = 66.6, df = 12, p < 0.01), with the Mountain and Coast ecoregions being the most unique places. Standardized residuals showed sites in the Mountain ecoregion were either not changing (*r* = 6.1) or exhibited increasing trends (*r* = 2.5). Further, standardized residuals from the Coast ecoregion showed sites were significantly decreasing (*r* = 3.5).

Within the context of an overall pattern of regional drying (Table 4.1), sites in the Mountains were either not changing or wetter than expected, and sites in the Coast were even drier than expected (Table 4.2).

Streamflow changes were correlated with both drainage area and ecoregion, which covaried themselves. Drainage area ($km^2$) analysis indicated a significant (Figure 4.2a; ANOVA: $F_{4,184} = 6.4$, $p < 0.01$) relationship between discharge trends and drainage areas. Gages that were significantly decreasing in discharge had the largest drainage areas, averaging 7,140 ± 1,437 $km^2$, followed by those with a decreasing trend in discharge (2,916 ± 489 $km^2$). Stream gages with an increasing trend in discharge (1,464 ± 1,130 $km^2$) were ranked third and those with no change were ranked fourth in watershed size (1,178 ± 335 $km^2$). Streams with significantly increasing discharge had the smallest drainage areas, averaging 59 ± 21 $km^2$. Ecoregions had significantly different drainage areas (Figure 4.2b; ANOVA: $F_{3,185} = 13.4$, $p < 0.01$): the Mountain ecoregion had the smallest drainage areas (1,410 ± 343 $km^2$) and the Southeastern Plains ecoregion had the largest drainage areas (7,049 ± 1,222 $km^2$). Streams from the Piedmont (1,500 ± 227 $km^2$) and Coast (6,542 ± 2,166 $km^2$) ecoregions had drainage areas in between the other two ecoregions (with the Coast being the most variable place, with both small and very large drainage-area streams co-occurring).

### *3.2 Mountains: environmental factors linked to changing streamflow*

In the Mountain ecoregion, average annual groundwater level (Appendix 4.B: Figure 4.1) analysis (n = 4 wells) revealed that one site was significantly decreasing (25%), two sites had increasing trends (50%) and one site was significantly increasing (25%) (Mann-Kendall). A Chi-square test of independence between groundwater levels and stream discharges showed that groundwater measures were biased towards wetter conditions, whereas discharge measures showed no changes and thus, were independent of each other (Table 4.3; $p = 0.05$). Discharge was increasing at 21% of stream gages whereas groundwater levels were increasing at 75% of groundwater wells.

Total annual precipitation (n = 48 gages) analysis revealed that eight sites were significantly decreasing (17%), 16 sites had decreasing trends (33%), four sites were not changing (8%), 17 sites had

increasing trends (35%) and three sites were significantly increasing (6%) (Appendix 4.B: Figure 4.2). Trends for total annual precipitation and discharge were independent (Table 4.3; $p < 0.01$); discharge showed drier conditions at 29% of stream gages, showed no changes at 50% of stream gages and showed wetter conditions at 42% of stream gages, whereas total precipitation showed drier conditions at 50% of rain gages, no changes at 8% of rain gages and wetter conditions at 42% of the rain gages.

In the Mountains, average annual temperature maximum analysis (n = 36 sites) revealed that four sites were significantly decreasing (11%), five sites had decreasing trends (14%), two sites were not changing (6%), eight sites had increasing trends (22%) and 17 sites were significantly increasing (47%) (Appendix 4.B: Figure 4.3). Trends in average annual temperature maximums (with decreasing temperatures indicating wetter stream conditions and increasing temperatures indicating drier stream conditions) and stream discharge were independent of each other (Table 4.3; $p < 0.01$); discharge showed drier conditions at 29% of stream gages whereas temperature maximums showed drier conditions at 70% of weather stations. Average annual temperature minimum (n = 36) analysis in the Mountains revealed that two sites were significantly decreasing (6%), one site had decreasing trends (3%), one site was not changing (3%), two sites had increasing trends (6%) and 30 sites were significantly increasing (83%) (Appendix 4.B: Figure 4.4). Similar to temperature maximums, minimum temperatures were independent from discharge trends (Table 4.3; $p < 0.01$); 50% of stream gages showed no changes, but temperature minimums showed drier conditions at 89% of weather stations.

In summary, discharge patterns in the Mountains (predominantly unchanging) did not reflect changes in precipitation or temperature. Changes in discharge were somewhat similar to changes in groundwater measures but this was based on a very limited groundwater data set.

### *3.3 Piedmont: environmental factors linked to changing discharge*

In the Piedmont, average annual groundwater level analysis (n = 9 wells) revealed that four sites were significantly decreasing (44%), one site had decreasing trends (11%), one site was not changing (11%), two sites had increasing trends (22%) and one site was significantly increasing (11%) (Appendix

4.B: Figure 4.1). A Chi-square test of independence between groundwater levels and stream discharges showed that groundwater measures were weakly associated to discharge (Table 4.4; $p = 0.27$); discharge showed drier conditions at 75% of stream gages whereas groundwater showed drier conditions at 55% of the groundwater wells.

Total annual precipitation ($n = 115$ gages) analysis revealed that 30 sites were significantly decreasing (26%), 57 sites had decreasing trends (50%), eight sites were not changing (7%), 17 sites had increasing trends (15%) and three sites was significantly increasing (3%) (Appendix 4.B: Figure 4.2). Trends for total annual precipitation and discharge were weakly associated (Table 4.4; $p = 0.39$); discharge showed drier conditions at 75% of stream gages whereas total precipitation showed drier conditions at 76% of rain gages (the p-value was depressed by differences in the no-change and wetter condition categories).

In the Piedmont, average annual temperature maximum ($n = 80$ sites) analysis revealed that seven sites were significantly decreasing (9%), 12 sites had decreasing trends (15%), four sites were not changing (5%), 13 sites had an increasing trend (16%) and 44 sites were significantly increasing (55%) (Appendix 4.B: Figure 4.3). Trends in average annual temperature maximums and stream discharge were weakly associated (Table 4.4; $p = 0.09$); discharge showed drier conditions at 75% of stream gages and maximum temperatures showed drier conditions at 71% of weather stations (the p-value was depressed by differences in the no-change and wetter condition categories). Average annual temperature minimum ($n = 78$) analysis revealed that two sites were significantly decreasing (3%), nine sites had decreasing trends (12%), seven sites had increasing trends (9%) and 60 sites were significantly increasing (77%) (Appendix 4.B: Figure 4.4). Trends for minimum temperatures were independent from discharge changes (Table 4.4; $p < 0.01$); 75% of stream gages showed drier conditions whereas temperature minimums showed drier conditions at 86% of weather stations (temperature minimums were skewed towards drier conditions even more so than discharge indicated).

In summary, discharge patterns in the Piedmont (predominantly decreases) were most closely associated with decreases in precipitation, and secondarily to decreases in groundwater levels.

Temperature was not consistent with changes in discharge and appeared to be even more strongly biased towards drying conditions. This may indicate that discharge changes are lagging behind temperature changes.

### *3.4 Southeastern Plains: environmental factors linked to changing streamflow*

In the Southeastern Plains, average annual groundwater level analysis (n = 79 wells) revealed that 28 sites were significantly decreasing (35%), 28 site had decreasing trends (35%), four sites were not changing (5%), 14 sites had increasing trends (18%) and five sites were significantly increasing (6%) (Appendix 4.B: Figure 4.1). A Chi-square test of independence between groundwater levels and stream discharges showed that groundwater measures were independent of discharge changes (Table 4.5; $p = 0.03$); discharge showed drier conditions at 88% of stream gages whereas groundwater levels showed drier conditions at only 71% of the groundwater wells.

Total annual precipitation (n = 70 gages) analysis revealed that 10 sites were significantly decreasing (14%), 31 sites had decreasing trends (44%), 13 sites were not changing (19%), 14 sites had increasing trends (20%) and two sites were significantly increasing (3%) (Appendix 4.B: Figure 4.2). Trends for total annual precipitation and discharge were independent of each other (Table 4.5; $p < 0.01$); discharge showed drier conditions at 88% of stream gages and total precipitation showed drier conditions at only 59% of rain gages.

In the Southeastern Plains, average annual temperature maximum analysis (n = 54 sites) revealed that five sites were significantly decreasing (9%), seven sites had decreasing trends (13%), two sites were not changing (4%), 15 sites had increasing trends (28%) and 25 sites were significantly increasing (46%) (Appendix 4.B: Figure 4.3). Trends in average annual temperature maximums and discharge were independent (Table 4.5; $p = 0.04$); discharge showed drier conditions at 88% of stream gages and temperature maximums showed drier conditions at 74% of weather stations. Average annual temperature minimum (n = 53) analysis in the Southeastern Plains revealed that one site was significantly decreasing (2%), four sites had decreasing trends (8%), four sites were not changing (8%), 11 sites had increasing

trends (21%) and 33 sites were significantly increasing (62%) (Appendix 4.B: Figure 4.4). Trends in average annual temperature minimums and discharge were strongly associated (Table 4.5; $p = 0.67$); discharge showed drier conditions at 88% of stream gages and temperature minimums showed drier conditions at 83% of weather stations.

In summary, discharge changes in the Southeastern Plains (predominantly decreases) were most closely associated with changes in temperature minimums (increasing temperature levels were linked to decreasing discharge). Other potential causative factors (groundwater, total precipitation and temperature maximums) were not consistent with decreases in streamflow. Although these potential causative factors showed primarily decreases, these decreases were not as strong as those observed for discharge levels.

### *3.5 Coast: environmental factors linked to changing streamflow*

In the Coast ecoregion, average annual groundwater level (n = 52) analysis revealed that 21 sites were significantly decreasing (40%), four site had decreasing trends (8%), two sites were not changing (4%), eight sites had increasing trends (15%) and 17 sites were significantly increasing (33%) (Appendix 4.B: Figure 4.1). A Chi-square test of independence between groundwater levels and stream discharges showed that groundwater measures were independent from changes in discharge (Table 4.6; $p < 0.01$); discharge showed drier conditions at 100% of stream gages whereas groundwater levels showed drier conditions at only 48% of the groundwater wells.

Total annual precipitation (n = 42 gages) analysis revealed that 12 sites were significantly decreasing (29%), 13 sites had decreasing trends (31%), four sites were not changing (10%), 11 sites had increasing trends (26%) and two sites were significantly increasing (5%) (Appendix 4.B: Figure 4.2). Trends for total annual precipitation and discharge were independent (Table 4.6; $p < 0.01$); discharge showed drier conditions at 100% of stream gages and total precipitation showed drier conditions at only 60% of rain gages.

In the Coast ecoregion, average annual temperature maximum analysis (n = 37 sites) revealed that one site was significantly decreasing (3%), six sites had decreasing trends (16%), one site was not

changing (3%), six sites had increasing trends (16%) and 23 sites were significantly increasing (62%) (Appendix 4.B: Figure 4.3). Trends in average annual temperature maximums and stream discharge were weakly associated (Table 4.6; $p = 0.05$); discharge showed drier conditions at 100% of stream gages whereas temperature maximums suggested drier conditions at 78% of the weather stations. Average annual temperature minimum ($n = 37$) analysis revealed that five sites had decreasing trends (14%), two sites had increasing trends (5%) and 30 sites were significantly increasing (81%) (Appendix 4.B: Figure 4.4). Minimum temperatures were weakly associated with discharge changes (Table 4.6; $p = 0.06$); 100% of stream gages showed drier conditions where temperature minimums showed drier conditions at 86% of weather stations.

In summary, discharge changes in the Coast (decreases) were most closely associated with changes in temperature; both maximum and minimum temperatures were broadly increasing to mirror the universal decreases in discharge. Precipitation was not consistent with changes in discharge; while precipitation indicated a bias towards drier conditions, it was not as strongly biased as those of discharge. Finally, groundwater was not consistent with changes in discharge and showed an approximate equal proportion of wetting and drying conditions.

## 4 DISCUSSION

Changes to climate and anthropogenic drivers are expected to alter hydrological cycling, freshwater levels and water budgets (USGCRP, 2017; Paul et al., 2019). We assessed streamflow in the Southeastern U.S. to further understand changing hydrological regimes, hypothesizing that streamflow would show declines across the region, corresponding with increases in population, consumption, air temperature, evapotranspiration rates, as well as changes in precipitation patterns, groundwater levels and land use (USGCRP, 2017). We found that declines were evident across the region, but streamflow patterns and causative factors were ecoregion specific.

### *4.1 Overall streamflow changes*

Streamflows across the study area were primarily declining, consistent with our hypothesis. These decreases, however, were more evident in the lower reaches of the study area and towards the Coast, contrary to our original hypothesis. We found that declines were amplified from the Mountains to the Coast, aligned with streamflow direction (i.e., Piedmont showed declines at 75% of locations, Southeastern Plains showed declines at 88% of locations and the Coast showed declines at all locations). Rodgers et al. (2020) also found widespread declines in streamflows in the Southeastern U.S., but declines in our study were not uniform, being region specific. We found that the Coast had the strongest declines, which was unexpected due to unchanging groundwater levels and more frequent occurrences of coastal storm surge (Wahl et al., 2015; Curtis, 2019). Our observations may result from the cumulative effects of the declines observed upstream within the Piedmont and Southeastern Plains, rather than localized coastal controls.

We hypothesized that streamflows would show declines across the entire region. This was generally true, although we found that streamflows in the Mountain ecoregion were not changing. Most streamflow changes in the Mountains were negligible. For those Mountain locations that had > 2% change, changes were both increasing or decreasing at similar rates. Our results indicate that discharge changes are ecoregion specific and more complex than originally hypothesized.

### *4.2 Mountain ecoregion*

We had expected that the Mountain ecoregion would show the greatest decreases in streamflow because climate changes elsewhere have been most pronounced at high latitudes and inland areas (USGCRP, 2017; Paul et al., 2019). We instead found that streamflows in the Mountains has not changed at most locations. Groundwater measurements indicated mostly increasing groundwater levels (albeit based on a small data set). Climate conditions in the Mountains appeared to be changing in unexpected ways. Total precipitation showed an equal proportion of increasing and decreasing levels. However, temperatures increased at most sites, indicating drying effects. Changes in streamflow in the Mountains

did not closely track groundwater or climate changes, which would suggest other factors are involved (see following).

### *4.3 Piedmont ecoregion*

Across the Piedmont ecoregion, streamflows were declining at most locations. Groundwater level and precipitation showed similar decreases to streamflow. Groundwater declines in Georgia have been reported by Sutton et al. (2021) and declines in ground water elsewhere have been linked to changing streamflow patterns (Zipper et al., 2022). Further, land cover change has been relatively high in the Piedmont (i.e., 14.5% land cover change from 1973 – 2000), compared to other eastern U.S. ecoregions, mostly due to silviculture (Ingram et al., 2013; Sayler et al., 2016). Additionally, while temperature maximums in our analysis were weakly associated with streamflow changes and temperature minimums were independent from streamflow changes, those deviations suggested that discharge decreases should have been even more pronounced than our data indicate. This, coupled with groundwater and precipitation changes, may suggest that streamflow declines in the Piedmont may accelerate in the future.

### *4.4 Southeastern Plains ecoregion*

Streamflow decreases in the Southeastern Plains ecoregion exceeded those in the Piedmont. Hydrologic and climate factors all indicated drying conditions in this ecoregion. Compared to other Southeastern U.S. ecoregions, groundwater declines (Sutton et al., 2021) and land cover change (i.e., 20.4% land cover change from 1973 – 2000) (Ingram et al., 2013; Sayler et al., 2016) are more pronounced in the Southeastern Plains. We found that temperature minimums were most closely associated with the decreases in streamflow, and thus, may be a primary driver of changes in streamflow in the Southeastern Plains ecoregion. Additionally, groundwater levels and temperature maximums were weakly associated with streamflow changes here. Precipitation, however, did not mirror changes in streamflow, as it did in the upstream Piedmont ecoregion. Some streams in the Southeastern Plains are likely integrating impacts to the Piedmont.

### *4.5 Coast ecoregion*

We had hypothesized that the Coast ecoregion would show the smallest changes to streamflow compared to those in inland areas away (USGCRP, 2017; Paul et al., 2019). We rejected that hypothesis. Streamflow declines across the Coast were the strongest of all ecoregions (100% declines). Higher amounts of precipitation have been reported along much of the Atlantic Coast due to sea breeze circulation and extreme precipitation events (Ingram et al. 2013, Curtis, 2019). However, our data indicated annual precipitation has decreased in the Coast ecoregion, although not as drastically as streamflows have declined. The streamflow in the Coast ecoregion is likely influenced by the combined upstream effects of the other ecoregions. Localized hydrologic and climate factors may not affect streamflows strongly. Intrusion from sea level increases (USGCRP, 2017; Sweet et al., 2017; Reidmiller et al., 2017), population increases (Crossett, 2004; Sayler et al., 2016), land use changes (18% change in the Middle Atlantic Coast and 13.2% change in the Southern Coastal Plains; Sayler et al., 2016), disruption in precipitation patterns (Shepherd et al., 2010; Qian et al., 2022) and others, may be complicating factors influencing streamflow in the Coast ecoregion.

### *4.6 Variability in streamflow changes*

Several authors report that changes in streamflows are driven by a combination of climate and anthropogenic factors (Rodgers et al., 2020; Silva et al., 2021; Shi et al., 2022). Our Southeastern U.S. study also indicates that a combination of factors are associated with observed changes of streamflows, with different controls operating in different ecoregions.

Climate in many places has been linked to changes in streamflow through factors such as temperature and precipitation variability (Vicente-Serrano et al., 2019; Tian et al., 2020; Shi et al., 2022), including the Southeastern U.S. (Paul et al., 2019). Precipitation is a strong driver of streamflow changes (Franzen et al., 2020). For example, Berton et al. (2016) found increased annual precipitation was the dominant driver of streamflow changes in the Merrimack Watershed of the Northeastern U.S., with river

regulation and land use being other influences. Historic records (1986 – 2016) indicate precipitation has decreased across the Southeastern U.S. by 5 – 10% overall, especially during the spring season (USGCRP, 2017). Our observations suggest a relationship of streamflow with precipitation at higher elevations and further inland, in the Mountains and the Piedmont.

However, at lower elevations and towards the Coast, temperature appeared a more widespread control of streamflow changes. Temperature alters streamflows through evapotranspiration and soil moisture (Krakauer and Fung, 2008; Paul et al., 2019). We found consistent increases in temperature across the region over the last 50+ years (higher temperatures being associated with increased evapotranspiration), and these drier temperature conditions were primarily associated with streamflow changes in the Piedmont and Southeastern Plains.

Anthropogenic changes can influence changes in streamflows (mostly decreases) through mechanisms, such as reservoir impoundments (Chai et al., 2019; Brogan et al., 2022), population growth (Ingram et al., 2013; Ahn and Merwade, 2014), decreased vegetation (Coats and Jackson, 2020; Zhang et al., 2022), consumption (Lin et al., 2019), land use changes (Vincent-Serrano et al., 2019; Silva et al., 2021) and groundwater pumping (de Graaf et al., 2019). A combination of anthropogenic impacts and climate changes can alter streamflow patterns. For example, Patterson et al. (2013) found that human-induced impacts were equivalent to climate impacts on streamflow, and Shi et al. (2022) and Vincent-Serrano et al. (2019) found that while climate explained most of the streamflow declines in upstream regions, human activities played a more important role in the downstream regions. This may, in part, explain why discharge patterns were different between the Mountains and the lower ecoregions in our study. The Coast and the Southeastern Plains have experienced considerable land use changes (the highest and second-highest percent land cover change across the Southeastern U.S., respectively), whereas the Mountain ecoregion has experienced less land use change (Sayler et al., 2016). Additionally, the Piedmont and Southern Coastal Plain ecoregions have experienced the greatest loss of forests (-4.8 and - 4.2%, respectively) (Sayler et al.2016). Further, many major impoundments occur at the transition between the

Piedmont and Southeastern Plains ecoregions, and flow alteration increases with impoundment density (Brogan et al., 2022).

Water usage may be another strong driver of streamflow changes in the downstream ecoregions. Groundwater pumping can decrease streamflows, especially in intensively irrigated areas (Zipper et al., 2022). Irrigation in the Piedmont and Southeastern Plains ecoregions of Georgia is common, with approximately 2.8 million liters being pumped daily (as of 2015) for crop rotations of corn, cotton, peanuts and soybean (USGS, 2016; Sutton et al., 2021). Also, substantial population growth (from 1970 – 2000) has occurred in the Piedmont (82%), Southeastern Plains (29%) and Coast (Southern Coastal Plains: 140%) ecoregions and population growth has been linked to streamflow changes (Ahn and Merwade, 2014). Thus, while climate may explain some streamflow changes, human activities may explain many streamflow changes in the mid to lower ecoregions.

Our study highlights the complexity of interactions between streamflow, climate factors and anthropogenic drivers. The Southeastern U.S. has experienced substantial declines in streamflows, but these declines are not consistent across the entire region. Streamflow changes will have implications for water quantity management, and water quantity will ultimately affect water quality, biota and human consumption. Understanding how long-term streamflows are changing on a region-wide scale is important for guiding and implementing solutions to reduce growing water resource problems. However, our study suggests that local goals and solutions for water resource management may be more appropriate than region-wide, large-scale solutions; a one-size-fits all approach would not be appropriate in the Southeastern U.S.

## REFERENCES

Ahn, K-H and Merwade, V., 2014. Quantifying the relative impact of climate and human activities on streamflow. J Hydrol, 515: 257-266, https://doi.org/10.1016/j.jhydrol.2014.04.062.

Alfieri, L., Lorini, V., Hirpa, F.A., Harrigan, S., Zsoter, E., Prudhomme, C. and Salamon, P., 2020. A global streamflow reanalysis for 1980–2018. J Hydrol X, 6: 100049. https://doi.org/10.1016/j.hydroa.2019.100049

Allawi, M.F., Binti Othman, F., Afan, H.A., Ahmed, A.N., Hossain, M.S., Fai, C.M. and El-Shafie, A., 2019. Reservoir evaporation prediction modeling based on artificial intelligence methods. Water, 11(6): 1226. https://doi.org/10.3390/w11061226

Andréassian, V., 2004. Waters and forests: from historical controversy to scientific debate. J Hydrol, 291(1-2): 1-27. http://doi.org/10.1016/j.jhydrol.2003.12.015

Aragaw, H.M., Goel, M.K. and Mishra, S.K., 2021. Hydrological responses to human-induced land use/land cover changes in the Gidabo River basin, Ethiopia. Hydrol Sci J, 66(4): 640-655. https://doi.org/10.1080/02626667.2021.1890328

Bales, R. C., Goulden, M. L., Hunsaker, C. T., Conklin, M. H., Hartsough, P. C., O' Geen, A. T., Hopmans, J.W. and Mohammad, S., 2018. Mechanisms controlling the impact of multi-year drought on mountain hydrology. Sci Rep, 8(1): 690. https://doi.org/10.1038/s41598-017-19007-0

Berton, R., Driscoll, C.T. and Chandler, D.G., 2016. Changing climate increases discharge and attenuates its seasonal distribution in the northeastern United States. J Hydrol Reg Stud, 5:164-178. https://doi.org/10.1016/j.ejrh.2015.12.057

Botero-Acosta, A., Ficklin, D.L., Ehsani, N. and Knouft, J.H., 2022. Climate induced changes in streamflow and water temperature in basins across the Atlantic Coast of the United States: An opportunity for nature-based regional management. J Hydrol Reg Stud, 44: 101202. https://doi.org/10.1016/j.ejrh.2022.101202

Brogan, C., Burgholzer, R., Keys, T., Kleiner, J., Shortridge, J. and Scott, D., 2022. The Cumulative Role of Impoundments in Streamflow Alteration. J Am Water Resour Assoc, 58(1): 119-133. https://doi.org/10.1111/1752-1688.12979

Chai, Y., Li, Y., Yang, Y., Zhu, B., Li, S., Xu, C. and Liu, C., 2019. Influence of climate variability and reservoir operation on streamflow in the Yangtze River. Sci Rep, 9(1): 5060. https://doi.org/10.1038/s41598-019-41583-6

Coats, W.A. and Jackson, C.R., 2020. Riparian canopy openings on mountain streams: Landscape controls upon temperature increases within openings and cooling downstream. Hydrol Process, 34(8): 1966-1980. https://doi.org/10.1002/hyp.13706

Cooley, S.W., Ryan, J.C. and Smith, L.C., 2021. Human alteration of global surface water storage variability. Nat, 591 (1): 78–81. https://doi.org/10.1038/s41586-021-03262-3

Crossett, K.M., 2004. Population trends along the coastal United States: 1980-2008 (Vol. 55). US Department of Commerce, National Oceanic and Atmospheric Administration, National Ocean Service, Management and Budget Office, Special Projects. 20 Aug 2023. https://repository.library.noaa.gov/view/noaa/1765/noaa_1765_DS1.pdf

Curtis, S., 2019. Means and long-term trends of global coastal zone precipitation. Sci Rep, 9(1):1-9. https://doi.org/10.1038/s41598-019-41878-8 1

De Cicco L.A., Lorenz, D., Hirsch, R.M., Watkins, W., Johnson, M., 2022. dataRetrieval: R packages for discovering and retrieving water data available from U.S. federal hydrologic web. http://doi.org/10.5066/P9X4L3GE, https://code.usgs.gov/water/dataRetrieval.

de Graaf, I.E., Gleeson, T., Van Beek, L.P.H., Sutanudjaja, E.H. and Bierkens, M.F., 2019. Environmental flow limits to global groundwater pumping. Nat, 574(7776): 90-94. https://doi.org/10.1038/s41586-019-1594-4

Douville, H., Ribes, A., Decharme, B., Alkama, R. and Sheffield, J., 2013. Anthropogenic influence on multidecadal changes in reconstructed global evapotranspiration. Nat Clim Chang, 3(1): 59-62. https://doi.org/10.1038/nclimate1632

Downing, J.A., Prairie, Y.T., Cole, J.J., Duarte, C.M., Tranvik, L.J., Striegl, R.G., McDowell, W.H., Kortelainen, P., Caraco, N.F., Melack, J.M., and Middleburd, J.J., 2006. The Global Abundance and Size Distribution of Lakes, Ponds, and Impoundments. Limnol Oceanogr, 51(5): 2388–97. https://doi.org/10.4319/lo.2006.51.5.2388

Dudley, R.W., Hirsch, R.M., Archfield, S.A., Blum, A.G. and Renard, B., 2020. Low streamflow trends at human-impacted and reference basins in the United States. J Hydrol, 580: 124254. https://doi.org/10.1016/j.jhydrol.2019.124254

Franzen, S.E., Farahani, M.A., and Goodwell, A.E., 2020. Information flows: Characterizing precipitation-streamflow dependencies in the Colorado Headwaters with an information theory approach. Water Resour Res, 56(10): e2019WR026133. https://doi.org/10.1029/2019WR026133

Heerspink, B.P., Kendall, A.D., Coe, M.T. and Hyndman, D.W., 2020. Trends in streamflow, evapotranspiration, and groundwater storage across the Amazon Basin linked to changing precipitation and land cover. J Hydrol Reg Stud, 32:100755. https://doi.org/10.1016/j.ejrh.2020.100755

Helsel, D.R., Hirsch, R.M., Ryberg, K.R., Archfield, S.A. and Gilroy, E.J., 2020. Statistical methods in water resources: U.S. Geological Survey Techniques and Methods, 4(A3): 458. https://doi.org/10.3133/tm4a3.

Hodgkins, G.A., Dudley, R.W., Russell, A.M. and LaFontaine, J.H., 2020. Comparing trends in modeled and observed streamflows at minimally altered basins in the United States. Water, 12(6): 1728. https://doi.org/10.3390/w12061728

Ingram, K.T., Dow, K., Carter, L., Anderson, J. and Sommer, E.K., 2013.Climate of the Southeast United States: variability, change, impacts, and vulnerability. Washington, DC: Island Press/Center for Resource Economics. ISBN: 978-1-59726-427-3

Kayitesi, N.M., Guzha, A.C. and Mariethoz, G., 2022. Impacts of land use land cover change and climate change on river hydro-morphology-a review of research studies in tropical regions. J Hydrol, 615(A): 128702. https://doi.org/10.1016/j.jhydrol.2022.128702

Krakauer, N.Y. and Fung, I., 2008. Mapping and attribution of change in streamflow in the coterminous United States. Hydrol Earth Syst Sci, 12(4):1111-1120. https://doi.org/10.5194/hess-12-1111-2008

Lin, C.C., Liou, K.Y., Lee, M. and Chiueh, P.T., 2019. Impacts of urban water consumption under climate change: an adaptation measure of rainwater harvesting system. J Hydrol, 572: 160-168. https://doi.org/10.1016/j.jhydrol.2019.02.032

Menne, M.J., Durre, I., Vose, R.S., Gleason, B.E. and Houston, T.G., 2012a. An overview of the Global Historical Climatology Network-Daily Database. J Atmos Ocean Technol, 29: 897-910. https://doi.org/10.1175/JTECH-D-11-00103.1

Menne, M.J., Durre, I., Korzeniewski, B., McNeill, S., Thomas, K., Yin, X., Anthony, S., Ray, R., Vose, R.S., Gleason, B.E. and Houston, T.G., 2012b. Global Historical Climatology Network - Daily (GHCN-Daily), Version 3. NOAA National Climatic Data Center. https://doi.org/10.7289/V5D21VHZ [2022].

*National Wild and Scenic Rivers System (NWSRS), 2022. River mileage classification for components of the national wild and scenic rivers system. https://www.rivers.gov/documents/rivers-table.pdf*

Mohan, C., Gleeson, T., Forstner, T., Famiglietti, J.S. and de Graaf, I., 2023. Quantifying groundwater's contribution to regional environmental-flows in diverse hydrologic landscapes. Water Resour Res, 59(6): e2022WR033153. https://doi.org/10.1029/2022WR033153

Omernik, J.M. and Griffith, G.E., 2014. Ecoregions of the Conterminous United States: Evolution of a Hierarchical Spatial Framework. Environ Manag. 54: 1249–1266. https://doi.org/10.1007/s00267-014-0364-1

Patterson, L.A., Lutz, B. and Doyle, M.W., 2013. Climate and direct human contributions to changes in mean annual streamflow in the South Atlantic, USA. Water Resour Res, 49(11): 7278-7291. https://doi.org/10.1002/2013WR014618

Paul, M.J., Coffey, R., Stamp, J. and Johnson, T., 2019. A review of water quality responses to air temperature and precipitation changes 1: Flow, water temperature, saltwater intrusion. J Am Water Resour Assoc, 55(4): 824-843. https://doi.org/10.1111/1752-1688.12710

Poff, N.L., Allan, J.D., Bain, M.B., Karr, J.R., Prestegaard, K.L., Richter, B.D., Sparks, R.E. and Stromberg, J.C., 1997. The Natural Flow Regime. BioSci, 47(11): 769–784. https://doi.org/10.2307/1313099

QGIS Development Team, 2009. QGIS Geographic Information System. Open Source Geospatial Foundation. 30 Aug 2023. http://qgis.org

Qian, Y., Chakraborty, T.C., Li, J., Li, D., He, C., Sarangi, C., Chen, F., Yang, X. and Leung, L.R., 2022. Urbanization impact on regional climate and extreme weather: Current understanding, uncertainties, and future research directions. Adv in Atmos Sci, 39(6): 819-860. https://doi.org/10.1007/s00376-021-1371-9

R Core Team, 2013. R: A language and environment for statistical computing. R Foundation for Statistical Computing, Vienna, Austria. ISBN 3-900051-07-0, URL http://www.R-project.org/.

Reidmiller, D.R., Avery, C.W., Easterling, D.R., Kunkel, K.E., Lewis, K.L., Maycock, T.K. and Stewart, B.C., 2017. Impacts, risks, and adaptation in the United States: Fourth national climate assessment, volume II, Chapter 19: Southeast. U.S. Global Change Research Program; National Oceanic and Atmospheric Administration; National Aeronuatics and Space Administration. http://doi.org/10.7930/NCA4.2018

Rice, J. S., Emanuel, R.E., Vose, J.M. and Nelson, S.A.C, 2015. Continental U.S. streamflow trends from 1940 to 2009 and their relationships with watershed spatial characteristics. Water Resour Res, 51: 6262–6275. https://doi.org/10.1002/2014WR016367

Rodgers, K., Roland, V., Hoos, A., Crowley-Ornelas, E. and Knight, R., 2020. An analysis of streamflow trends in the southern and southeastern US from 1950–2015. Water, 12(12): 3345. https://doi.org/10.3390/w12123345

RStudio Team (2020). RStudio: Integrated Development for R. RStudio, PBC, Boston, MA. http://www.rstudio.com/.

Sagarika, S., Kalra, A. and Ahmad, S., 2014. Evaluating the effect of persistence on long-term trends and analyzing step changes in streamflows of the continental United States. J. Hydrol, 517: 36–53. http://doi.org/10.1016/j.jhydrol.2014.05.002

Sayler, K.L., Acevedo, W. and Taylor, J.L., 2016. Status and trends of land change in the Eastern United States—1973 to 2000: U.S. Geological Survey Professional Paper 1794–D:195, http://doi.org/10.3133/pp1794D

Sharpe, D., 2015. Chi-square test is statistically significant: Now what? Pract Assess Res Eval, 20(8). https://doi.org/10.7275/tbfa-x148

Shepherd, J.M., Carter, M., Manyin, M., Messen, D. and Burian, S., 2010. The impact of urbanization on current and future coastal precipitation: a case study for Houston. Environment and planning B: Planning and Design, 37(2):284-304. https://doi.org/10.1068/b34102t

Shi, R., Wang, T., Yang, D. and Yang, Y., 2022. Streamflow decline threatens water security in the upper Yangtze river. J Hydrol, 606: 127448. https://doi.org/10.1016/j.jhydrol.2022.127448

Silva, A.L.D., Souza, S.A.D., Coelho Filho, O., Eloy, L., Salmona, Y.B. and Passos, C.J.S., 2021. Water appropriation on the agricultural frontier in western Bahia and its contribution to streamflow reduction: revisiting the debate in the Brazilian Cerrado. Water, 13(8): 1054. https://doi.org/10.3390/w13081054

Stephens, T.A. and Bledsoe, B.P., 2020. Low-flow trends at Southeast United States streamflow gauges. J Water Resour Plan Manag, 146(6): 04020032. https://doi.org/10.1016/j.ancene.2019.100231

Sutton, C., Kumar, S., Lee, M.K. and Davis, E., 2021. Human imprint of water withdrawals in the wet environment: A case study of declining groundwater in Georgia, USA. J Hydrol Reg Stud, 35:100813. https://doi.org/10.1016/j.ejrh.2021.100813

Sweet, W.V., Kopp, R.E., Weaver, C.P., Obeysekera, J., Horton, R.M., Thieler, E.R. and Zervas, C., 2017. Global and Regional Sea Level Rise Scenarios for the United States. NOAA Technical Report

NOS CO-OPS 083. Washington, D.C.: National Oceanographic and Atmospheric Administration. https://tidesandcurrents.noaa.gov/publications/techrpt83_Global_and_Regional_SLR_Scenarios_for_the_US_final.pdf

Tian, P., Lu, H., Feng, W., Guan, Y. and Xue, Y., 2020. Large decrease in streamflow and sediment load of Qinghai–Tibetan Plateau driven by future climate change: A case study in Lhasa River Basin. Catena.187:104340. https://doi.org/10.1016/j.catena.2019.104340

U.S. Global Change Research Program (USGCRP), 2017. Climate Science Special Report: Fourth National Climate Assessment (Volume I), edited by D.J. Wuebbles, D.W. Fahey, K.A. Hibbard, D.J. Dokken, B.C. Stewart, and T.K. Maycock. Washington,D.C. https://doi.org/10.7930/j0j964j6

U.S. Geological Survey (USGS). 2016. National Water Information System data available on the World Wide Web (USGS Water Data for the Nation). http://waterdata.usgs.gov/nwis/

van Vliet, M.T., Franssen, W.H., Yearsley, J.R., Ludwig, F., Haddeland, I., Lettenmaier, D.P. and Kabat, P., 2013. Global river discharge and water temperature under climate change. Glob Environ Change, 23(2): 450-464. https://doi.org/10.1016/j.gloenvcha.2012.11.002

Vicente-Serrano, S.M., Peña-Gallardo, M., Hannaford, J., Murphy, C., Lorenzo-Lacruz, J., Dominguez-Castro, F., López-Moreno, J.I., Beguería, S., Noguera, I., Harrigan, S. and Vidal, J.P., 2019. Climate, irrigation, and land cover change explain streamflow trends in countries bordering the northeast Atlantic. Geophys Res Lett, 46(19): 10821-10833. https://doi.org/10.1029/2019GL084084

Wahl, T., Jain, S., Bender, J., Meyers, S.D. and Luther, M.E., 2015. Increasing risk of compound flooding from storm surge and rainfall for major US cities. Nat Clim Chang, 5(12): 1093-1097. https://doi.org/10.1038/nclimate2736

Wickham, H., 2016. Ggplot2: Elegant Graphics for Data Analysis. Springer-Verlag New York, 2016.

Williams, G.P. and Wolman, M.G, 1984. Downstream Effects of Dams on Alluvial Rivers. United State Geologic Survey Professional Paper 1286. https://doi.org/10.1126/science.277.5322.9j

Younger, S.E., Jackson, C.R. and Rasmussen, T.C., 2020. Relationships among forest type, watershed characteristics, and watershed ET in rural basins of the Southeastern US. J Hydrol, 591: 125316. https://doi.org/10.1016/j.jhydrol.2020.125316

Zhang, X., Yi, H., Xue, F., Bruijnzeel, L.A., Cheng, Z. and Liu, B., 2022. Stability and variability of long-term streamflow and its components in watersheds under vegetation restoration on the Chinese Loess Plateau. Hydrol Process, 36(4): e14543. https://doi.org/10.1002/hyp.14543

Zhao, G., Li, Y., Zhou, L. and Gao, H., 2022. Evaporative water loss of 1.42 million global lakes. Nat Commun, 13: 3686. https://doi.org/10.1038/s41467-022-31125-6

Zipper, S.C., Farmer, W.H., Brookfield, A., Ajami, H., Reeves, H.W., Wardropper, C., Hammond, J.C., Gleeson, T. and Deines, J.M., 2022. Quantifying streamflow depletion from groundwater pumping: a practical review of past and emerging approaches for water management. J Am Water Resour Assoc, 58(2): 289-312. https://doi.org/10.1111/1752-1688.12998

Table 4.1: Number of sites (n =189) for long-term (50+ years) discharge ($m^3 s^{-1}$) that are decreasing (significantly decreasing and decreasing trend), not changing (no changes) or increasing (increasing trend and significantly increasing). Chi-square goodness of fit test, with a hypothesized even distribution among decreasing, no change and increasing discharge, indicated ($X^2 = 177.4$, df = 11, $p < 0.01$) observations of discharge were not evenly distributed among ecoregions. Standardized residuals (*r*) for Chi-squared test are shown with significant contributions in bold.

| **Ecoregion** | **Decreasing** | | **No changes** | | **Increasing** | |
|---|---|---|---|---|---|---|
| | Sites | *r* | Sites | *r* | Sites | *r* |
| Mountains | 11 | - 0.5 | 19 | 1.8 | 8 | - 1.4 |
| Piedmont | 63 | **7.2** | 10 | **- 3.7** | 11 | **- 3.5** |
| Southeastern Plains | 38 | **6.5** | 3 | **- 3.1** | 2 | **- 3.4** |
| Coast | 24 | **5.8** | 0 | **- 2.9** | 0 | **- 2.9** |

Table 4.2: Number of sites (n =189) for long-term (50+ years) discharge ($m^3 s^{-1}$) that are significantly decreasing, decreasing trend, no change, increasing trend or significantly increasing for ecoregions in the Southeastern U.S. including Mountains, Piedmont, Southeastern Plains and Coast. Pearson's Chi-squared test of independence indicated ($X^2 = 66.6$, df = 12, $p < 0.01$) a significant association between ecoregion and discharge trends. Standardized residuals (*r*) for Chi-squared test are shown with significant contributions in bold.

| **Ecoregion** | **Significantly Decreasing** | | **Decreasing trend** | | **No changes** | | **Increasing trend** | | **Significantly Increasing** | |
|---|---|---|---|---|---|---|---|---|---|---|
| | Sites | *r* | Sites | *r* | Sites | *r* | Sites | *r* | Sites | *r* |
| Mountains | 0 | **- 3.7** | 11 | **- 2.9** | 19 | **6.1** | 8 | **2.5** | 0 | - 0.7 |
| Piedmont | 16 | - 0.9 | 47 | 1.5 | 10 | - 1.6 | 9 | 0.3 | 2 | 1.6 |
| Southeastern Plains | 14 | 1.9 | 24 | 0.9 | 3 | **- 2.0** | 2 | - 1.3 | 0 | - 0.8 |
| Coast | 12 | **3.5** | 12 | 0.0 | 0 | **- 2.4** | 0 | - 1.8 | 0 | - 0.5 |

Table 4.3: Number of sites in the Mountain ecoregion for discharge (n = 38) contrasted individually with number of sites that showed drier conditions (Mann-Kendall decreasing over time), no changes ($\tau$ between -2% and +2%) or wetter conditions (Mann-Kendall increasing over time) for groundwater (n = 4), total precipitation (n = 48), temperature maximum (n = 36) and temperature minimum (n = 36). Temperature maximum and temperature minimum were reversed for drier conditions (decreasing over time) and wetter conditions (increasing over time). Chi-square test p-value are shown for individual contrasts.

| | **Drier Conditions** | **No Changes** | **Wetter Conditions** | **p-value of $X^2$ test** |
|---|---|---|---|---|
| Discharge | 11 | 19 | 8 | — |
| Groundwater | 1 | 0 | 3 | 0.05 |
| Total Precipitation | 24 | 4 | 20 | < 0.01 |
| Temp Max | 25 | 2 | 9 | < 0.01 |
| Temp Min | 32 | 1 | 3 | < 0.01 |

Table 4.4: Number of sites in the Piedmont ecoregion for discharge (n = 84) contrasted individually with number of sites that showed drier conditions (Mann-Kendall decreasing over time), no changes ($\tau$ between -2% and +2%) or wetter conditions (Mann-Kendall increasing over time) for groundwater (n = 9), total precipitation (n = 115), temperature maximum (n = 80) and temperature minimum (n = 78). Temperature maximum and temperature minimum were reversed for drier conditions (decreasing over time) and wetter conditions (increasing over time). Chi-square test p-value are shown for individual contrasts.

| | **Drier Conditions** | **No Changes** | **Wetter Conditions** | **p-value of $X^2$ test** |
|---|---|---|---|---|
| Discharge | 63 | 10 | 11 | — |
| Groundwater | 5 | 1 | 3 | 0.27 |
| Total Precipitation | 87 | 8 | 20 | 0.39 |
| Temp Max | 57 | 4 | 19 | 0.09 |
| Temp Min | 67 | 0 | 11 | < 0.01 |

Table 4.5: Number of sites in the Southeastern Plains ecoregion for discharge (n = 43) contrasted individually with number of sites that showed drier conditions (Mann-Kendall decreasing over time), no changes (τ between -2% and +2%) or wetter conditions (Mann-Kendall increasing over time) for groundwater (n =79), total precipitation (n = 70), temperature maximum (n = 54) and temperature minimum (n = 53). Temperature maximum and temperature minimum were reversed for drier conditions (decreasing over time) and wetter conditions (increasing over time). Chi-square test p-value are shown for individual contrasts.

| | **Drier Conditions** | **No Changes** | **Wetter Conditions** | **p-value of $X^2$ test** |
|---|---|---|---|---|
| Discharge | 38 | 3 | 2 | — |
| Groundwater | 56 | 4 | 19 | 0.03 |
| Total Precipitation | 41 | 13 | 16 | < 0.01 |
| Temp Max | 40 | 2 | 12 | 0.04 |
| Temp Min | 44 | 4 | 5 | **0.67** |

Table 4.6: Number of sites in the Coast ecoregion for discharge (n = 24) contrasted individually with number of sites that showed drier conditions (Mann-Kendall decreasing over time), no changes (τ between -2% and +2%) or wetter conditions (Mann-Kendall increasing over time) for groundwater (n = 52), total precipitation (n = 42), temperature maximum (n = 37) and temperature minimum (n = 37). Temperature maximum and temperature minimum were reversed for drier conditions (decreasing over time) and wetter conditions (increasing over time). Chi-square test p-value are shown for individual contrasts.

| | **Drier Conditions** | **No Changes** | **Wetter Conditions** | **p-value of $X^2$ test** |
|---|---|---|---|---|
| Discharge | 24 | 0 | 0 | — |
| Groundwater | 25 | 2 | 25 | < 0.01 |
| Total Precipitation | 25 | 4 | 13 | < 0.01 |
| Temp Max | 29 | 1 | 7 | 0.05 |
| Temp Min | 32 | 0 | 5 | 0.06 |

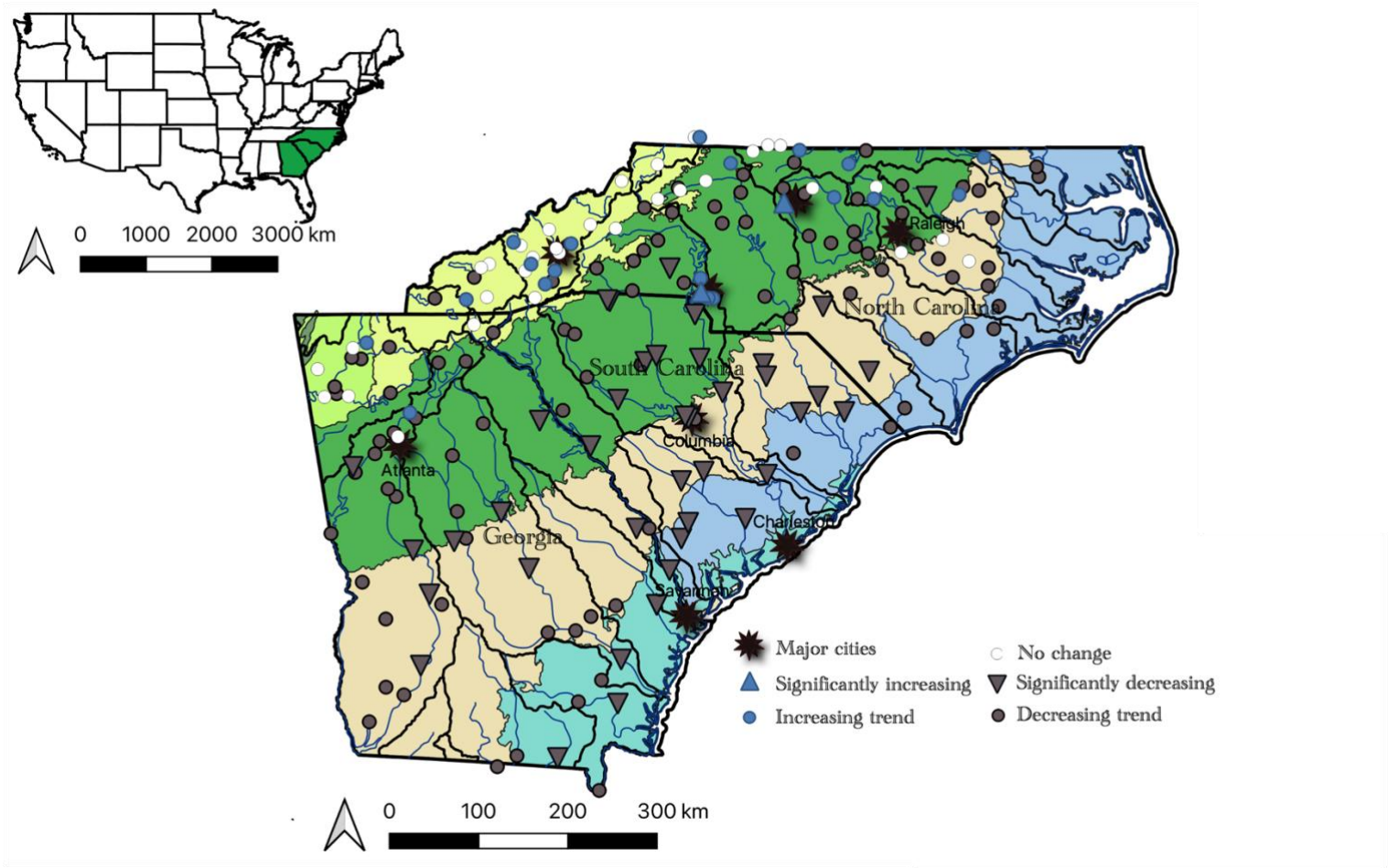


Figure 4.1: Average annual discharge ($m^3s^{-1}$, n=189) trends (50+ years) including significantly decreasing (gray triangle), decreasing trend (gray circles), no change (white circle), increasing trend (blue circle) and significantly increasing sites (blue triangle). North Carolina, South Carolina and Georgia are split by level III ecoregions represented by gray lines and include the Mountains [Ridge and Valley (light green) and Blue Ridge

(yellow)], Piedmont (green), Southeastern Plains (tan) and Coast [Southern Coastal Plains (aqua) and Middle Atlantic Coastal Plains (blue)]. Thin black lines indicate drainage basins.

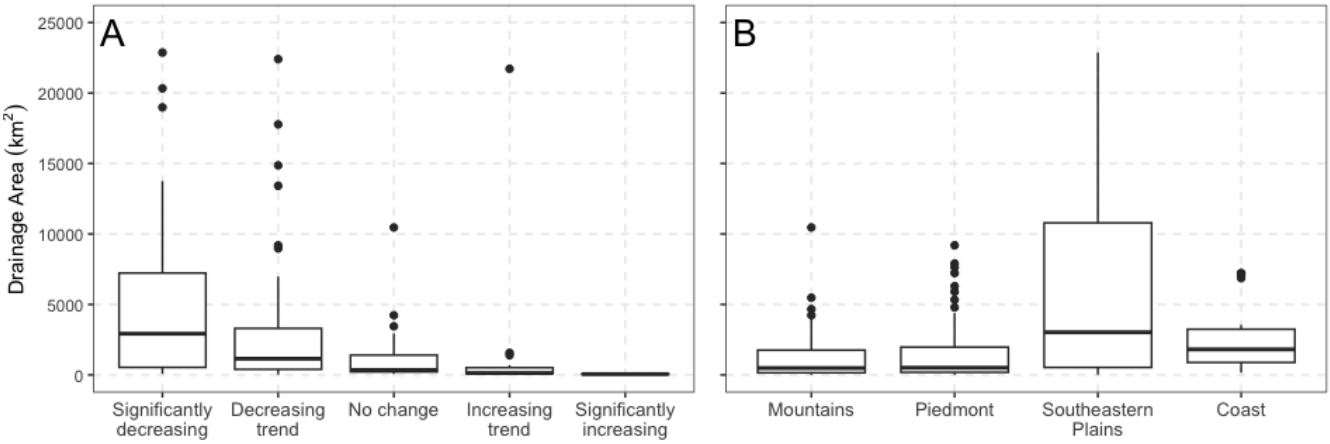


Figure 4.2: **(A)** Drainage area ($km^2$) for each trend including significantly decreasing (n = 42), decreasing trend (n = 92), no change (n =32), increasing trend (n = 19) and significantly increasing (n = 2) at discharge gages and **(B)** drainage area ($km^2$) for ecoregions including Mountains (n = 38), Piedmont (n=84), Southeastern Plains (n = 43) and Coast (n = 24). We removed 3 outliers from significantly decreasing and 1 outlier from decreasing trend for figure A clarity and 3 outliers from Coast ecoregion and 1 from Southeastern Plains ecoregion for figure B clarity. ANOVA indicated a significant difference between drainage area and trend ($F_{4,184} = 6.4$, $p < 0.01$) and indicated a significant difference between drainage area and ecoregion ($F_{3,185} = 13.4$, $p < 0.01$)

# CHAPTER 5

## EVALUATION OF STREAMFLOW TRENDS IN THE SOUTH ATLANTIC-GULF DRAINAGE BASIN AND THE DRIVERS OF LONG-TERM CHANGE

Wilbanks, K.A. and D.P. Batzer. Submitted to Freshwater Science, December 1, 2024.

**ABSTRACT**

Growing water demands and climate change are altering the timing and magnitude of streamflows. To further understand how streamflows are changing over time, we assessed long-term streamflow trends for 33 basins in the South Atlantic-Gulf Drainage located in the southeastern United States. Mann-Kendall analysis was used to determine streamflow ($m^3/s$; n = 374 streamflow gages) change ($\tau$) over time by averaging daily streamflows (n = 365 days) for 65 years (1957 – 2022) (n = 50 minimum of years). Using regression analysis and AIC model selection, we assessed the relationship between average streamflow change and potential causative metrics for each basin. Our results indicated that streamflows are generally decreasing across the study region but are spatially variable; streamflows were increasing in the western and southern portions but decreasing in the larger central portion of the region over time. We also assessed precipitation (mm, n = 463), drainage area ($km^2$; n = 358), annual temperature maximums (ºC, n = 357), annual temperature minimums (ºC, n = 355), population density (# individuals/$km^2$; n = 664), streamflow changes within ecoregions ($m^3/s$; n = 374) and groundwater level (depth (m) below surface level; n = 391 wells) to determine the causative factors of streamflow change We found that total precipitation explained 39% of streamflow variation and drainage area explained 13%. Temperatures and population levels increased uniformly across the region but were not related to variation in streamflow changes. Understanding the contributions of different drivers of streamflow changes provides insight for more effective management of water resources.

**Key words:** rivers, streams, water quantity, climate, anthropogenic, precipitation, discharge, groundwater, population

Several recent global (Dai et al. 2009, van Vliet et al. 2013, Hansford et al. 2020, Zhang et al. 2023), national (Rice et al. 2015, Dudley et al., 2020; Hodgkins et al., 2020) and regional (Rodgers et al 2020, Stephens and Bledsoe 2020, Gaines et al. 2022, Botero-Acosta et al. 2022) studies have documented changes in streamflows (also referred to as streamflow, which we use interchangeably with discharge in the manuscript) over the last century. Despite differences in streamflow trends, there is an emerging consensus that streamflows have changed and will continue to change with growing water demands and a changing climate (Milly et al. 2005, Rice et al. 2015, Yang et al. 2021). Recent reports of declines in low-flows (van Vliet et al. 2013, Stephens and Bledsoe 2020), extreme weather events causing both floods and droughts (Ingram et al. 2013), spatially variable precipitation patterns (Ingram et al. 2013, USCGPR 2017) and uncertainties regarding future climate projections have elucidated a need for comprehensive and continued investigations into streamflow changes.

Streamflows are modified by both alterations in climate and anthropogenic activities. Climate change is altering and intensifying precipitation across the globe (Trenberth 2011, Dai 2013). Precipitation is a direct driver of streamflow change (Rice et al. 2015) and many studies have observed a direct relationship between precipitation and streamflow (Berton et al. 2016, Engström and Waylen 2021, Franzen et al. 2020). The general conclusion of these studies was that an increase in precipitation has resulted in an increase in low flows, annual minimum, annual median, annual maximum and average annual streamflows across much of the United States (U.S.) (McCabe and Wolock 2002, Sadri et al. 2016). However, precipitation demonstrates significant spatial heterogeneity and temporal variability related to the proximities of the coast, influence of topography, sea breeze circulation, tropical cyclones, drought persistence, and other climate and local factors (Ingram et al. 2013, Konapala et al. 2020).

Additionally, average annual air temperatures have increased in the southeastern U.S. by 0.7 –1.0 °C from 1986 – 2016 and are projected to increase by 1.4 °C by 2050 (Ingram et al. 2013, USGCPR 2017, Carter et al. 2018). Increased air temperatures lead to increased evapotranspiration rates, increased water temperatures, and plant and soil water losses. Evapotranspiration rates play an important role in water holding capacities and water budgets that ultimately effect streamflow quantities (Konapala et al. 2020, Massari et al. 2022).

Human activities, such as land use changes (Aragaw et al. 2021; Kayitesi et al. 2022), surface and groundwater withdrawals (de Graaf et al. 2019), reservoirs (Chai et al. 2019, Allawi et al. 2019; Brogan et al. 2022), consumption (Lin et al. 2019) and urbanization (Bhaskar et al. 2020) affect the timing and quantity of streamflows. Rapid population growth, especially over the last half century, intensifies these anthropogenic drivers (Ingram et al. 2013, US REAP 2024). Direct human activities have been observed modifying the timing, magnitude and seasonality of streamflows (Ahn and Merwade 2014). Further, reservoirs directly alter the hydrograph by attenuating and disrupting downstream flows and increasing surface evaporation rates (Cooley et al. 2021, Zhao et al. 2022). Rapid population growth and the subsequent anthropogenic activities are changing streamflows.

Groundwater is the world's largest available freshwater resource and streamflows are determined by a balance among precipitation, groundwater storage and evapotranspiration (Zipper et al. 2022, Mohan et al. 2023). A decrease in groundwater level can alter streamflows in hydrologically connected systems (Bierkens and Wada 2019, Zipper et al. 2022), especially in agricultural areas or where pumping exceeds the rates of recharge (de Graaf et al. 2019, Zipper et al. 2022, Mohan et al. 2023). With climate change, increased water demands and the increased

frequency of drought, the dependence on groundwater is expected to further increase in the future.

Several global (Dai et al. 2009, van Vliet et al. 2013, Hansford et al. 2020, Zhang et al. 2023) and national studies (Wang and Hejazi 2011, Brauer et al. 2015, Ficklin et al. 2018) have documented climate as the primary driver of streamflow change. However, at the basin- and local- level, anthropogenic activities appear to outweigh the influence of climate and are seemingly a stronger driver of streamflow change (Ahn and Merwade 2014, Xue et al. 2017, Khan et al. 2021). Others have found that climate explained most of the streamflow changes in upstream regions, but that anthropogenic activities played a more important role in downstream regions (Vincent-Serrano et al. 2019, Shi et al. 2022). Alternatively, some have found that human-impacts and climate changes had an equivalent impact on streamflows (Patterson et al. 2013). Understanding the contributions of these different drivers of streamflow changes provides insight for the effective management of water resources.

We assessed long-term average annual streamflow patterns over a 65-year period gain insight into patterns of streamflow change in the southeastern U.S. and aimed to further explore the spatial variability of streamflows. We hypothesized that (1) long-term streamflows patterns would show regional drying and streamflow drying trends would be exacerbated from northern to southern basins, consistent with predicted annual precipitation patterns [i.e., Mean annual precipitation is predicted to increase across the northern portion of the Southeast and decrease across the southern portion of the Southeast throughout the 21$^{st}$ century (Ingram et al. 2013, Sadri et al. 2016)]. We also assessed precipitation, drainage area, annual temperature maximum, annual temperature minimum, population density, streamflow changes within ecoregions and groundwater level to determine the causative factors of streamflow change and hypothesized that

(2) both climate change (i.e., increases in both temperatures and evapotranspiration rates) and anthropogenic drivers (e.g., increased groundwater withdrawals and population growth) would be linked to regional drying patterns.

## METHODS

### Study area

Our study area focused on streams and rivers in the South Atlantic-Gulf Drainage, at the resolution of the six-digit hydrologic unit codes for watersheds assigned by the United States Geological Survey (hereafter, "HUC" or "drainage basin"). The overall South Atlantic-Gulf Drainage (03 HUC) spans an area of 367,740 $km^2$ in the southeastern U.S, and encompasses the states of Florida and South Carolina, and parts of Alabama, Georgia, Louisiana, Mississippi, North Carolina, Tennessee and Virginia (Figure 1; USGS 2024). The 33 basins (6-unit HUC) of the South Atlantic-Gulf Drainage were used to group sites in the following analyses (USGS 2013). Drainage basins ranged in size with the largest being the Apalachicola (HUC 031300) at 52,264 $km^2$ and the smallest being East Florida Coastal (HUC 030802) at 4,053 $km^2$ (Table 5.1; USGS 2024). The highest elevation was Mt. Mitchell (2,037 m above sea level), located in western North Carolina, just outside of the Edisto-Santee drainage basin and the lowest elevation was sea level at the mouth of each basin. Population in the South Atlantic-Gulf drainage basin was approximately 48,718,547 as of 2022 and has increased 12.7% over the last 10 years (2012 – 2022) (U.S. Census Bureau 2023).

The climate of the South Atlantic-Gulf Drainage is influenced by its diverse topography. The Appalachian Mountain range runs from eastern Alabama to central Virginia and ranged from 90 m to 2,037 m in elevation (USDA 2024). In the eastern and southern portion of the South

Atlantic-Gulf Drainage, rolling plateaus transition to extensive coastal plains. The climate is characterized by a semi-Permanent high-pressure system, known as the Bermuda High, which results in a humid, subtropical climate, but also causes extreme weather events like heat waves, cold temperature outbreaks, flooding, drought, hurricanes and tornados (Ingram et al. 2013). Temperatures have steadily increased across the southeastern U.S. since 1970, with an increase in the number of days where maximum temperatures have exceeded 35 °C and minimum temperatures have exceeded 24 °C (Ingram et al. 2013, Carter et al. 2018).

**Data collection**

Daily average discharge ($m^3/s$) (also referred to as streamflow, which we use interchangeably with discharge in the manuscript) and groundwater level (depth (m) to water level) were gathered from the United States Geological Survey (hereafter, USGS) (USGS 2016). For discharge, time series data was gathered from 1957 (the date when most major dam building in the Southeast was complete) to 2022, for gauges where at least 50 years of data were available. Time periods in the dataset ranged from 50 years at a minimum, to 66 years maximum across a total of 374 streamflow gauges. Average annual discharge was continuous with no data gaps for 83% of sites; 17% of gauges had gaps that ranged from 1 to 15 years of missing data, although linear trends remained evident despite gaps. Further, data sets from gauges where flows were largely affected by major dams (defined as gauges where discharge through a dam contributed to > 50% of flows) were not included in the analyses. Daily groundwater level and groundwater field measurements were collected from sites with a minimum of 30 years of data, spanning from 1957 at the earliest to 2022, for a total of 391 groundwater wells. Information including site number, drainage area ($km^2$), watershed hydrologic unit code (HUC) and GPS

coordinates were collected from the USGS National Water Information System (USGS 2016). Discharge and groundwater data were downloaded using the dataRetrieval package in R (RStudio Team, 2020; De Cicco et al. 2022).

Daily average summaries for climate data, including total precipitation (mm), total snowfall (mm), average temperature maximum (°C) and average temperature minimum (°C) were gathered from the National Oceanic and Atmospheric Administration (NOAA) National Centers for Environmental Information (Menne et al. 2012a). Stations with a minimum of 50 years of data, spanning between 1957 at the earliest to 2022, were utilized for a total of 463 stations for total precipitation, 357 stations for temperature maximum and 355 stations for temperature minimum. Daily average precipitation and snowfall were combined into a single precipitation metric for analyses. The Global Historical Climatological Network daily (GHCNd) package was used to download and summarize climate data in R (Menne et al. 2012b, RStudio Team, 2020).

Ecoregions, or areas where ecosystems are generally similar in geology, landforms, soil, vegetation, climate, land use and hydrology, were used to investigate patterns of streamflow change. Environmental Protection Agency (EPA) level II ecoregions were delineated for each basin and included the Mississippi Alluvial and Southeast USA Coastal Plains (USEPA 8.5; hereafter, Coastal Plains), Ozark, Ouachita-Appalachian Forests (USEPA 8.4; hereafter, Appalachian Forests), Southeastern USA Plains (USEPA 8.3; hereafter, Plains) and Everglades (USEPA 15.4) (Omernik 1987, US EPA 2024).

We used population change as an indicator of changes in human activities. Total population for each county was collected by aggregating decennial population estimates from the U.S. Census Bureau (U.S. Census Bureau 2007, 2021, 2023). The total number of individuals in

each county were summed and that total was divided by basin area ($km^2$) to determine average population density (# individuals/$km^2$) for individual basins. On occasion, portions of a county occurred outside a focal watershed, which lead to a level of imprecision of population density, but general patterns of population change could still be determined.

Data were mapped using QGIS software (version 3.8.2 - Zanzibar, QGIS Development Team, 2009). The Watershed Boundary Dataset at a 1:24,000 topographic scale and a 6-unit HUC were used to delineate drainage basins in the South Atlantic-Gulf Drainage (USGS NGTOC 2016). QGIS was used to estimate basin size, calculate elevation, determine ecoregion, delineate counties within basins and create maps. A 1-meter digital elevation model was used with GPS coordinates in QGIS to estimate elevation (USGS 2023).

**Data analyses**

Data were summarized into annual means or annual totals to describe temporal trends. Averages were reported with standard errors (mean ± SE). Mann-Kendall analysis (Helsel et al., 2020), a non-parametric regression, was used to statistically (*a priori* $\alpha = 0.05$) describe trends of discharge ($m^3/s$; n = 374 stream gauges) total precipitation (mm, n = 463 rain gauges), population density (# individuals/$km^2$; n = 664 counties), temperature maximums (ºC, n = 357 weather stations), temperature minimums (ºC, n = 355 weather stations) and groundwater level (depth (m) below surface level; n = 391 wells), over time (years of record). Mann-Kendall slopes was then averaged for each of the 33 basins. Mann-Kendall results with a negative slope ($-\tau$) indicated a decreasing trend, a zero slope ($\tau = 0.00$) indicated no changes and a positive slope ($+\tau$) indicated an increasing trend in streamflow over time.

Linear regression analysis was used to describe the relationship between average streamflow changes (Mann-Kendall slope (τ)) and potential causative metrics, including total precipitation change (Mann-Kendall (τ)), average drainage area ($km^2$), temperature maximum change (Mann-Kendall (τ)), temperature minimum change (Mann-Kendall (τ)), population change (Mann-Kendall (τ)), elevation, streamflows for ecoregions and groundwater change (Mann-Kendall (τ)) for each basin. Average drainage area was square root transformed and elevation was log transformed prior to analysis to meet the linearity assumption of linear regression analysis. We compared linear regression model results with Akaike's information criterion (AIC; Akaike, 1998). Models with larger AIC values indicated a more parsimonious description of streamflow change. R studio (version 2024.04.1+748; Posit team 2024) with the R Stats Package was used to run all data analyses (R Core Team, 2024) and the ggplot2 package was used to make figures (Wickham 2016).

## RESULTS

### Streamflow trends for the South Atlantic-Gulf Drainage

Long-term (1957 – 2022) streamflow (m3/s; n = 374 total gauges) trends in the South Atlantic-Gulf Drainage (HUC-03) showed negative Mann-Kendall slopes of at least 1% at 237 (63.1%) streamflow gauges, of which 58 (15.5 %) were significantly ($p \leq 0.05$) decreasing. Additionally, 13 (3.5 %) streamflow gauges had slopes that were unchanging (between –1 and 1% τ). On-the-other-hand, 124 (33.2%) streamflow gauges had >1% positive slopes, of which 22 (5.9%) were significantly increasing. Overall, streamflow slopes averaged $–0.04 \pm 0.01$ τ indicating a 4% decline in flows across all basins in the South Atlantic-Gulf Drainage (Fig. 1).

Changes in streamflow varied spatially (ANOVA: $F_{32,343}$ =11.19, $p < 0.01$) among the 33 drainage basins (Table 5.1, Fig. 5.2). Twenty-three basins (69.7%) averaged a decreasing streamflow slope (– τ) from 1957 – 2022. Two drainage basins (6.1%) averaged an unchanging streamflow slope (τ = 0.00) and eight drainage basins (24.2%) averaged an increasing streamflow slope (+ τ) over time. Drainage basins in the western portion of our study area averaged increasing streamflow over time and included the Black Warrior-Tombigbee, Pascagoula and Pearl Drainage Basins. Additionally, drainage basins in the southern portion of our study area averaged increasing streamflows over time and included the Kissimmee, Southern Florida and Peace Drainage Basins. Lastly, the Roanoke Drainage Basin, located in the upper portion of our study area, averaged increasing streamflows over time.

In summary, declines in streamflows were evident across most of the South Atlantic-Gulf Drainage. Over two-thirds of the drainage basins exhibited declines in average annual streamflow from 1957 – 2022 (Fig. 2). However, not all basins in the South Atlantic-Guld Drainage were declining. Basins in the western portion of the South Atlantic-Gulf Drainage and basins in the southern portion of Florida exhibited increased flows over time (Fig. 2). Furthermore, the Roanoke Drainage Basin was another isolated place with flow increases.

**Factors linked to changing streamflows**

Precipitation and drainage area were linked to changing streamflow patterns (Table 5.1). Regression analysis of average total precipitation slope (τ) for the 33 drainage basins indicated there was a relationship to streamflow changes ($F_{1,30}$ = 20.45, $p < 0.01$) that explained 39% of streamflow variation ($R^2$ = 0.39) (Table 5.2, Fig. 5.3A). We found total precipitation had the largest AIC value (AIC = 61.72), which indicated the best fit model. Additionally, regression

analysis of drainage area ($km^2$) indicated there was a relationship to streamflow changes ($F_{1,31}$ = 5.64, p = 0.02) that explained 13% of streamflow variation ($R^2$ = 0.13) (Table 5.2, Fig. 5.3B). Drainage area followed precipitation in AIC value (AIC = 53.04), and it was the second-best fitting model.

Long-term (1957 – 2022) total precipitation (mm; n = 463 rain gauges) trends in the South Atlantic-Gulf Drainage averaged – 0.03 ± 0.01 τ indicating a 3% decline across all basins in the South Atlantic-Gulf Drainage. Changes in precipitation varied across the South Atlantic-Gulf Drainage (Fig. 4A). Seventeen basins (n = 31, 54.8%) were found to have a decreasing total precipitation slope (– τ) from 1957 – 2022 and fourteen drainage basins (45.2%) were found to have an increasing total precipitation slope (+ τ) over time. Total precipitation was markedly variable between drainage basins (Appendix 4.A: Fig. 1A). Drainage basins in the western portion of our study area averaged an increasing total precipitation over time and included the Black Warrior-Tombigbee, Escambia, Pearl, Mobile Bay-Tombigbee, Pascagoula and Coosa-Tallapoosa Drainage Basins. Additionally, drainage basins in the southern portion of our study averaged an increasing total precipitation over time and included the East Florida Coastal, Kissimmee, Peace and Tampa Bay Drainage Basins. Finally, drainage basins in the northern portion of our study area averaged an increasing total precipitation over time and included the Neuse, Roanoke and Albemarle-Chowan Drainage Basins.

In summary, streamflow changes were closely mirrored by total precipitation changes (Fig. 2, 4A). Basins in the central portion of our study area showed declines in streamflow and total precipitation, whereas basins in the northern, southern and western portion of our study area showed increases in streamflow and total precipitation over time. Drainage area was found also

associated with streamflow changes (large watersheds declined the most in flows), but to a lesser extent.

**Other factors not significantly linked to changing streamflows**

Long term (1957 – 2022) temperature maximum trends, temperature minimum trends and decennial (1950 – 2020) population trends all increased uniformly across the South Atlantic-Gulf Drainage, but degree of changes were not directly related to changing streamflow patterns (Table 5.2). Temperature maximum slope averaged a 0.15 ± 0.01 $\tau$ increase (Figure 5.4B), temperature minimum slope averaged a 0.27 ± 0.01 $\tau$ increase (Figure 5.4C) and population density slope averaged a 0.99 ± < 0.01 $\tau$ increase (Figure 5.4D) across basins in the South Atlantic-Gulf Drainage (Appendix 5.A: Table 5.S1, Figs. 2A, 2B, 2C). Elevation (Appendix 5.A: Table 5.1, Fig. 5.2D) and ecoregions (Appendix 5.A: Table 5.2, Fig. 5.3) were variable for basins but were not related to changing streamflows. Finally, long term (1957 – 2022) groundwater level slope averaged a – 0.13 ± 0.02 $\tau$ decline across all basins in the South Atlantic-Gulf Drainage (Table 5.2, Fig. 5.4E). Groundwater level was variable for basins, but consistent patterns were not evident nor were they related to variation in streamflows (Appendix 5.A: Table 5.1, Fig. 5.2E).

**DISCUSSION**

Climate change and anthropogenic drivers alter hydrological cycling, freshwater levels, and the timing and magnitude of flows (Rodgers et al., 2020; Silva et al., 2021; Shi et al., 2022). We assessed streamflows in the South Atlantic-Gulf Drainage to further understand the spatial variability of changing streamflows and identify the most likely causative factors driving these changes. First, we hypothesized that declines in streamflows would be widespread and

correspond with climate change (i.e., increased air temperature leading to higher evapotranspiration rates and changes in precipitation patterns) and anthropogenic drivers (i.e., population growth, groundwater withdrawals, urbanization, land use changes, etc.) (USGCPR 2017). This hypothesis was supported. Second, we hypothesized that declines would be less severe in the northern portion of the South Atlantic-Gulf Drainage and more severe in more southern portion, corresponding to previously reported annual precipitation patterns (Sadri et al. 2016). This hypothesis was only partially supported.

**Overall streamflow changes**

As predicted, we found that streamflows in the South Atlantic-Gulf Drainage were primarily declining. Our results were similar to other observations of decreased streamflows in the southeastern U.S. (Patterson et al. 2013, Sadri et al. 2016, Kam and Sheffield 2016, Stephens and Bledsoe 2019, Paul et al. 2019, Dudley et al. 2020, Rodgers et al. 2020). However, we unexpectedly found increased streamflows in some places; streamflows have increased in the southern portion of Florida, the western portion of our study area, and in the Roanoke Drainage Basin, a northern basin. In the northeastern U.S, others (Sadri et al. 2016, Dudley et al. 2020, Botero-Acosta et al. 2022) have found streamflows to be increasing, but streamflows appear to be decreasing in southeastern portion of the U.S. (Stephens and Bledsoe 2019, Paul et al. 2019, Dudley et al. 2020). The increased flow in the Roanoke Drainage Basin of our study was likely consistent with the observed patterns of streamflows in the adjacent northeastern U.S. (Ficklin et al. 2018, Dudley et al. 2019).

**Causative factors linked to streamflow patterns**

Several studies exploring streamflow trends report increases coinciding with a change in precipitation (Tomer and Schilling 2009, Patterson et al. 2012, Rodgers et al. 20201). McCabe and Wolock (2002) and Rodgers et al. (2020) suggest that increased precipitation can mitigate decreases in streamflows from increased temperatures, evapotranspiration and anthropogenic water use. Precipitation is a strong driver of streamflow change globally [China watersheds (Zhang et al. 2011, Shi et al. 2022), the Amazon River Basin (Heerspink et al. 2020), across multiple countries (Wu et al. 2021, Zhang et al. 2022, Zhang et al. 2023)], in the U.S. (Dougherty et al. 2021, Sazib et al. 2020, Franzen et al. 2020) including parts of the southeastern U.S. (Botero-Acosta et al. 2020, Rogers et al. 2020). We found precipitation to be the strongest driver of regional streamflow changes. Precipitation in the western, northern and southern portions of our study area were increasing and conversely, precipitation in the central portions of our study area were decreasing over time, coinciding with observed patterns of streamflows in those areas. Precipitation changes in the U.S. have a spatial component with less precipitation in the southeast and more precipitation in northeastern U.S. from 1951–2015 (Bartels et al. 2020). In the northeastern U.S., both precipitation and streamflows are increasing (Berton et al. 2016, Dudley et al. 2016), largely the opposite of what we found across most of the southeastern U.S.

In addition to precipitation, drainage area was found associated with streamflow changes. We had hypothesized that larger drainage basins would show a larger magnitude of streamflow change and smaller drainage basins would show a smaller magnitude of streamflow change. Do et al. (2017) found that flows in small drainage areas tended to increase and conversely, flows in larger drainage areas tended to decrease, as we did. However, the connection between basin size and streamflow change in our study was fairly weak, and several factors associated with drainage area size could explain its effect on streamflow trends (Hansford et al. 2020).

**Alternative drivers of streamflow change**

Streamflows can be altered through many human activities and climate factors (Ahn and Merwade 2014, Paul et al. 2019), beyond the effects of precipitation. We found air temperatures and population were changing uniformly across the South Atlantic-Gulf Drainage. Air temperatures alter streamflows through evapotranspiration and soil moisture (Patterson et al. 2022, Zhang et al. 2023). We found increased temperature across the region for both maximums and minimums. This is consistent with historic records of increasing average annual temperatures (USGCPR 2017), longer summer heat waves (Smith et al. 2013), enhanced metropolitan heat island effects (Rizwan et al. 2008) and an increase in warm nights (Cater et al. 2018, Fall et al. 2021). This should lead to increased evapotranspiration rates, reduced surface waters (Konapala et al. 2020) and declines in groundwater (Codon et al. 2020). In addition, population increases often amplify groundwater withdrawals (de Graaf et al. 2019, Mohan et al. 2023), land use changes (Zheng et al. 2009, Vincent-Serrano et al., 2019; Silva et al., 2021), consumption (Lin et al. 2019) and reservoir storage volumes (Chai et al., 2019; Brogan et al., 2022). Sun et al. (2008) showed that population density correlated to a higher impact of human activities (i.e., domestic and thermoelectric water use) on streamflows in the southeastern U.S.

Groundwater is a major component of water resource management and environmental flow sustainability (de Graaf et al. 2019, Zipper et al., 2022, Mohan et al. 2023). Although we found declines in groundwater level, many basins had few groundwater wells, especially in the western portion of our study area. As such, groundwater levels associated with our streamflow records were not comprehensive. However, others have found declining groundwater level associated with water withdrawals, hydrogeologic characteristics and precipitation variability,

with declines being particularly evident in areas of heavy irrigation (Sutton et al. 2021, Zipper et al., 2022, Mohan et al. 2023). Groundwater declines ultimately effect streamflows through these mechanisms and is an important component of the water budget.

Overall changes in air temperatures, population growth and groundwater level were not associated with regional patterns of streamflow change. However, these factors undoubtedly influence streamflows, and all likely contributed to the general trend for decreasing streamflows across the southeastern U.S. Where precipitation was decreasing these other factors likely amplified streamflow declines, and where precipitation was increasing these factors likely muted streamflow declines (see also Rodgers et al. 2020). At smaller scales (catchments, reaches), temperature and anthropogenic factors may have a more obvious control over streamflows (Rodgers et al. 2020, Shi et al. 2022).

**Conclusions**

This study investigated long-term streamflow change in the South Atlantic-Gulf Drainage of the southeastern U.S. Understanding the patterns of streamflow change is particularly challenging due to uncertainty about local climate and interactions with anthropogenic drivers. Our results indicated that changes in streamflows are spatially variable, and complex given the interactions among hydrologic processes, climate and human influences. Precipitation appeared to be the dominant driver of streamflow change regionally, with the potential of increased floods in areas experiencing increased precipitation and streamflow, and increased droughts in areas experiencing decreased precipitation and streamflows. Undoubtedly, numerous factors influence patterns of streamflows, and it is prudent to consider all factors at a variety of spatial and temporal scales. Our findings compliment previous studies performed in the South Atlantic-Gulf

Drainage and contribute to a broader understanding of streamflow changes and the causative factors that influence them.

**ACKNOWLEDGEMENTS**

Author contributions: KAW conceptualized, designed, created visualizations, and analyzed and interpreted the data; and wrote the manuscript. DPB conceptualized, designed, interpreted data, and reviewed and edited the manuscript.

We are grateful for the manuscript improvements from anonymous reviewers. This work was supported by the Georgia Environmental Protection Division, Regional Water Plan SEED Grant [Contract Number: 761–200119], and in part by the U.S. Department of Agriculture Hatch Program.

**LITERATURE CITED**

Ahn, K-H., and V. Merwade. 2014. Quantifying the relative impact of climate and human activities on streamflow. Journal of Hydrology 515:257−266. https://doi.org/10.1016/j.jhydrol.2014.04.062

Akaike, H.1998. Information theory and an extension of the maximum likelihood principle. In Selected papers of Hirotugu Akaike. pp. 199-213. New York, NY: Springer New York.

Allawi, M. F., F. Binti Othman, H. A. Afan, A. N. Ahmed, M. S. Hossain, C. M. Fai, and A. El-Shafie. 2019. Reservoir evaporation prediction modeling based on artificial intelligence methods. Water 11:1226. https://doi.org/10.3390/w11061226

Aragaw, H. M., M. K. Goel, and S. K. Mishra. 2021. Hydrological responses to human-induced land use/land cover changes in the Gidabo River basin, Ethiopia. Hydrological Sciences Journal 66: 640-655. https://doi.org/10.1080/02626667.2021.1890328

Bartels, R. J., A. W. Black, and B. D. Keim. 2020. Trends in precipitation days in the United States. International Journal of Climatology 40:1038-1048. https://doi.org/10.1002/joc.6254

Berton, R., C. T. Driscoll, and D. G. Chandler. 2016. Changing climate increases discharge and attenuates its seasonal distribution in the northeastern United States. Journal of Hydrology Regional Studies 5:164-178. https://doi.org/10.1016/j.ejrh.2015.12.057

Bhaskar, A.S., K. G. Hopkins, B. K. Smith, T. A. Stephens, and A. J. Miller. 2020. Hydrologic signals and surprises in US streamflow records during urbanization. Water Resources Research 56. https://doi.org/10.1029/2019WR027039

Bierkens, M. F., and Y. Wada. 2019. Non-renewable groundwater use and groundwater depletion: a review. Environmental Research Letters. 14:063002. **https://doi.org/**10.1088/1748-9326/ab1a5f

Botero-Acosta, A., D. L. Ficklin, N. Ehsani, and , J. H. Knouft. 2022. Climate induced changes in streamflow and water temperature in basins across the Atlantic Coast of the United States: An opportunity for nature-based regional management. Journal of Hydrology: Regional Studies 44:101202. https://doi.org/10.1016/j.ejrh.2022.101202

Brauer, D., R. L. Baumhardt, D. Gitz, P. Gowda, and J. Mahan. (2015) Characterization of trends in reservoir storage, streamflow, and precipitation in the Canadian River watershed in New Mexico and Texas. Lake and Reservoir Management 31:64-79. http://doi.org/10.1080/10402381.2015.1006348

Brogan, C., R. Burgholzer, T. Keys, J. Kleiner, J. Shortridge, and D. Scott. 2022. The cumulative role of impoundments in streamflow alteration. Journal of the American Water Resources Association 58:119-133. https://doi.org/10.1111/1752-1688.12979

Carter, L., A. Terando, K. Dow, K. Hiers, K. E. Kunkel, A. Lascurain, D. Marcy, M. Osland, and P. Schramm. 2018: Southeast. In Impacts, Risks, and Adaptation in the United States: Fourth National Climate Assessment, Volume II [Reidmiller, D.R., C.W. Avery, D.R. Easterling, K.E. Kunkel, K.L.M. Lewis, T.K. Maycock, and B.C. Stewart (eds.)]. U.S. Global Change Research Program, Washington, DC, USA, pp. 743–808. doi: 10.7930/NCA4.2018.CH19

Chai, Y., Y. Li, Y. Yang, B. Zhu, S. Li, C. Xu, and C. Liu. 2019. Influence of climate variability and reservoir operation on streamflow in the Yangtze River. Scientific Reports 9: 5060. https://doi.org/10.1038/s41598-019-41583-6

Condon, L.E., A.L. Atchley, and R. M. Maxwell. 2020. Evapotranspiration depletes groundwater under warming over the contiguous United States. Nature communications 11:873. https://doi.org/10.1038/s41467-020-14688-0

Cooley, S.W., J. C. Ryan, and L. C. Smith. 2021. Human alteration of global surface water storage variability. Nature 591:78–81. https://doi.org/10.1038/s41586-021-03262-3

Dai, A., T. Qian, K. E. Trenberth, and J. D.Milliman. 2009. Changes in continental freshwater discharge from 1948 to 2004. Journal of climate 22:2773-2792. https://doi.org/10.1175/2008JCLI2592.1

Dai, A. 2013. Increasing drought under global warming in observations and models. Nature Climate Change 3:52-58. https://doi.org/10.1038/nclimate1633

De Cicco L.A., D. Lorenz, R. M. Hirsch, W. Watkins, and M. Johnson. 2022. dataRetrieval: R packages for discovering and retrieving water data available from U.S. federal hydrologic web. http://doi.org/10.5066/P9X4L3GE, https://code.usgs.gov/water/dataRetrieval.

de Graaf, I.E., T. Gleeson, L. P. H. Van Beek, E. H. Sutanudjaja, and M. F. Bierkens. 2019. Environmental flow limits to global groundwater pumping. Nature 574:90-94. https://doi.org/10.1038/s41586-019-1594-4

Do, H. X., S. Westra, and M. Leonard. 2017. A global-scale investigation of trends in annual maximum streamflow. Journal of Hydrology 552:28-43. https://doi.org/10.1016/j.jhydrol.2017.06.015

Dougherty, E., R. Morrison, and K. Rasmussen. 2021. High-resolution flood precipitation and streamflow relationships in two US river basins. Meteorological Applications 28:e1979. https://doi.org/10.1002/met.1979

Dudley, R. W., R. M. Hirsch, S. A. Archfield, A. G. Blum, and B. Renard. 2020. Low streamflow trends at human-impacted and reference basins in the United States. Journal of Hydrology 580:124254. https://doi.org/10.1016/j.jhydrol.2019.124254

Engström, J. and P. Waylen. 2017. The changing hydroclimatology of Southeastern US. Journal of Hydrology 548:16-23. https://doi.org/10.1016/j.jhydrol.2017.02.039

Fall, S., Coulibaly, K.M., Quansah, J.E., El Afandi, G. and Ankumah, R., 2021. Observed Daily Temperature Variability and Extremes over Southeastern USA (1978–2017). Climate 2021, 9, 110. https://doi.org/10.3390/cli9070110

Ficklin, D.L., J. T. Abatzoglou, S. M. Robeson, S. E. Null, and J. H. Knouft. 2018. Natural and managed watersheds show similar responses to recent climate change. Proceedings of the National Academy of Sciences 115:8553-8557. http://doi.org/10.1073/pnas.1801026115

Franzen, S.E., M. A. Farahani, and A. E. Goodwell. 2020. Information flows: Characterizing precipitation-streamflow dependencies in the Colorado Headwaters with an information theory approach. Water Resources Research 56:e2019WR026133. https://doi.org/10.1029/2019WR026133

Gaines, M. D., M. G. Tulbure, and V. Perin. 2022. Effects of climate and anthropogenic drivers on surface water area in the southeastern United States. Water Resources Research 58:e2021WR031484. https://doi.org/10.1029/2021WR031484

Hansford, M. R., P. Plink-Björklund, and E. R. Jones. 2020. Global quantitative analyses of river discharge variability and hydrograph shape with respect to climate types. Earth-science reviews 200:102977. https://doi.org/10.1016/j.earscirev.2019.102977

Heerspink, B. P., A. D. Kendall, M. T. Coe, and D. W. Hyndman. 2020. Trends in streamflow, evapotranspiration, and groundwater storage across the Amazon Basin linked to changing

precipitation and land cover. Journal of Hydrology: Regional Studies 32:100755. https://doi.org/10.1016/j.ejrh.2020.100755

Ingram, K. T., K. Dow, L. Carter, J. Anderson, and E. K. Sommer. 2013.Climate of the Southeast United States: variability, change, impacts, and vulnerability. Washington, DC: Island Press/Center for Resource Economics. ISBN: 978-1-59726-427-3

Kam, J., and J. Sheffield. 2016. Changes in the low flow regime over the eastern United States (1962–2011): variability, trends, and attributions. Climatic Change 135:639-653. https://doi.org/10.1007/s10584-015-1574-0

Kayitesi, N. M., A. C. Guzha, and G. Mariethoz. 2022. Impacts of land use land cover change and climate change on river hydro-morphology-a review of research studies in tropical regions. Journal of Hydrology 615:128702. https://doi.org/10.1016/j.jhydrol.2022.128702

Khan, M., V. Dahal, H. Jeong, M. Markus, and R. Bhattarai. 2021. Relative Contribution of Climate Change and Anthropogenic Activities to Streamflow Alterations in Illinois. Water 13:3226. https://doi.org/10.3390/w13223226

Konapala, G., A. K. Mishra, Y. Wada, and M. E. Mann. 2020. Climate change will affect global water availability through compounding changes in seasonal precipitation and evaporation. Nature Communications 11:3044. https://doi.org/10.1038/s41467-020-16757-w

Lin, C.C., K. Y. Liou, M. Lee, and P. T. Chiueh. 2019. Impacts of urban water consumption under climate change: an adaptation measure of rainwater harvesting system. Journal of Hydrology 572:160-168. https://doi.org/10.1016/j.jhydrol.2019.02.032

Massari, C., F. Avanzi, G. Bruno, S. Gabellani, D. Penna, and S. Camici. 2022. Evaporation enhancement drives the European water-budget deficit during multi-year droughts.

Hydrology and Earth System Sciences 26:1527-1543. https://doi.org/10.5194/hess-26-1527-2022

McCabe, G. J. and D. M. Wolock. 2002. A step increase in streamflow in the conterminous United States. Geophysical Research Letters 29:38-1. https://doi.org/10.1029/2002GL015999

Menne, M. J., I. Durre, B. Korzeniewski, S. McNeill, K. Thomas, X. Yin, S. Anthony, R. Ray, R. S. Vose, B. E. Gleason, and T. G. Houston. 2012a. Global Historical Climatology Network - Daily (GHCN-Daily), Version 3. NOAA National Climatic Data Center. https://doi.org/10.7289/V5D21VHZ [2022].

Menne, M. J., I. Durre, R. S. Vose, B. E. Gleason, and T. G. Houston. 2012b. An overview of the Global Historical Climatology Network-Daily Database. Journal of Atmospheric and Ocean Technology 29:897-910. https://doi.org/10.1175/JTECH-D-11-00103.1

Milly, P. C., K. A. Dunne, and A. V. Vecchia. 2005. Global pattern of trends in streamflow and water availability in a changing climate. Nature 438:347-350. http://doi.org/10.1038/nature04312

Mohan, C., T. Gleeson, T. Forstner, J. S. Famiglietti, and I. de Graaf. 2023. Quantifying groundwater's contribution to regional environmental-flows in diverse hydrologic landscapes. Water Resources Research 59:e2022WR033153. https://doi.org/10.1029/2022WR033153

Omernik, J. M. 1987. Ecoregions of the conterminous United States. Map (scale 1:7,500,000). Annals of the Association of American Geographers 77:118-125. https://doi.org/10.1007/s00267-014-0364-1

Paul, M. J., R. Coffey, J. Stamp, and T. Johnson. 2019. A review of water quality responses to air temperature and precipitation changes 1: Flow, water temperature, saltwater intrusion. Journal of American Water Resource Association 55:824-843. https://doi.org/10.1111/1752-1688.12710

Patterson, L. A., B. Lutz, and M. W. Doyle. 2013. Climate and direct human contributions to changes in mean annual streamflow in the South Atlantic, USA. Water Resource Research 49:7278-7291. https://doi.org/10.1002/2013WR014618

Patterson, N. K., B. A. Lane, S. Sandoval- Solis, G. G. Persad, and J. P. Ortiz-Partida. 2022. Projected effects of temperature and precipitation variability change on streamflow patterns using a functional flows approach. Earth's Future 10:e2021EF002631. https://doi. org/10.1029/2021EF002631

Posit team. 2024. RStudio: Integrated Development Environment for R. Posit Software, PBC, Boston, MA. http://www.posit.co/

QGIS (Quantum Geographic Information System). Development Team. 2009. QGIS Geographic Information System. Open Source Geospatial Foundation. 30 Jun 2024. http://qgis.org

R Core Team. 2024. R: A Language and Environment for Statistical Computing. R Foundation for Statistical Computing, Vienna, Austria. https://www.R-project.org/

Rice, J. S., R. E. Emanuel, J. M. Vose, and S. A. C. Nelson. 2015. Continental U.S. streamflow trends from 1940 to 2009 and their relationships with watershed spatial characteristics. Water Resource Research 51:6262–6275. http://doi.org/10.1002/2014WR016367

Rizwan, A. M., L. Y. Dennis, and L. I. U. Chunho. 2008. A review on the generation, determination and mitigation of Urban Heat Island. Journal of Environmental Sciences 20:120-128. https://doi.org/10.1016/S1001-0742(08)60019-4

RStudio Team. 2020. RStudio: Integrated Development for R. RStudio, PBC, Boston, MA. http://www.rstudio.com/.

Rodgers, K., V. Roland, A. Hoos, E. Crowley-Ornelas, and R. Knight. 2020. An analysis of streamflow trends in the southern and southeastern US from 1950–2015. Water 12:3345. https://doi.org/10.3390/w12123345

Sazib, N., J. Bolten, and I. Mladenova. 2020. Exploring spatiotemporal relations between soil moisture, precipitation, and streamflow for a large set of watersheds using Google Earth Engine. Water 12:1371. https://doi.org/10.3390/w12051371

Sadri, S., J. Kam, and J. Sheffield. 2016. Nonstationarity of low flows and their timing in the eastern United States. Hydrology and Earth System Sciences 20:633-649. https://doi.org/10.5194/hess-20-633-2016

Shi, R., T. Wang, D. Yang, and Y. Yang. 2022. Streamflow decline threatens water security in the upper Yangtze river. Journal of Hydrology 606:127448. https://doi.org/10.1016/j.jhydrol.2022.127448

Silva, A. L. D., S. A. D Souza, O. Coelho Filho, L. Eloy, Y. B. Salmona, and C. J. S. Passos. 2021. Water appropriation on the agricultural frontier in western Bahia and its contribution to streamflow reduction: revisiting the debate in the Brazilian Cerrado. Water 13:1054. https://doi.org/10.3390/w13081054

Smith, T.T., B. F. Zaitchik, and J. M. Gohlke. 2013. Heat waves in the United States: definitions, patterns and trends. Climatic change 118:811-825. https://doi.org/10.1007/s10584-012-0659-2

Stephens, T.A., and B. P. Bledsoe. 2020. Low-flow trends at Southeast United States streamflow gauges. Journal of Water Resource Planning Management 146:04020032. https://doi.org/10.1061/(ASCE)WR.1943-5452.0001212

Sun, G., S. G., McNulty, J. A. Moore Myers, and E. C. Cohen. 2008. Impacts of multiple stresses on water demand and supply across the Southeastern United States 1. Journal of the American Water Resources Association 44:1441-1457. https://doi.org/10.1111/j.1752-1688.2008.00250.x

Sutton, C., S. Kumar, M. K. Lee, and E. Davis. 2021. Human imprint of water withdrawals in the wet environment: A case study of declining groundwater in Georgia, USA. Journal of Hydrology: Regional Studies 35:100813. https://doi.org/10.1016/j.ejrh.2021.100813

Trenberth, K.E. 2011. Changes in precipitation with climate change. Climate Research 47:123-138. https://doi.org/10.3354/cr00953

U.S. Census Bureau. 2007. Census U.S. decennial county population data, 1900-1990. *Accessed 1 April 2024.* https://www.nber.org/research/data/census-us-decennial-county-population-data-1900-1990

U.S. Census Bureau. 2021. (CO-2000-8) County Population Estimates and Demographic Components of Population Change: Annual Time Series, April 1, 1990 Census to July 1, 2000 Estimate. Accessed 1 April 2024. Retrieved from https://www.census.gov/data/tables/time-series/demo/popest/estimates-and-change-1990-2000.html

U.S. Census Bureau. 2023. County Population Totals 2010 - 2019: Annual estimates of the Resident Population for Counties: April 1, 2010 to July 1, 2019. Accessed 1 April *2024.* Retrieved from https://www.census.gov/data/datasets/time-

series/demo/popest/2010s-counties-total.html.*U.S. Geologic Survey (USGS), 2013.* Boundary Descriptions and Names of Regions, Subregions, Accounting Units and Cataloging Units from the 1987 USGS Water-Supply Paper 2294. Retrieved January 17, 2024. https://water.usgs.gov/GIS/wbd_huc8.pdf

USDA (United States Forest Service, Department of Agriculture). 2024. M221 Central Appalachian Broadleaf Forest. Department of Agriculture. Accessed 28 Jun 2024. https://www.fs.usda.gov/land/ecosysmgmt/colorimagemap/images/m221.html#:~:text=The%20relief%20is%20high%20(up,Pisgah%20National%20Forest%2C%20North%20Carolina.

U.S. EPA (United States Environmental Protection Agency). 2024. Ecoregions of North America. https://gaftp.epa.gov/EPADataCommons/ORD/Ecoregions/cec_na/NA_LEVEL_II.pdf

USGCRP (United States Global Change Research Program). 2017. Climate Science Special Report: Fourth National Climate Assessment (Volume I), edited by D.J. Wuebbles, D.W. Fahey, K.A. Hibbard, D.J. Dokken, B.C. Stewart, and T.K. Maycock. Washington,D.C. https://doi.org/10.7930/j0j964j6

USGS (United States Geological Survey). 2024. Science in your watershed. U.S. Department of the Interior. Retrieved 31 Jun 2024. https://water.usgs.gov/wsc/

USGS (United States Geological Survey). 2016. National Water Information System data available on the World Wide Web (USGS Water Data for the Nation). http://waterdata.usgs.gov/nwis/

USGS NGTOC (United States Geological Survey, National Geospatial Technical Operations Center). 2016. USGS National Watershed Boundary Dataset (WBD) Downloadable Data

Collection - National Geospatial Data Asset (NGDA) Watershed Boundary Dataset (WBD): U.S. Geological Survey.

USGS (U.S. Geological Survey). 2023. 1 meter Digital Elevation Models (DEMs) - USGS National Map 3DEP Downloadable Data Collection: U.S. Geological Survey.

US REAP (United States Regional Economic Analysis Project). 2024. Southeast vs. United States comparative trend analysis population growth and change, 1958-2023. Regional income and product division of the Bureau of Economic Analysis, U.S. Department of Commerce. 27 Jun 2024. https://united-states.reaproject.org/analysis/comparative-trends-analysis/population/tools/950000/0/#:~:text=During%20this%2066%2Dyear%20period,of%2050%2C242%2C050%2C%20or%20134.21%25.

Van Vliet, M. T., W. H. Franssen, J. R. Yearsley, F. Ludwig, I. Haddeland, D. P. Lettenmaier, and P. Kabat. 2013. Global river discharge and water temperature under climate change. Global Environmental Change 23:450-464. https://doi.org/10.1016/j.gloenvcha.2012.11.002

Vicente-Serrano, S.M., M. Peña-Gallardo, J. Hannaford, C. Murphy, J. Lorenzo-Lacruz, F. Dominguez-Castro, J. I. López-Moreno, S. Beguería, I. Noguera, S. Harrigan, and J. P. Vidal. 2019. Climate, irrigation, and land cover change explain streamflow trends in countries bordering the northeast Atlantic. Geophysical Research Letters 46:10821-10833. https://doi.org/10.1029/2019GL084084

Wang, D., and M. Hejazi. 2011. Quantifying the relative contribution of the climate and direct human impacts on mean annual streamflow in the contiguous United States. Water Resources Research 47:W00J12. https://doi.org/10.1029/2010WR010283

Wickham, H. 2016. Ggplot2: Elegant Graphics for Data Analysis. Springer-Verlag New York, 2016.

Wu, J., X. Chen, X. Yuan, H. Yao, Y. Zhao, and A. AghaKouchak. 2021. The interactions between hydrological drought evolution and precipitation-streamflow relationship. Journal of Hydrology 597:126210. https://doi.org/10.1016/j.jhydrol.2021.126210

Xue, L., F. Yang, C. Yang, X. Chen, L. Zhang, Y. Chi, and G. Yang. 2017. Identification of potential impacts of climate change and anthropogenic activities on streamflow alterations in the Tarim River Basin, China. Scientific Reports 7:8254. DOI:10.1038/s41598-017-09215-z

Yang, D., Y. Yang, and J. Xia, 2021. Hydrological cycle and water resources in a changing world: A review. Geography and Sustainability 2:115-122. https://doi.org/10.1016/j.geosus.2021.05.003

Zhang, Z., X. Chen, C. Y. Xu, L. Yuan, B. Yong, and S. Yan. 2011. Evaluating the non-stationary relationship between precipitation and streamflow in nine major basins of China during the past 50 years. Journal of Hydrology, 409(1-2), pp.81-93.

Zhang, Y., A. Viglione, and G. Blöschl. 2022. Temporal scaling of streamflow elasticity to precipitation: a global analysis. Water Resources Research 58:e2021WR030601.

Zhang, Y., H. Zheng, X. Zhang, L. R. Leung, C. Liu, C. Zheng, Y. Guo, F. H. Chiew, D. Post, D. Kong, and H. E. Beck. 2023. Future global streamflow declines are probably more severe than previously estimated. Nature Water 1:261-271 https://doi.org/10.1038/s44221-023-00030-7

Zhao, G., Y. Li, L. Zhou, and H. Gao. 2022. Evaporative water loss of 1.42 million global lakes. Nature Communications 13:3686. https://doi.org/10.1038/s41467-022-31125-6

Zheng, H. L. Zhang, R. Zhu, C. Liu, Y. Sato, and Y. Fukushima. 2009. Responses of streamflow to climate and land surface change in the headwaters of the Yellow River Basin. Water Resources Research 45:W00A19. https://doi.org/10.1029/2007WR006665

Zipper, S.C., W. H. Farmer, A. Brookfield, H. Ajami, H. W. Reeves, C. Wardropper, J. C. Hammond, T. Gleeson, and J. M. Deines. 2022. Quantifying streamflow depletion from groundwater pumping: a practical review of past and emerging approaches for water management. Journal of the American Water Resource Association 58:289-312. https://doi.org/10.1111/1752-1688.129

Table 5.1: Hydrologic unit codes (HUC), number of samples (n) and average ± standard error (SE) for Mann-Kendall streamflow slope (τ), Mann-Kendall total precipitation slope (τ) and drainage area ($km^2$) for individual basins.

| Basins | HUC | Streamflow | | Total precp | | Drainage area | |
|---|---|---|---|---|---|---|---|
| | | n | τ | n | τ | n | average |
| Alabama | 031502 | 5 | –0.01 ± 0.03 | 11 | –0.00 ± 0.04 | 5 | 9,517 ± 7,425 |
| Albemarle-Chowan | 030102 | 11 | –0.09 ± 0.01 | 14 | 0.05 ± 0.04 | 11 | 1,175 ± 316 |
| Altamaha | 030701 | 11 | –0.15 ± 0.02 | 13 | –0.09 ± 0.03 | 11 | 9,869 ± 3,672 |
| Apalachicola | 031300 | 26 | –0.10 ± 0.02 | 32 | –0.08 ± 0.02 | 26 | 8,670 ± 3,772 |
| Aucilla-Waccasassa | 031101 | 4 | –0.08 ± 0.02 | 4 | –0.07 ± 0.04 | 4 | 1,134 ± 380 |
| Black Warrior-Tombigbee | 031601 | 14 | 0.01 ± 0.02 | 34 | 0.04 ± 0.03 | 14 | 2,771 ± 833 |
| Cape Fear | 030300 | 14 | –0.06 ± 0.03 | 19 | –0.01 ± 0.03 | 14 | 1,611 ± 654 |
| Choctawhatchee | 031402 | 4 | –0.05 ± 0.01 | 7 | –0.02 ± 0.05 | 4 | 8,981 ± 4,367 |
| Coosa-Tallapoosa | 031501 | 19 | –0.03 ± 0.02 | 24 | 0.03 ± 0.03 | 19 | 2,341 ± 605 |
| East Florida Coastal | 030802 | 5 | 0.00 ± 0.10 | 7 | 0.05 ± 0.04 | 5 | 230 ± 57 |
| Escambia | 031403 | 4 | –0.06 ± 0.02 | 8 | 0.03 ± 0.03 | 4 | 1,696 ± 732 |
| Florida Panhandle Coastal | 031401 | 6 | 0.00 ± 0.01 | 8 | –0.01 ± 0.05 | 6 | 1,198 ± 372 |
| Kissimmee | 030901 | 12 | 0.26 ± 0.04 | 7 | 0.03 ± 0.08 | 12 | 529 ± 140 |
| Lower Pee Dee | 030402 | 11 | –0.19 ± 0.03 | 23 | –0.05 ± 0.02 | 11 | 5,709 ± 2,281 |
| Mobile Bay-Tombigbee | 031602 | 5 | 0.04 ± 0.02 | 8 | 0.03 ± 0.05 | 5 | 10,032 ± 9,420 |
| Neuse | 030202 | 13 | –0.05 ± 0.01 | 15 | 0.07 ± 0.03 | 13 | 1,784 ± 639 |
| Ochlockonee | 031200 | 5 | –0.13 ± 0.01 | 2 | –0.20 ± 0.02 | 5 | 3,004 ± 1,287 |

| | | | | | | | |
|---|---|---|---|---|---|---|---|
| Ogeechee | 030602 | 2 | –0.20 ± 0.04 | 6 | –0.13 ± 0.05 | 2 | 6,864 ± 0 |
| Onslow Bay | 030203 | 1 | –0.05 ± NA | – | – | 1 | 236 ± NA |
| Pamlico | 030201 | 6 | –0.10 ± 0.05 | 10 | –0.01 ± 0.04 | 6 | 1,573 ± 832 |
| Pascagoula | 031700 | 17 | 0.05 ± 0.01 | 11 | 0.06 ± 0.02 | 17 | 4,745 ± 1,723 |
| Peace | 031001 | 12 | 0.04 ± 0.03 | 4 | 0.06 ± 0.07 | 12 | 1,556 ± 444 |
| Pearl | 031800 | 8 | 0.04 ± 0.02 | 12 | 0.03 ± 0.03 | 8 | 9,509 ± 3,511 |
| Roanoke | 030101 | 29 | 0.05 ± 0.01 | 28 | 0.11 ± 0.01 | 29 | 2,022 ± 796 |
| Santee | 030601 | 30 | –0.13 ± 0.03 | 39 | –0.16 ± 0.02 | 5 | 3,634 ± 1,449 |
| Savannah | 030502 | 9 | –0.17 ± 0.03 | 23 | –0.12 ± 0.02 | 30 | 8,323 ± 3,552 |
| S. Edisto-SC Coastal | 030501 | 5 | –0.29 ± 0.02 | 14 | –0.10 ± 0.03 | 9 | 2,423 ± 1,190 |
| Southern Florida | 030902 | 11 | 0.19 ± 0.04 | 19 | –0.02 ± 0.03 | 1 | 0.00 ± NA |
| St. Johns | 030702 | 16 | –0.05 ± 0.04 | 7 | –0.03 ± 0.05 | 16 | 2,530 ± 868 |
| St. Marys-Satilla | 030801 | 5 | –0.14 ± 0.01 | 11 | –0.12 ± 0.02 | 5 | 3,146 ± 1,116 |
| Suwanee | 031102 | 10 | –0.16 ± 0.01 | 13 | –0.10 ± 0.02 | 10 | 13,455 ± 4,658 |
| Tampa Bay | 031002 | 33 | –0.07 ± 0.03 | 15 | 0.03 ± 0.03 | 33 | 1,461 ± 384 |
| Upper Pee Dee | 030401 | 13 | –0.04 ± 0.01 | 15 | –0.06 ± 0.04 | 13 | 1,541 ± 531 |

Table 5.2: Regression results including degrees of freedom (df), F-statistic, p-value, $R^2$ and Akaike information criterion (AIC) for causative factors including average Mann-Kendall total precipitation slope (τ), drainage area ($\sqrt{km^2}$), population slope (τ), elevation (m above sea level), temperature minimum slope (τ), temperature maximum slope (τ), ecoregion and groundwater level slope (τ). Elevation was log transformed and drainage area was square root transformed prior to analysis to improve linearity.

| | df | F-statistic | p-value | $R^2$ | AIC |
|---|---|---|---|---|---|
| Total precipitation | 1, 30 | 20.45 | < 0.01 | 0.39 | 61.72 |
| Drainage area | 1, 31 | 5.64 | 0.02 | 0.13 | 50.79 |
| Population | 1, 31 | 2.30 | 0.14 | 0.04 | 50.12 |
| Elevation | 1, 31 | 0.70 | 0.41 | < 0.01 | 47.90 |
| Temperature minimum | 1, 30 | 0.60 | 0.45 | 0.01 | 45.72 |
| Temperature maximum | 1, 30 | 0.01 | 0.93 | 0.03 | 45.10 |
| Ecoregion | 5, 27 | 0.22 | 0.95 | 0.04 | 37.46 |
| Groundwater | 1, 24 | 1.41 | 0.25 | 0.02 | 32.97 |

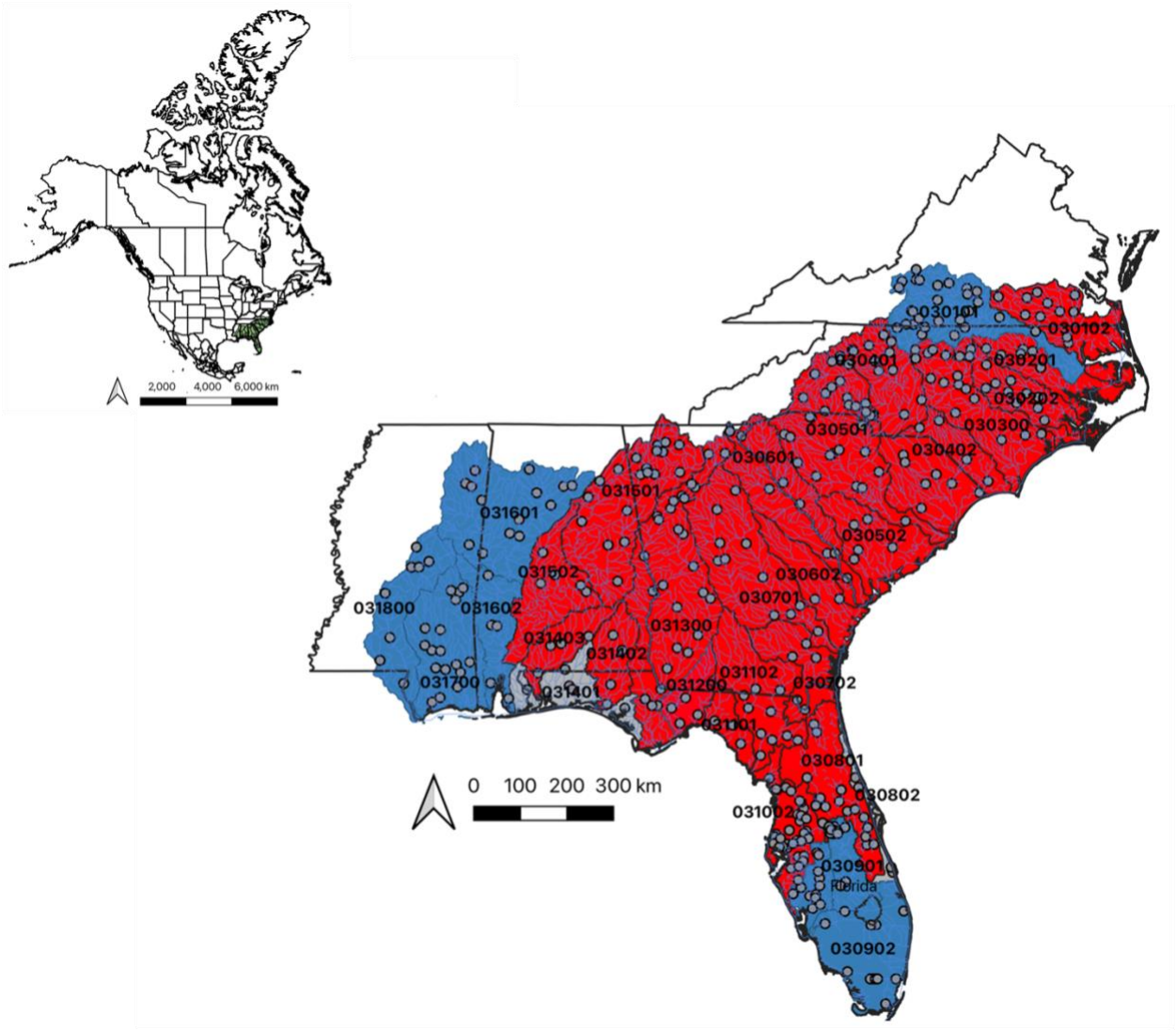


Figure 5.1: Streamflow ($m^3/s$, n = 377) sites (50+ years) for the 33 drainage basins in the South Atlantic-Gulf Drainage (HUC-03) indicated by gray dots. Average decreasing slope (– τ) for individual basins are indicated by red, no change in slope (τ =0.00) are indicated by gray and increasing slope (+ τ) are indicated by blue. Basin numbers correspond to 6-digit hydrologic unit codes (HUCs) assigned by the USGS.

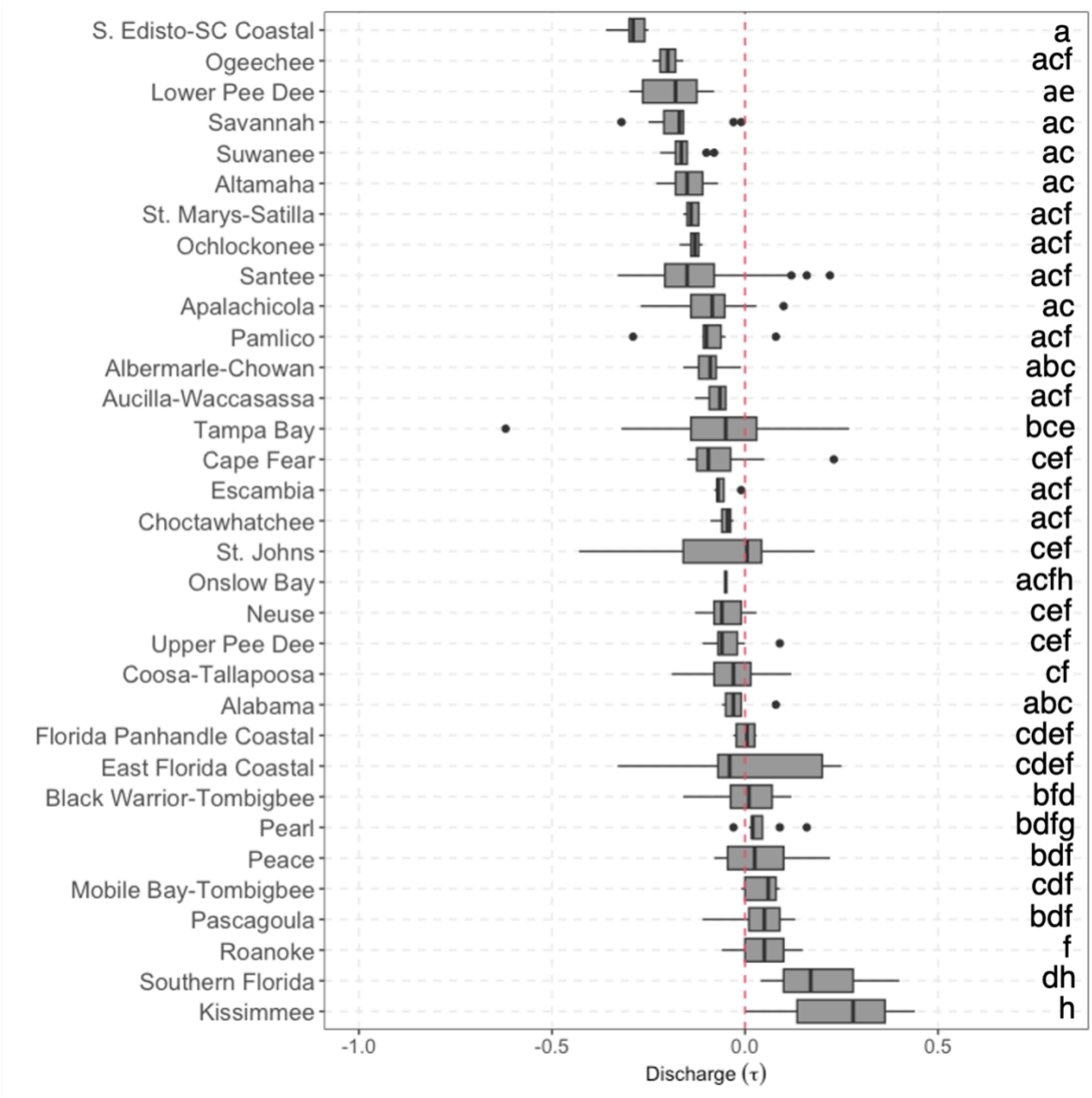


Figure 5.2: Mann-Kendall discharge slope (τ) for drainage basins. Box and whisker plots indicate that the bottom and top of each box are the 25$^{th}$ and 75$^{th}$ percentiles and the line in the middle of each box is the median, whiskers extend above and below each box to 1.5 times the interquartile range, and observations beyond the whisker length are marked as outliers with an individual symbol. Regression analysis indicated a significant ($F_{32,343}$ =11.19, $p < 0.01$, $R^2$ =

0.47) difference among drainage basins, and Tukey-HSD tests were used to separate means (indicated by small letters on the right).

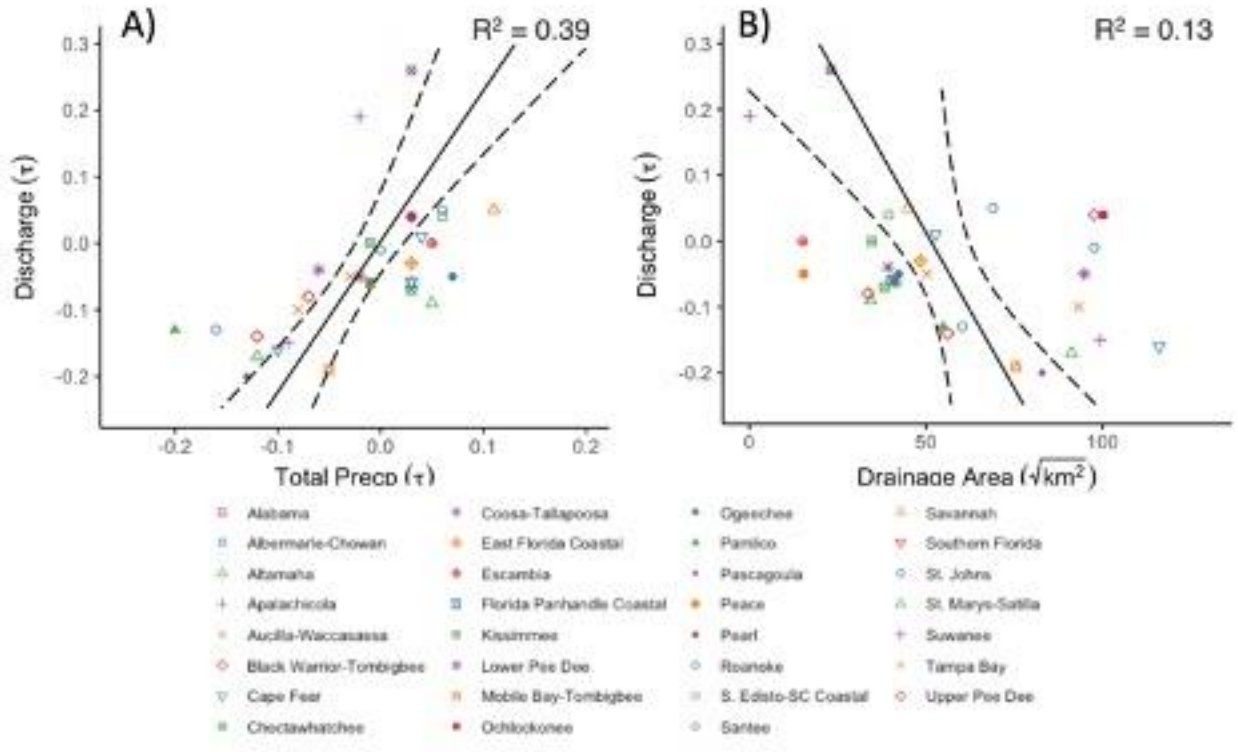


Figure 5.3: Average Mann-Kendall discharge slope (τ) over time (1957 – 2022) for drainage basins contrasted with average A.— Mann-Kendall total precipitation slope (τ) and B.— drainage area ($\sqrt{km^2}$) over time (1957–2022).

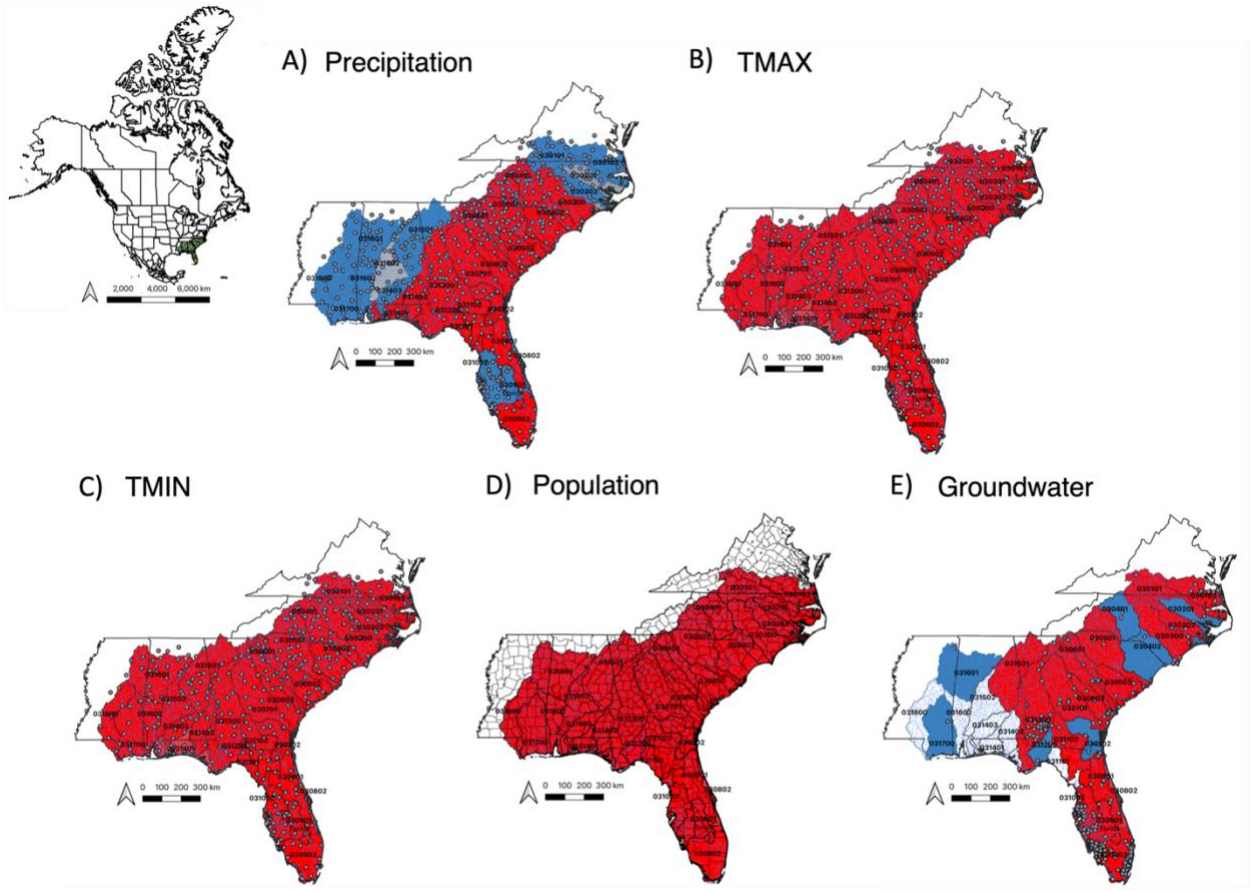


Figure 5.4: Average Mann-Kendall A.— total precipitation slope (τ), B.— temperature maximum (TMAX) slope (τ), C.— temperature minimum (TMIN) slope (τ), D.— population slope (τ) from 1950 – 2020, and E.— groundwater level slope (τ) from 1957 – 2022. Average decreasing slope (– τ) for basins are indicated by red, no changes in slope (τ = 0.00) are indicated by gray, no data are indicated by white and increasing slopes (+ τ) are indicated by blue

# CHAPTER 6

## CONCLUSIONS

Freshwater ecosystems, including streams, rivers and floodplains, are among the most threatened in the world, while providing critically important ecosystem services (Vári et al. 2021). Hydrological drought alters the timing and magnitude of flows, which ultimately effect the physical, physiochemical, biogeochemical, nutrient and biological function of lotic systems (Boulton and Lake 2008, Mosley et al. 2015). This effects ecosystem services including nutrient cycling, water purification, waste breakdown, hydropower generation, enhancing soil health, carbon storage, food supply, recreation, protection from floods and droughts and more (Dodds and Whiles 2019, Petsch et al. 2023). These services are estimated at 58 trillion/year in 2023 and thus, research is vital to understanding the changing future of water resources and sustaining them (DeWit 2021).

In the oxbow lakes of the Savannah River floodplain, we found that hydrological connectivity had less than expected control on the assemblage of aquatic invertebrates. Connectivity to the main river channel did not dramatically affect macroinvertebrates. However, a large flood did have clear impacts on the assemblage, but the invertebrate fauna quickly reestablished and appeared to be well adapted to seasonal hydrological variability. This study highlights that invertebrate assemblages in oxbow lakes are unique and resilient and that oxbow lakes are not simply ecotones between river channels and floodplains but are unique and valuable habitats.

In the main river channel of the Savannah River, we found that a drought period had not only a great effect on physicochemical conditions, but also on the dynamics of important nutrients and carbon. Drought conditions caused a shift in flow dynamics, which effected the concentration and flux of nutrients. Our results were somewhat unexpected. We found levels of pH, dissolved oxygen, and nitrate-nitrite were higher during drought, but total nitrogen and carbon levels were lower during drought. These complex changes could be attributed to volume reductions coupled with an increase in the percentage of total flow originating from groundwater as well as limnetic reservoir inputs, persistent point source pollution, reduced natural catchment inputs and/or reduced floodplain interactions.

In the ecoregions of Georgia, South Carolina and North Carolina, we found streamflows were broadly declining, but patterns of streamflow declines were spatially complex. The mountains showed unchanging streamflows that were associated with precipitation patterns. The Piedmont, Southeastern Plains and Coast showed drying trends that were associated with a combination of groundwater and climate factors. Streamflow changes will have implications for water quantity management, and water quantity will ultimately affect water quality, biota and human consumption.

In the 33 basins of the South Atlantic-Gulf Drainage, our results indicated that long-term streamflows were generally decreasing over time but changes were spatially variable. Streamflows were increasing in the western and southern portions of the region but decreasing in the larger central portion of the region. We found precipitation was related to streamflow changes and had a similar spatial patterns to those of streamflow. We also found that drainage area was related to streamflow changes, but to a lesser extent. Understanding the contributions of different drivers of streamflow changes provides insight for more effective management of water

resources. Drought and changes to water quantities will impact the physical, physicochemical, chemical and ultimately be disruptive to aquatic biological communities. Our results highlight the need for water resource management and policies to include framework addressing a future with a high level of streamflow variability, increased drought, and uncertainty regarding climate change predictions.

# LITERATURE CITED

Boulton, A.J. and Lake, P.S., 2008. Effects of drought on stream insects and its ecological consequences. In Aquatic insects: Challenges to populations (pp. 81-102). Wallingford UK: CABI.

DeWit, W., J. Lawson-Johns, F. Lottner, and J-C. Guinchard. 2021. High cost of cheap water: the true value of water and freshwater ecosystems to the people and planet. World Wildlife Fund for Nature. Gland Switzerland. Accessed from: https://wwfint.awsassets.panda.org/downloads/wwf-high-cost-of-cheap-water--final-lr-for-web-.pdf

Dodds, W. and Whiles, M. 2019. Freshwater Ecology: Concepts and Environmental Applications of Limnology. 3rd Edition Academic Press, Chapter 1 p.9. ISBN: 9780128132555

Mosley, L.M., 2015. Drought impacts on the water quality of freshwater systems; review and integration. Earth-Science Reviews, 140, pp.203-214.

Vári, Á., Podschun, S.A., Erős, T., Hein, T., Pataki, B., Iojă, I.C., Adamescu, C.M., Gerhardt, A., Gruber, T., Dedić, A. and Ćirić, M., 2022. Freshwater systems and ecosystem services: Challenges and chances for cross-fertilization of disciplines. Ambio, 51(1), pp.135-151.

# CHAPTER 2 APPENDCIES

## APPENDIX 2.A:

**Table 2.1:** Community description including relative abundance ($x_i$) and frequency (f) of taxa collected in high and low connectivity oxbow lakes for the 2015-2016 study period.

| | High | | Low | |
|---|---|---|---|---|
| Taxonomic Group | $x_i$ | f | $x_i$ | f |
| **Non-Insect** | | | | |
| Ancylidae | 0.01 | 0.21 | < 0.01 | 0.27 |
| Asellidae | 0.01 | 0.71 | 0.02 | 0.55 |
| Cambaridae | < 0.01 | 0.14 | < 0.01 | 0.09 |
| Corbicula fluminea | 0.00 | 0.14 | 0.01 | 0.36 |
| Crangonyx | 0.01 | 0.36 | 0.02 | 0.18 |
| Hirudinea | 0.03 | 0.50 | 0.01 | 0.36 |
| Hyalella | 0.05 | 0.64 | 0.05 | 1.00 |
| Lymnaeidae | < 0.01 | 0.07 | < 0.01 | 0.18 |
| Oligochaeta | 0.03 | 0.50 | 0.03 | 0.73 |
| Palaemonidae | 0.00 | 0.21 | 0.01 | 0.45 |
| Planorbidae | 0.01 | 0.71 | 0.01 | 0.73 |
| Trombidiformes | 0.02 | 0.50 | 0.04 | 0.73 |
| Turbellaria | < 0.01 | 0.21 | < 0.01 | 0.27 |
| **Ephemeroptera** | | | | |

| | | | | |
|---|---|---|---|---|
| *Baetis* | < 0.01 | 0.36 | < 0.01 | 0.18 |
| *Caenis* | 0.02 | 0.50 | 0.04 | 0.73 |
| *Ephemerella* | < 0.01 | 0.14 | < 0.01 | 0.18 |
| *Eurylophella* | < 0.01 | 0.07 | < 0.01 | 0.18 |
| *Heptagenia* | < 0.01 | 0.07 | < 0.01 | 0.18 |
| *Isonychia* | < 0.01 | 0.07 | — | — |
| *Leptophlebia* | < 0.01 | 0.07 | < 0.01 | 0.09 |
| *Stenonema* | < 0.01 | 0.14 | 0.01 | 0.18 |
| *Siphloplecton* | | | < 0.01 | 0.09 |
| **Odonata** | | | | |
| *Enallagma* | 0.02 | 0.57 | 0.04 | 0.73 |
| *Epitheca* | — | — | < 0.01 | 0.09 |
| *Hagenius* | < 0.01 | 0.07 | — | — |
| *Ischnura* | < 0.01 | 0.07 | < 0.01 | 0.09 |
| *Nasiaeschna* | < 0.01 | 0.29 | < 0.01 | 0.36 |
| *Perithemis* | — | — | < 0.01 | 0.18 |
| *Stylurus* | < 0.01 | 0.07 | — | — |
| **Plecoptera** | | | | |
| *Perlesta* | — | — | < 0.01 | 0.09 |
| **Hemiptera** | | | | |
| *Belostoma/Abedus* | < 0.01 | 0.07 | 0.01 | 0.36 |
| Corixidae | 0.01 | 0.57 | 0.01 | 0.45 |

| | | | | |
|---|---|---|---|---|
| *Hydrometra* | < 0.01 | 0.07 | < 0.01 | 0.09 |
| *Limnoporus* | < 0.01 | 0.14 | — | — |
| *Microvelia* | 0.01 | 0.36 | 0.01 | 0.55 |
| *Pelocoris* | < 0.01 | 0.07 | < 0.01 | 0.09 |
| *Rheumatobates* | 0.09 | 0.57 | 0.01 | 0.36 |
| *Trepobates* | 0.04 | 0.43 | 0.02 | 0.45 |
| **Lepidoptera** | | | | |
| Muscidae | — | — | < 0.01 | 0.09 |
| Noctuidae | — | — | < 0.01 | 0.09 |
| **Coleoptera** | | | | |
| *Coptotomus* | 0.00 | 0.21 | 0.00 | 0.09 |
| *Cyphon* | 0.02 | 0.57 | 0.03 | 0.73 |
| *Dineutus* | 0.00 | 0.07 | < 0.01 | 0.18 |
| *Dryopidae* | 0.00 | 0.07 | — | — |
| *Dubiraphia* | 0.01 | 0.36 | — | — |
| *Enochrus* | 0.00 | 0.07 | — | — |
| *Gyrinus* | < 0.01 | 0.14 | < 0.01 | 0.09 |
| *Helochares* | < 0.01 | 0.07 | < 0.01 | 0.27 |
| *Hydrovatus* | — | — | < 0.01 | 0.18 |
| *Laccophilus* | < 0.01 | 0.07 | — | — |
| *Neoporus* | < 0.01 | 0.43 | < 0.01 | 0.18 |
| *Peltodytes* | < 0.01 | 0.21 | < 0.01 | 0.09 |
| *Stenelmis* | < 0.01 | 0.07 | < 0.01 | 0.09 |

| | | | | |
|---|---|---|---|---|
| *Tropisternus* | < 0.01 | 0.14 | — | — |
| **Megaloptera** | | | | |
| *Chauliodes* | — | — | 0.01 | 0.09 |
| **Trichoptera** | | | | |
| *Ceraclea* | < 0.01 | 0.07 | — | — |
| *Cyrnellus* | 0.00 | 0.14 | — | — |
| *Nectopsyche* | — | — | < 0.01 | 0.09 |
| *Nyctiophylax* | 0.00 | 0.14 | — | — |
| *Oecetis* | 0.01 | 0.36 | 0.01 | 0.73 |
| *Orthotrichia* | 0.00 | 0.14 | 0.01 | 0.27 |
| *Oxythira* | 0.00 | 0.07 | < 0.01 | 0.09 |
| **Diptera** | | | | |
| **(Non-Chironomidae)** | | | | |
| *Aedes* | 0.01 | 0.14 | < 0.01 | 0.09 |
| *Anopheles* | < 0.01 | 0.07 | < 0.01 | 0.09 |
| *Atrichopogon* | < 0.01 | 0.43 | 0.01 | 0.55 |
| *Bezzia* | 0.02 | 0.86 | 0.03 | 0.91 |
| *Chaoborus* | < 0.01 | 0.14 | 0.00 | 0.09 |
| *Forcipomyia* | < 0.01 | 0.07 | < 0.01 | 0.18 |
| *Hemerodromia* | — | — | < 0.01 | 0.09 |
| Tabanidae | < 0.01 | 0.07 | — | — |
| **(Chironomidae)** | | | | |

| | | | | |
|---|---|---|---|---|
| *Ablabesmyia* | 0.01 | 0.43 | < 0.01 | 0.27 |
| *Clinotanypus* | — | — | 0.00 | 0.18 |
| *Corynoneura* | 0.02 | 0.21 | 0.00 | 0.09 |
| *Cricotopus/Orthocladius complex* | 0.01 | 0.21 | — | — |
| *Cryptochironomus* | 0.00 | 0.14 | — | — |
| *Cryptotendipes* | 0.00 | 0.07 | < 0.01 | 0.09 |
| *Dicrotendipes* | 0.03 | 0.79 | 0.03 | 0.73 |
| *Einfeldia* | — | — | 0.00 | 0.18 |
| *Endochironomus* | 0.11 | 1.00 | 0.09 | 1.00 |
| *Glyptotendipes* | 0.05 | 0.71 | 0.12 | 0.82 |
| *Hydrobaenus* | < 0.01 | 0.14 | — | — |
| *Labrundinia* | 0.02 | 0.50 | 0.01 | 0.45 |
| *Limonia* | < 0.01 | 0.07 | — | — |
| *Macropelopia* | < 0.01 | 0.07 | — | — |
| *Nanocladius* | 0.02 | 0.57 | 0.02 | 0.55 |
| *Parachironomus* | 0.01 | 0.36 | 0.01 | 0.73 |
| *Parakiefferiella* | < 0.01 | 0.14 | 0.00 | 0.09 |
| *Paramerina* | < 0.01 | 0.07 | — | — |
| *Polypedilum* | 0.17 | 0.93 | 0.10 | 1.00 |
| *Potthastia* | | | < 0.01 | 0.09 |
| *Procladius* | 0.01 | 0.14 | 0.02 | 0.55 |
| *Pseudochironomus* | < 0.01 | 0.14 | < 0.01 | 0.09 |
| *Rheocricotopus* | < 0.01 | 0.07 | | |
| *Rheotanytarsus* | | | < 0.01 | 0.09 |
| *Stenochironomus* | < 0.01 | 0.36 | < 0.01 | 0.09 |

| | | | | |
|---|---|---|---|---|
| *Tanypus* | — | — | < 0.01 | 0.18 |
| *Tanytarsus* | 0.01 | 0.29 | 0.01 | 0.45 |
| *Thienemanniella* | < 0.01 | 0.07 | — | — |
| *Zavreliella* | < 0.01 | 0.07 | 0.02 | 0.45 |

**Table 2.2**: Mean (± SE) water quality parameters in high connectivity (i.e., Miller and Whirligig) and low connectivity (i.e., Conyers and Possum Eddy) oxbow lakes before, during and after the flood stage. Water quality parameters include temperature (°C), conductivity (μS $cm^{-1}$), pH and dissolved oxygen (DO) in (mg $L^{-1}$ and % saturation)

| Connectivity | Flood Stage | Temperature (°C) | Conductivity (μS $cm^{-1}$) | pH | DO (mg $L^{-1}$) | DO (% saturation) |
|---|---|---|---|---|---|---|
| High | Before | 25.2 ± 3.1 | 91 ± 2.9 | 7.5 ± 0.3 | 7.9 ± 1.1 | 97.7 ± 19.4 |
| Low | | 25.9 ± 3.3 | 76.5 ± 3.7 | 9.0 ± 0.6 | 8.8 ± 1.3 | 108.9 ± 17.7 |
| High | During | 12.0 ± 1.3 | 70.8 ± 9.5 | 7.1 ± 0.1 | 9.4 ± 0.8 | 87.6 ± 7.0 |
| Low | | 12.2 ± 0.4 | 64.5 ± 0.5 | 7.3 ± 0.1 | 10.0 ± 0.0 | 93.8 ± 0.7 |
| High | After | 25.2 ± 1.8 | 96.3 ± 6.2 | 7.1 ± 0.3 | 9.0 ± 0.8 | 111.3 ± 11.6 |
| Low | | 28.0 ± 2.0 | 94.1± 3.6 | 7.3 ± 0.4 | 9.7 ± 1.1 | 125.0 ± 17.4 |

# CHAPTER 3 APPENDICES

**Appendix 3.A** Location of study sites on the Savannah River including the GPS coordinates, river kilometers (RKM) from the mouth and number of sampling events.

| Study Sites | GPS coordinates | RKM | Nearest USGS Station ID | No. Samples |
|---|---|---|---|---|
| Site 1 | 33.50277, -81.99067 | 325 | #02197000 & #02196690 | 50 |
| Site 2 | 33.38391, -81.93174 | 306 | #02197000 | 49 |
| Site 3 | 33.31791, -81.89093 | 288 | #02197000 | 46 |
| Site 4 | 33.11608, -81.69772 | 235 | #021973269 | 46 |
| Site 5 | 32.52474, -81.26239 | 98 | #021973269 | 36 |

**Appendix 3.B** Daily air temperature (°C) including number of samples (n), average maximum (max ± SE), average minimum (min ± SE) and coefficient of variation (CV) from Augusta Bushfield Airport GA, US (NOAA Stations #USW00003820) for the drought period (2006–2008) and the normal period (2016–2019). Air temperature minimum was found to be significantly ($F_{1,2554} = 21.86$, $p < 0.01$) lower during the drought period.

| | | n | Average | CV |
|---|---|---|---|---|
| Drought | Max | 1096 | 25.6 ± 0.8 | 30.3 |
| | Min | 943 | 10.8 ± 0.4 | 77.6 |
| Normal | Max | 1461 | 26.2 ± 0.2 | 30.3 |
| | Min | 1314 | 12.4 ± 0.2 | 68.4 |

**Appendix 3.C** Average water temperature (°C) including number of samples (n), average (± SE) and coefficient of variation (CV) from the Ogeechee River USGS station at GA 24, near Oliver (station #02202190).

| | n | Average | CV |
|---|---|---|---|
| Drought | 85 | 20.4 ± 0.8 | 36.8 |
| Normal | 114 | 19.3 ± 0.7 | 37.5 |

**Appendix 3.D** Averages (± standard error) of physicochemical metrics, and nutrient and carbon concentration (first row for each measure) and flux (second row for each measure) metrics for drought and normal hydrological conditions on the Savannah River for Sites 1, 2, 3, 4 and 5 (see Figure 3.1 and Appendix 3.A). Physicochemical metrics include temperature (ºC), DO (% and mg $L^{-1}$), conductivity (µS $cm^{-1}$) and pH. Nutrients include total nitrogen (TN), nitrate + nitrite ($NO_X$), ammonia ($NH_3$), total phosphorus (TP), total organic carbon (TOC) and dissolved organic carbon (DOC) concentration (mg $L^{-1}$) and flux (kg $day^{-1}$).

| | Site 1 | | Site 2 | | Site 3 | | Site 4 | | Site 5 | |
|---|---|---|---|---|---|---|---|---|---|---|
| | Drought | Normal | Drought | Normal | Drought | Normal | Drought | Normal | Drought | Normal |
| Temp (ºC) | 17.7 ± 1.0 | 18.5 ± 1.0 | 17.8 ± 1.1 | 19.1 ± 1.1 | 18.3 ± 1.2 | 20.2 ± 1.2 | 18.5 ± 1.2 | 20.2 ± 1.2 | 17.9 ± 1.8 | 21.0 ± 1.2 |
| DO (%) | 105.2 ± 0.9 | 101.9 ± 1.8 | 99.6 ± 1.4 | 92.8 ± 1.2 | 97.0 ± 1.9 | 98.8 ± 0.9 | 91.0 ± 1.6 | 88.7 ± 1.1 | 90.6 ± 1.5 | 89.7 ± 1.1 |
| DO (mg $L^{-1}$) | 10.1 ± 0.3 | 9.6 ± 0.2 | 9.6 ± 0.3 | 8.7 ± 0.3 | 9.3 ± 0.3 | 9.1 ± 0.3 | 8.7 ± 0.4 | 8.2 ± 0.3 | 8.8 ± 0.4 | 7.6 ± 0.3 |
| Conductivity (uS $cm^{-1}$) | 48.7 ± 0.7 | 50.7 ± 1.4 | 55.5 ± 1.6 | 55.0 ± 1.7 | 99.0 ± 4.2 | 79.5 ± 3.4 | 97.8 ± 3.7 | 78.7 ± 3.3 | 107.6 ± 3.5 | 85.6 ± 3.3 |
| pH | 6.8 ± 0.2 | 6.8 ± 0.1 | 7.0 ± 0.1 | 6.3 ± 0.1 | 6.9 ± 0.1 | 6.7 ± 0.1 | 6.8 ± 0.2 | 6.6 ± 0.1 | 7.0 ± 0.2 | 6.7 ± 0.1 |
| TN (mg-N $L^{-1}$) | 0.261 ± 0.04 | 0.332 ± 0.04 | 0.299 ± 0.07 | 0.428 ± 0.04 | 0.494 ± 0.11 | 0.766 ± 0.25 | 0.345 ± 0.04 | 0.498 ± 0.03 | 0.403 ± 0.06 | 0.466 ± 0.03 |
| TN (kg-N $day^{-1}$) | 5,077 ± 1,476 | 7,657 ± 1,663 | 5,820 ± 1,726 | 9,496 ± 1,714 | 7,543 ±1,542 | 11,623 ± 2,777 | 6,421 ± 1,176 | 9,592 ± 1,269 | 5,120 ± 935 | 10,611 ± 1,269 |
| $NO_x$ (mg-N $L^{-1}$) | 0.124 ± 0.01 | 0.149 ± 0.02 | 0.199 ±0.02 | 0.196 ± 0.02 | 0.248 ± 0.01 | 0.205 ± 0.02 | 0.279 ± 0.01 | 0.242 ± 0.02 | 0.325 ± 0.02 | 0.256 ± 0.02 |
| $NO_x$ (kg-N $day^{-1}$) | 2,210 ± 510 | 2,963 ± 494 | 3,181 ± 441 | 4,219 ± 801 | 3,859 ± 448 | 4,007 ± 1,001 | 4,607 ± 394 | 4,916 ± 841 | 3,997 ± 314 | 5,501 ± 841 |

| | | | | | | | | | | |
|---|---|---|---|---|---|---|---|---|---|---|
| $NH_3$ (mg-N $L^{-1}$) | 0.054 ± 0.01 | 0.021 ± 0.01 | 0.096 ± 0.02 | 0.049 ± 0.01 | 0.115 ± 0.02 | 0.082 ± 0.01 | 0.098 ± 0.02 | 0.184 ± 0.09 | 0.084 ± 0.02 | 0.089 ± 0.09 |
| $NH_3$ (kg-N $day^{-1}$) | 942 ± 348 | 379 ± 152 | 1,555 ± 370 | 842 ± 227 | 1,922 ± 606 | 1,441 ± 353 | 1,706 ± 385 | 2,720 ± 1,252 | 1078 ± 234 | 1,850 ± 1,252 |
| TP (mg-P $L^{-1}$) | 0.073 ± 0.06 | 0.023 ± 0.69 | 0.051 ± 0.01 | 0.036 ± 0.01 | 0.133 ± 0.01 | 0.114 ± 0.02 | 0.126 ± 0.01 | 0.146 ± 0.06 | 0.133 ± 0.01 | 0.098 ± 0.06 |
| TP (kg-P $day^{-1}$) | 1,250 ± 941 | 371 ±162 | 832 ± 151 | 555 ± 225 | 2,020 ± 236 | 1,752 ± 510 | 2,132 ± 279 | 1,898 ± 754 | 1639 ± 127 | 1,708 ± 754 |
| TOC (mg-C $L^{-1}$) | 2.4 ± 0.2 | 4.7 ± 0.7 | 2.6 ± 0.1 | 4.2 ± 0.5 | 4.0 ± 0.1 | 5.6 ± 0.6 | 3.7 ± 0.1 | 5.3 ± 0.4 | 3.9 ±0.2 | 6.7 ± 0.4 |
| TOC (kg-C $day^{-1}$) | 38,934 ± 6,339 | 102,344 ± 23,930 | 43,821 ± 6,972 | 98,646 ± 21,882 | 62,947 ± 7,539 | 105,344 ± 24,825 | 63,043 ± 6,090 | 112,957 ± 22,907 | 48,568 ± 4,186 | 159,436 ± 22,907 |
| DOC (mg-C $L^{-1}$) | 2.7 ± 0.1 | 4.5 ± 0.7 | 2.7 ± 0.1 | 3.9 ± 0.5 | 3.9 ± 0.1 | 4.9 ± 0.5 | 3.8 ± 0.1 | 5.0 ± 0.4 | 3.9 ± 0.2 | 6.1 ± 0.4 |
| DOC (kg-C $day^{-1}$) | 43,601 ± 7,682 | 106,580 ± 28,956 | 44,946 ± 6,888 | 92,507 ± 21,133 | 61,603 ± 7,429 | 99,081 ± 26,322 | 63,677 ± 6,277 | 105,915 ± 21,176 | 49,254 ± 4,171 | 140,030 ± 21,176 |

**Appendix 3.E** Coefficient of variation (CV) (%) of water temperature (ºC) for drought and normal hydrological conditions on the Savannah River for Sites 1, 2, 3, 4 and 5.

| Site 1 | | Site 2 | | Site 3 | | Site 4 | | Site 5 | |
|---|---|---|---|---|---|---|---|---|---|
| Drought | Normal | Drought | Normal | Drought | Normal | Drought | Normal | Drought | Normal |
| 69.9 | 72.1 | 68.5 | 80.4 | 74.1 | 103.9 | 53.3 | 73.8 | 17.7 | 50.7 |

# CHAPTER 4 APPENDICIES

**APPENDIX 4.A:**

**Appendix 4.A. Table 4.1:** Sites (n=189) for long-term discharge including state, river, location, GPS coordinates, USGS gage number, ecoregion, trend, total number of years and time span.

| State | River | Location | GPS coordinates | USGS gage | Ecoregion | Trend | # years | Time span |
|---|---|---|---|---|---|---|---|---|
| GA | Etowah River | Canton | 34.240194, -84.494528 | 02392000 | Mountain | Decreasing trend | 66 | 1957-2022 |
| GA | Coosawattee River | Ellijay | 34.675861, -84.506833 | 02380500 | Mountain | Decreasing trend | 60 | 1963-2022 |
| NC | French Broad River | Blantyre | 35.299167, -82.623889 | 03443000 | Mountain | Decreasing trend | 66 | 1957-2022 |
| NC | Yadkin River | Patterson | 35.990833, -81.558333 | 02111000 | Mountain | Decreasing trend | 66 | 1957-2022 |
| NC | Little Tennessee River | Needmore | 35.336389, -83.526944 | 03503000 | Mountain | Decreasing trend | 65 | 1957-1981, 1983-2022 |
| NC | Valley River | Tomotla | 35.138889, -83.980556 | 03550000 | Mountain | Decreasing trend | 66 | 1957-2022 |
| SC | Chattooga River | Clayton | 34.813889, -83.306111 | 02177000 | Mountain | Decreasing trend | 66 | 1957-2022 |
| GA | Etowah River | Rome | 34.232111, -85.116944 | 02395980 | Mountain | Decreasing trend | 66 | 1957-2022 |
| GA | Coosawattee River | Pine Chapel | 34.564167, -84.833056 | 02383500 | Mountain | Decreasing trend | 66 | 1957-2022 |
| GA | Oostanaula River | Rome | 34.298972, -85.138000 | 02388500 | Mountain | Decreasing trend | 66 | 1957-2022 |
| GA | Oostanaula River | Resaca | 34.577111, -84.941853 | 02387500 | Mountain | Decreasing trend | 66 | 1957-2022 |
| NC | West Fork Pigeon River | Hazelwood | 35.396111, -82.937500 | 03455500 | Mountain | No change | 66 | 1957-2022 |

| | | | | | | | | |
|---|---|---|---|---|---|---|---|---|
| NC | French Broad River | Marshall | 35.786389, -82.660833 | 03453500 | Mountain | No change | 66 | 1957-2022 |
| NC | New River | Galax | 36.647222, -80.979167 | 03164000 | Mountain | No change | 66 | 1957-2022 |
| NC | French Broad River | Rosman | 35.143333, -82.824722 | 03439000 | Mountain | No change | 66 | 1957-2022 |
| NC | Little Tennessee River | Prentiss | 35.150000, -83.379722 | 03500000 | Mountain | No change | 66 | 1957-2022 |
| GA | Tallulah River | Clayton | 34.889972, -83.530639 | 02178400 | Mountain | No change | 59 | 1964-2022 |
| NC | Oconaluftee River | Birdtown | 35.461389, -83.353611 | 03512000 | Mountain | No change | 66 | 1957-2022 |
| NC | Pigeon River | Hepco | 35.635000, -82.990000 | 03459500 | Mountain | No change | 66 | 1957-2022 |
| NC | South Toe River | Celo | 35.831389, -82.184167 | 03463300 | Mountain | No change | 66 | 1957-2022 |
| NC | Tuckasegee River | Bryson | 35.427500, -83.446944 | 03513000 | Mountain | No change | 65 | 1957-1981, 1983-2022 |
| NC | Watauga River | sugar grove | 36.239167, -81.822222 | 03479000 | Mountain | No change | 66 | 1957-2022 |
| NC | Swannanoa River | Biltmore | 35.568333, -82.544722 | 03451000 | Mountain | No change | 66 | 1957-2022 |
| NC | South Fork New River | Jefferson | 36.393333, -81.406944 | 03161000 | Mountain | No change | 66 | 1957-2022 |
| NC | French Broad River | Asheville | 35.608889, -82.578056 | 03451500 | Mountain | No change | 66 | 1957-2022 |
| NC | Pigeon River | Canton | 35.521944, -82.848056 | 03456991 | Mountain | No change | 66 | 1957-2022 |
| GA | Coosa River | Rome | 34.200500, -85.256417 | 02397000 | Mountain | No change | 63 | 1957-1958, 1962-2022 |
| GA | Chattooga River | Summerville | 34.466389, -85.336111 | 02398000 | Mountain | No change | 66 | 1957-2022 |
| GA | Etowah River | Kingston | 34.209306, -84.978750 | 02395000 | Mountain | No change | 54 | 1957-1995, 2008-2022 |
| GA | Conasauga River | Tilton | 34.666917, -84.927917 | 02387000 | Mountain | No change | 66 | 1957-2022 |

| | | | | | | | | |
|---|---|---|---|---|---|---|---|---|
| GA | Holy Creek | Chatsworth | 34.716667, -84.770000 | 02385800 | Mountain | Increasing trend | 63 | 1960-2022 |
| NC | East Fork Pigeon River | Canton | 35.461667, -82.869722 | 03456500 | Mountain | Increasing trend | 66 | 1957-2022 |
| NC | Mills River | Mills | 35.398056, -82.595000 | 03446000 | Mountain | Increasing trend | 66 | 1957-2022 |
| NC | Cataloochee Creek | Cataloochee | 35.667222, -83.072778 | 03460000 | Mountain | Increasing trend | 61 | 1962-2022 |
| NC | Davidson River | Brevard | 35.273056, -82.705833 | 03441000 | Mountain | Increasing trend | 64 | 1957-1990, 1992-2022 |
| NC | Beetree Creek | Swannanoa | 35.653056, -82.405278 | 03450000 | Mountain | Increasing trend | 60 | 1957-1975, 1979-1981, 1985-2022 |
| NC | Nantahala River | Rainbow Springs | 35.127500, -83.618611 | 03504000 | Mountain | Increasing trend | 66 | 1957-2022 |
| NC | Chestnut Creek | Galax | 36.645833, -80.919444 | 03165000 | Mountain | Increasing trend | 66 | 1957-2022 |
| SC | Rocky Creek | Great Falls | 34.565278, -80.920000 | 02147500 | Piedmont | Significantly decreasing | 62 | 1957-1981, 1986-2022 |
| NC | Long Creek | Bessemer | 35.306389, -81.234722 | 02144000 | Piedmont | Significantly decreasing | 66 | 1957-2022 |
| SC | Tyger River | Delta | 34.535278, -81.548333 | 02160105 | Piedmont | Significantly decreasing | 50 | 1973-2022 |
| NC | Tar River | Louisburg | 36.093056, -78.296111 | 02081747 | Piedmont | Significantly decreasing | 60 | 1963-2022 |
| GA | Snake Creek | Whitesburg | 33.529306, -84.928722 | 02337500 | Piedmont | Significantly decreasing | 66 | 1957-2022 |
| SC | Broad River | Carlisle | 34.595000, -81.421389 | 02156500 | Piedmont | Significantly decreasing | 66 | 1957-2022 |
| GA | Stevens Creek | Modoc | 33.729167, -82.181944 | 02196000 | Piedmont | Significantly decreasing | 62 | 1957-1978, 1983-2022 |
| GA | Tobesofkee Creek | near Macon | 32.808889, -83.758333 | 02213500 | Piedmont | Significantly decreasing | 66 | 1957-2022 |
| SC | Saluda River | Chappells | 34.174444, -81.864167 | 02167000 | Piedmont | Significantly decreasing | 66 | 1957-2022 |

| | | | | | | | | |
|---|---|---|---|---|---|---|---|---|
| GA | Flint River | Carsonville | 32.721389, -84.232500 | 02347500 | Piedmont | Significantly decreasing | 66 | 1957-2022 |
| NC | Indian Creek | Laboratory | 35.420556, -81.265278 | 02143500 | Piedmont | Significantly decreasing | 66 | 1957-2022 |
| SC | Pacolet River | Fingerling | 35.109722, -81.959722 | 02155500 | Piedmont | Significantly decreasing | 66 | 1957-2022 |
| NC | Catawba River | Rock Hill | 34.984722, -80.974167 | 02146000 | Piedmont | Significantly decreasing | 66 | 1957-2022 |
| GA | Oconee River | Milledgeville | 33.090167, -83.214778 | 02223000 | Piedmont | Significantly decreasing | 66 | 1957-2022 |
| SC | North Pacolet River | Fingerling | 35.120833, -81.986111 | 02154500 | Piedmont | Significantly decreasing | 66 | 1957-2022 |
| GA | Broad River | Bell | 33.974167, -82.770000 | 02192000 | Piedmont | Significantly decreasing | 66 | 1957-2022 |
| SC | Enoree River | Whitemire | 34.509167, -81.598333 | 02160700 | Piedmont | Decreasing trend | 50 | 1973-2022 |
| SC | Little River | Mt. Carmel | 34.072444, -82.500917 | 02192500 | Piedmont | Decreasing trend | 51 | 1967-1970, 1986-2022 |
| GA | Flint River | Griffin | 33.244167, -84.429167 | 02344500 | Piedmont | Decreasing trend | 66 | 1957-2022 |
| SC | Broad River | Boiling Springs | 35.210833, -81.697500 | 02151500 | Piedmont | Decreasing trend | 66 | 1957-2022 |
| NC | Deep River | Moncure | 35.626944, -79.116111 | 02102000 | Piedmont | Decreasing trend | 66 | 1957-2022 |
| NC | Buckhorn Creek | Corinth | 35.559722, -78.973611 | 02102192 | Piedmont | Decreasing trend | 51 | 1972-2022 |
| GA | Middle Oconee River | Athens | 33.946667, -83.422778 | 02217500 | Piedmont | Decreasing trend | 66 | 1957-2022 |
| SC | Saluda River | Greenville | 34.842222, -82.480833 | 02162500 | Piedmont | Decreasing trend | 55 | 1957-1978, 1990-2022 |
| SC | Saluda River | Ware Shoals | 34.391667, -82.223611 | 02163500 | Piedmont | Decreasing trend | 66 | 1957-2022 |
| NC | Tick Creek | Mt Vernon springs | 35.659722, -79.401667 | 02101800 | Piedmont | Decreasing trend | 53 | 1958-1981, 1994-2022 |
| GA | Falling Creek | Juliette | 33.100306, -83.723167 | 02212600 | Piedmont | Decreasing trend | 59 | 1964-2022 |

| | | | | | | | | |
|---|---|---|---|---|---|---|---|---|
| NC | Neuse River | Falls | 35.940000, -78.580833 | 02087183 | Piedmont | Decreasing trend | 53 | 1970-2022 |
| NC | Rocky River | Norwood | 35.156997, -80.165772 | 02126000 | Piedmont | Decreasing trend | 66 | 1957-2022 |
| NC | Little Fishing River | White Oak | 36.183333, -77.876111 | 02082950 | Piedmont | Decreasing trend | 64 | 1959-2022 |
| SC | Reedy River | Greenville | 34.800000, -82.365278 | 02164000 | Piedmont | Decreasing trend | 51 | 1957-1971, 1988-2022 |
| NC | Henry Fork | Henry River | 35.684444, -81.403333v | 02143000 | Piedmont | Decreasing trend | 66 | 1957-2022 |
| NC | Little River | Star | 35.387222, -79.831389 | 02128000 | Piedmont | Decreasing trend | 66 | 1957-2022 |
| NC | North Buffalo Creek | Greensboro | 36.120556, -79.708056 | 02095500 | Piedmont | Decreasing trend | 59 | 1957-1990, 1998-2022 |
| NC | First Broad River | Casar | 35.493056, -81.682222 | 02152100 | Piedmont | Decreasing trend | 64 | 1959-2022 |
| GA | Chattahoochee River | Norcross | 33.997222, -84.201944 | 02335000 | Piedmont | Decreasing trend | 66 | 1957-2022 |
| GA | Alcovy River | Covington | 33.639389, -83.778417 | 02208450 | Piedmont | Decreasing trend | 51 | 1972-2022 |
| NC | Hunting Creek | Harmony | 36.000556, -80.745556 | 02118500 | Piedmont | Decreasing trend | 66 | 1957-2022 |
| GA | Chattahoochee River | Fairburn | 33.656667, -84.673611 | 02337170 | Piedmont | Decreasing trend | 58 | 1965-2022 |
| NC | Eno River | Hillsborough | 36.071111, -79.095556 | 02085000 | Piedmont | Decreasing trend | 53 | 1957-1971, 1985-2022 |
| NC | Jacob Fork | Ramsey | 35.590556, -81.566944 | 02143040 | Piedmont | Decreasing trend | 62 | 1961-2022 |
| NC | Lower Little River | Healing Springs | 35.945556, -81.236944 | 02142000 | Piedmont | Decreasing trend | 65 | 1957-1995, 1997-2022 |
| GA | Chattahoochee River | Cornelia | 34.540722, -83.622775 | 02331600 | Piedmont | Decreasing trend | 66 | 1957-2022 |
| NC | Deep River | Ramseur | 35.726389, -79.655556 | 02100500 | Piedmont | Decreasing trend | 66 | 1957-2022 |
| GA | Chattahoochee River | Whitesburg | 33.476528, -84.901194 | 02338000 | Piedmont | Decreasing trend | 58 | 1965-2022 |

| | | | | | | | | |
|---|---|---|---|---|---|---|---|---|
| NC | South Yadkin River | Mocksville | 35.845000, -80.658889 | 02118000 | Piedmont | Decreasing trend | 66 | 1957-2022 |
| NC | South Fork Catawba | Lowell | 35.285278, -81.101111 | 02145000 | Piedmont | Decreasing trend | 54 | 1957-1971, 1983-1996, 1997-2021 |
| GA | Sweetwater Creek | Austell | 33.776778, -84.615500 | 02337000 | Piedmont | Decreasing trend | 66 | 1957-2022 |
| NC | Yadkin River | Yadkin College | 35.856667, -80.386944 | 02116500 | Piedmont | Decreasing trend | 66 | 1957-2022 |
| NC | Dan River | Wentworth | 36.412500, -79.826111 | 02071000 | Piedmont | Decreasing trend | 66 | 1957-2022 |
| NC | Reedies River | North Wilkesboro | 36.175000, -81.168889 | 02111500 | Piedmont | Decreasing trend | 66 | 1957-2022 |
| NC | Neuse River | Clayton | 35.647222, -78.405278 | 02087500 | Piedmont | Decreasing trend | 66 | 1957-2022 |
| NC | Reedy Fork | Oak Ridge | 36.172500, -79.952778 | 02093800 | Piedmont | Decreasing trend | 66 | 1957-2022 |
| NC | Tar River | Tar | 36.194167, -78.583056 | 02081500 | Piedmont | Decreasing trend | 66 | 1957-2022 |
| NC | Little Yadkin River | Dalton | 36.299167, -80.414722 | 02114450 | Piedmont | Decreasing trend | 63 | 1960-2022 |
| NC | Hyco River | Mcgehees Mill | 36.522722, -78.997056 | 02077303 | Piedmont | Decreasing trend | 50 | 1973-2022 |
| GA | Chattahoochee River | Atlanta | 33.859167, -84.454444 | 02336000 | Piedmont | Decreasing trend | 66 | 1957-2022 |
| GA | Chestatee River | Dahlonega | 34.528056, -83.939722 | 02333500 | Piedmont | Decreasing trend | 66 | 1957-2022 |
| NC | Cove Creek | Lake Lure | 35.423333, -82.111667 | 02149000 | Piedmont | Decreasing trend | 66 | 1957-2022 |
| GA | Chattahoochee River | West Point | 32.886639, -85.181583 | 02339500 | Piedmont | Decreasing trend | 66 | 1957-2022 |
| GA | Line Creek River | Senoia | 33.319167, -84.522222 | 02344700 | Piedmont | Decreasing trend | 59 | 1964-2022 |
| NC | Yadkin River | Enon | 36.132886, -80.445275 | 02115360 | Piedmont | Decreasing trend | 59 | 1964-2022 |

| | | | | | | | | |
|---|---|---|---|---|---|---|---|---|
| NC | Haw River | Bynum | 35.765278, -79.135833 | 02096960 | Piedmont | Decreasing trend | 50 | 1973-2022 |
| NC | North Mayo River | Spencer | 36.568056, -79.987500 | 02070000 | Piedmont | No change | 66 | 1957-2022 |
| NC | Yadkin River | Wilkesboro | 36.152500, -81.145556 | 02112000 | Piedmont | No change | 66 | 1957-2022 |
| NC | Flat River | Bahama | 36.182778, -78.878889 | 02085500 | Piedmont | No change | 66 | 1957-2022 |
| GA | Peachtree Creek | Atlanta | 33.820306, -84.407639 | 02336300 | Piedmont | No change | 65 | 1958-2022 |
| NC | Elk Creek | Elkville | 36.071389, -81.403056 | 02111180 | Piedmont | No change | 58 | 1965-2022 |
| NC | Dan River | Fransisco | 36.515000, -80.303056 | 02068500 | Piedmont | No change | 63 | 1957-1987, 1991-2022 |
| NC | Yadkin River | Elkin | 36.241039, -80.849111 | 02112250 | Piedmont | No change | 59 | 1964-2022 |
| NC | Reedy Fork | Gibsonville | 36.173056, -79.614167 | 02094500 | Piedmont | No change | 66 | 1957-2022 |
| NC | Linville River | Nebo | 35.795556, -81.891111 | 02138500 | Piedmont | No change | 66 | 1957-2022 |
| NC | South Mayo River | Nettleridge | 36.570833, -80.129722 | 02069700 | Piedmont | No change | 61 | 1962-2022 |
| NC | Eno River | Durham | 36.072222, -78.907778 | 02085070 | Piedmont | Increasing trend | 60 | 1963-2022 |
| NC | Haw River | Haw River | 36.087222, -79.366111 | 02096500 | Piedmont | Increasing trend | 66 | 1957-2022 |
| NC | Hyco Creek | Leasburg | 36.397778, -79.196667 | 02077200 | Piedmont | Increasing trend | 59 | 1964-2022 |
| NC | Ararat River | Ararat | 36.404389, -80.561694 | 02113850 | Piedmont | Increasing trend | 59 | 1964-2022 |
| NC | Smith River | Eden | 36.525556, -79.765556 | 02074000 | Piedmont | Increasing trend | 66 | 1957-2022 |
| GA | Big Creek | Alpharetta | 34.050556, -84.269444 | 02335700 | Piedmont | Increasing trend | 63 | 1960-2022 |
| NC | Mcalpine Creek | Charlotte | 35.137778, -80.767500 | 02146600 | Piedmont | Increasing trend | 61 | 1962-2022 |

| | | | | | | | | |
|---|---|---|---|---|---|---|---|---|
| NC | Long Creek | Paw Creek | 35.328611, -80.909722 | 02142900 | Piedmont | Increasing trend | 58 | 1965-2022 |
| NC | McMullen Creek | Sharon View | 35.140833, -80.820000 | 02146700 | Piedmont | Increasing trend | 61 | 1962-2022 |
| NC | Irwin Creek | Charlotte | 35.197778, -80.904444 | 02146300 | Piedmont | Significantly increasing | 61 | 1962-2022 |
| NC | East Fork Deep River | High Point | 36.037222, -79.945556 | 02099000 | Piedmont | Significantly increasing | 64 | 1957-1994, 1997-2022 |
| SC | North Fork Edisto River | Orangeburg | 33.483333, -80.873611 | 02173500 | Southeastern Plains | Significantly decreasing | 66 | 1957-2022 |
| SC | Black Creek | McBee | 34.513889, -80.183333 | 02130900 | Southeastern Plains | Significantly decreasing | 64 | 1959-2022 |
| SC | Black Creek | Hartsville | 34.397222, -80.150000 | 02130910 | Southeastern Plains | Significantly decreasing | 63 | 1960-2022 |
| SC | South Fork Edisto River | Denmark | 33.393056, -81.133333 | 02173000 | Southeastern Plains | Significantly decreasing | 58 | 1957-1971, 1980-2022 |
| NC | Drowning Creek | Hoffman | 35.061111, -79.493889 | 02133500 | Southeastern Plains | Significantly decreasing | 66 | 1957-2022 |
| SC | Congaree River | Columbia | 33.993056, -81.050000 | 02169500 | Southeastern Plains | Significantly decreasing | 66 | 1957-2022 |
| SC | Saluda River | Columbia | 34.013889, -81.088056 | 02169000 | Southeastern Plains | Significantly decreasing | 66 | 1957-2022 |
| GA | Oconee River | Dublin | 32.543944, -82.892972 | 02223500 | Southeastern Plains | Significantly decreasing | 66 | 1957-2022 |
| GA | Flint River | Albany | 31.594167, -84.144167 | 02352500 | Southeastern Plains | Significantly decreasing | 66 | 1957-2022 |
| GA | Flint River | Montezuma | 32.293056, -84.043611 | 02349605 | Southeastern Plains | Significantly decreasing | 66 | 1957-2022 |
| SC | Wateree River | Camden | 34.244444, -80.654167 | 02148000 | Southeastern Plains | Significantly decreasing | 66 | 1957-2022 |
| GA | Savannah River | Augusta | 33.372528, -81.942083 | 02197000 | Southeastern Plains | Significantly decreasing | 66 | 1957-2022 |
| NC | Lumber River | Broadman | 34.442500, -78.960278 | 02134500 | Southeastern Plains | Significantly decreasing | 66 | 1957-2022 |
| SC | Pee Dee River | Pee Dee | 34.204167, -79.548611 | 02131000 | Southeastern Plains | Significantly decreasing | 66 | 1957-2022 |

| | | | | | | | | |
|---|---|---|---|---|---|---|---|---|
| GA | Savannah River | Burton's Ferry | 32.936444, -81.502528 | 02197500 | Southeastern Plains | Decreasing trend | 55 | 1957-1970, 1982-2022 |
| GA | Flint River | Newton | 31.306944, -84.338889 | 02353000 | Southeastern Plains | Decreasing trend | 66 | 1957-2022 |
| GA | Canoochee River | Claxton | 32.184361, -81.889222 | 02203000 | Southeastern Plains | Decreasing trend | 66 | 1957-2022 |
| GA | Ohoopee River | Reidsville | 32.077139, -82.176500 | 02225500 | Southeastern Plains | Decreasing trend | 66 | 1957-2022 |
| SC | Gills Creek | Columbia | 33.989444, -80.974444 | 02169570 | Southeastern Plains | Decreasing trend | 57 | 1966-2022 |
| GA | Kinchafoonee Creek | Preston | 32.052500, -84.548333 | 02350600 | Southeastern Plains | Decreasing trend | 52 | 1957-1977, 1986-2002, 2009-2022 |
| GA | Ichawaynochaway Creek | Milford | 31.382778, -84.546389 | 02353500 | Southeastern Plains | Decreasing trend | 66 | 1957-2022 |
| NC | Little River | Princeton | 35.511389, -78.160278 | 02088500 | Southeastern Plains | Decreasing trend | 66 | 1957-2022 |
| GA | Ocmulgee River | Lumber City | 31.919917, -82.674056 | 02215500 | Southeastern Plains | Decreasing trend | 66 | 1957-2022 |
| GA | Turkey Creek | Byromville | 32.195556, -83.902222 | 02349900 | Southeastern Plains | Decreasing trend | 65 | 1958-2022 |
| NC | Flat Creek | Inverness | 35.182778, -79.177500 | 02102908 | Southeastern Plains | Decreasing trend | 55 | 1968-2022 |
| NC | Cape Fear River | Lillington | 35.406111, -78.813333 | 02102500 | Southeastern Plains | Decreasing trend | 66 | 1957-2022 |
| NC | Tar River | Tarboro | 35.894444, -77.533056 | 02083500 | Southeastern Plains | Decreasing trend | 66 | 1957-2022 |
| NC | Fishing Creek | Enfield | 36.150556, -77.693056 | 02083000 | Southeastern Plains | Decreasing trend | 66 | 1957-2022 |
| GA | Withlacoochee River | near Pinetta | 30.595278, -83.259722 | 02319000 | Southeastern Plains | Decreasing trend | 66 | 1957-2022 |
| GA | Altamaha River | Baxley | 31.938889, -82.353611 | 02225000 | Southeastern Plains | Decreasing trend | 53 | 1970-2022 |
| NC | Pee Dee River | Rockingham | 34.945833, -79.869722 | 02129000 | Southeastern Plains | Decreasing trend | 66 | 1957-2022 |

| | | | | | | | | |
|---|---|---|---|---|---|---|---|---|
| NC | Black River | Tomahawk | 34.755000, -78.288611 | 02106500 | Southeastern Plains | Decreasing trend | 66 | 1957-2022 |
| GA | Spring Creek | Iron City | 31.040278, -84.740000 | 02357000 | Southeastern Plains | Decreasing trend | 59 | 1957-1971, 1976-2022 |
| GA | Ocmulgee River | Macon | 32.838611, -83.620556 | 02213000 | Southeastern Plains | Decreasing trend | 66 | 1957-2022 |
| NC | Neuse River | Kinston | 35.257778, -77.585556 | 02089500 | Southeastern Plains | Decreasing trend | 66 | 1957-2022 |
| GA | Upatoi Creek | Columbus | 32.413000, -84.820000 | 02341800 | Southeastern Plains | Decreasing trend | 55 | 1968-2022 |
| NC | Neuse River | Goldsboro | 35.337500, -77.997500 | 02089000 | Southeastern Plains | Decreasing trend | 66 | 1957-2022 |
| NC | Contentnea Creek | Hookerton | 35.428889, -77.582500 | 02091500 | Southeastern Plains | Decreasing trend | 66 | 1957-2022 |
| NC | Contentnea Creek | Lucama | 35.691111, -78.109722 | 02090380 | Southeastern Plains | No change | 59 | 1964-2022 |
| NC | Nahunta Swamp | Shine | 35.488889, -77.806111 | 02091000 | Southeastern Plains | No change | 66 | 1957-2022 |
| NC | Middle Creek | Clayton | 35.570833, -78.590556 | 02088000 | Southeastern Plains | No change | 66 | 1957-2022 |
| NC | Roanoke River | Roanoke Rapids | 36.460000, -77.633611 | 02080500 | Southeastern Plains | Increasing trend | 66 | 1957-2022 |
| NC | Swift Creek | Hilliardston | 36.112222, -77.920000 | 02082770 | Southeastern Plains | Increasing trend | 60 | 1963-2022 |
| SC | Coosawhatchie River | Hampton | 32.836111, -81.131944 | 02176500 | Coast | Significantly decreasing | 66 | 1957-2022 |
| SC | Salkehatchie River | Miley | 32.988889, -81.052778 | 02175500 | Coast | Significantly decreasing | 66 | 1957-2022 |
| SC | Edisto River | Givhans | 33.027778, -80.391667 | 02175000 | Coast | Significantly decreasing | 66 | 1957-2022 |
| SC | Little Pee Dee River | Galivants | 34.056944, -79.247222 | 02135000 | Coast | Significantly decreasing | 66 | 1957-2022 |
| SC | Lynches River | Effingham | 34.051389, -79.754167 | 02132000 | Coast | Significantly decreasing | 66 | 1957-2022 |
| SC | Santee River | Pineville | 33.454167, -80.141667 | 02171500 | Coast | Significantly decreasing | 66 | 1957-2022 |

| | | | | | | | | |
|---|---|---|---|---|---|---|---|---|
| GA | Brier Creek | Millhaven | 32.933333, -81.650667 | 02198000 | Coast | Significantly decreasing | 66 | 1957-2022 |
| GA | Ogeechee River | Eden | 32.190111, -81.415861 | 02202500 | Coast | Significantly decreasing | 66 | 1957-2022 |
| GA | Savannah River | Clyo | 32.528556, -81.268333 | 02198500 | Coast | Significantly decreasing | 66 | 1957-2022 |
| GA | Altamaha River | Doctortown | 31.654667, -81.827500 | 02226000 | Coast | Significantly decreasing | 66 | 1957-2022 |
| GA | Suwannee River | Fargo | 30.680556, -82.560556 | 02314500 | Coast | Significantly decreasing | 66 | 1957-2022 |
| GA | Satilla River | Atkinson | 31.219583, -81.866444 | 02228000 | Coast | Significantly decreasing | 66 | 1957-2022 |
| GA | Satilla River | Waycross | 31.238444, -82.322833 | 02226500 | Coast | Decreasing trend | 66 | 1957-2022 |
| GA | St Mary's River | Macclenny | 30.358611, -82.081667 | 02231000 | Coast | Decreasing trend | 66 | 1957-2022 |
| GA | Little Satilla River | Offerman | 31.452139, -82.054333 | 02227500 | Coast | Decreasing trend | 66 | 1957-2022 |
| GA | Alapaha River | Statenville | 30.703833, -83.032667 | 02317500 | Coast | Decreasing trend | 66 | 1957-2022 |
| SC | Black River | Kingstree | 33.662250, -79.836139 | 02136000 | Coast | Decreasing trend | 66 | 1957-2022 |
| NC | Ahoskie Creek | Ahoskie | 36.280278, -76.999444 | 02053500 | Coast | Decreasing trend | 66 | 1957-2022 |
| NC | Northeast Cape Fear River | Chinquapin | 34.828889, -77.832222 | 02108000 | Coast | Decreasing trend | 66 | 1957-2022 |
| NC | Waccamaw River | Freeland | 34.095000, -78.548333 | 02109500 | Coast | Decreasing trend | 66 | 1957-2022 |
| NC | Trent River | Trenton | 35.064167, -77.461389 | 02092500 | Coast | Decreasing trend | 66 | 1957-2022 |
| NC | Potecasi Creek | Union | 36.370833, -77.025556 | 02053200 | Coast | Decreasing trend | 65 | 1958-2022 |
| SC | Waccamaw River | Longs | 33.912500, -78.715278 | 02110500 | Coast | Decreasing trend | 66 | 1957-2022 |
| NC | New River | Gum Branch | 34.849167, -77.519444 | 02093000 | Coast | Decreasing trend | 53 | 1957-1973, 1987-2022 |

**APPENDIX B:**

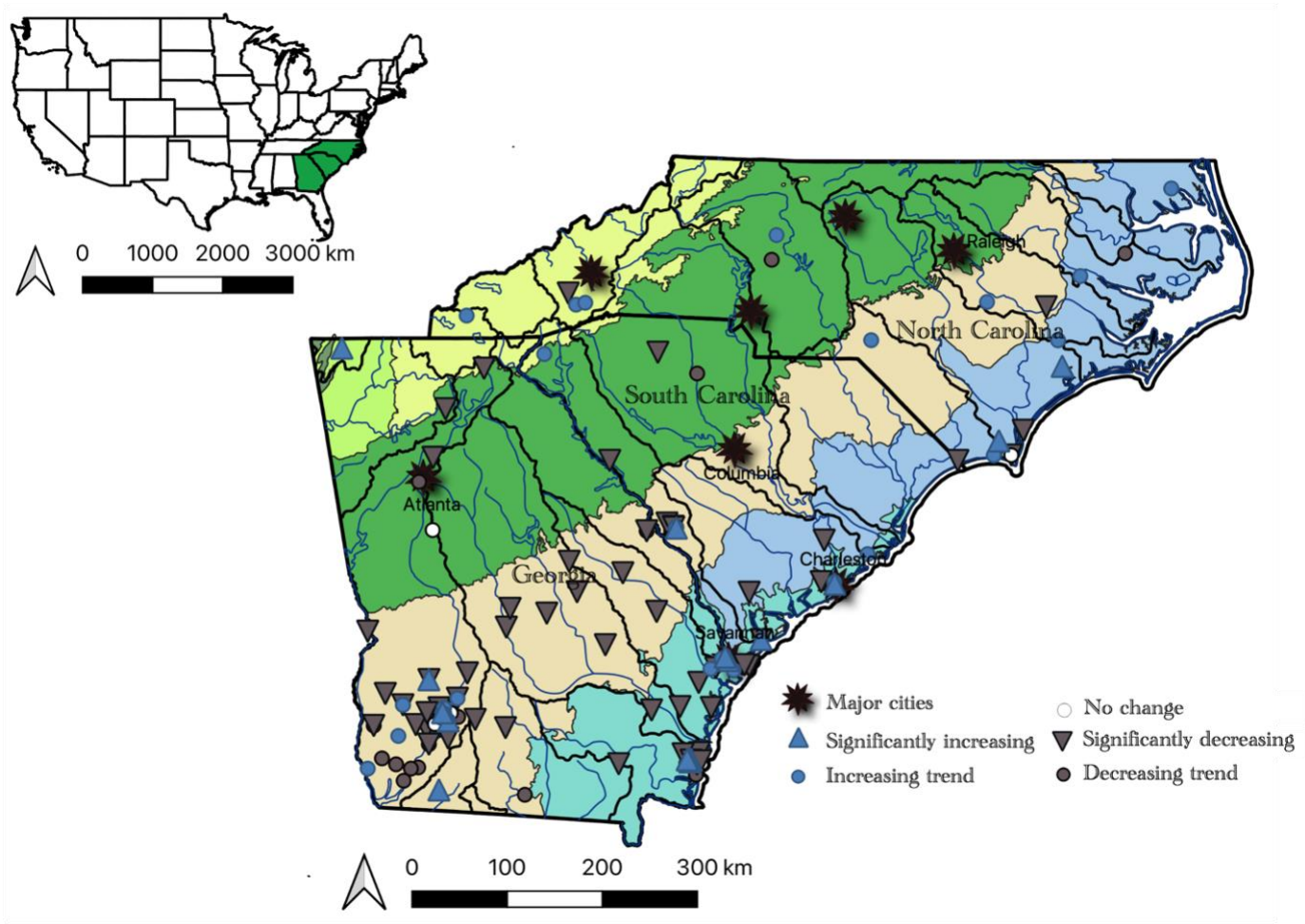
0 1000 2000 3000 km
Raleigh
North Carolina
South Carolina
Columbia
Atlanta
Charleston
Georgia
Savannah
Major cities
Significantly increasing
Increasing trend
No change
Significantly decreasing
Decreasing trend
0 100 200 300 km

**Figure 4.1:** Average annual groundwater (depth (m) below surface; n = 143) trends (30+ years) including significantly decreasing (gray triangle), decreasing trend (gray circles), no change (white circle), increasing trend (blue circle) and significantly increasing sites (blue triangle). North Carolina, South Carolina and Georgia are split by level III ecoregions represented by gray lines and include the Mountains [Ridge and Valley (light green) and Blue Ridge (yellow)], Piedmont (green), Southeastern Plains (tan) and Coast [Southern Coastal Plains (aqua) and Middle Atlantic Coastal Plains (blue)]. Thin black lines indicate drainage basins.

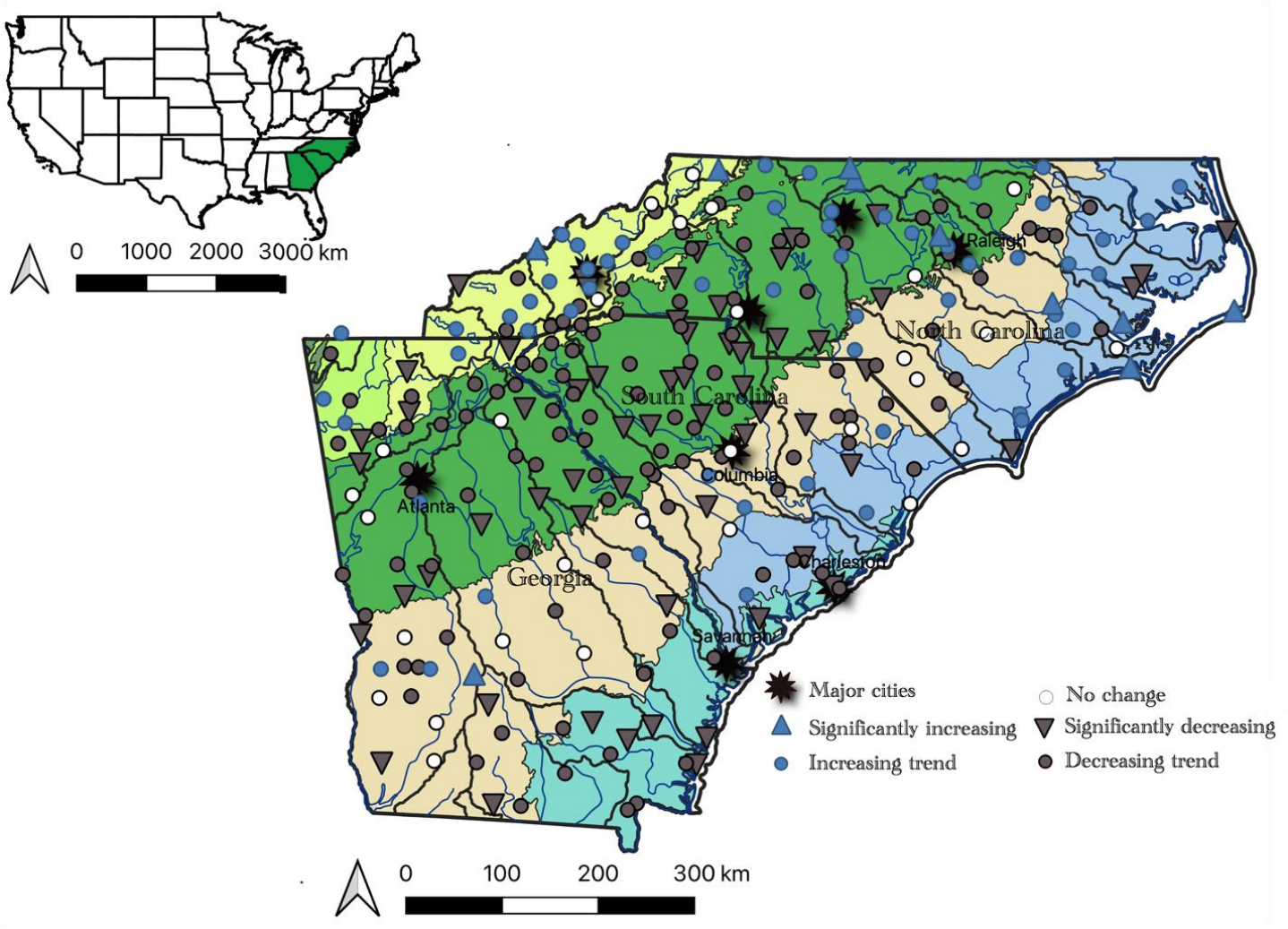


**Figure 4.2:** Total annual precipitation (mm) and snow (mm) (n = 275) trends (50+ years) including significantly decreasing (gray triangle), decreasing trend (gray circles), no change (white circle), increasing trend (blue circle) and significantly increasing sites (blue triangle). North Carolina, South Carolina and Georgia are split by level III ecoregions represented by gray lines include the Mountains [Ridge and Valley (light green) and Blue Ridge (yellow)], Piedmont (green), Southeastern Plains (tan) and Coast [Southern Coastal Plains (aqua) and Middle Atlantic Coastal Plains (blue)]. Thin black lines indicate drainage basins.

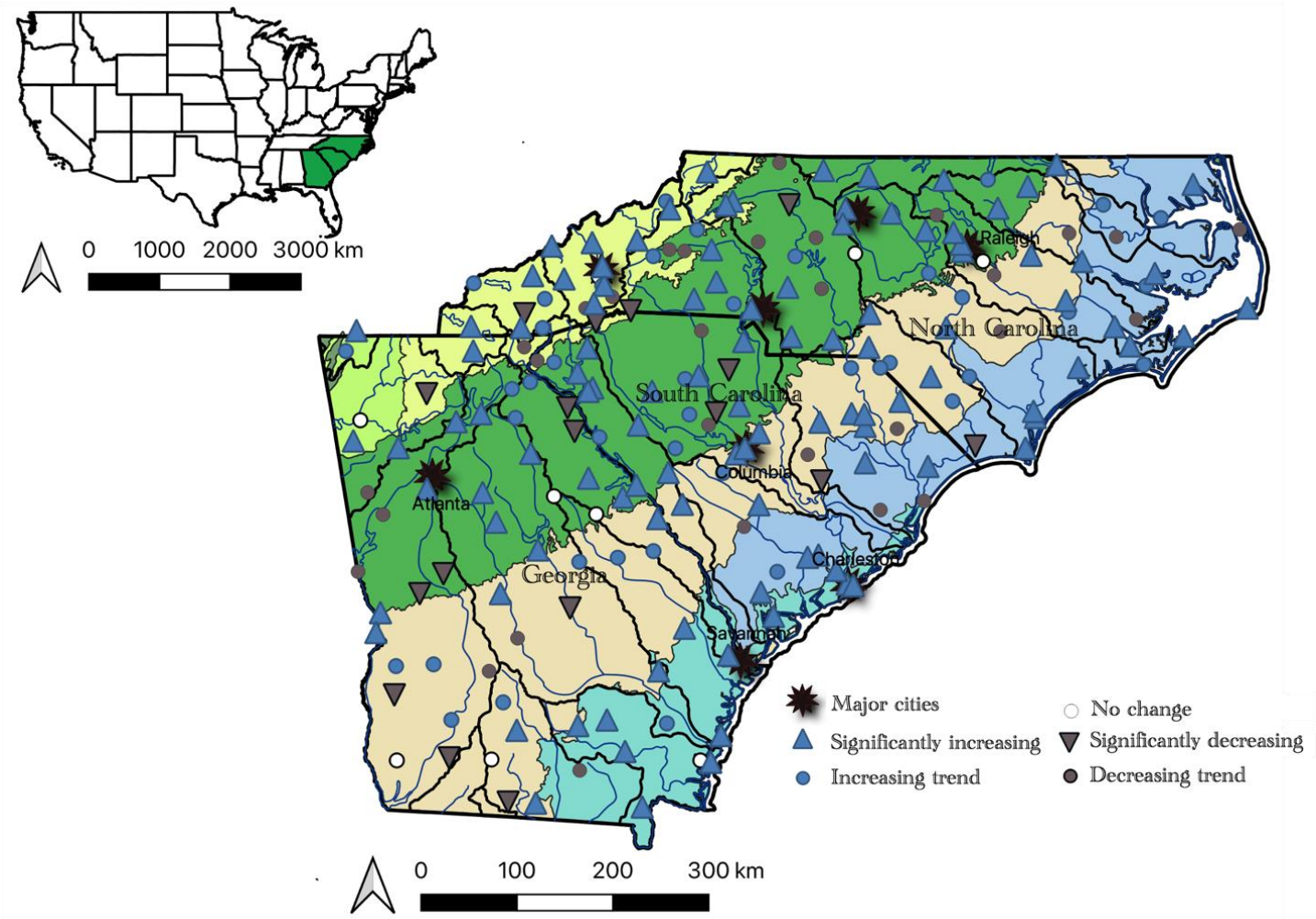


**Figure 4.3:** Average annual temperature maximum (°C, n = 207) trends (50+ years) including significantly decreasing (gray triangle), decreasing trend (gray circles), no change (white circle), increasing trend (blue circle) and significantly increasing sites (blue triangle). North Carolina, South Carolina and Georgia are split by level III ecoregions represented by gray lines and include the Mountains [Ridge and Valley (light green) and Blue Ridge (yellow)], Piedmont (green), Southeastern Plains (tan) and Coast [Southern Coastal Plains (aqua) and Middle Atlantic Coastal Plains (blue)]. Thin black lines indicate drainage basins.

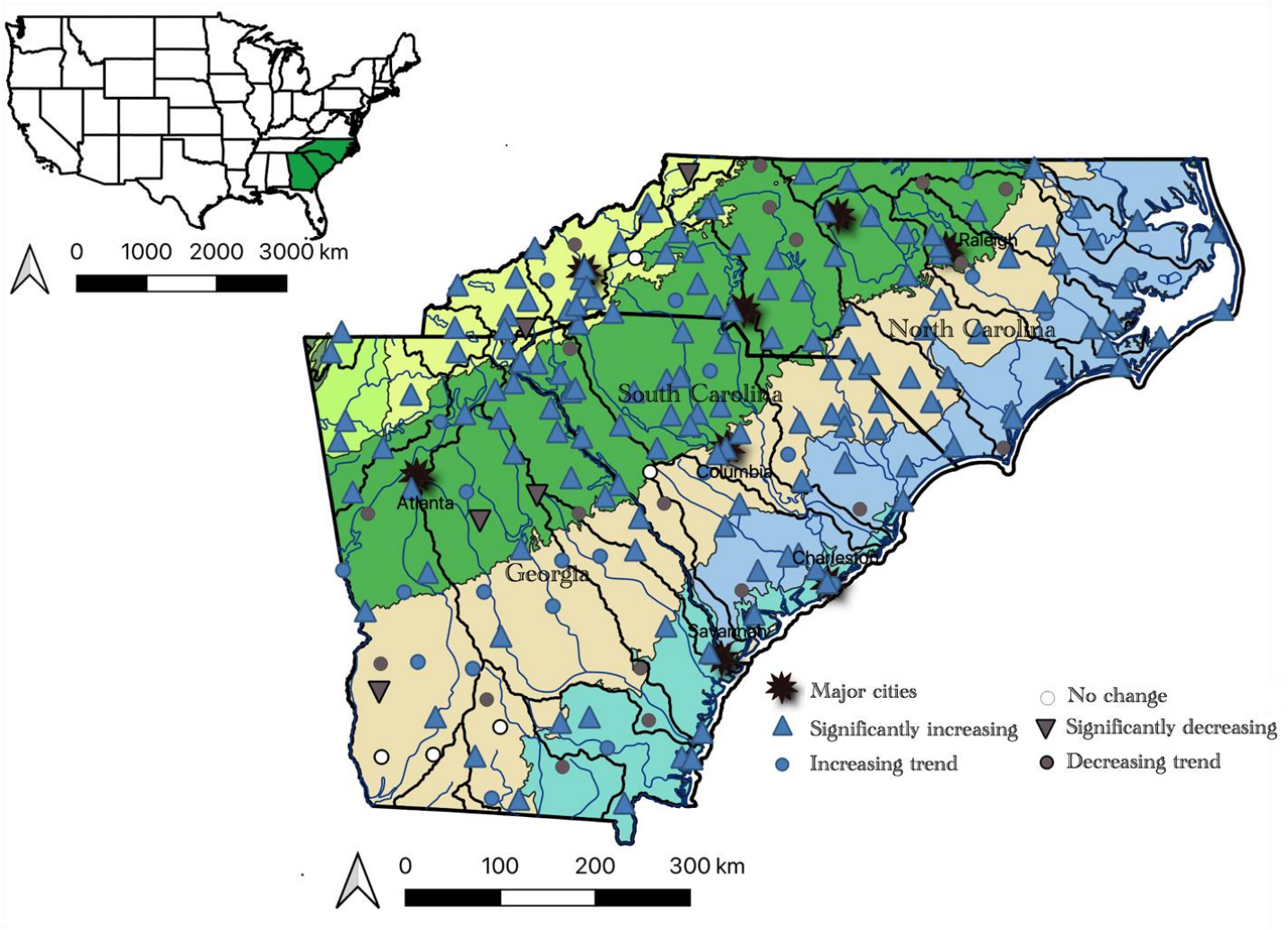


**Figure 4.4:** Average annual temperature minimum (°C, n = 204) trends (50+ years) including significantly decreasing (gray triangle), decreasing trend (gray circles), no change (white circles), increasing trend (blue circle) and significantly increasing sites (blue triangle). North Carolina, South Carolina and Georgia are split by level III ecoregions represented by gray lines and include the Mountains [Ridge and Valley (light green) and Blue Ridge (yellow)], Piedmont (green), Southeastern Plains (tan) and Coast [Southern Coastal Plains (aqua) and Middle Atlantic Coastal Plains (blue)]. Thin black lines indicate drainage basins.

**APPENDIX 4.C: Mountain ecoregion discharge plots**

***Significantly decreasing***

None

***Decreasing trend***

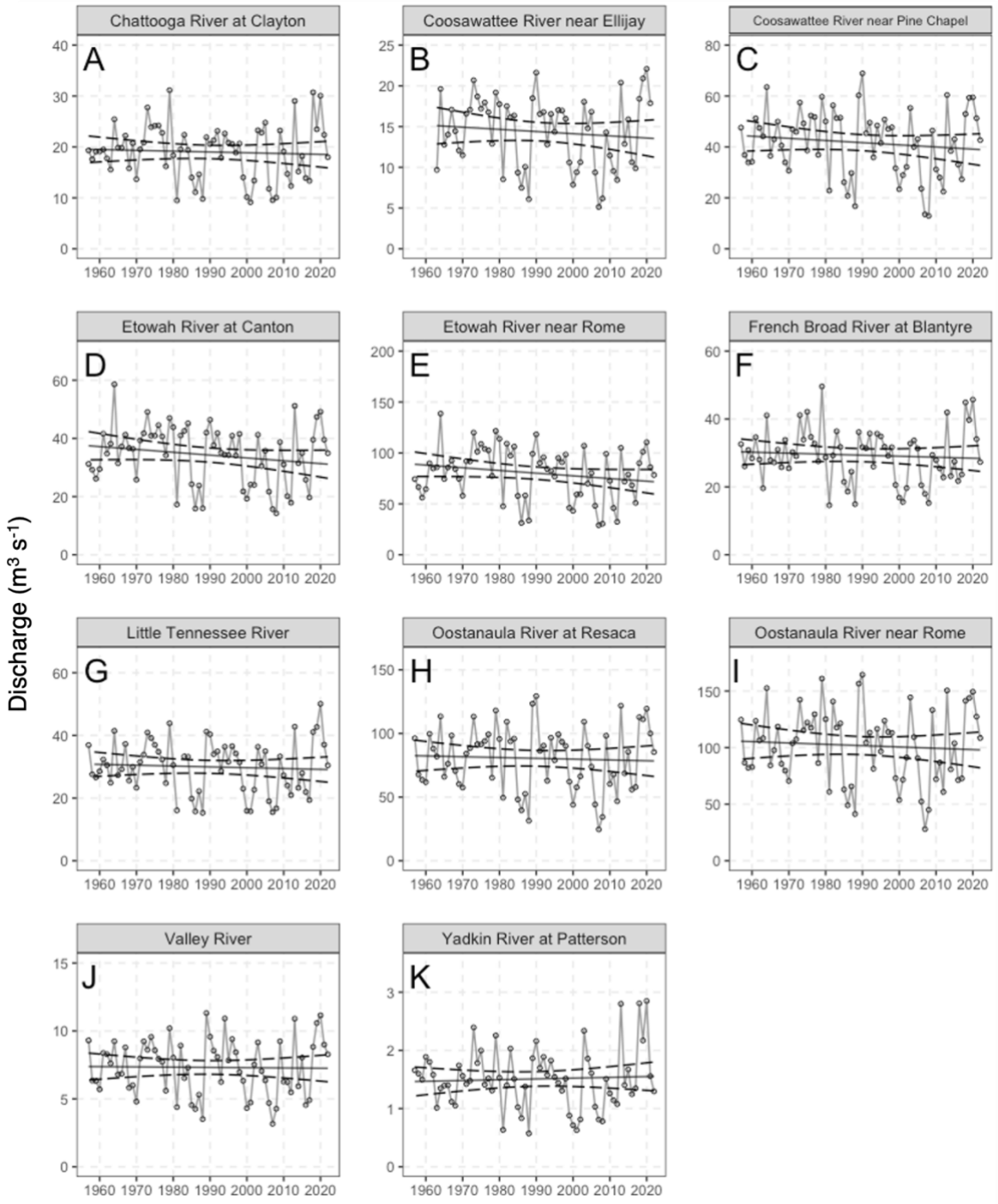

**Figure 4.C1:** Average annual discharge ($m^3$ $s^{-1}$) for sites in the Mountain ecoregion that showed a decreasing trend. USGS gage number, GPS coordinates and Mann-Kendall results can be found in the table below.

**Table 4.C1:** Sites located in the Mountain ecoregion that showed a decreasing trend including discharge plot tag, stream name, site name, USGS gage number, Mann-Kendall tau and p-value.

| Tag | Stream | Site | USGS Gage | Tau | p-value |
|---|---|---|---|---|---|
| A | Chattooga River | Clayton | 02177000 | -0.03 | 0.76 |
| B | Coosawattee River | Ellijay | 02380500 | -0.08 | 0.38 |
| C | Coosawattee River | Pine Chapel | 02383500 | -0.08 | 0.38 |
| D | Etowah River | Canton | 02392000 | -0.11 | 0.21 |
| E | Etowah River | Rome | 02395980 | -0.10 | 0.25 |
| F | French Broad River | Blantyre | 03443000 | -0.07 | 0.39 |
| G | Little Tennessee River | Needmore | 03503000 | -0.04 | 0.61 |
| H | Oostanaula River | Resaca | 02387500 | -0.03 | 0.74 |
| I | Oostanaula River | Rome | 02388500 | -0.05 | 0.59 |
| J | Valley River | Tomotla | 03550000 | -0.04 | 0.67 |
| K | Yadkin River | Patterson | 02111000 | -0.06 | 0.50 |

***No Change***

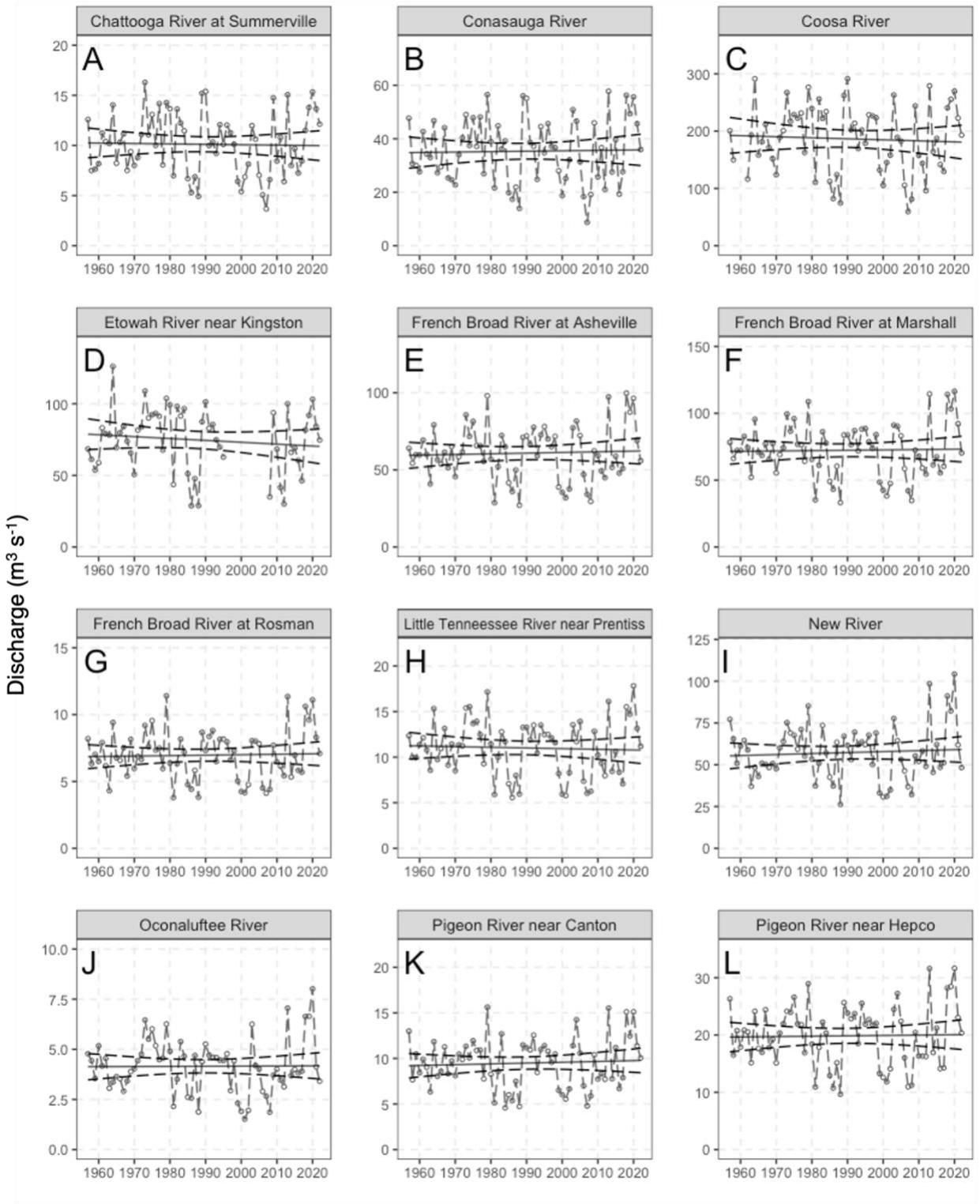
Chattooga River at Summerville
A
Conasauga River
B
Coosa River
C
Etowah River near Kingston
D
French Broad River at Asheville
E
French Broad River at Marshall
F
French Broad River at Rosman
G
Little Tenneessee River near Prentiss
H
New River
I
Oconaluftee River
J
Pigeon River near Canton
K
Pigeon River near Hepco
L
Discharge ($m^3 s^{-1}$)
1960 1970 1980 1990 2000 2010 2020

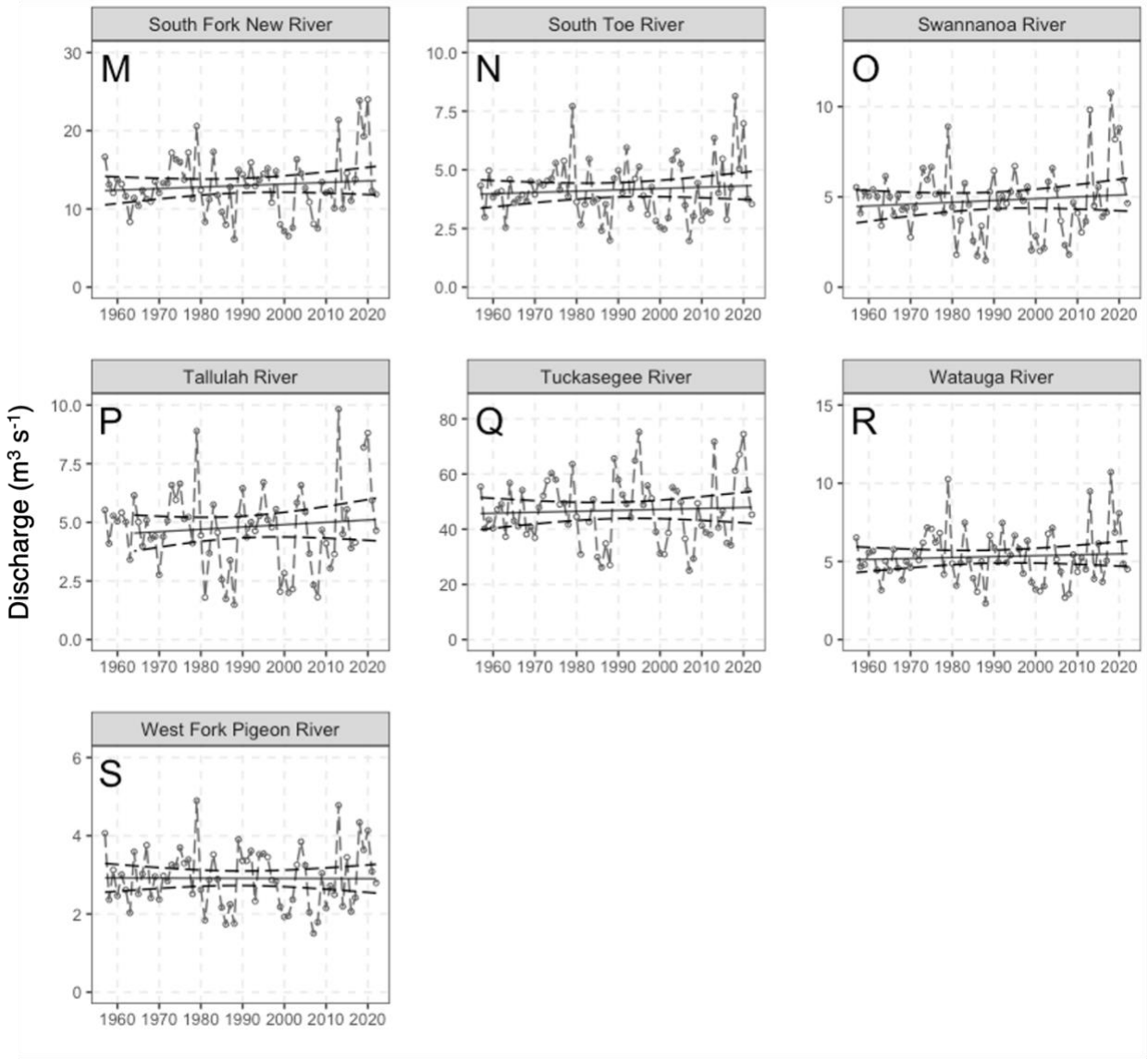


**Figure 4.C2:** Average annual discharge ($m^3$ $s^{-1}$) for sites in the Mountain ecoregion that showed no change. USGS gage number, GPS coordinates and Mann-Kendall results can be found in the table below.

**Table 4.C2:** Sites located in the Mountain ecoregion that showed no changes including discharge plot tag, stream name, site name, USGS gage number, Mann-Kendall tau and p-value.

| Tag | Stream | Site | USGS Gage | Tau | p-value |
|---|---|---|---|---|---|
| A | Chattooga River | Summerville | 02398000 | -0.02 | 0.82 |
| B | Conasauga River | Tilton | 02387000 | < 0.01 | 0.97 |
| C | Coosa River | Rome | 02397000 | -0.02 | 0.80 |
| D | Etowah River | Kingston | 02395000 | -0.01 | 0.89 |
| E | French Broad River | Asheville | 03451500 | 0.02 | 0.86 |
| F | French Broad River | Marshall | 03453500 | -0.02 | 0.83 |
| G | French Broad River | Rosman | 03439000 | -0.01 | 0.87 |
| H | Little Tennessee River | Prentiss | 03500000 | -0.01 | 0.87 |
| I | New River | Galax | 03164000 | -0.02 | 0.84 |
| J | Oconaluftee River | Birdtown | 03512000 | -0.01 | 0.94 |
| K | Pigeon River | Canton | 03456991 | 0.02 | 0.80 |
| L | Pigeon River | Hepco | 03459500 | -0.01 | 0.96 |
| M | South Fork New River | Jefferson | 03161000 | 0.01 | 0.89 |
| N | South Toe River | Celo | 03463300 | < 0.01 | 0.96 |
| O | Swannanoa River | Biltmore | 03451000 | 0.01 | 0.90 |
| P | Tallulah River | Clayton | 02178400 | -0.01 | 0.92 |
| Q | Tuckasegee River | Bryson | 03513000 | 0.01 | 0.92 |
| R | Watauga River | Sugar Grove | 03479000 | 0.01 | 0.91 |
| S | West Fork Pigeon River | Hazelwood | 03455500 | -0.02 | 0.80 |

***Increasing trend***

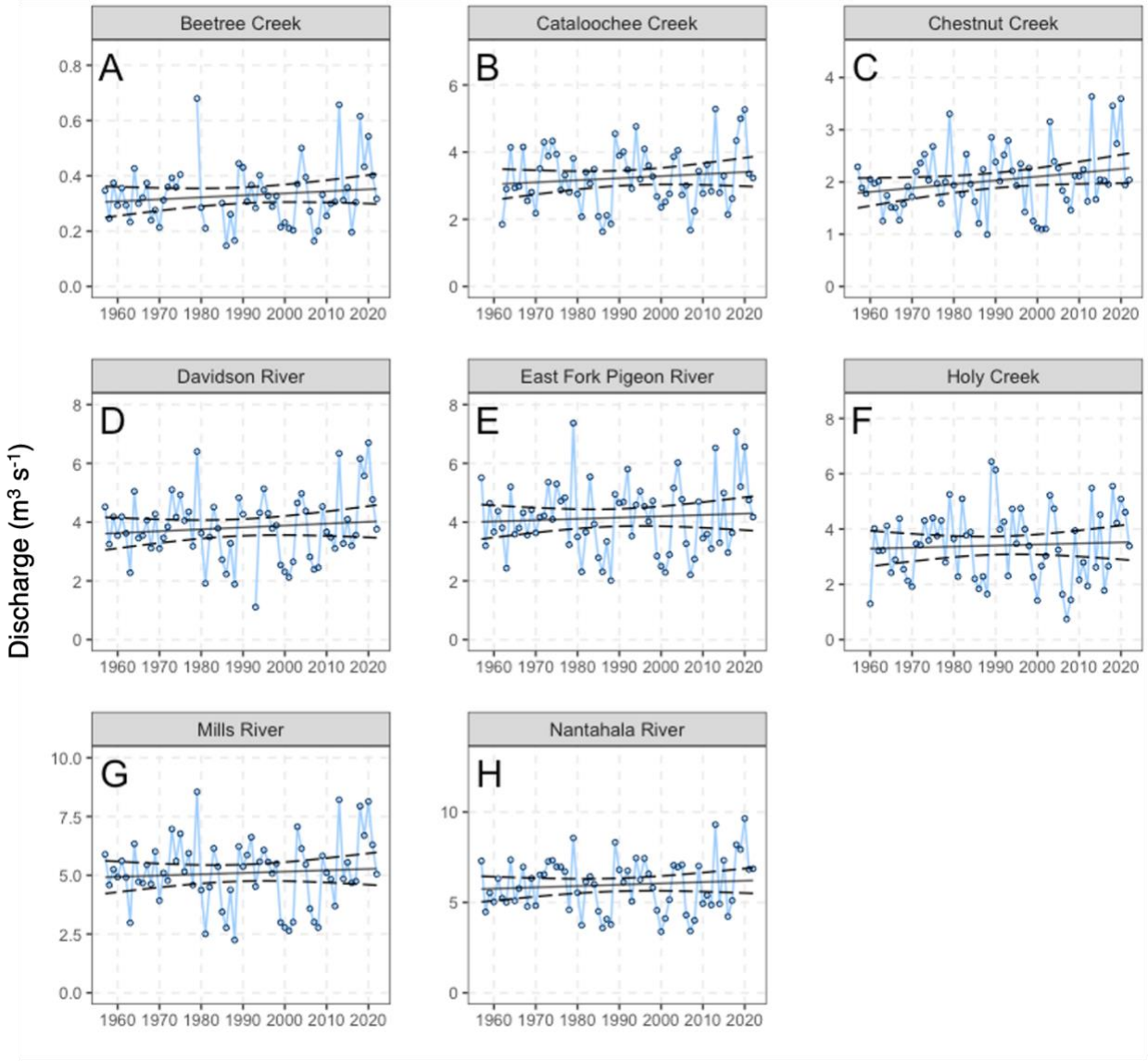


**Figure 4.C3:** Average annual discharge ($m^3$ $s^{-1}$) for sites in the Mountain ecoregion that showed an increasing trend. USGS gage number, GPS coordinates and Mann-Kendall results can be found in the table below.

**Table 4.C3:** Sites located in the Mountain ecoregion that showed an increasing trend including discharge plot tag, stream name, site name, USGS gage number, Mann-Kendall tau and p-value.

| Tag | Stream | Site | USGS Gage | Tau | p-value |
|---|---|---|---|---|---|
| A | Beetree Creek | Swannanoa | 03450000 | 0.05 | 0.59 |
| B | Cataloochee Creek | Cataloochee | 03460000 | 0.04 | 0.68 |
| C | Chestnut Creek | Galax | 03165000 | 0.12 | 0.15 |
| D | Davidson River | Brevard | 03441000 | 0.04 | 0.61 |
| E | East Fork Pigeon River | Canton | 03456500 | 0.03 | 0.77 |
| F | Holy Creek | Chatsworth | 02385800 | 0.03 | 0.70 |
| G | Mills River | Mills | 03446000 | 0.03 | 0.73 |
| H | Nantahala River | Rainbow Springs | 03504000 | 0.05 | 0.56 |

***Significantly Increasing***

None

**APPENDIX 4.D: Piedmont ecoregion discharge plots**

***Significantly decreasing***

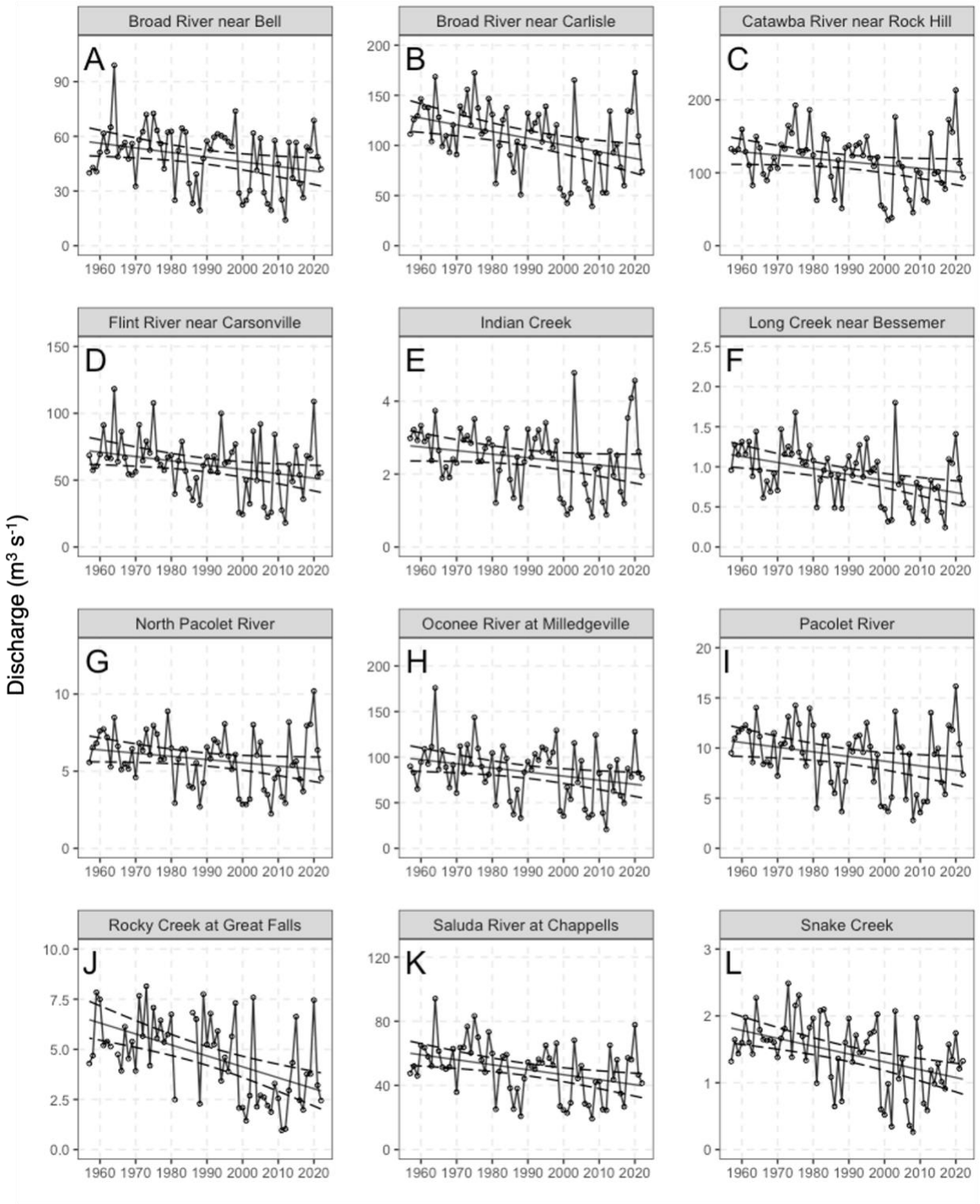

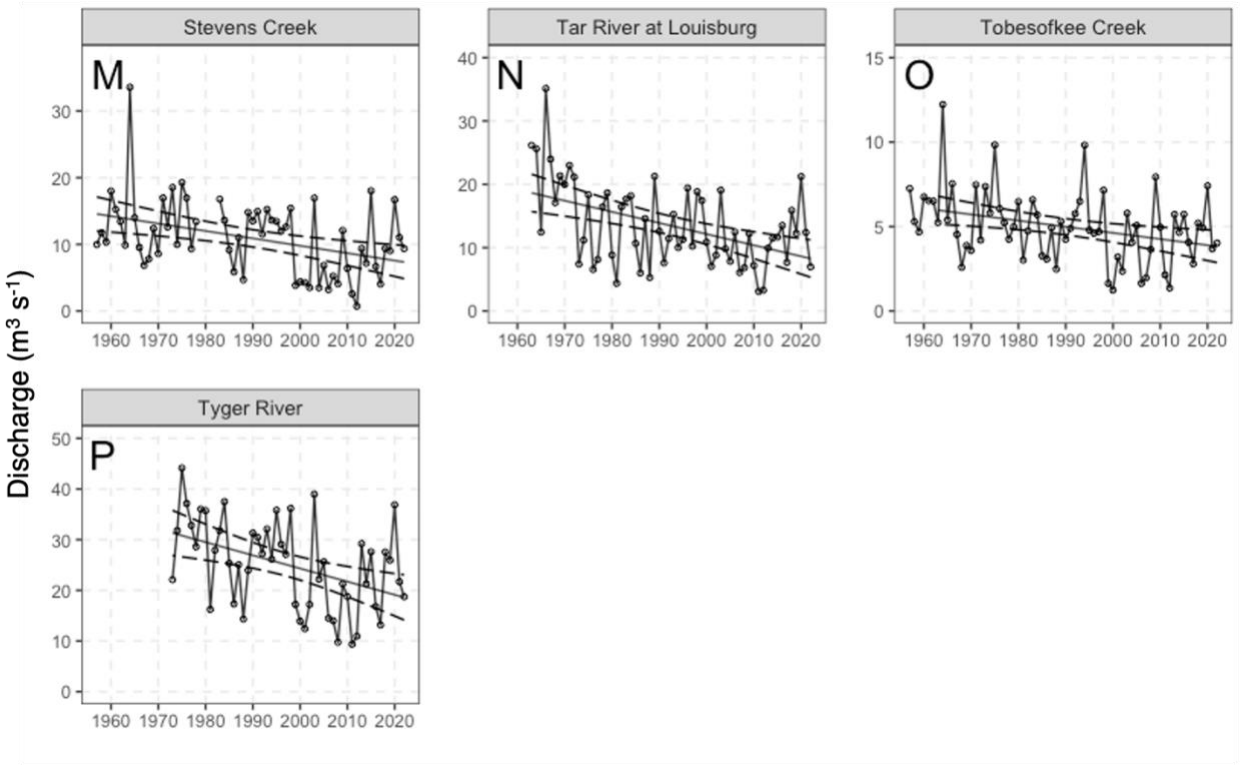


**Figure 4.D1:** Average annual discharge ($m^3$ $s^{-1}$) for sites in the Piedmont ecoregion that were significantly decreasing. USGS gage number, GPS coordinates and Mann-Kendall results can be found in the table below.

**Table 4.D1:** Sites located in the Piedmont ecoregion that were significantly decreasing including discharge plot tag, stream name, site name, USGS gage number, Mann-Kendall tau and p-value.

| Tag | Stream | Site | USGS Gage | Tau | p-value |
|---|---|---|---|---|---|
| A | Broad River | Bell | 02192000 | -0.16 | 0.05 |
| B | Broad River | Carlisle | 02156500 | -0.26 | < 0.01 |
| C | Catawba River | Rock Hill | 02146000 | -0.19 | 0.03 |
| D | Flint River | Carsonville | 02347500 | -0.21 | 0.01 |
| E | Indian Creek | Laboratory | 02143500 | -0.20 | 0.02 |
| F | Long Creek | Bessemer | 02144000 | -0.32 | < 0.01 |
| G | North Pacolet River | Fingerling | 02154500 | -0.17 | 0.05 |
| H | Oconee River | Milledgeville | 02223000 | -0.17 | 0.04 |
| I | Pacolet River | Fingerling | 02155500 | -0.20 | 0.02 |
| J | Rocky Creek | Great Falls | 02147500 | -0.33 | < 0.01 |
| K | Saluda River | Chappells | 02167000 | -0.22 | 0.01 |
| L | Snake Creek | Whitesburg | 02337500 | -0.27 | < 0.01 |
| M | Stevens Creek | Modoc | 02196000 | -0.25 | < 0.01 |
| N | Tar River | Louisburg | 02081747 | -0.29 | < 0.01 |
| O | Tobesofkee Creek | Macon | 02213500 | -0.23 | 0.01 |
| P | Tyger River | Delta | 02160105 | -0.30 | < 0.01 |

***Decreasing trend***

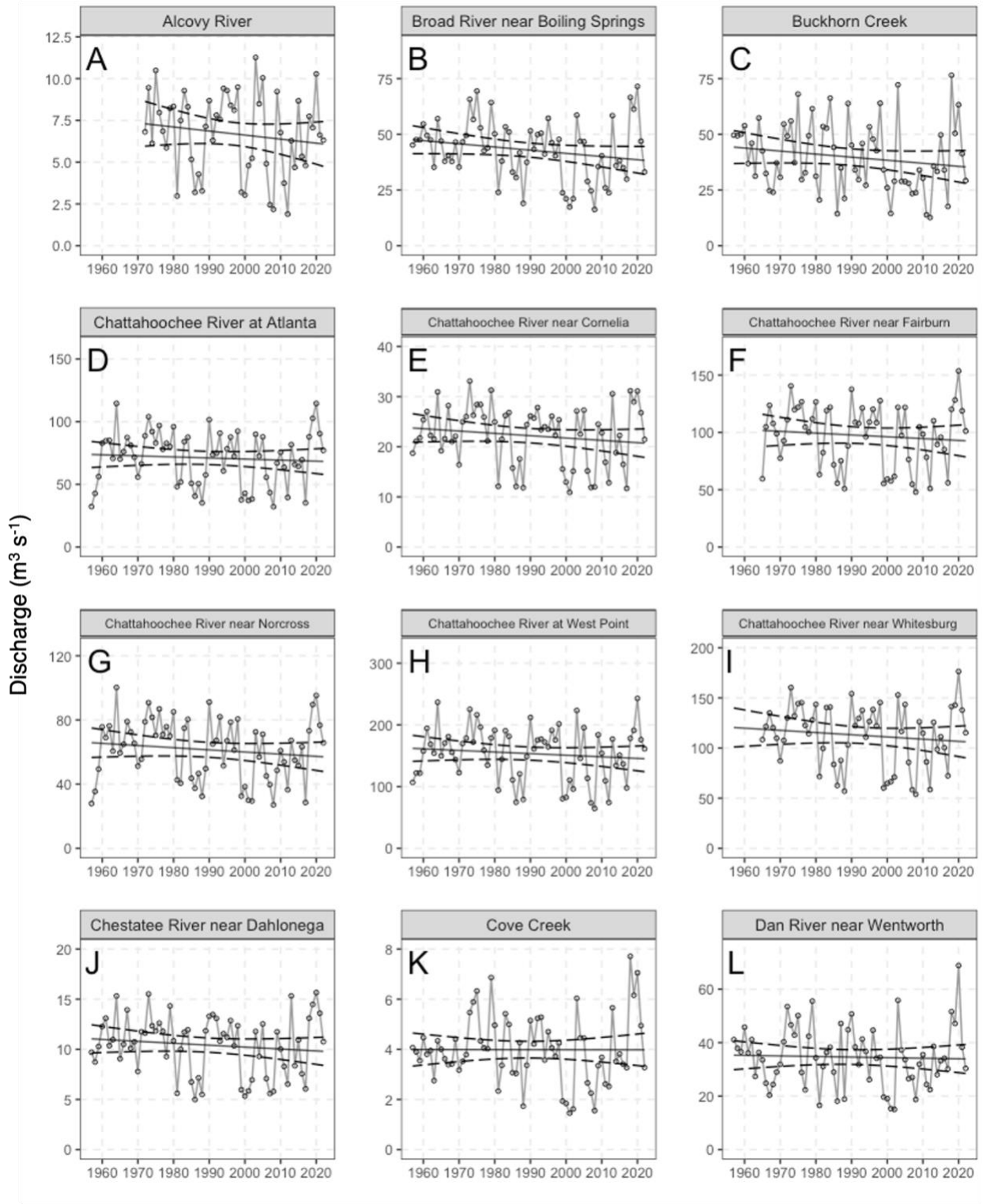

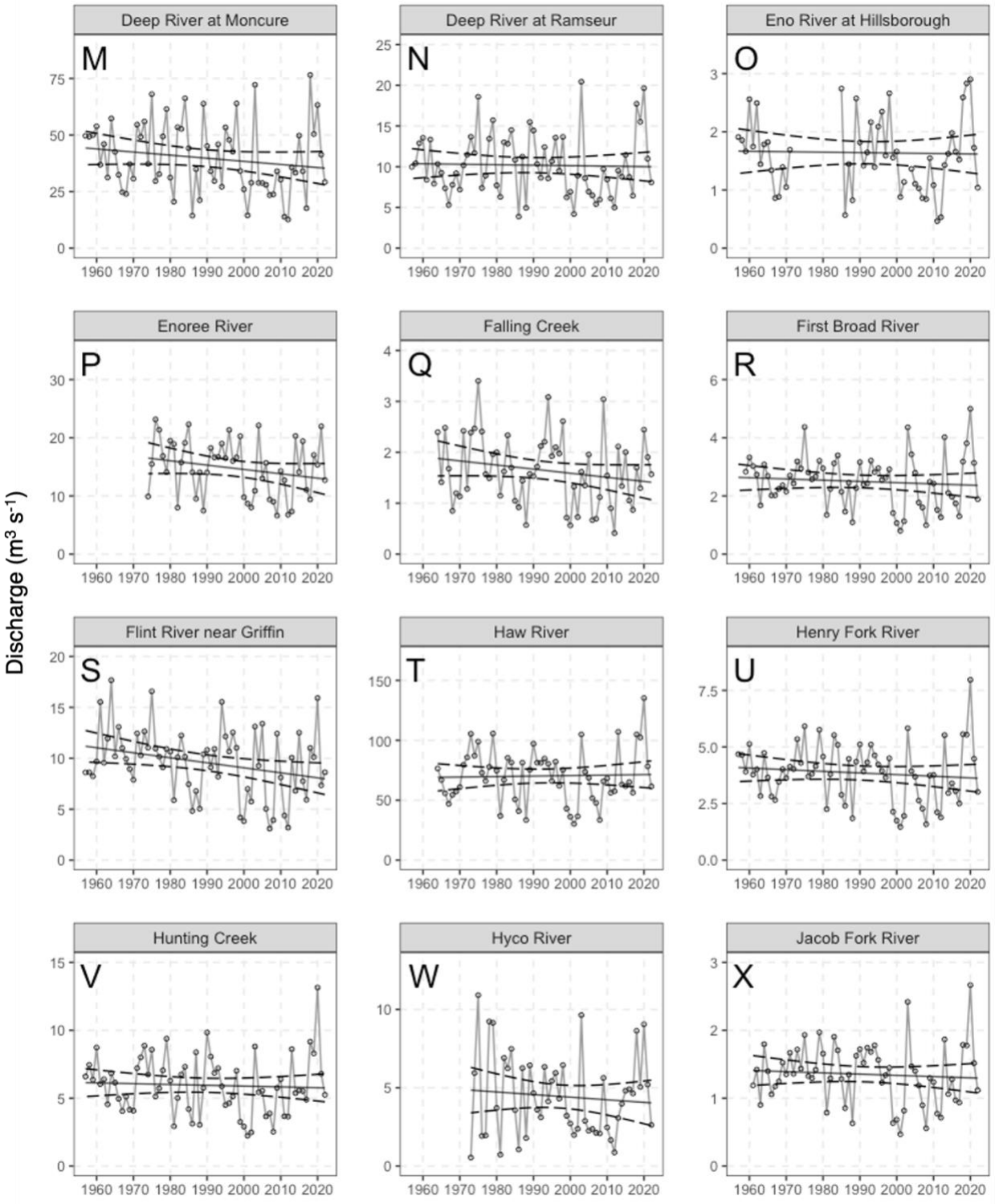
Deep River at Moncure
M
Deep River at Ramseur
N
Eno River at Hillsborough
O
Enoree River
P
Falling Creek
Q
First Broad River
R
Flint River near Griffin
S
Haw River
T
Henry Fork River
U
Hunting Creek
V
Hyco River
W
Jacob Fork River
X
Discharge (m3 s-1)
1960 1970 1980 1990 2000 2010 2020

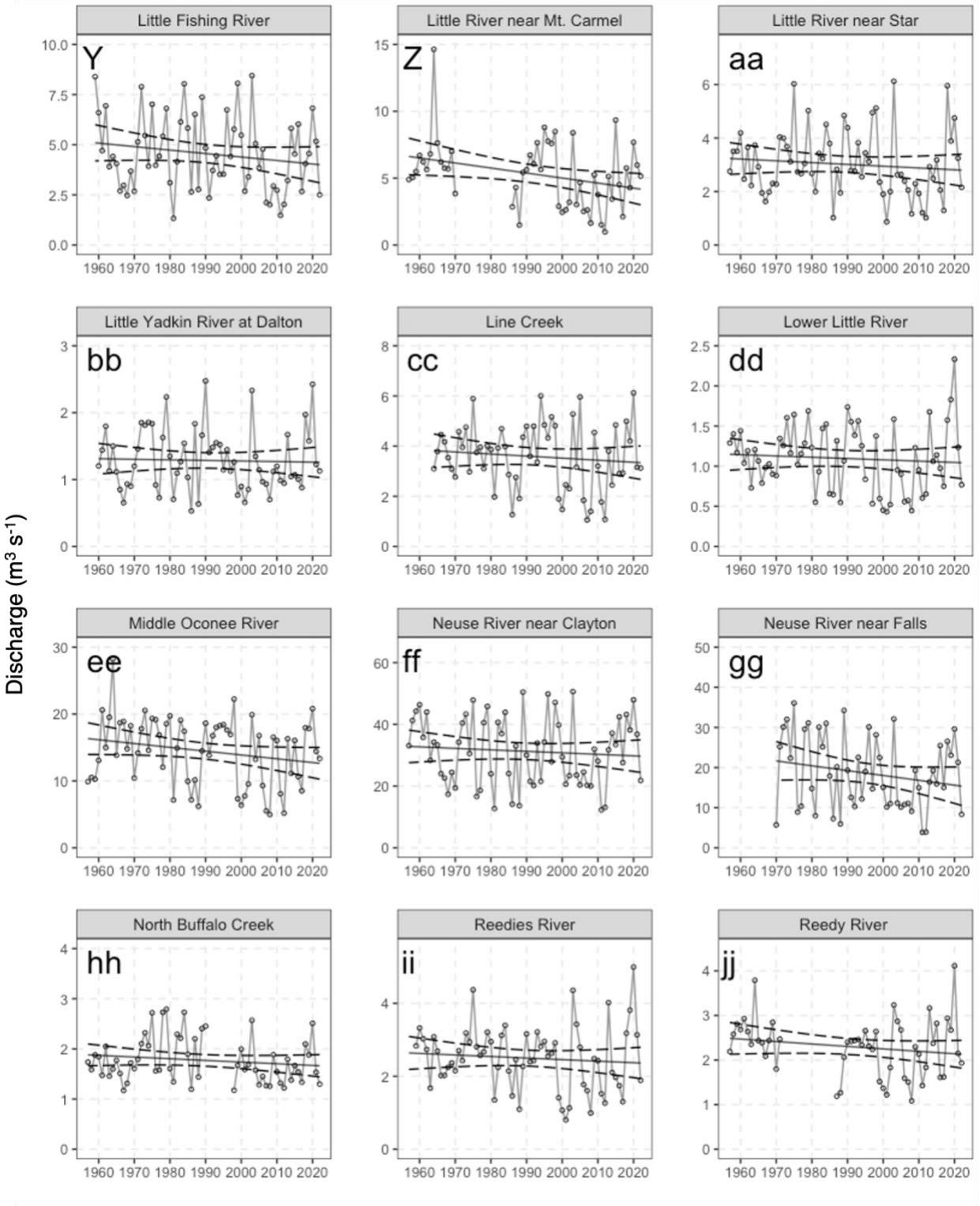
Little Fishing River
Y
Little River near Mt. Carmel
Z
Little River near Star
aa
Little Yadkin River at Dalton
bb
Line Creek
cc
Lower Little River
dd
Middle Oconee River
ee
Neuse River near Clayton
ff
Neuse River near Falls
gg
North Buffalo Creek
hh
Reedies River
ii
Reedy River
jj
Discharge (m3 s-1)
1960 1970 1980 1990 2000 2010 2020

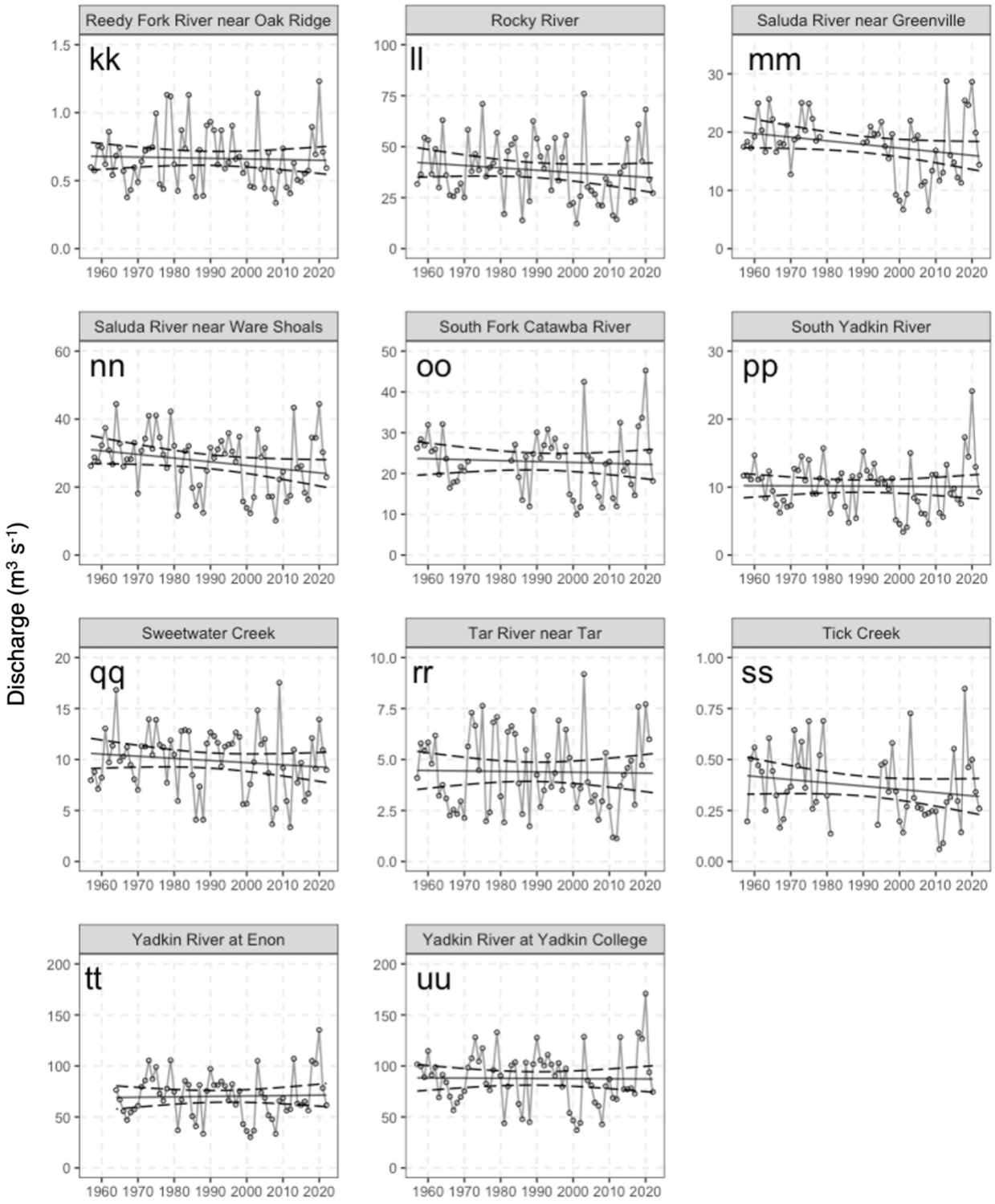
Reedy Fork River near Oak Ridge
kk
Rocky River
ll
Saluda River near Greenville
mm
Saluda River near Ware Shoals
nn
South Fork Catawba River
oo
South Yadkin River
pp
Sweetwater Creek
qq
Tar River near Tar
rr
Tick Creek
ss
Yadkin River at Enon
tt
Yadkin River at Yadkin College
uu
Discharge (m3 s-1)
1960 1970 1980 1990 2000 2010 2020

**Figure 4.D2:** Average annual discharge ($m^3$ $s^{-1}$) for sites in the Piedmont ecoregion that showed a decreasing trend. USGS gage number, GPS coordinates and Mann-Kendall results can be found in the table below.

**Table 4.D2:** Sites located in the Piedmont ecoregion that showed a decreasing trend including discharge plot tag, stream name, site name, USGS gage number, Mann-Kendall tau and p-value.

| Tag | Stream | Site | USGS Gage | Tau | p-value |
|---|---|---|---|---|---|
| A | Alcovy River | Covington | 02208450 | -0.08 | 0.40 |
| B | Broad River | Boiling Springs | 02151500 | -0.15 | 0.07 |
| C | Buckhorn Creek | Corinth | 02102192 | -0.15 | 0.12 |
| D | Chattahoochee River | Atlanta | 02336000 | -0.05 | 0.57 |
| E | Chattahoochee River | Cornelia | 02331600 | -0.07 | 0.39 |
| F | Chattahoochee River | Fairburn | 02337170 | -0.08 | 0.38 |
| G | Chattahoochee River | Norcross | 02335000 | -0.09 | 0.31 |
| H | Chattahoochee River | West Point | 02339500 | -0.05 | 0.59 |
| I | Chattahoochee River | Whitesburg | 02338000 | -0.07 | 0.44 |
| J | Chestatee River | Dahlonega | 02333500 | -0.05 | 0.57 |
| K | Cove Creek | Lake Lure | 02149000 | -0.05 | 0.58 |
| L | Dan River | Wentworth | 02071000 | -0.06 | 0.47 |
| M | Deep River | Moncure | 02102000 | -0.15 | 0.07 |
| N | Deep River | Ramseur | 02100500 | -0.07 | 0.41 |
| O | Eno River | Hillsborough | 02085000 | -0.08 | 0.42 |
| P | Enoree River | Whitemire | 02160700 | -0.16 | 0.09 |
| Q | Falling Creek | Juliette | 02212600 | -0.14 | 0.13 |
| R | First Broad River | Casar | 02152100 | -0.09 | 0.29 |
| S | Flint River | Griffin | 02344500 | -0.16 | 0.06 |
| T | Haw River | Bynum | 02096960 | -0.03 | 0.74 |
| U | Henry Fork | Henry River | 02143000 | -0.11 | 0.21 |
| V | Hunting Creek | Harmony | 02118500 | -0.08 | 0.34 |

| | | | | | |
|---|---|---|---|---|---|
| W | Hyco River | Mcgehees Mill | 02077303 | -0.05 | 0.63 |
| X | Jacob Fork | Ramsey | 02143040 | -0.08 | 0.38 |
| Y | Little Fishing River | White Oak | 02082950 | -0.11 | 0.20 |
| Z | Little River | Mt. Carmel | 02192500 | -0.16 | 0.09 |
| aa | Little River | Star | 02128000 | -0.10 | 0.22 |
| bb | Little Yadkin River | Dalton | 02114450 | -0.05 | 0.57 |
| cc | Line Creek | Senoia | 02344700 | -0.04 | 0.63 |
| dd | Lower Little River | Healing Springs | 02142000 | -0.08 | 0.37 |
| ee | Middle Oconee River | Athens | 02217500 | -0.15 | 0.08 |
| ff | Neuse River | Clayton | 02087500 | -0.06 | 0.47 |
| gg | Neuse River | Falls | 02087183 | -0.11 | 0.23 |
| hh | North Buffalo Creek | Greensboro | 02095500 | -0.10 | 0.26 |
| ii | Reedies River | North Wilkesboro | 02111500 | -0.06 | 0.47 |
| jj | Reedy River | Greenville | 02164000 | -0.11 | 0.26 |
| kk | Reedy Fork | Oak Ridge | 02093800 | -0.06 | 0.47 |
| ll | Rocky River | Norwood | 02126000 | -0.11 | 0.18 |
| mm | Saluda River | Greenville | 02162500 | -0.15 | 0.12 |
| nn | Saluda River | Ware Shoals | 02163500 | -0.14 | 0.09 |
| oo | South Fork Catawba | Lowell | 02145000 | -0.07 | 0.49 |
| pp | South Yadkin River | Mocksville | 02118000 | -0.07 | 0.44 |
| qq | Sweetwater Creek | Austell | 02337000 | -0.06 | 0.45 |
| rr | Tar River | Tar | 02081500 | -0.05 | 0.52 |
| ss | Tick Creek | Mt Vernon Springs | 02101800 | -0.14 | 0.14 |
| tt | Yadkin River | Enon | 02115360 | -0.04 | 0.69 |
| uu | Yadkin River | Yadkin College | 02116500 | -0.06 | 0.46 |

***No Change***

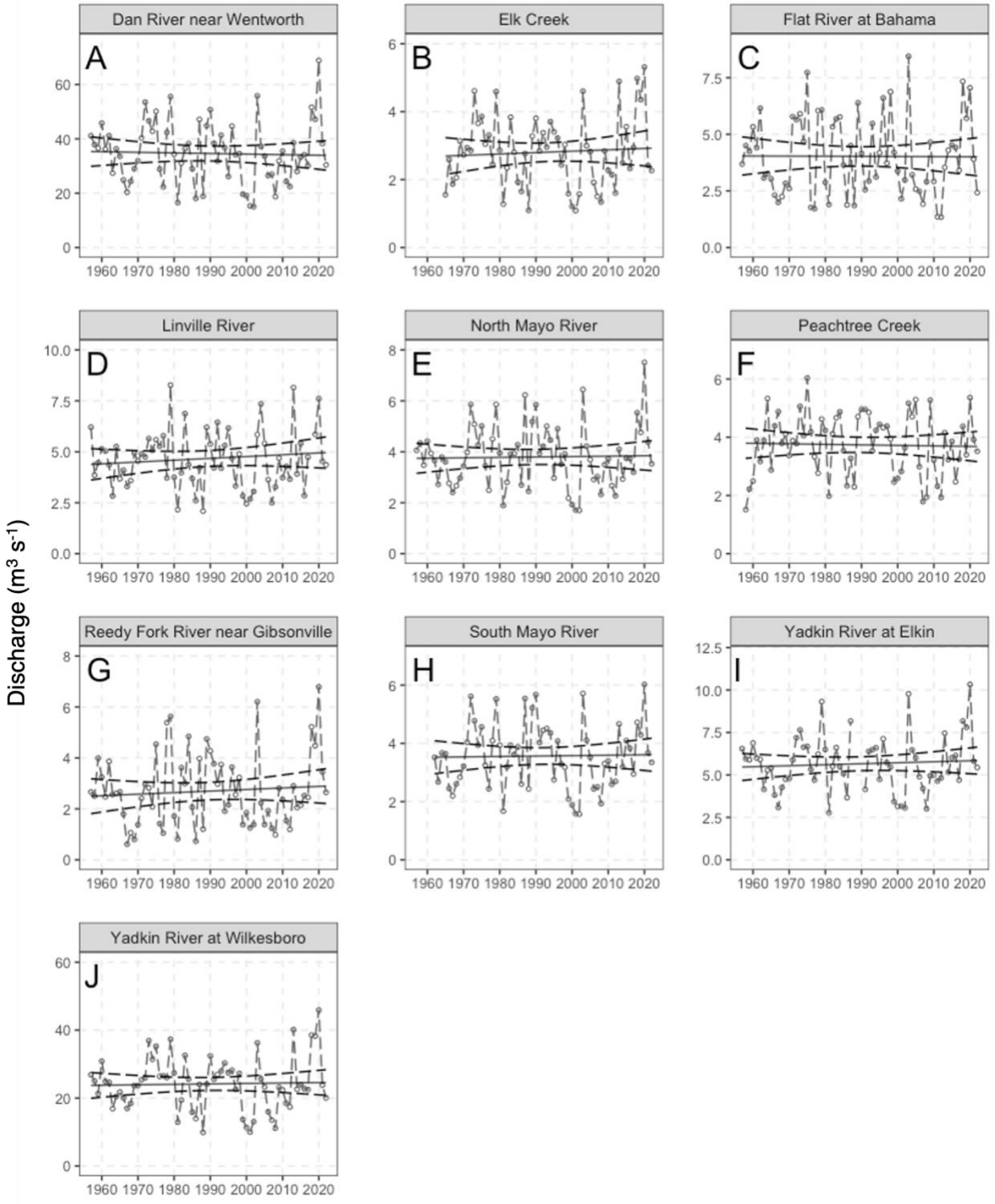
Dan River near Wentworth
A
Elk Creek
B
Flat River at Bahama
C
Linville River
D
North Mayo River
E
Peachtree Creek
F
Reedy Fork River near Gibsonville
G
South Mayo River
H
Yadkin River at Elkin
I
Yadkin River at Wilkesboro
J
Discharge (m³ s⁻¹)
1960 1970 1980 1990 2000 2010 2020

**Figure 4.D3:** Average annual discharge ($m^3$ $s^{-1}$) for sites in the Piedmont ecoregion that showed no changes. USGS gage number, GPS coordinates and Mann-Kendall results can be found in the table below.

**Table 4.D3:** Sites located in the Piedmont ecoregion that showed no changes including discharge plot tag, stream name, site name, USGS gage number, Mann-Kendall tau and p-value.

| Tag | Stream | Site | USGS Gage | Tau | p-value |
|---|---|---|---|---|---|
| A | Dan River | Fransisco | 02068500 | < 0.01 | 0.99 |
| B | Elk Creek | Elkville | 02111180 | < 0.01 | 0.99 |
| C | Flat River | Bahama | 02085500 | -0.02 | 0.86 |
| D | Linville River | Nebo | 02138500 | 0.02 | 0.79 |
| E | North Mayo River | Spencer | 02070000 | -0.02 | 0.82 |
| F | Peachtree Creek | Atlanta | 02336300 | -0.01 | 0.91 |
| G | Reedy Fork | Gibsonville | 02094500 | 0.02 | 0.86 |
| H | South Mayo River | Nettleridge | 02069700 | 0.02 | 0.80 |
| I | Yadkin River | Elkin | 02112250 | < 0.01 | 0.97 |
| J | Yadkin River | Wilkesboro | 02112000 | -0.02 | 0.84 |

***Increasing trend***

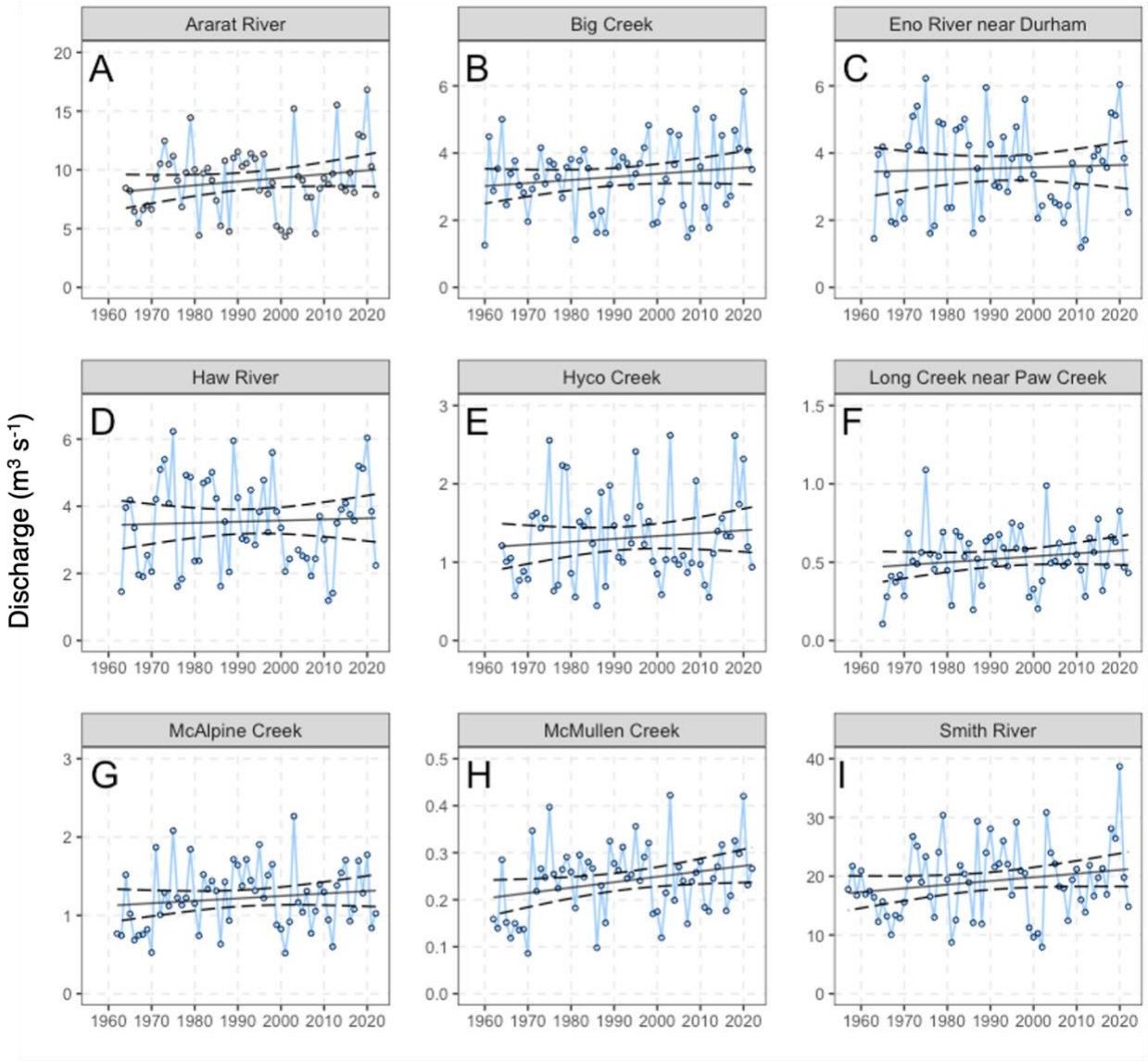


**Figure 4.D4:** Average annual discharge ($m^3$ $s^{-1}$) for sites in the Piedmont ecoregion that showed an increasing trend. USGS gage number, GPS coordinates and Mann-Kendall results can be found in the table below.

**Table 4.D4:** Sites located in the Piedmont ecoregion that showed an increasing trend including discharge plot tag, stream name, site name, USGS gage number, Mann-Kendall tau and p-value.

| Tag | Stream | Site | USGS Gage | Tau | p-value |
|---|---|---|---|---|---|
| A | Ararat River | Ararat | 02113850 | 0.09 | 0.30 |
| B | Big Creek | Alpharetta | 02335700 | 0.10 | 0.24 |
| C | Eno River | Durham | 02085070 | 0.03 | 0.74 |
| D | Haw River | Haw River | 02096500 | 0.05 | 0.58 |
| E | Hyco Creek | Leasburg | 02077200 | 0.06 | 0.49 |
| F | Long Creek | Paw Creek | 02142900 | 0.12 | 0.18 |
| G | Mcalpine Creek | Charlotte | 02146600 | 0.11 | 0.22 |
| H | McMullen Creek | Sharon View | 02146700 | 0.16 | 0.07 |
| I | Smith River | Eden | 02074000 | 0.10 | 0.25 |

***Significantly increasing***

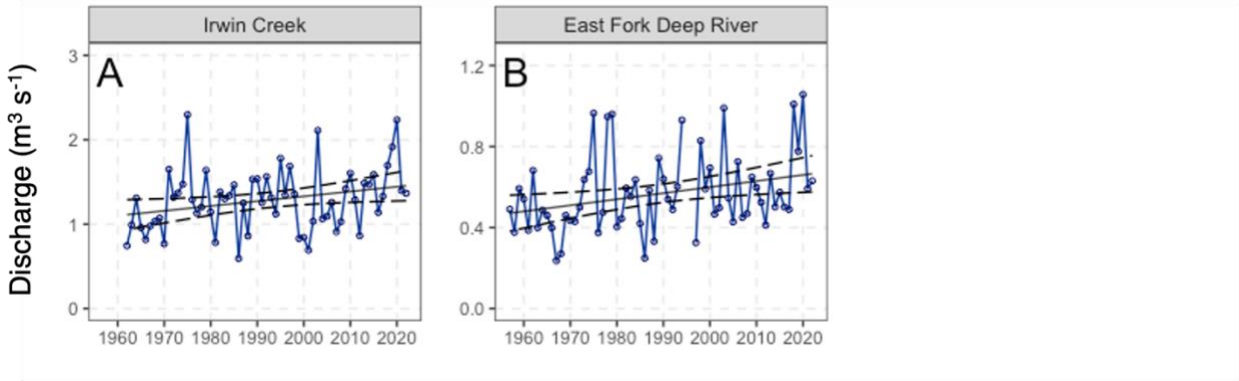


**Figure 4.D5:** Average annual discharge ($m^3$ $s^{-1}$) for sites in the Piedmont ecoregion that were significantly increasing. USGS gage number, GPS coordinates and Mann-Kendall results can be found in the table below.

**Table 4.D5:** Sites located in the Piedmont ecoregion that were significantly increasing including discharge plot tag, stream name, site name, USGS gage number, Mann-Kendall tau and p-value.

| Tag | Stream | Site | USGS Gage | Tau | p-value |
|---|---|---|---|---|---|
| A | Irwin Creek | Charlotte | 02146300 | 0.22 | 0.01 |
| B | East Fork Deep River | High Point | 02099000 | 0.23 | 0.01 |

**APPENDIX 4.E: Southeastern Plains ecoregion discharge plots**

***Significantly decreasing***

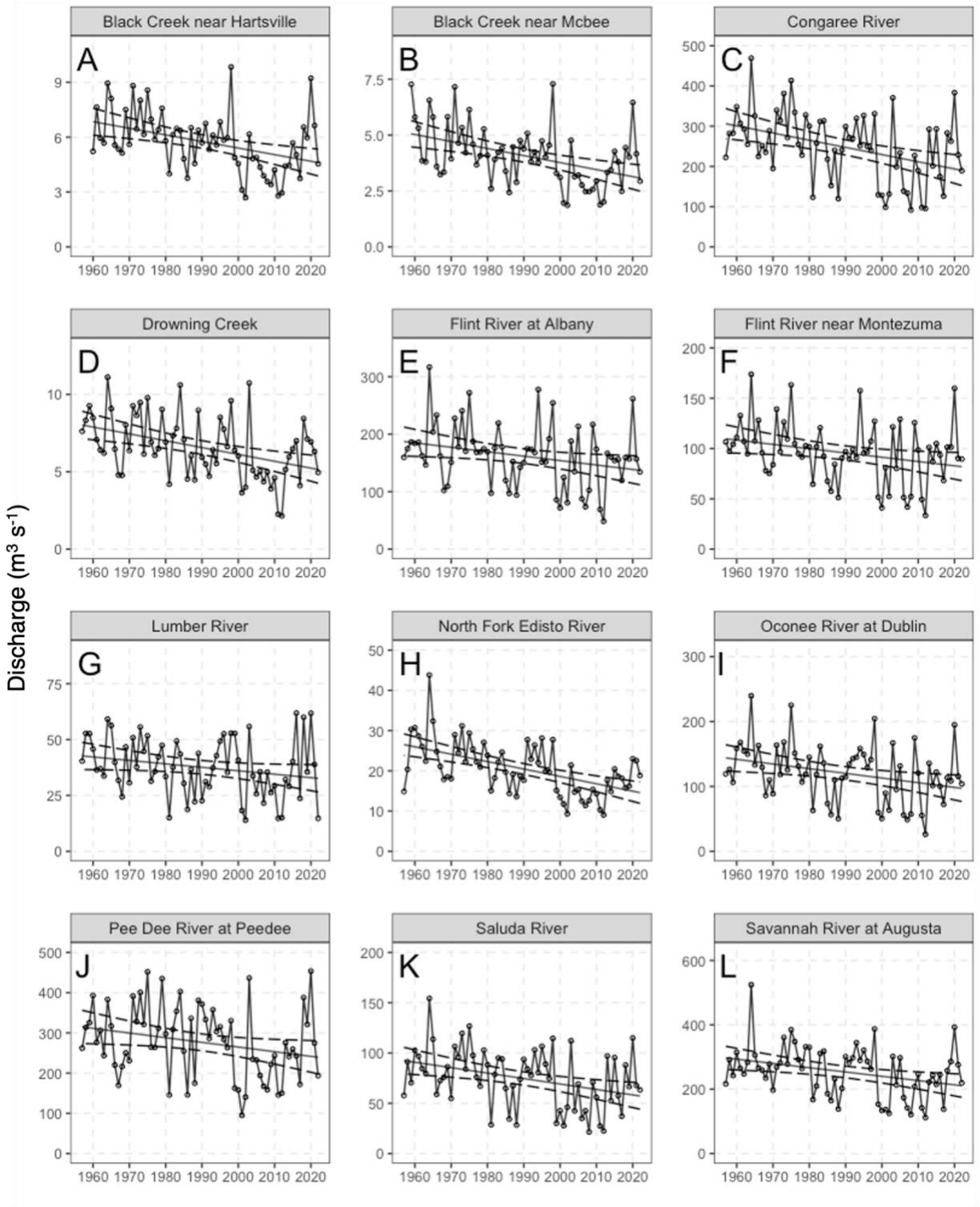

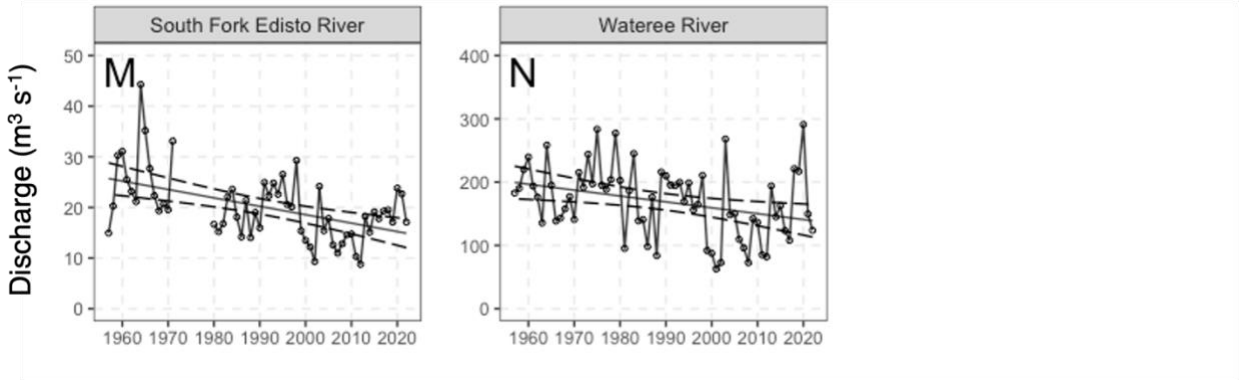


**Figure 4.E1:** Average annual discharge ($m^3$ $s^{-1}$) for sites in the Southeastern Plains ecoregion that were significantly decreasing. USGS gage number, GPS coordinates and Mann-Kendall results can be found in the table below.

**Table 4.E1:** Sites located in the Southeastern Plains ecoregion that were significantly decreasing including discharge plot tag, stream name, site name, USGS gage number, Mann-Kendall tau and p-value.

| Tag | Stream | Site | USGS Gage | Tau | p-value |
|---|---|---|---|---|---|
| A | Black Creek | McBee | 02130900 | -0.30 | < 0.01 |
| B | Black Creek | Hartsville | 02130910 | -0.30 | < 0.01 |
| C | Congaree River | Columbia | 02169500 | -0.27 | < 0.01 |
| D | Drowning Creek | Hoffman | 02133500 | -0.29 | < 0.01 |
| E | Flint River | Albany | 02352500 | -0.21 | 0.01 |
| F | Flint River | Montezuma | 02349605 | -0.21 | 0.01 |
| G | Lumber River | Broadman | 02134500 | -0.18 | 0.04 |
| H | North Fork Edisto River | Orangeburg | 02173500 | -0.36 | < 0.01 |
| I | Oconee River | Dublin | 02223500 | -0.22 | 0.01 |
| J | Pee Dee River | Pee Dee | 02131000 | -0.18 | 0.04 |
| K | Saluda River | Columbia | 02169000 | -0.23 | 0.01 |
| L | Savannah River | Augusta | 02197000 | -0.20 | 0.02 |

| | | | | | |
|---|---|---|---|---|---|
| M | South Fork Edisto River | Denmark | 02173000 | -0.29 | < 0.01 |
| N | Wateree River | Camden | 02148000 | -0.21 | 0.01 |

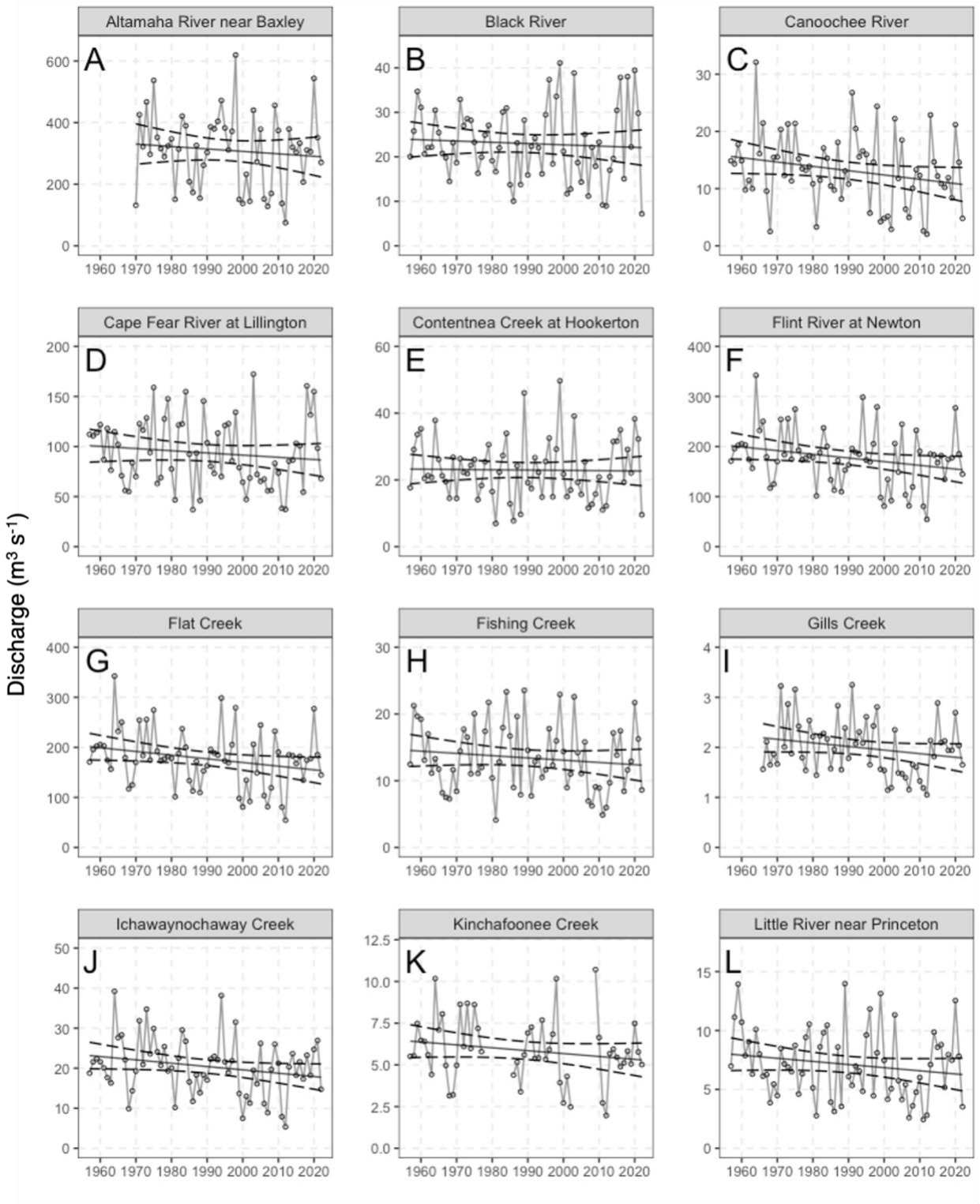
Altamaha River near Baxley
A
Black River
B
Canoochee River
C
Cape Fear River at Lillington
D
Contentnea Creek at Hookerton
E
Flint River at Newton
F
Flat Creek
G
Fishing Creek
H
Gills Creek
I
Ichawaynochaway Creek
J
Kinchafoonee Creek
K
Little River near Princeton
L
Discharge (m3 s-1)
1960 1970 1980 1990 2000 2010 2020

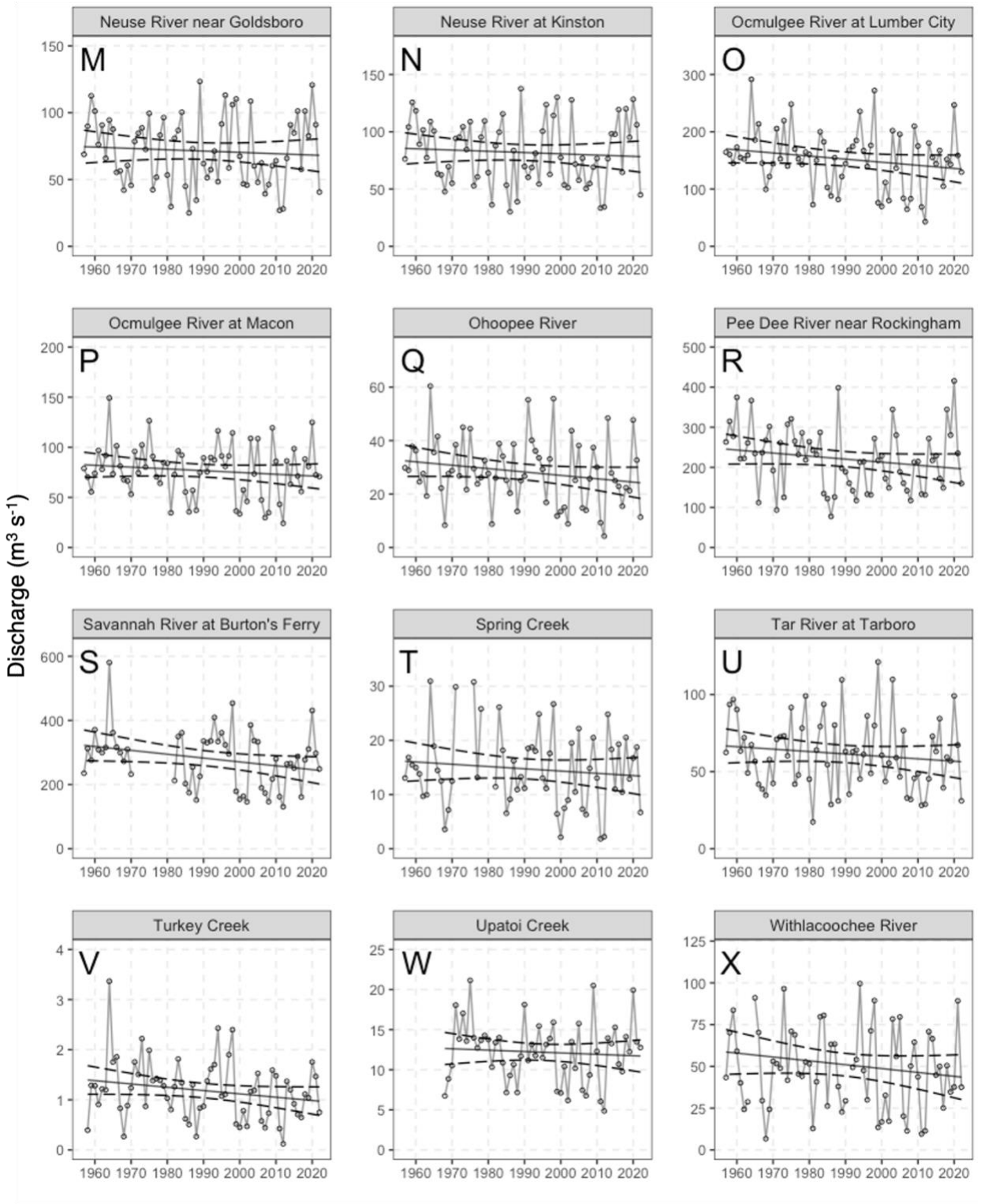
Neuse River near Goldsboro
M
Neuse River at Kinston
N
Ocmulgee River at Lumber City
O
Ocmulgee River at Macon
P
Ohoopee River
Q
Pee Dee River near Rockingham
R
Savannah River at Burton's Ferry
S
Spring Creek
T
Tar River at Tarboro
U
Turkey Creek
V
Upatoi Creek
W
Withlacoochee River
X
Discharge (m3 s-1)
1960 1970 1980 1990 2000 2010 2020

**Figure 4.E2:** Average annual discharge ($m^3$ $s^{-1}$) for sites in the Southeastern Plains ecoregion that showed a decreasing trend. USGS gage number, GPS coordinates and Mann-Kendall results can be found in the table below.

**Table 4.E2:** Sites located in the Southeastern Plains ecoregion that showed a decreasing trend including discharge plot tag, stream name, site name, USGS gage number, Mann-Kendall tau and p-value.

| Tag | Stream | Site | USGS Gage | Tau | p-value |
|---|---|---|---|---|---|
| A | Altamaha River | Baxley | 02225000 | -0.09 | 0.34 |
| B | Black River | Tomahawk | 02106500 | -0.09 | 0.31 |
| C | Canoochee River | Claxton | 02203000 | -0.16 | 0.06 |
| D | Cape Fear River | Lillington | 02102500 | -0.10 | 0.23 |
| E | Contentnea Creek | Hookerton | 02091500 | -0.03 | 0.68 |
| F | Flint River | Newton | 02353000 | -0.16 | 0.06 |
| G | Flat Creek | Inverness | 02102908 | -0.11 | 0.24 |
| H | Fishing Creek | Enfield | 02083000 | -0.10 | 0.24 |
| I | Gills Creek | Columbia | 02169570 | -0.14 | 0.12 |
| J | Ichawaynochaway Creek | Milford | 02353500 | -0.13 | 0.11 |
| K | Kinchafoonee Creek | Preston | 02350600 | -0.14 | 0.14 |
| L | Little River | Princeton | 02088500 | -0.13 | 0.11 |
| M | Neuse River | Goldsboro | 02089000 | -0.06 | 0.51 |
| N | Neuse River | Kinston | 02089500 | -0.06 | 0.45 |
| O | Ocmulgee River | Lumber City | 02215500 | -0.13 | 0.12 |
| P | Ocmulgee River | Macon | 02213000 | -0.07 | 0.43 |
| Q | Ohoopee River | Reidsville | 02225500 | -0.15 | 0.08 |
| R | Pee Dee River | Rockingham | 02129000 | -0.09 | 0.30 |
| S | Savannah River | Burton’s Ferry | 02197500 | -0.17 | 0.07 |
| T | Spring Creek | Iron City | 02357000 | -0.07 | 0.43 |
| U | Tar River | Tarboro | 02083500 | -0.10 | 0.23 |
| V | Turkey Creek | Byromville | 02349900 | -0.13 | 0.12 |

| | | | | | |
|---|---|---|---|---|---|
| W | Upatoi Creek | Columbus | 02341800 | -0.06 | 0.51 |
| X | Withlacoochee River | Pinetta | 02319000 | -0.10 | 0.24 |

***No Change***

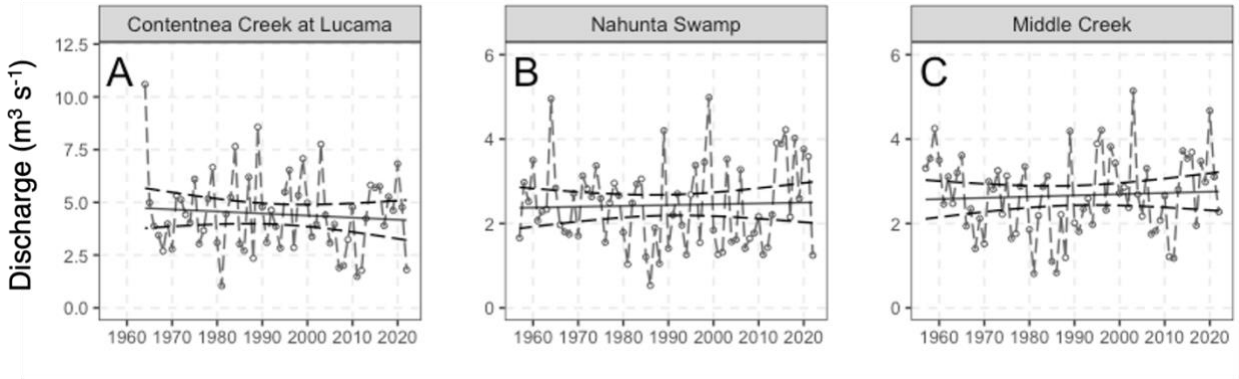


**Figure 4.E3:** Average annual discharge ($m^3$ $s^{-1}$) for sites in the Southeastern Plains ecoregion that showed no changes. USGS gage number, GPS coordinates and Mann-Kendall results can be found in the table below.

**Table 4.E3:** Sites located in the Southeastern Plains ecoregion that showed no changes including discharge plot tag, stream name, site name, USGS gage number, Mann-Kendall tau and p-value.

| Tag | Stream | Site | USGS Gage | Tau | p-value |
|---|---|---|---|---|---|
| NC | Contentnea Creek | Lucama | 02090380 | -0.01 | 0.89 |
| NC | Nahunta Swamp | Shine | 02091000 | < 0.01 | 0.98 |
| NC | Middle Creek | Clayton | 02088000 | 0.01 | 0.89 |

***Increasing trend***

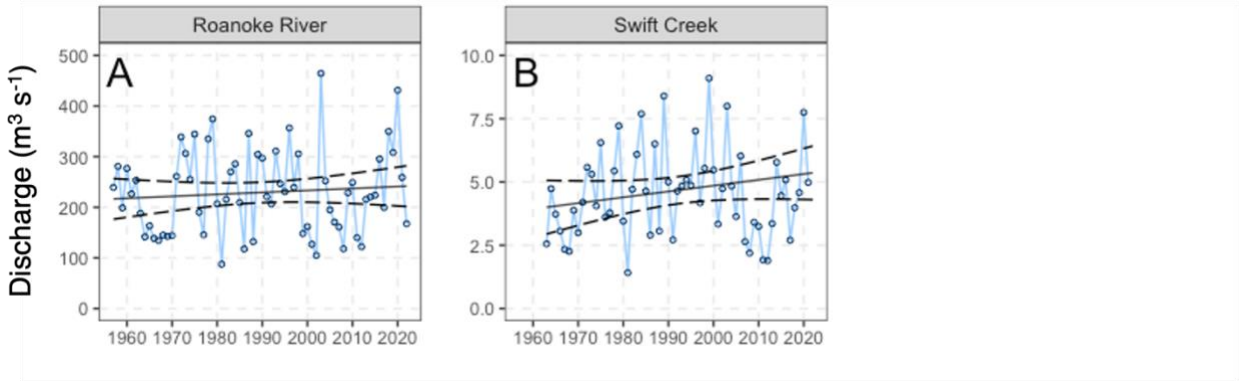


**Figure 4.E4:** Average annual discharge ($m^3$ $s^{-1}$) for sites in the Southeastern Plains ecoregion that showed increasing trend. USGS gage number, GPS coordinates and Mann-Kendall results can be found in the table below.

**Table 4.E4:** Sites located in the Southeastern Plains ecoregion that showed an increasing trend including discharge plot tag, stream name, site name, USGS gage number, Mann-Kendall tau and p-value.

| Tag | Stream | Site | USGS Gage | Tau | p-value |
|---|---|---|---|---|---|
| A | Roanoke River | Roanoke Rapids | 02080500 | 0.04 | 0.63 |
| B | Swift Creek | Hilliardston | 02082770 | 0.08 | 0.35 |

***Significantly increasing***

None

**APPENDIX 4.F: Coast ecoregion discharge plots**

***Significantly decreasing***

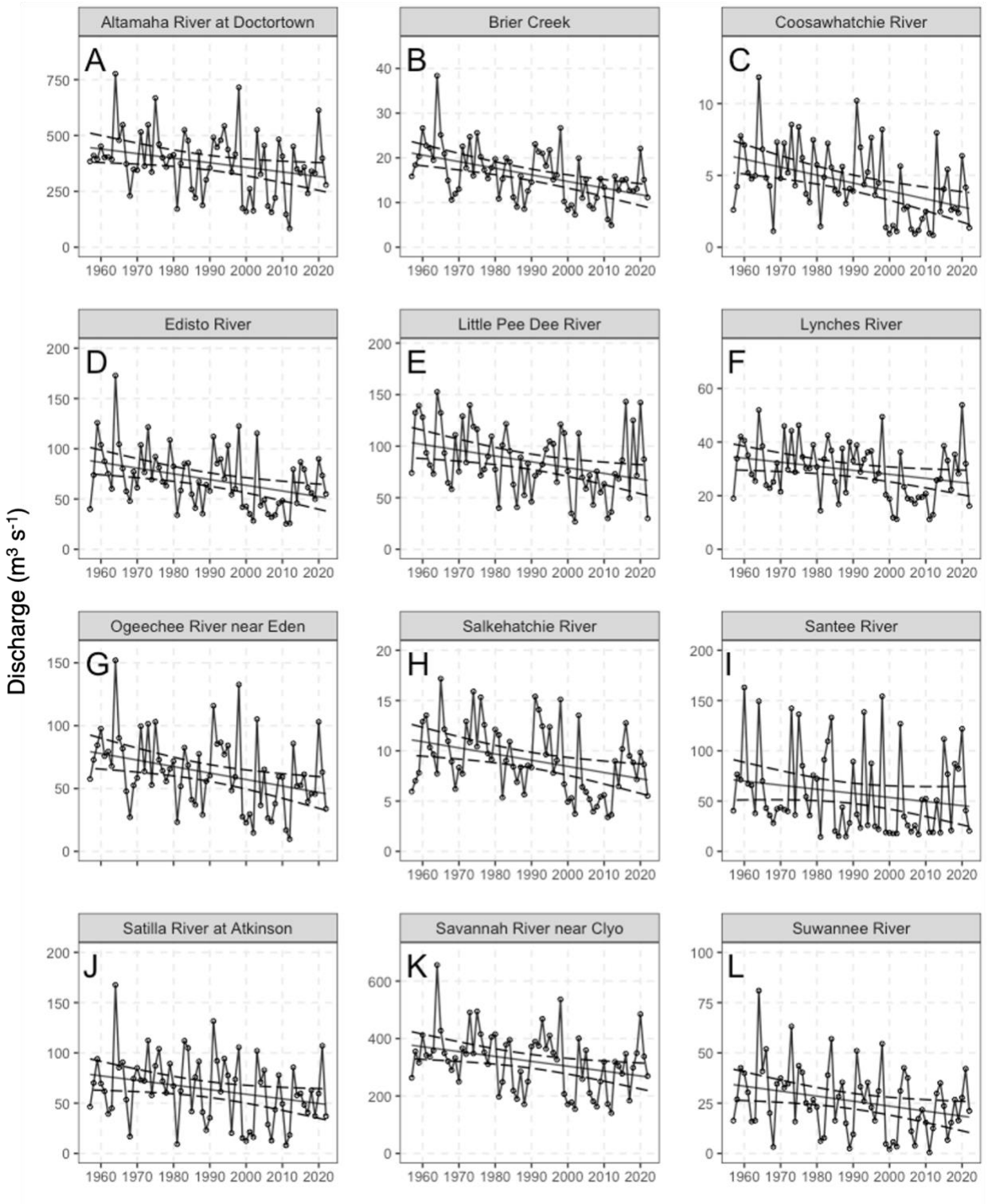

**Figure 4.F1:** Average annual discharge ($m^3$ $s^{-1}$) for sites in the Coast ecoregion that were significantly decreasing. USGS gage number, GPS coordinates and Mann-Kendall results can be found in the table below.

**Table 4.F1:** Sites located in the Coast ecoregion that were significantly decreasing including discharge plot tag, stream name, site name, USGS gage number, Mann-Kendall tau and p-value.

| Tag | Stream | Site | USGS Gage | Tau | p-value |
|---|---|---|---|---|---|
| A | Altamaha River | Doctortown | 02226000 | -0.19 | 0.02 |
| B | Brier Creek | Millhaven | 02198000 | -0.32 | < 0.01 |
| C | Coosawhatchie River | Hampton | 02176500 | -0.30 | < 0.01 |
| D | Edisto River | Givhans | 02175000 | -0.25 | < 0.01 |
| E | Little Pee Dee River | Galivants | 02135000 | -0.24 | < 0.01 |
| F | Lynches River | Effingham | 02132000 | -0.20 | 0.02 |
| G | Ogeechee River | Eden | 02202500 | -0.24 | 0.01 |
| H | Salkehatchie River | Miley | 02175500 | -0.26 | < 0.01 |
| I | Santee River | Pineville | 02171500 | -0.17 | 0.04 |
| J | Satilla River | Atkinson | 02228000 | -0.16 | 0.05 |
| K | Savannah River | Clyo | 02198500 | -0.21 | 0.01 |
| L | Suwannee River | Fargo | 02314500 | -0.18 | 0.03 |

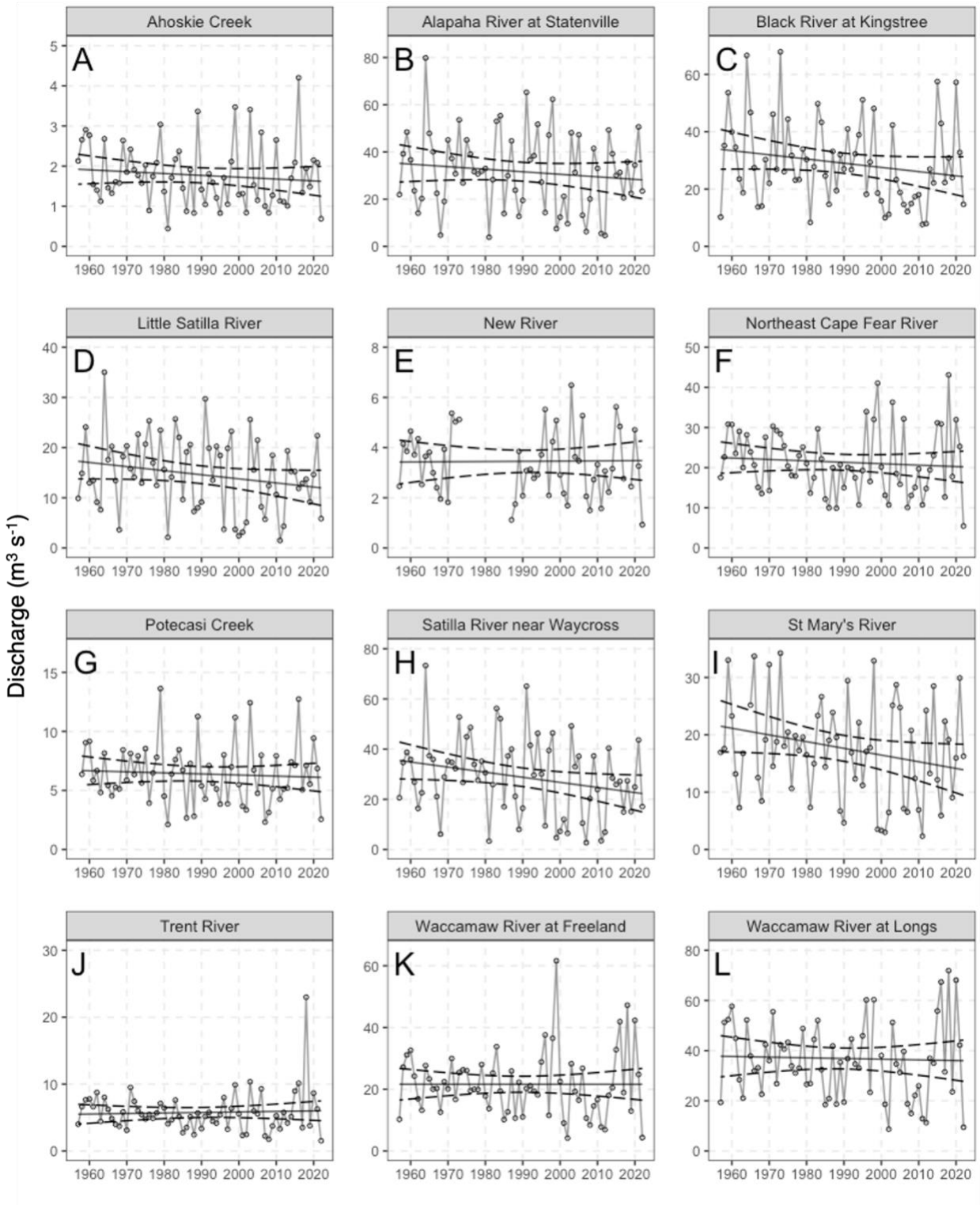


**Figure 4.F2:** Average annual discharge ($m^3$ $s^{-1}$) for sites in the Coast ecoregion that showed a decreasing trend. USGS gage number, GPS coordinates and Mann-Kendall results can be found in the table below.

**Table 4.F2:** Sites located in the Coast ecoregion that showed a decreasing trend including discharge plot tag, stream name, site name, USGS gage number, Mann-Kendall tau and p-value.

| Tag | Stream | Site | USGS Gage | Tau | p-value |
|---|---|---|---|---|---|
| A | Ahoskie Creek | Ahoskie | 02053500 | -0.13 | 0.11 |
| B | Alapaha River | Statenville | 02317500 | -0.08 | 0.38 |
| C | Black River | Kingstree | 02136000 | -0.15 | 0.08 |
| D | Little Satilla River | Offerman | 02227500 | -0.12 | 0.14 |
| E | New River | Gum Branch | 02093000 | -0.05 | 0.58 |
| F | Northeast Cape Fear River | Chinquapin | 02108000 | -0.13 | 0.13 |
| G | Potecasi Creek | Union | 02053200 | -0.08 | 0.32 |
| H | Satilla River | Waycross | 02226500 | -0.15 | 0.08 |
| I | St Mary's River | Macclenny | 02231000 | -0.14 | 0.10 |
| J | Trent River | Trenton | 02092500 | -0.09 | 0.28 |
| K | Waccamaw River | Freeland | 02109500 | -0.10 | 0.26 |
| L | Waccamaw River | Longs | 02110500 | -0.08 | 0.36 |

***No Change***

None

***Increasing Trend***

None

***Significantly increasing***

None

# CHAPTER 5 APPENDICIES

## APPENDIX 5.A:

**Table 5.1:** Number of samples (n) and average Mann-Kendall slope ± standard error (SE) for temperature maximum (°C), temperature minimum (°C), population density (# individuals/km$^2$), elevation (m above sea level) and groundwater level (depth (m) to water level) for individual basins in the South Atlantic-Gulf Drainage.

| Basin | TMAX | | TMIN | | Population | | Elevation | | Groundwater | |
|---|---|---|---|---|---|---|---|---|---|---|
| | n | average | n | average | n | average | n | average | n | average |
| Alabama | 11 | 0.02 ± 0.08 | 11 | 0.32 ± 0.03 | 1 | 1.00 | 5 | 47.2 ± 7.8 | – | – |
| Albemarle-Chowan | 14 | 0.20 ± 0.06 | 14 | 0.38 ± 0.04 | 1 | 0.86 | 11 | 33.1 ± 9.8 | 17 | –0.10 ± 0.09 |
| Altamaha | 13 | 0.20 ± 0.07 | 13 | 0.12 ± 0.06 | 1 | 1.00 | 11 | 81.7 ± 20.2 | 9 | –0.64 ± 0.09 |
| Apalachicola | 32 | 0.09 ± 0.05 | 32 | 0.15 ± 0.04 | 1 | 1.00 | 26 | 153.8 ± 21.9 | 53 | –0.18 ± 0.04 |
| Aucilla-Waccasassa | 4 | 0.11 ± 0.03 | 4 | 0.26 ± 0.03 | 1 | 1.00 | 4 | 12.5 ± 5.9 | 5 | –0.52 ± 0.17 |
| Black Warrior-Tombigbee | 34 | 0.10 ± 0.04 | 34 | 0.36 ± 0.03 | 1 | 1.00 | 14 | 93.0 ± 13.1 | 1 | 0.16 ± NA |
| Cape Fear | 19 | 0.21 ± 0.03 | 19 | 0.33 ± 0.04 | 1 | 1.00 | 14 | 119.9 ± 22.4 | 4 | –0.31 ± 0.18 |

| | | | | | | | | | | |
|---|---|---|---|---|---|---|---|---|---|---|
| Choctawhatchee | 7 | 0.19 ± 0.07 | 7 | 0.17 ± 0.06 | 1 | 1.00 | 4 | 41.0 ± 19.2 | 1 | – |
| Coosa-Tallapoosa | 24 | 0.11 ± 0.03 | 24 | 0.31± 0.04 | 1 | 1.00 | 19 | 197.5 ± 13.5 | 1 | –0.36 ± NA |
| East Florida Coastal | 7 | 0.24 ± 0.09 | 7 | 0.40 ± 0.07 | 1 | 1.00 | 5 | 8.8 ± 2.6 | 2 | –0.43 ± 0.07 |
| Escambia | 8 | 0.02 ± 0.05 | 8 | 0.03 ± 0.08 | 1 | 1.00 | 4 | 53.8 ± 13.6 | – | – |
| Florida Panhandle Coastal | 8 | 0.24 ± 0.06 | 8 | 0.18 ± 0.07 | 1 | 1.00 | 6 | 16.8 ± 3.7 | – | – |
| Kissimmee | 7 | 0.30 ± 0.07 | 7 | 0.21 ± 0.06 | 1 | 1.00 | 12 | 24.3 ± 2.7 | 2 | –0.06 ± 0.26 |
| Lower Pee Dee | 23 | 0.13 ± 0.05 | 23 | 0.32 ± 0.03 | 1 | 1.00 | 11 | 32.5 ± 8.2 | 5 | 0.08 ± 0.19 |
| Mobile Bay-Tombigbee | 8 | 0.07 ± 0.06 | 8 | 0.13 ± 0.10 | 1 | 1.00 | 5 | 21.2 ± 5.6 | – | – |
| Neuse | 15 | 0.19 ± 0.05 | 15 | 0.27 ± 0.06 | 1 | 1.00 | 13 | 54.6 ± 13.5 | 4 | –0.16 ± 0.21 |
| Ochlockonee | 2 | 0.39 ± 0.07 | 2 | 0.17 ± 0.15 | 1 | 1.00 | 5 | 21.2 ± 5.6 | 2 | 0.08 ± 0.16 |
| Ogeechee | 6 | 0.22 ± 0.08 | 6 | 0.13 ± 0.12 | 1 | 1.00 | 2 | 20.5 ± 11.5 | 9 | –0.42 ± 0.12 |
| Onslow Bay | – | – | – | – | 1 | 0.93 | 1 | 2.0 ± NA | 1 | 0.43 ± NA |
| Pamlico | 10 | 0.16 ± 0.05 | 10 | 0.30 ± 0.07 | 1 | 0.93 | 6 | 47.5 ± 12.2 | 2 | 0.01 ± 0.11 |
| Pascagoula | 11 | 0.05 ± 0.08 | 11 | 0.17 ± 0.06 | 1 | 1.00 | 17 | 48.8 ± 7.6 | 1 | 0.23 ± 0.05 |
| Peace | 4 | 0.33 ± 0.05 | 4 | 0.40 ± 0.04 | 1 | 1.00 | 12 | 15.8 ± 2.9 | 36 | –0.21 ± 0.05 |

| | | | | | | | | | | |
|---|---|---|---|---|---|---|---|---|---|---|
| Pearl | 12 | 0.02 ± 0.05 | 12 | 0.10 ± 0.04 | 1 | 1.00 | 8 | 82.3 ± 10.9 | – | – |
| Roanoke | 28 | 0.12 ± 0.04 | 28 | 0.30 ± 0.03 | 1 | 0.93 | 29 | 198.4 ± 17.7 | 1 | –0.49 ± NA |
| Santee | 39 | 0.15 ± 0.04 | 39 | 0.35 ± 0.02 | 1 | 1.00 | 5 | 188.5 ± 7.5 | 2 | –0.32 ± 0.15 |
| Savannah | 23 | 0.14 ± 0.05 | 23 | 0.29 ± 0.04 | 1 | 1.00 | 30 | 153.2 ± 64.6 | 26 | –0.07 ± 0.07 |
| S. Edisto-SC Coastal | 14 | 0.30 ± 0.05 | 14 | 0.28 ± 0.05 | 1 | 1.00 | 9 | 39.0 ± 7.5 | 8 | –0.41 ± 0.18 |
| Southern Florida | 19 | 0.25± 0.03 | 19 | 0.39 ± 0.03 | 1 | 0.86 | 11 | 7.2 ± 1.3 | 132 | –0.02 ± 0.03 |
| St. Johns | 7 | 0.00 ± 0.10 | 7 | 0.29 ± 0.06 | 1 | 1.00 | 16 | 14.4 ± 2.3 | 12 | –0.34 ± 0.09 |
| St. Marys-Satilla | 11 | 0.19 ± 0.05 | 11 | 0.26 ± 0.05 | 1 | 1.00 | 5 | 20.0 ± 3.8 | 23 | 0.08 ± 0.10 |
| Suwannee | 13 | 0.06 ± 0.06 | 13 | 0.09 ± 0.05 | 1 | 1.00 | 10 | 25.3 ± 3.8 | – | – |
| Tampa Bay | 15 | 0.16 ± 0.07 | 15 | 0.32 ± 0.06 | 1 | 1.00 | 33 | 19.9 ± 1.6 | 30 | -0.16 ± 0.05 |
| Upper Pee Dee | 15 | 0.03± 0.05 | 15 | 0.25 ± 0.06 | 1 | 1.00 | 13 | 243.2 ± 23.8 | 2 | 0.01 ± 0.11 |

**Table 5.2**: Number of samples (n) and average Mann-Kendall streamflow slope (τ) ± standard error (SE) for ecoregions in individual basins. Ecoregions included the Plains (EPA ecoregion 8.3; n = 213), Coastal Plains (EPA ecoregion 8.5; n = 124), Appalachian Forests (EPA ecoregion 8.4; n = 28) and Everglades (EPA ecoregion 15.4; n = 9).

| Basin | Ecoregion | n | Discharge |
|---|---|---|---|
| Alabama | Plains | 5 | –0.01 ± 0.03 |
| Albemarle-Chowan | Coastal Plains | 4 | –0.10 ± 0.03 |
| | Plains | 7 | –0.08 ± 0.01 |
| Altamaha | Coastal Plains | 1 | –0.19 ± NA |
| | Plains | 10 | –0.14 ± 0.02 |
| Apalachicola | Plains | 26 | –0.10 ± 0.02 |
| Aucilla-Waccasassa | Coastal Plains | 4 | –0.08 ± 0.02 |
| Black Warrior-Tombigbee | Appalachian Forests | 5 | 0.08 ± 0.02 |
| | Plains | 9 | –0.03 ± 0.03 |
| Cape Fear | Coastal Plains | 1 | –0.13 ± NA |
| | Plains | 13 | –0.05 ± 0.03 |
| Choctawhatchee | Coastal Plains | 1 | –0.04 ± NA |
| | Plains | 3 | –0.06 ± 0.02 |
| Coosa-Tallapoosa | Appalachian Forests | 15 | –0.02 ± 0.02 |
| | Plains | 4 | –0.08 ± 0.05 |
| East Florida Coastal | Coastal Plains | 5 | 0.00 ± 0.10 |
| Escambia | Plains | 4 | –0.06 ± 0.02 |
| Florida Panhandle Coastal | Coastal Plains | 1 | 0.03 ± NA |

| | | | |
|---|---|---|---|
| | Plains | 5 | 0.00 ± 0.01 |
| Kissimmee | Coastal Plains | 12 | 0.26 ± 0.04 |
| Lower Pee Dee | Coastal Plains | 5 | –0.15 ± 0.03 |
| | Plains | 6 | –0.22 ± 0.04 |
| Mobile Bay-Tombigbee | Plains | 5 | 0.04 ± 0.02 |
| Neuse | Coastal Plains | 1 | –0.09 ± NA |
| | Plains | 12 | –0.04 ± 0.01 |
| Ochlockonee | Coastal Plains | 3 | –0.13 ± 0.01 |
| | Plains | 2 | –0.14 ± 0.03 |
| Ogeechee | Coastal Plains | 1 | –0.24 ± NA |
| | Plains | 1 | –0.16 ± NA |
| Onslow Bay | Coastal Plains | 1 | –0.05 ± NA |
| Pamlico | Plains | 6 | –0.10 ± 0.05 |
| Pascagoula | Coastal Plains | 4 | –0.03 ± 0.03 |
| | Plains | 13 | 0.07 ± 0.01 |
| Peace | Coastal Plains | 12 | 0.04 ± 0.03 |
| Pearl | Plains | 8 | 0.04 ± 0.02 |
| Roanoke | Appalachian Forests | 5 | 0.11 ± 0.01 |
| | Plains | 22 | 0.04 ± 0.01 |
| S. Edisto-SC Coastal | Coastal Plains | 1 | –0.25 ± NA |
| | Plains | 4 | –0.30 ± 0.02 |
| Santee | Appalachian Forests | 2 | –0.10 ± 0.12 |
| | Plains | 28 | –0.13 ± 0.03 |

| | | | |
|---|---|---|---|
| Savannah | Coastal Plains | 5 | –0.19 ± 0.02 |
| | Plains | 4 | –0.14 ± 0.02 |
| Southern Florida | Coastal Plains | 2 | 0.25 ± 0.08 |
| | Everglades | 9 | 0.18 ± 0.04 |
| St. Johns | Coastal Plains | 16 | –0.05 ± 0.04 |
| St. Marys-Satilla | Coastal Plains | 5 | –0.14 ± 0.01 |
| Suwannee | Coastal Plains | 6 | –0.17 ± 0.02 |
| | Plains | 4 | –0.15 ± 0.02 |
| Tampa Bay | Coastal Plains | 33 | –0.07 ± 0.03 |
| Upper Pee Dee | Appalachian Forests | 1 | –0.06 ± NA |
| | Plains | 12 | –0.04 ± 0.02 |

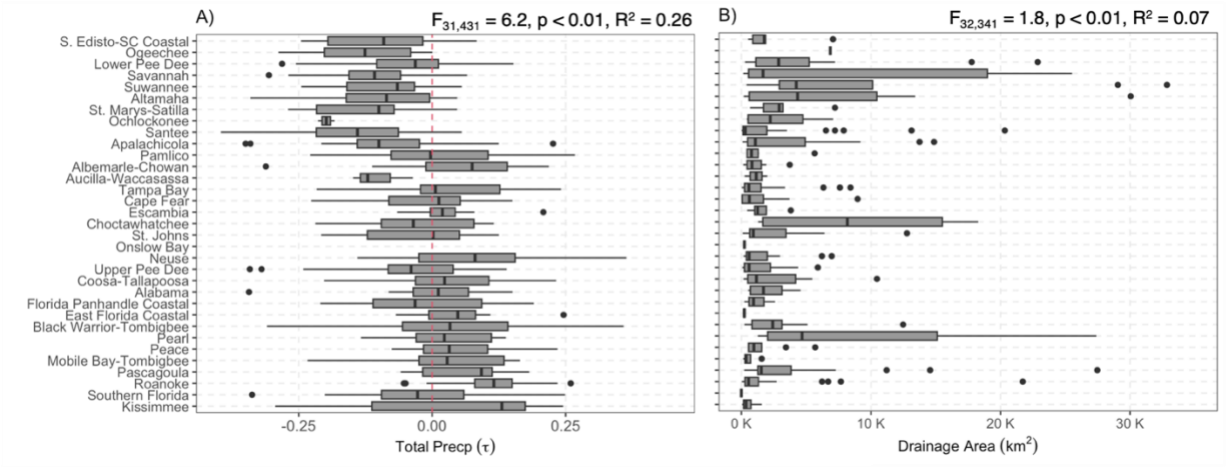


**Figure 5.1:** A) Mann-Kendall total precipitation slope (τ) and B) drainage area (km$^2$) for drainage basins from 1957 – 2022. Box and whisker plots indicate that the bottom and top of each box are the 25$^{th}$ and 75$^{th}$ percentiles and the line in the middle of each box is the median, whiskers extend above and below each box to 1.5 times the interquartile range, and observations beyond the whisker length are marked as outliers with an individual symbol. ANOVA indicated a significant difference for A) total precipitation slope ($F_{31,432}$ =6.2, $p < 0.01$) and B) drainage area ($F_{32,326}$ = 1.8, $p < 0.01$).

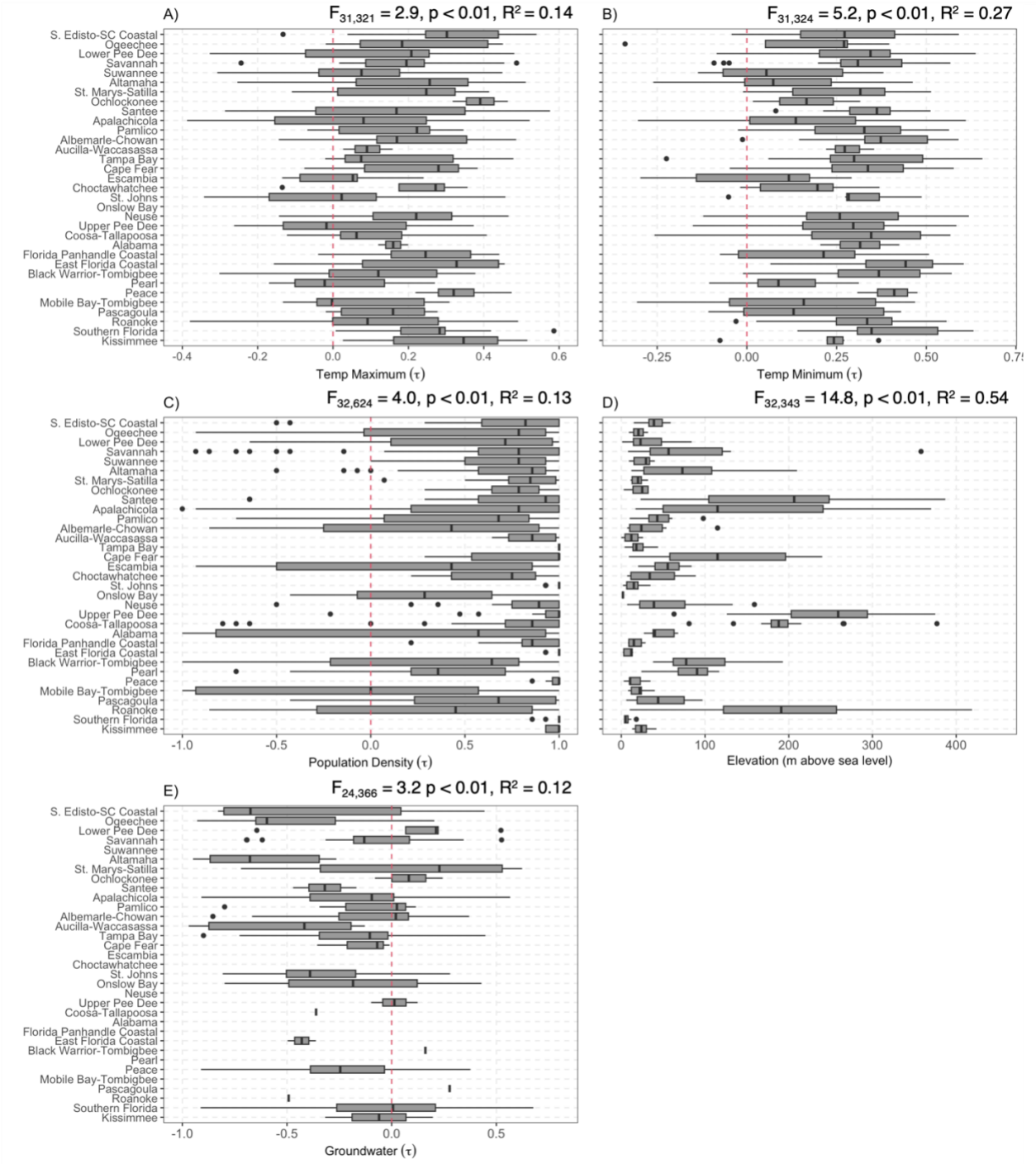


**Figure 5.2:** Mann-Kendall A) Temperature maximum slope (τ), B) temperature minimum slope (τ), C) population density slope (τ), D) elevation (m above sea level) and E) groundwater slope (τ) for drainage basins from 1957 – 2022. Box and whisker plots indicate that the bottom and top

of each box are the 25$^{th}$ and 75$^{th}$ percentiles and the line in the middle of each box is the median, whiskers extend above and below each box to 1.5 times the interquartile range, and observations beyond the whisker length are marked as outliers with an individual symbol. ANOVA indicated a significant difference for A) temperature maximum slope ($F_{31,324}$ =5.2, $p < 0.01$), B) temperature minimum slope ($F_{31, 321}$ = 2.9, $p < 0.01$), C) population density slope ($F_{32,624}$ = 4.3, $p < 0.01$), D) elevation ($F_{32,343}$ = 14.8, $p < 0.01$) and E) groundwater slope ($F_{24,366}$ = 3.2, $p < 0.01$).

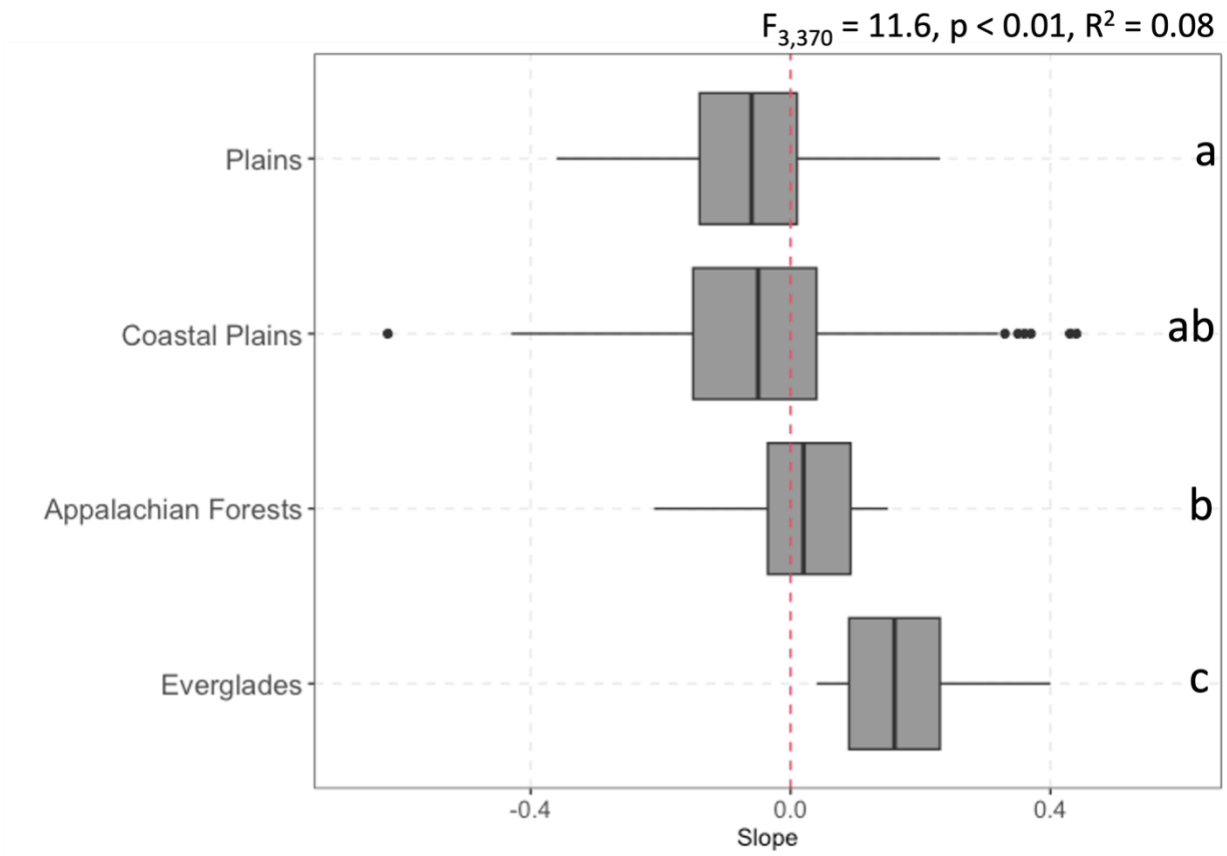


**Figure 5.3:** Mann-Kendall discharge slope (τ) for ecoregions in the South Atlantic-Gulf Drainage (HUC – 03) from 1957 – 2022. Ecoregions included EPA Southeastern USA Plains (Plains, n = 213), Mississippi Alluvial and Southeastern USA Coastal Plains (Coastal Plains, n = 124), Appalachian Forests (n =28) and Everglades (n = 9). Box and whisker plots indicate that the bottom and top of each box are the 25$^{th}$ and 75$^{th}$ percentiles and the line in the middle of each box is the median, whiskers extend above and below each box to 1.5 times the interquartile range, and observations beyond the whisker length are marked as outliers with an individual symbol. Regression results indicated a significant ($F_{3,370}$ = 11.6, p < 0.01, $R^2$ =0.08) difference between ecoregions and Tukey-HSD tests were used to separate means (indicated by small letters).

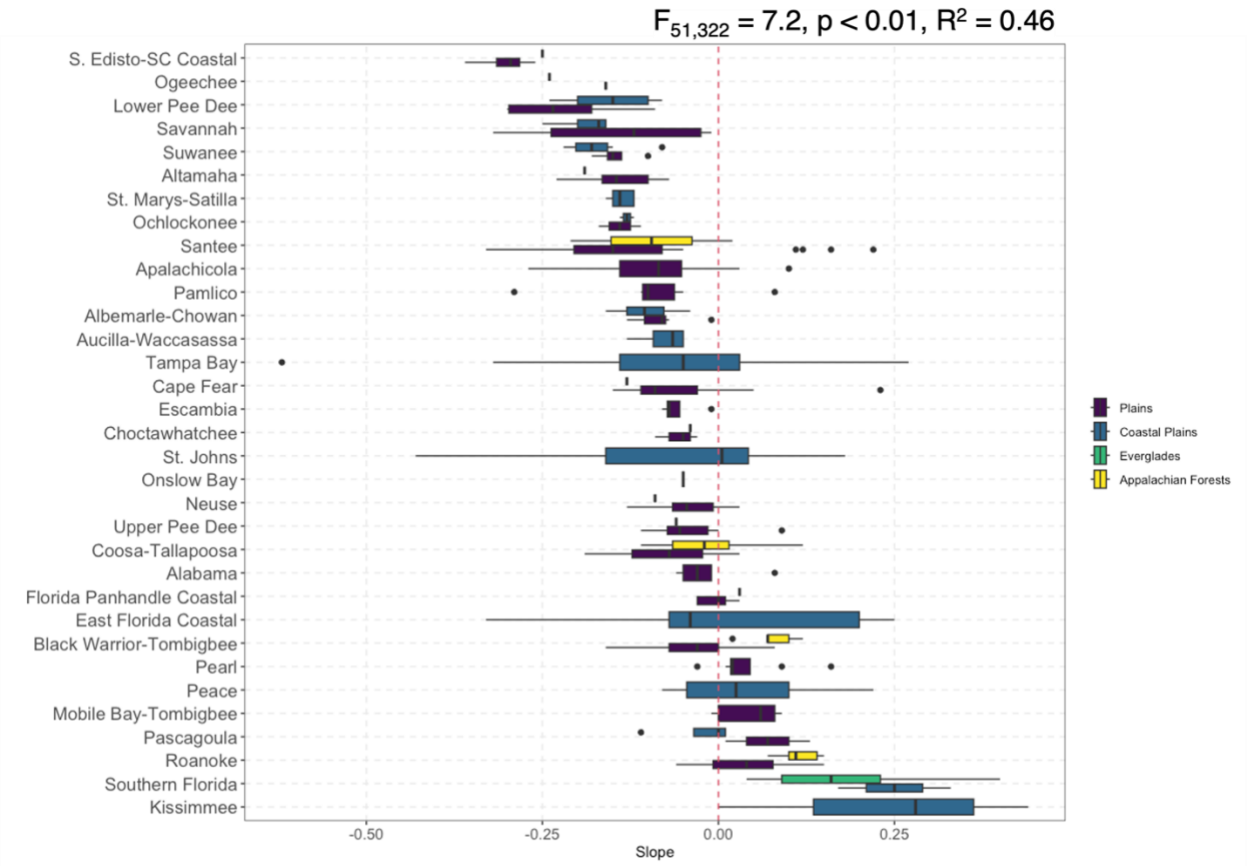


**Figure 5.4.** Mann-Kendall discharge slope (τ) of ecoregions for individual basins from 1957 – 2022. Ecoregions included EPA Southeastern USA Plains (Plains), Mississippi Alluvial and Southeastern USA Coastal Plains (Coastal Plains), Appalachian Forests and Everglades. Box and whisker plots indicate that the bottom and top of each box are the 25$^{th}$ and 75$^{th}$ percentiles and the line in the middle of each box is the median, whiskers extend above and below each box to 1.5 times the interquartile range, and observations beyond the whisker length are marked as outliers with an individual symbol. The plains ecoregion is indicated by dark purple, the coastal plains ecoregion is indicated by dark blue, the everglades ecoregion is indicated by green and the Appalachian Forest ecoregion is indicated by yellow.

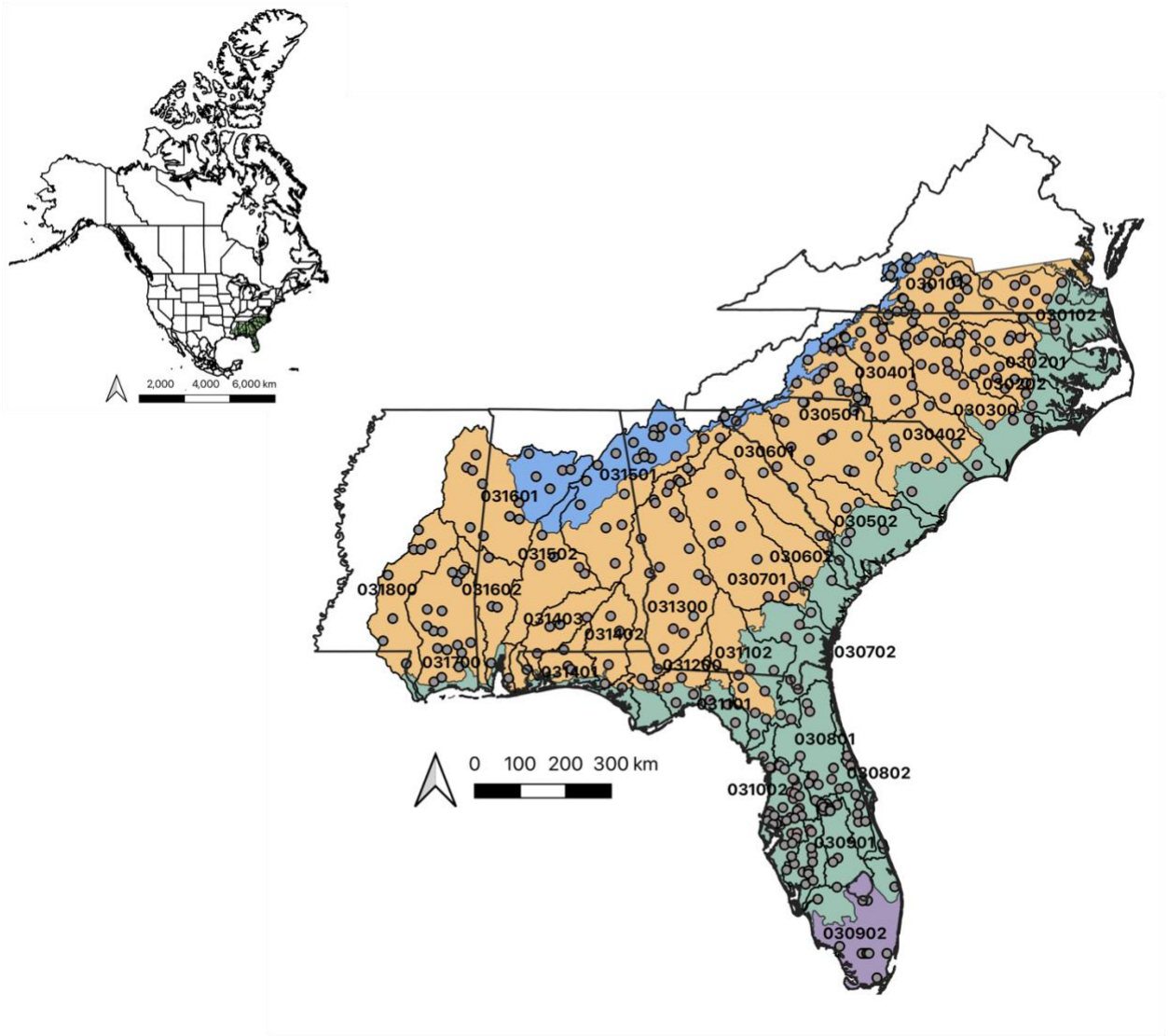


**Figure 5.5**: Streamflow ($m^3/s$, n = 377) sites (50+ years) for ecoregions for the 33 drainage basins in the South Atlantic-Gulf Drainage (HUC-03). Streamflow sites are indicated by gray dots. Basin numbers correspond to 6-digit hydrologic unit codes (HUCs) assigned by the USGS. Blue indicates Ozark, Ouachita-Appalachian Forests (USEPA 8.4; hereafter, Appalachian Forests), gold indicates the Southeastern USA Plains (USEPA 8.3; hereafter, Plains), green indicates the Mississippi Alluvial and Southeast USA Coastal Plains (USEPA 8.5; hereafter, Coastal Plains), and purple indicates the Everglades (USEPA 15.4).